Reactive Power Compensation by Soft-Computing Techniques in Deregulated Environment

Thesis

Submitted by

Syamasree Biswas (Raha)

Doctor of Philosophy

(Engineering)

Department of Power Engineering

Faculty Council of Engineering & Technology

Jadavpur University

Kolkata, India

July 2016

INDEX NO. 255/09/E

1. **Title of the Thesis:** Reactive Power Compensation by Soft-Computing Techniques in Deregulated Environment

2. Name, Designation & Institution of the Supervisor/s:

I. Dr. Niladri Chakraborty.

Professor, Department of Power Engineering, Jadavpur University, Saltlake Campus, Kolkata-700098.

II. Dr. Kamal Krishna Mandal.

Professor, Department of Power Engineering, Jadavpur University, Saltlake Campus, Kolkata-700098.

3. List of Patents: No

4. List of Publications:

Journal Publications:

i. **Biswas (Raha) S**, Mandal K. K., Chakraborty N, "Hybrid SMES based Reactive Power Dispatch by Cuckoo Search Algorithm", Accepted for publication in the IEEE Industry Application Magazine, 13th September, 2017.

ii. **Biswas (Raha) S**, Mandal K. K., Chakraborty N, "Pareto Efficient Double Auction Power Transactions for Economic Reactive Power Dispatch", Applied Energy, 2016, 168: 610-627.

iii. **Biswas (Raha) S**, Chakraborty N, Mandal K.K., "Differential Evolution Technique with Random Localization for Tuned Reactive Power Dispatch Problem", Electric Power Components and Systems, Taylor & Francis Group, LLC, 2013, 41: 500–518.

iv. **Biswas (Raha) S**, Mandal K.K., Chakraborty N, "Constriction Factor based Particle Swarm Optimization for Analyzing Tuned Reactive Power Dispatch", Frontiers in Energy (Springer), 2013, 7(2): 174-181.

v. **Biswas (Raha) S**, Chakraborty N, "Tuned Reactive Power Dispatch Through Modified Differential Evolution Technique", Frontiers in Energy (Springer), 2012, 6(2): 138-147.

vi. **Biswas (Raha) S**, Mandal K.K., Chakraborty N", "Modified Differential Evolution based Multi-Objective Congestion Management in Deregulatory Power Environment", International Journal of Electrical, Electronics and Computer Engineering, 2012, 1(2): 93-97.

vii. **Biswas (Raha) S**, Mandal K. K., Chakraborty N, "Global Welfare Analysis for Modified Differential Evolution based Multilateral Power Transactions with Spot Pricing", **Communicated to Applied Soft-computing.**

viii. **Biswas (Raha) S**, Mandal K. K., Chakraborty N, "Hybrid Pareto efficient Multilateral Power Transactions for Real and Reactive Power Dispatch", C**ommunicated to Applied Energy.**

ix. **Biswas (Raha) S**, Mandal K. K., Chakraborty N, "Comparable Var Compensation for Reactive Power Dispatch in Deregulated Scenario", **Communicated to Electrical Power Components and Systems.**

Conference/Summit Publication:

i. **Biswas (Raha) S**, Mandal K. K., Chakraborty N, "Hybrid SMES based Reactive Power Dispatch by Cuckoo Search Algorithm", International Conference on Power Electronics, Intelligent Control and Energy Systems (ICPEICES) July 2016, IEEE, Delhi.

ii. **Biswas (Raha) S**, Mandal K. K., Chakraborty N, "Modified Differential Evolution based Reactive Power Dispatch Problem involving Multilateral Power Transactions in Deregulated Power Scenario", Power, Communication and Information Technology Conference (PCITC) Oct, 2015, IEEE, Bhubaneswar.

iii. **Biswas (Raha) S**, Mandal K. K., Chakraborty N, "Impact of Modified Differential Evolution Strategy on Reactive Power Dispatch Problem", India Conference (INDICON), 2014 Annual IEEE.DOI:10.1109/INDICON.2014.7030534. Publication Year: 2014, Page(s): 1 – 5.

iv. **Biswas (Raha) S**, Som T., Mandal K. K., Chakraborty N, "Cuckoo Search Algorithm based Optimal Reactive Power Dispatch", Control, Instrumentation, Energy and Communication (CIEC), 2014 International IEEE Conference, DOI: 10.1109/CIEC.2014.6959121.Publication Year: 2014 , Page(s): 412 – 416.

v. **Biswas (Raha) S**, Mandal K.K., Chakraborty N, "Parametric Variation based Simulated Annealing for Reactive Power Dispatch" In proceedings of Sustainable energy & intelligent System (SEISCON 2013), December, 2013, IET, Chennai.

vi. **Biswas (Raha) S**, Mandal K.K., Chakraborty N, "Simulated Annealing Based Real Power Loss Minimization Aspect for a Large Power Network", Swarm, Evolutionary, and Memetic Computing Lecture Notes in Computer Science, 2013, Volume 8297, 345-35.

vii. **Biswas (Raha) S**, Mandal K.K., Chakraborty N, "Modified Differential Evolution based Congestion Management in Deregulatory Power environment", Michael Faraday IET India Summit-2012, (MFIIS-12) 25th Nov, 2012 , Kolkata.

viii. **Biswas (Raha) S**, Chakraborty N, "Reactive Power Generation Minimization Aspect in Deregulatory Power Scenario Using Particle Swarm Optimization Technique", In proceedings of International Conference on Energy, Automation and Signal (ICEAS 2011), Dec, 2011, IEEE, Bhubaneswar.

ix. **Raha S**, Som T, Chakraborty N, Constriction Factor Based Particle Swarm Optimization Applied to Reactive Power Dispatch in Transmission System, In proceedings of Sustainable energy & intelligent System (SEISCON 2011), July, 2011, 2: 335-339, IET, Chennai.

x. **Raha S**, Som T, Chakraborty N., Exploration of Simulated Annealing Technique in Reactive Power Dispatch Domain, In proceedings of National conference on Recent Developments in Electrical Engineering, NCRDEE (2011), 2011, 92-97, Jalpaiguri, West Bengal.

5. List of presentations in National/International Conferences:

i. **Biswas (Raha) S**, Mandal K. K., Chakraborty N, "Hybrid SMES based Reactive Power Dispatch by Cuckoo Search Algorithm", International Conference on Power

Electronics, Intelligent Control and Energy Systems (ICPEICES) July 2016, IEEE, Delhi.

ii. **Biswas (Raha) S**, Mandal K. K., Chakraborty N, "Modified Differential Evolution based Reactive Power Dispatch Problem involving Multilateral Power Transactions in Deregulated Power Scenario", Power, Communication and Information Technology Conference (PCITC) Oct, 2015, IEEE, Bhubaneswar.

iii. **Biswas (Raha) S**, Mandal K. K., Chakraborty N, "Impact of Modified Differential Evolution Strategy on Reactive Power Dispatch Problem", India Conference (INDICON), 2014 Annual IEEE.DOI:10.1109/INDICON.2014.7030534. Publication Year: 2014, Page(s): 1 – 5.

iv. **Biswas (Raha) S**, Som T., Mandal K. K., Chakraborty N, "Cuckoo Search Algorithm based Optimal Reactive Power Dispatch", Control, Instrumentation, Energy and Communication (CIEC), 2014 International IEEE Conference, DOI: 10.1109/CIEC.2014.6959121.Publication Year: 2014 , Page(s): 412 – 416.

v. **Biswas (Raha) S**, Mandal K.K., Chakraborty N, "Parametric Variation based Simulated Annealing for Reactive Power Dispatch" In proceedings of Sustainable energy & intelligent System (SEISCON 2013), December, 2013, IET, Chennai.

vi. **Biswas (Raha) S**, Mandal K.K., Chakraborty N, "Modified Differential Evolution based Congestion Management in Deregulatory Power environment", Michael Faraday IET India Summit-2012, (MFIIS-12) 25th Nov, 2012 , Kolkata.

vii. **Biswas (Raha) S**, Chakraborty N, "Reactive Power Generation Minimization Aspect in Deregulatory Power Scenario Using Particle Swarm Optimization Technique", In proceedings of International Conference on Energy, Automation and Signal (ICEAS 2011), Dec, 2011, IEEE, Bhubaneswar.

viii. **Raha S**, Som T, Chakraborty N, Constriction Factor Based Particle Swarm Optimization Applied to Reactive Power Dispatch in Transmission System, In proceedings of Sustainable energy & intelligent System (SEISCON 2011), July, 2011, 2: 335-339, IET, Chennai.

ix. **Raha S**, Som T, Chakraborty N., Exploration of Simulated Annealing Technique in Reactive Power Dispatch Domain, In proceedings of National conference on Recent Developments in Electrical Engineering, NCRDEE (2011), 2011, 92-97, Jalpaiguri, West Bengal.

DEPARTMENT OF POWER ENGINEERING

FACULTY OF ENGINEERING & TECHNOLOGY

JADAVPUR UNIVERSITY

KOLKATA, INDIA

This is to certify that the thesis entitled "Restructured Reactive Power Compensation by Soft-Computing Techniques in Deregulated Environment" submitted by Smt Syamasree Biswas (Raha), who got her name registered on 29.07.2009 for the award of Ph.D. (Engineering) degree of Jadavpur University is absolutely based upon her own work under the supervision of Prof. Niladri Chakraborty and Prof. Kamal Krishna Mandal and that neither her thesis nor any part of the thesis has been submitted for any degree/diploma or any other academic award anywhere before.

(Prof. Niladri Chakraborty)	(Prof. Kamal Krishna Mandal)
Signature of the Supervisor	Signature of the Supervisor
Date with Official Seal	Date with Official Seal

The thesis is dedicated to the four auspicious females of my life;

Late Grand Mother

Mother

Mother-in-Law

Daughter

Acknowledgement

I would like to express my sincerest gratitude to my supervisors Prof. Niladri Chakraborty and Prof. Kamal Krishna Mandal, Department of Power Engineering, Jadavpur University for allowing and motivating me to work on a very promising area of the present research. I am very much grateful to their valuable suggestions, stimulating guidance and moral support during the full period of my research work.

I am obligated to the Registrar of Jadavpur University, Head, faculty members and office staff of the Department of Power Engineering, the office staff of the FET and TEQIP Cell, the Librarians and the staff of the Research Sections of the Jadavpur University for their kind help and cooperation extended as and when needed.

I also acknowledge DST INSPIRE FELLOWSHIP Programme Divisions, Ministry of Human Resource and Development, Government of India for funding towards my doctoral research.

My sincere thanks are due to my former and present colleagues and friends for their help and support.

I would always be grateful to my parent-in-laws as well as my parents for their affections and moral support for extending conducive and cordial environment for my work. I would also like to express my sincere thanks to my elder brother, brother-in-law and their families for their continuous support to my work.

Last but not the least, I would like to express my heartfelt gratitude to my husband, Sri. Debasish Biswas for his incessant help, cooperation, and motivations. I also acknowledge my 2 year's old little daughter Miss. Kaushani whose innocent support also helped this work to reach at its present form.

Abstract:

Restructured reactive power dispatches and the associated economics have been mainly focussed in this work. The dispatches have been realised by a number of *var* compensators likely Synchronous Condensers, Thyristor Controlled Series Capacitors (TCSC), Superconducting Magnetic Energy Storage (SMES) and some of their combination with capacitors. The work was considered on IEEE 14, 30, 57 and 118-bus network. One real time Indian 62-bus systems is also considered. Performance of a single as well as variable 12-hour, a day ahead double auction bilateral and multi-lateral power transactions have been studied with some of the larger networks. Effect of such on the global welfare is observed while solving the reactive power dispatch (RPD) by different *var* compensators. The sitting and sizing of these *var* compensators are optimised herewith by different soft-computing techniques. These are Simulated Annealing (SA), Particle Swarm Optimisation (PSO), Differential Evolution with Localisation around the Best Vector (DELB), Differential Evolution with Random Localization (DERL) and Cuckoo Search Algorithm (CSA) etc. Initially SA was applied to solve the fundamental RPD problem without considering the complexities of the deregulated power scenario. For SA, the optimum solutions were generated by capacitive *var* compensations only. However due to the limitations such as single solution based approach, SA had faced few challenges. In this ground, PSO was further applied to solve the proposed RPD. The PSO based observations showed improved solutions over the SA in terms optimised real power losses. However, the PSO based solutions were found frequently suffering from the premature convergence problem. By incorporating the constriction factor to the fundamental PSO, the problem was handled to some extent. However, further modifications were required to obtain the desired solutions compared to that obtained by the PSO. Hence, Differential Evolution (DE) was considered to solve the proposed problem. Alike the PSO, fundamental DE based optimisations showed improved responses. However, DE based solutions were frequently found suffering from the problem of slow convergence. To manage the issue, two types of modified DE were considered here to solve the proposed problem of reactive power dispatch. These techniques were namely the DELB and DERL. Amongst them, the DERL showed faster global convergence to optimise the power loss value. Although the DERL generated the desired solutions, but it required higher populations. In this situation, one advanced swarm intelligence based meta-heuristics namely CSA were considered to solve the problem again. The CSA technique was able to generate globally converging data with moderate sized optimal parameters.

Now, amongst these meta-heuristics, the DERL and CSA have been observed to generate better results for the fundamental RPD problems due to their different strengths. Therefore, the RPD issues

involving restructured power transactions were majorly investigated using these two methods. Since the economics is a very important aspects of the deregulated power scenario, the case studies to identify the Pareto efficient transactions were reconciled by planed bidding. These transactions have provided the maximum global welfare every time. Even the transactions which were very close to the Pareto efficient points have been found to generate significant global welfare. Moreover, the power mismatch during the restructured power transactions was also considered which has a major impact in global welfare. This impact in terms of spot pricing was determined and observed to play an important role to effect the global welfare in different scenario. Now, the global welfare was further improved by cumulating the reduced merchandising surplus caused by the *var* compensators. Considering these, three cases on RPD involving deregulated power scenario were investigated.

The first study comparatively analysed performances of the different *var* compensators such as capacitor, synchronous condenser (SC), SMES and some of their combinations considering the bilateral transactions in IEEE 118-bus network. This provided maximum percent global welfare improvement to a value of 0.0452 for the capacitor-SMES combination compared to the case study with no *var* compensators. In the second case study for a 12-h variable bilateral power transactions considering IEEE 57-bus systems, it had been found that the combined capacitor-SMES based *var* compensations were able to reduce 7.41% more power loss and achieve 2.5 times improved economic benefit over the singular capacitor placement. This further realised 0.069% profit enhancement in connection to the fundamental global welfare. Moreover, the investigations considering a day ahead (24-h) multilateral power transactions for a 62-bus Indian utility showed that the combined *var* compensations by capacitor-SMES were able to reduce 11.72% more power loss with 7.5 times improved economic benefit over the singular capacitor placement. This further provided 0.20% profit enhancement in relation to the fundamental global welfare. Here, the optimal parameters were found to be sufficiently able to tackle the dynamic voltage limit crossover problem to maintain the voltage of the network in the desired range for all the case studies.

List of Figures

List of Tables

Table of Contents

Chapter 1

1 Introduction

Reactive power is a fundamental component of power system operation. Its existence can be measured only when reactive elements or loads are presents. By convention inductive loads absorb reactive power where capacitive loads provide the reactive power. When large consumers are present in the network i.e., the amount of inductive loads is high, the power factor of the system goes down. This causes additional losses with extra voltage drop. This in turn affects the customers billing. In this regards the reactive power compensating devices like capacitor banks, overexcited synchronous motor, flexible AC transmission (FACTs) devices, energy storage systems (ESS) are incorporated in the network to improve the power factor, voltage profile and to reduce real power losses. Thus the stability and reliability aspects of any power system are maintained by the adequate reactive power flow. This situation however may be affected due to the change in the power scenario in the challenging environment.

1.1 Power Scenario

The power scenario is facing few challenges amongst which the network security issues involving stable real and reactive power flows are very important. It is therefore very much essential to maintain a balance between the generation and the ever-mounting load demand. Success will depend on how public policies are adopting the innovative techniques likely the low-emitting energy generation technologies to reduce greenhouse gas emission, incorporation of the sustainable *var* compensating devices etc in to the system. This is happening throughout the world. Before implementing it throughout in Indian power scenario, it is therefore very much essential to review the present worldwide power scenario.

1.1.1 Worldwide Power Scenario

The world net electricity generation has been exceeded to 21531.709 Billion Kilowatthours whereas the net consumptions is reported to be 19710.36 Billion Kilowatthours [1]. Hence, a loss of 1835.111 Billion Kilowatthours has been realised. In this direction, Asia & Oceania has generated 8761.581 Billion Kilowatthours of electricity from which 8108.104 Billion Kilowatthours has been consumed as load. More specifically, India generated 1052.499 Billion Kilowatthours of electricity amongst which 864.709 Billion Kilowatthours has been consumed as active load [1]. This however has caused

a significant amount of loss of 192.579 Billion Kilowatthours in India. This losses being very high needs more attention in the Indian perspective.

1.1.2 Recent Indian Power Scenario

The electricity sector of India has a current installed capacity of 301.965 GW by end of March, 2016 [2]. India has got third position in power generation in 2013 with 4.8% global share setting aside Japan and Russia [3, 4]. Although India is the world's fourth largest energy consumer after United States, China and Russia [5], Indian power scenarios are facing several challenges due to shortages in power generation and supply constraints over a rapid growth and development of various exposures. The few of the problems are very important. They are shortage of fuel mainly coal and natural gases as and when required, poor and old connectivity to accumulate the fuel to its destination, theft of power, losses in the connector system, losses in the transmission, distribution and consumers level, lack of pollution free energy efficient sources etc. The present deregulated situations are facing issues like excess demand against lack of supply, transmission and distribution losses above the specified level, low plant load factor, peak demand and energy shortage etc. Poor financial conditions of the State Electricity Boards (SEBs) and severe other resource mismanagements are however addressed by new central and state legislations.

The power sector in the country has already undergone reforms. Consequently privatization was introduced in the generation, transmission and distribution. Hence several complexities arose and adequate controls are necessary to handle the deregulated environment. In this deregulated environment, Ministry of Power (MoP) and Ministry of Non-conventional Energy Sources (MNES) are encouraging various renewable energy sources like wind, small hydro and biomass, tidal energy resources to participate and to generate energy to support the grid at this critical period of requirement. As of November 2015, India has an installed renewable capacity of about 44.059 GW where grid connected power is 42.73 GW and off-grid or captive power generation is about 1.329 GW [6]. As evidenced, India's electricity sector has been reorganized by several aspects. Amongst them, the one of the major issues is the minimization of the real power losses. This demands adequate attention in the deregulated power scenario.

1.2 Generation of Real Power and Loss issue

The power i.e., the energy generated or consumed per unit time is the key entity of an electrical network. Whenever an electric current flows through the transmission and distribution network which has some resistances, it creates heat in the form of losses which is most undesirable. Again these

networks have inductive and capacitive elements. Extra voltage drops do occur in them. This part can be handled by reactive power compensation by incorporating reactive power sources. With this the power factor of the circuit improves. With the improvement of power factor the real power loss is reduced. Thus, in practice, the problem of real power loss handling is analogous to that of reactive power dispatch and management.

1.3 Reactive Power Dispatch (RPD)

The reactive power dispatch (RPD) is addressed as a minimization of real power loss with stable voltage profile issue which helps to reduce grid congestion in a significant amount [7, 8]. In this regards, real power flow is mandatory to provide electricity to any consumers where the reactive power helps to support the real power flow. Now in the practical field, the presence of huge inductive load causes a large amount of voltage deviation or voltage fluctuation. This further gives birth to the grid congestion which can lead the network towards total shut down. Hence, the RPD needs to be solved by integrating various reactive power or *var* compensating devices in conjunction to the control of generator bus voltages and transformer tap-settings. The *var* compensators are generally used as capacitor banks, overexcited synchronous motor, flexible AC transmission (FACTs) devices, distributed generating units, wind mill etc. Recently, to obtain more sustainable performances, energy storage systems like battery energy storage (BES), superconducting magnetic energy storage (SMES), super capacitors, flow batteries and few other renewable energy sources are utilised as *var* compensators. Now, due to reliability reason, the dynamic voltage limit crossover issue as voltage deviation of the load buses can be optimized as a separate objective function. Alike the RPD issue, the voltage deviation can be optimized by incorporating different *var* improvement devices in the network. In this direction, the role of the reactive power support plays a vital role which helps to transmit the real power flow. The reactive power support can be divided into two components: one for supplying reactive demand to improve system security and controlling system voltage and the other for supporting real power transmission. The first part of the reactive power is treated as an important ancillary service provider in restructured power markets under certain constraints. The second part of the reactive power component is utilized to support real power flow of the network. This is usually arranged such a way that no excess generations of reactive power are required to support the real power flow although if required it will be procured under extra payment. In this case ISO will arrange the extra reactive power for which the responsible generator will be paid by the underperforming generator. Therefore, the reactive power issues draw significant attention in the deregulated power scenario.

1.4 Power Sector Deregulation

A number of electric utilities and power sectors are forced to switch their operating mode from vertically integrated network to open access market since the nineties [9]. There are few reasons behind this. Before deregulation, the single operating electrical industry has to obey the rules and regulation set by the Government while generating or transmitting or even distributing the electricity. These impose huge restrictions while serving a range of growing power demands with increasing cost. As a result, an imbalance was generated between the demand and supply which created dissatisfaction among the consumers. In this situation deregulation or restructuring in the power sector claimed an efficient, economic and reliable service at reasonable operating costs. But there were some complexities while implementing the same.

The main aspects of reformed power sector is to identify and distribute the various operation of a traditional organization part by part to different organizations or entities by introducing competition amongst themselves. The functional ability of the different entities of the deregulated power scenario is controlled by the individual system operator (ISO). Here, the customer is the entity who takes the most fundamental part by purchasing the electricity either directly from any Gencos or from the local distribution company of the power market. This helps to improve the efficiency and quality of service at the cheapest rate compared to monopolistic power system. As the operation handling in the deregulated power scenarios is comparatively complex compared to the monopolistic power network, it needs critical observation. In such scenario, the transmission and distribution loss minimization aspects involving restructured power transactions requires major attention.

1.5 Power Transactions

Power transactions are one of the very important aspects of deregulated power markets which are handled by several mechanisms. Amongst these mechanisms, bilateral/multilateral transactions are important trades which occur between multi-seller/multi-buyer systems or between individual buyers and sellers under a self-bargaining or private communicating system under the surveillance of ISO. Now, the transactions are operated based on an open access model. In open access model, both of the participants such as the buyers and sellers are well connected through energy auction phenomena.

In this context, it has been observed that whenever the double auction power transactions occur, the security constraints like the voltage profiles may fluctuate near the boundary values. Even sometimes, these constraints violate the stable operating limits and thereby causes dynamic voltage limit crossover issues leading to network congestions in terms of huge line current flow and power losses.

1.6 Dynamic Voltage Limit Crossover and Congestion Management

Dynamic voltage limit crossover leading to congestion is one of the major issue of deregulated power environment which may happen due to several reasons. A number of power transactions which occur in the electrical power network are sometimes forced to violate the operating limit of security constraint of the line leading to congestion. Moreover, the Gencos, who provide the real power at the lowest rate, are sometimes overloaded while delivering maximum demand. This may be one of the specific causes of congestion in the restructured power scenario. In addition to this the distance between the loads and the Gencos may also influence the network in the congestion issue. Further, the imbalance in loading, excess power demand, line outages may lead the network towards congestion. In the congested power network, ISO increases the price of electricity in terms of merchandising surplus. This further reduces the net benefit of the market players resulting to market inefficiency. Hence the congestion issue needs to be corrected by adopting convenient means.

There are several ways to solve the congestion management problem. Amongst them the incorporation of any *var* compensators such as shunt capacitor, synchronous condenser, FACTs device, or energy storage systems (ESS) in the existing network may help to accomplish the proposed problem efficiently. Although certain investment and operating cost of the proposed devices is always involved but the net monetary benefit due to the integration of the proposed devices ultimately helps to reduce the merchandising surplus [11]. This will further enhance the benefit of the market players in terms of improved global welfare.

1.7 Global Welfare

In the deregulated power market, the fundamental global welfare is quantified by the net benefits of the competing players of the market [11]. The net benefit of the participants are determined w.r.t the market clearing or the market equilibrium point (MEP). In this regards, the bidding of the market players has a great impact on market clearing which helps to derive the transactions at the MEP i.e., the Pareto efficient point. The Pareto efficient situation is addressed as the state of the restructured market where the economic benefits of any of the participants can be enhanced only by diminishing the benefits enjoyed by one of the other participants. Therefore, the market players will achieve maximum economic benefit at the Pareto efficient point. In this connection, if the transactions are occurred at other than MEP, the deadweight losses are found [11]. This reduces the global welfare. In this direction, the economics of the *var* compensators may help to reduce merchandising surplus having RPD solutions involving the power transactions. Hence, the net monetary benefits due to *var* compensators have significant role to improve the benefits of the market participants. This will further

enhance the global welfare of the system under observation. Therefore, the study in this domain draws more interest on the present scope of the research works.

1.8 Scope of the Present Work

From the above discussions, it has been found that there are a number of complexities in the present deregulated power network. Amongst them economic real power loss minimization issues involving power transactions and congestion management are the significant problems of recent power sector. Therefore, the study on the economic reactive power dispatch (RPD) considering monopoly as well as deregulated power scenarios needs closer investigations. In this work, the fundamental reactive power dispatch (RPD) is initially solved by controlling the generator bus voltages, transformer tap settings and shunt capacitor placement satisfying all major equality and inequality constraints. In this conjunction, minimization of the voltage deviation and the reactive power generation issue of the power network are also solved while maintaining stability and reliability criteria. Further, the RPD is considered in deregulated power scenario involving double auction bilateral and multi-lateral power transactions. During the power transactions, the security constraints such as bus voltages fluctuate nearly at their boundary values. Even few of the buses may violate the standard range of per unit values lying in between 0.95 p.u. - 1.10 p.u. This voltage limit violation in the form of dynamic voltage limit crossover may cause increased line current flow and power loss enhancement leading to the congestion.

Since, the congestion is an undesirable phenomenon at any circumstance, it needs major attention to be solved and addressed properly. Here the congestion matter is initially solved by shunt capacitor placements which showed marginal benefit. To obtain better response in the backdrop of deregulated power scenario, few dynamic *var* compensators are incorporated in the network. However the choice of the devices is a topic worth of investigation. These *var* compensators may be synchronous condensers (SC), thyristor controlled series capacitor (TCSC) as FACTs device, and integration of super-conducting magnetic energy storage (SMES) as ESS. To achieve more reliable, sustainable and economic benefit, the combinations of either devices likely capacitor-SC or capacitor-SMES may be accomplished to solve the proposed problem.

Since, economics is a prime factor of the deregulated power scenario, the economic impacts of the proposed *var* compensators to the global welfare of the system under consideration are also ascertained here. In this work, the net monetary benefit due to *var* compensations are determined and added to the fundamental global welfare. This helped to enhance the global welfare as well as the benefits of the participants of the considered network. The net monetary benefit due to *var*

compensation is termed as reduced merchandising surplus or congestion rent. This is distributed equally to the competing market players. In this regards the bidding of the market players has played a very vital role to fix the Pareto efficient transaction at MEP to procure the maximum global welfare [11].

As a test case IEEE 14, 30, 57 and 118 bus systems are initially considered to solve the RPD in a monopolistic market. Further, the RPD problem involving bilateral and multilateral power transactions are evaluated considering medium and large power network likely the IEEE 30, 57 and 118 bus systems. As the RPD is a non-linear, non-convex, non-differentiable optimization problem, soft-computing techniques are applied here for solution purpose. In this work, focus has been given to use modified differential evolution technique namely differential evolution technique with random localization (DERL) and Cuckoo Search Algorithm (CSA) due to their different strengths. In this context, it may be pointed out that the loss optimization is also a big issue in a developing country like India. Since the power sector in India already has undergone deregulation, the RPD requires special attention in the Indian context.

1.8.1 Scope of the Present Work in India

According to the statistics, the technical losses of recent transmission and distribution sector in India are 23.04% in 2014. This was 23.65 % in 2013 and 23.74% in 2012 [12]. A target is fixed to reduce it to 17.1% by 2017 [13]. In this connection the RPD in the backdrop of Indian deregulated power network can draw major attention to the researchers. Here, the proposed problem involving multilateral power transactions is solved considering a real 62-bus network having *var* compensation. As *var* compensators, shunt capacitor, TCSC, SMES and hybrid combinations of capacitor-SMES are utilised and comparatively analysed. Further, the economics of the *var* compensators as reduced merchandising surplus, improved global welfare including the spot pricing are also considered. This finally helped to add a notable contribution to the field of present power system research.

1.9 Contribution of the Present Work

The reactive power dispatches (RPD) have been solved since two decades passed. Although several advanced *var* compensators are incorporated to solve the problem, adequate economic solutions satisfying Pareto efficiency in the context of economics in deregulated environment are sparse in literature. Moreover, the investigations on the benefits of the market participants which are dependent majorly on the reduced merchandising surplus, the planned bidding and the spot pricing etc. are yet to be adequately ascertained. Therefore, the study on economic RPD by advanced *var* compensation for

Pareto efficient power transactions draws a major attention in the present deregulated electricity sectors.

The major contributions of the proposed work are stated below:

- This work is configured on the basis of RPD in deregulated power scenario. Here, the RPD problem is characterized by double auction bilateral/multilateral power transaction phenomena, dynamic voltage limits crossover and congestion management issues. These are solved to obtain new, reliable, sustainable and cost effective solutions which will be appropriate for the deregulated power environment.

- Besides the different *var* compensators, this work mainly focuses to solve the proposed problem by integrating one of the promising technology namely the SMES and combination of capacitor-SMES as advanced *var* compensators. This provided improved performances.

- Since, the economics is one of the prime issues of the competitive power market, the economic impact of the SMES has been considered in this work. Besides the loss minimization, the net monetary benefit due to combined capacitor-SMES based *var* compensation is determined and added to the fundamental global welfare of the system under considerations. This further helped to improve the economic welfare.

- The SMES based the fundamental global welfare are comparatively analyzed with respect to other advanced technology based economic solutions to ascertain the significant contribution of the proposed solution.

- In this work, bidding of the market participants are planned such a way that Pareto efficient transactions may be achieved. This will further help to provide maximum economic benefit to the system under consideration.

- This work is simulated considering medium and larger bus systems likely IEEE 57 and 118 bus systems. Again, a 12-hour variable power transaction in an interconnected network is also considered to derive the importance of Pareto efficient power transactions in a competitive power market. Moreover, a variable day ahead power transaction considering an inter-regional grid of real Indian 62-bus systems is considered to solve the proposed problem with few complexities likely the power mismatch during the power transactions and respective spot pricing etc.

Since, the proposed problem is a nonlinear, non-differentiable, non-convexed, multi-constrained types in nature, it was considered to solve it by several meta-heuristics. Now, there are a number of meta-heuristics methods amongst which the choice of suitable technique is a topic worth of investigation. This work initially considered SA and PSO but later modified differential evolution (DE) and cuckoo search algorithm (CSA) was considered to solve the proposed problem depending on applicability and strength of the techniques. While optimizing the control variables, both the techniques of DE and CSA strategically avoided the local convergence point and finally converged to the global optimal solution.

Therefore, the contributions of the work indicate some positive steps towards the economic and promising solutions in the deregulated power scenario while solving the Reactive Power Dispatch. Further, the work can be extended with economic multi-objective RPD analysis involving optimal power flow, economic power dispatch, and economic emission dispatch in competitive power scenarios. Focus can be given to utilize promising technologies likely flywheels, flow battery energy storage devices and sustainable renewable energy sources as advanced *var* compensators. Hybridisation of the two to three promising meta-heuristics can be incorporated to solve the proposed problem for faster optimisations. With these, the work is organised in the thesis form as enumerated below.

1.10 Organization of the Thesis

The thesis is organised into nine chapters followed by Reference and Appendix sections. Chapter 1 presents an overview to the restructured reactive power dispatch (RPD) for the global as well as the Indian power scenario. Additionally the scopes and contributions of the present work are also stated in the chapter 1. The chapter 2 shows the extensive research prospect of reactive power optimisations issue in three specified domains; reactive power dispatch, restructured power transactions and reactive power optimisations based congestion management. The economics of the proposed approaches are also outlined through the literature survey in this chapter. This chapter also pointed out the shortcomings of the current research which motivated the present work. Chapter 3 defines the fundamental reactive power dispatch; the constraints and their effects on the other parameters of the networks. Finally the working principles of the different *var* compensators are illustrated here. These are required to solve the RPD issue. Chapter 4 outlines the restructured power transactions in the backdrop of economics RPD issue. Here, the optimal bidding, economics of the market participants, Pareto efficient global welfare, impact of spot pricing, merchandising surplus and the impact of economics of the *var* compensations have been described with dynamic voltage limit crossover and the congestion issue. By combing the theoretical compositions of Chapter 3 and 4, Chapter 5

formulates the proposed RPD mathematically considering different cases. In this regard as solution methodology to the proposed problem, different stages of soft-computing techniques are discussed in the chapter 6. This chapter also expedites the importance of the chosen techniques to solve the proposed problem over the other metaheuristics methods. Moreover, the working principle of the chosen algorithms and their implementation to the present problem are presented. Chapter 7 portrays the result and discussion of all the considered cases. The investigations are illustrated in the tabular form as well as graphically in the chapter 7. Finally, chapter 8 draws the salient conclusions from the detailed results as demonstrated in chapter 7. Chapter 9 presents a brief outline towards the future scope of work. The References and the Appendixes are shown later in the Chapter 9.

With this overview of the power situation, a thorough review of the reactive power optimization in deregulated power scenario is essential for better understanding of the RPD. This has been elaborately explored in the next chapter.

Chapter 2

2 Reactive Power Optimization

Reactive power optimization is an important aspect of deregulated power system which helps to operate the network securely by maintaining the voltage profile of the network. Although real power is traded as an important commodity of the power market, reactive power support plays a vital role to conduct the smooth real power flow in the network and grid. Reactive power optimization has definite connection and particularly influenced few aspects of power system. These are likely the reactive power dispatch, restructured economic power transaction and economic congestion management issue.

2.1 Reactive Power Dispatch

Reactive power dispatch (RPD) is a major concern of the present day research which is defined as a real power loss minimization aspect bounded by stable voltage profile within the standard p.u. value. This can be achieved by controlling generator bus voltages, transformer tap settings and by integrating reactive power compensating devices in the network. These adjustments help to improve the power factor of the network which results reduced real power losses with enhanced voltage profile. Moreover, better performance in the associated transmission lines and distribution networks are achieved by this. Therefore, the knowledge on real power loss minimisation while solving the RPD in different scenario is a necessity from many aspects of reactive power dispatch.

2.1.1 Different Aspects of Fundamental RPD

The different aspects of fundamental RPD are comprised of loss minimisation issues, advanced technologies for loss handling, competitive power market based loss optimisations and stability enhancement due to security constraints.

2.1.1.1 Loss Minimisation at Different sized Power Network

Real power loss minimisation is one of the governing issue of a power network irrespective of its size. In this regards, Khazali et.al., [16] demonstrated a harmony search algorithm for optimal reactive power dispatch (ORPD) considering a medium sized networks of IEEE 30 and 57-bus systems. The obtained results were compared and found better in comparison to the evolutionary programs such as

simple genetic algorithm (SGA) and particle swarm optimization (PSO). In the field of advanced PSOs, Wang et.al., [17] proposed a hybrid topology scale-free Gaussian-dynamic particle swarm (HTSFGDPS) optimization algorithm for optimizing real power loss minimization. This work was composed of a new combination of swarm intelligence optimization and complex network theory while solving fundamental RPD problem of power system considering small networks like IEEE 14-Bus and 30-Bus power system. The numerical results, compared with other stochastic search algorithms showed that HTSFGDPS based solution were providing high-quality outputs with higher convergence speed and probability. In this direction, a newly developed teaching learning based optimization (TLBO) algorithm was considered to solve multi-objective optimal reactive power dispatch (ORPD) as described elsewhere [18]. The methods such as TLBO and quasi-oppositional TLBO (QOTLBO) were applied on two test systems such as IEEE 30-bus and IEEE 118-bus systems. The obtained data showed improved response in terms of solution quality of the proposed QOTLBO approach over the original TLBO and other optimization techniques. It further proved its potential to solve the ORPD problem. In this connection, Jovanović et.al., [29] considered the reactive power compensation and the power loss minimization of large radial power networks in the Serbian mine and smeltery industry. The work provided an efficient optimization procedure for positioning and sizing capacitors in large industrial systems based on a simple network analysis method. However, although the capacitor based *var* compensation provided good response; few advanced technologies are presently incorporated to solve the RPD problems for loss minimization and better optimisation.

2.1.1.2 Advanced Technologies for Loss Minimisation

In recent days optimal sitting and sizing of distributed generation (DG) and shunt capacitor at the distribution networks have been drawing much attention of researchers. It helps to reduce power flow in feeder lines while releasing stress on feeder loading which further increases their life. This also adds opportunity to use the existing facility to serve any increased load demand. In this context, the analytical approach based methods for optimal allocation (sizing and siting) of DG and capacitor were proposed [19]. This helped to minimize the total real power loss subjected to equality and inequality constraints in the distribution network. The sizing of the DG and capacitor were fixed considering a 12-bus and IEEE 33-bus test distribution systems. The obtained solutions showed that the combined placement of DG and capacitor provided a significant amount of loss reduction with better voltage profile. Further the reactive power dispatch problem in wind farms (WF) was considered to be solved [20] by particle swarm optimization (PSO), combined with a feasible solution search (FSSPSO). The algorithm was tested on a WF system with 12 wind turbines considering different control options and different real power output levels in the backdrop of competitive power scenario.

2.1.1.3 Competetitive Power Market based Loss Optimisation

A new method was introduced elsewhere [21] to allocate real and reactive losses in pool-based markets. Unlike other approaches, the proposed method could easily and effectively be optimised for the real and reactive power losses simultaneously without any additional calculation except the substitution of line reactance instead of resistance. The proposed method was validated considering the IEEE-14-bus and IEEE-30-bus systems. In this regards, Pourshafie et.al., proposed the optimal reactive power compensation scheme using shunt capacitors [22] at a deregulated distribution power network. By obtaining optimum location and number of capacitance, the distribution network operator solved the two main objectives. These were the reduction of the real power losses and maximizing the reverse on investment. As stability is interconnected to the RPD it should be considered for both the transmission and distribution network involving the RPD issue.

2.1.1.4 Stability Enhancement for Security Constraints

Stability in the power sector is a major issue of present day research which needs critical attention during RPD analysis. In this direction, an improved Genetic algorithm (GA) approach for voltage stability enhancement was formulated by minimizing the maximum of *L*-indices of load buses [14]. Generator voltages, switchable *var* sources and transformer tap changers were utilised here as optimization variables of this problem. The GA technique based performance analysis was examined on IEEE 30-bus and IEEE 57-bus test systems. These provided useful results. Moreover, Differential evolution (DE) based optimal power flow (OPF) was solved considering few issues like the improvement of voltage profile by the reactive power compensation [15]. The proposed DE algorithm determined control variable settings to be operated for active power loss minimization and voltage profile improvement in the transmission system. Here, voltage security margin was evaluated using continuation power flow (CPF), ensuring the feasibility of the optimal control variables setting. The method was validated considering IEEE 14 and IEEE RTS 24-bus systems. These results were further compared with sequential quadratic programming (SQP) method based results to compare improved power loss situation. This also included the voltage profile studies for both the networks.

2.1.2 Voltage Profile Improvements

Voltage profile improvement is an important aspect of the power system optimisation domain. This is majorly connected to the voltage stability emphasising limit crossover issue, handling of voltage security constraints and different *var* compensators for voltage stability improvement.

2.1.2.1 Voltage Stability Issues

Voltage stability including limit crossover issue which is one of the fundamental part of the RPD, was attentively considered by Varadarajan et.al., using the differential evolutionary algorithm [23]. The control variables were generator voltages, tap positions of tap changing transformers and the number of shunt reactive compensation devices for real power loss minimization in the transmission system. Here "penalty parameter less" approach was utilised to handle the inequality operational constraints. The algorithm was validated on standard IEEE 14, 30, 57 and 118-bus systems and the results were compared with conventional method. In this connection, Hamzaoglu et.al., proposed a method to find the location of series capacitors to minimize the total series reactive power loss (SRPL) of a power system [24]. A newly developed indicator was introduced to calculate the decrease in SRPL as a result of series compensation. The proposed method was applied to one and two-area systems and the obtained results were observed to be consistent. The proposed approach also helped to maintain voltage security constraints within their stable operating limit.

2.1.2.2 Voltage Security Constraints

One efficient method to evaluate voltage stability status having limit crossover consideration in both pre-contingency and post-contingency states using two outstanding techniques was developed elsewhere [25]. This work used the continuation method and the local analysis to bring the contingency effect. The proposed methods were tested on two practical systems; power networks of New Zealand and Iran showing the efficient performances. In this context, a preventive countermeasure to improve the voltage stability margin by managing the reactive power was also proposed [26]. While solving the same the effective generator reactive power reserve (EGRPR) was found to be maximized. Detailed models of the generators including the armature and field current limits were analysed to maximize the reactive power capability in emergency states. The proposed optimization procedure was tested on a 6-bus system and the New England 39-bus system to illustrate the effectiveness of the method. In this regards the multi-objective problem formulations for the minimizations of the reactive power provision and transmission loss, costs in addition to maximizing system voltage security margin were considered [27] by presenting a new algorithm. While maintaining the voltage profile of power system within the stable operating limit during server contingencies, all voltage control areas (VCA) of the system were detected and then optimal reactive power reserve was provided for each VCA. The simulation results showed the satisfactory output of the proposed algorithm by *var* compensations for IEEE-RTS test system

2.1.2.3 Different Var Compensators for Voltage Stability Improvement

In this regard to study voltage stability enhancement considering limit crossover, Yang et.al., [28] introduced an improved voltage stability index (*IVSI)* for reactive power compensation by hybrid differential evolution (HDE). The optimisation technique was applied to determine tap settings of on-load tap changing (OLTC) transformers, excitation settings of generators or synchronous condensers (SCs), and size and the locations of static *var* compensators (SVCs) to solve the proposed problem. The results showed that the HDE based improved voltage stability index was able to enhance the voltage stability of a system and reduced line losses considering IEEE 30-bus system as test case. In this context of improvement of the voltage profile, a comparative study of using secondary voltage regulation (SVR) versus shunt-connected controllers are shown elsewhere [29] considering the Italian power network. The comparisons were conducted on the basis of costs for improving voltage stability (VS) and the external transfer capability (TC). This showed that SVR could be seriously considered in practice when trying to improve VS and TC of power systems.

Since the RPD issue is involved with the real power loss minimisation including voltage stability it was found to be a non-linear, non-convex, non-differentiable problem. In this case it was frequently solved by meta-heuristics methods.

2.1.3 Meta-heuristics Techniques based Reactive Power Dispatch Problem

A number of fundamental and advanced meta-heuristics methods were applied to solve the reactive power dispatch.

2.1.3.1 Fundamental Meta-heuristics Methods based RPD

Different paradigms of the fundamental meta-heuristics techniques for RPD implementation are elaborated here. These are stochastic algorithm, evolutionary algorithm, physical algorithm, swarm algorithm and neural network based algorithm. Their implementations to the RPD problems are discussed.

2.1.3.1.1 RPD involved Stochastic Algorithms

Stochastic algorithm is one of the paradigm of the meta-heuristics methods which was considered by Naama et.al., [30] for solving security constrained economic dispatch (SCED) problem. This work applied the tabu search (TS) method to solve the SCED problem with and without considering the line flow constraints. As a test case IEEE-57 bus system was chosen. The TS based results were compared

and observed better w.r.t genetic algorithm (GA) and quasi-Newton method (QN) based observations. In this direction, Sahil et.al., [31] proposed a new approach to solve the optimal reactive power dispatch (ORPD) problem by hybrid algorithm. The hybridisations were performed by combining the particle swarm optimization (PSO) and tabu-search (TS) meta-heuristics (PSO-TS). Simulations were observed considering IEEE 30-bus systems. The observations of the present work were compared with the different evolutionary algorithms including the singular PSO and TS and better result in terms of loss minimization was observed.

2.1.3.1.2 Evolutionary Algorithms oriented RPD Issue

Evolutionary algorithms likely genetic algorithms, evolutionary programing, evolutionary strategies, differential algorithms were extensively applied to optimise RPD issues. In this direction, Varadarajan et.al., presented differential evolution to optimizes different control variable for solving the RPD [32]. The algorithm was validated w.r.t. PSO and SQP techniques considering standard IEEE 14, IEEE 30, and IEEE 118-bus test systems. Further, Abou El Ela et.al., [34] proposed an efficient and reliable soft-computing technique based approach to solve the RPD problem. Here, the power loss minimization, voltage profile improvement, and voltage stability enhancement were tested by the proposed approach considering the IEEE 30-bus test system. The results approved the potentiality of the proposed approach. Further, this showed its effectiveness, robustness to solve the RPD problem compared to other reported evolutionary technique based results. In this regards of evolutionary algorithms applied to solve the RPD problem, the self-adaptive real coded genetic algorithm (SARGA) technique was also considered [33]. The IEEE 14 and 30-bus systems were chosen as test systems to show the applicability and efficiency of the proposed method. The results showed the efficiency of the proposed SARGA method while solving the ORPD problem. Abou et.al., [34] on the other hand presented an efficient GA approach for modelling and solving RPD problem. In the proposed approach, the objectives function in terms of RPD problem was fuzzily described. As a test case standard IEEE 6-Generator 30-Bus System was used. In this connection, Wu et.al.[35] proposed an adaptive genetic algorithm (AGA) for optimal reactive power dispatch and voltage deviation control of power systems. The AGA method helped to refine the convergence performance of genetic algorithms while solving the optimal reactive power dispatch for an IEEE 30-bus power system.

Although the evolutionary algorithms were extensively considered to solve the RPD, the physical algorithms such as Simulated Annealing (SA), Harmony Search (HS) etc. were successfully applied to solve RPD issues.

2.1.3.1.3 Physical Algorithm based RPD

Being motivated by the successful implementation of the SA method in the power system domain, Roa-Sepulveda et.al., solved the optimal power flow (OPF) solutions by SA technique. The simulation results were obtained considering two test systems (IEEE 6 and 30 buses). The proposed results provided satisfactory responses over other meta-heuristics [36]. Further, SA method was considered by Gomes et.al., to validate the economic schedules obtained by market operators together with the injections from bilateral contracts [37]. Here, the SA was applied to optimise the control variables of the proposed problem for IEEE 118 bus system. Besides the SA, HS algorithms were widely applied to few power system optimisation problems including the optimal reactive power dispatch (ORPD) [38]. While solving these the equality constraint, the generator voltages, tap positions of tap changing transformers and the amount of reactive compensation devices were optimised. The proposed HS method helped to optimise the power transmission loss, voltage stability and voltage profile improvement separately considering IEEE 30 and 57-bus systems. The results were further validated by comparing with other evolutionary programs. In this regards, a modified HS algorithm solved economic load dispatch (ELD) and combined economic and emission load dispatch (CEELD) problems [39]. The effectiveness of the proposed algorithm was analysed by solving the proposed problem at various test systems. Even the obtained results were validated with classical HS algorithm and some of the most recent research works of the area.

Nevertheless, the physical algorithms handled the proposed problem efficiently, the swarm algorithm were also widely utilised in this domain to solve these types of problems.

2.1.3.1.4 RPD solved by Swarm Algorithms

In this direction to applications of swarm algorithms, Mahadevan et.al., applied the [40] fundamental PSO and advanced PSO to solve the RPD. In this work, the advanced approach namely comprehensive learning particle swarm optimization (CLPSO) has been proved to work satisfactorily over fundamental PSO while solving the proposed problem efficiently. As a test case, a standard IEEE 30-bus and 118-bus test systems were used. Besides this, it has been found that a number of modified swarm algorithms efficiently solved the proposed problem. In this regards, a new modified artificial Bee Colony algorithm (MABC) was proposed to solve the economic dispatch problem by Secui [41]. Here, the modification in the fundamental Bee Colony algorithm helped to avoid premature convergence while deriving the stable and high quality solutions. Several test cases were considered to compare the performances of the classical ABC algorithm and other optimization techniques. This showed better performance of the MABC algorithm over the others. Meanwhile, Huang et.al.,

proposed a hybrid swarm evolutionary approach to solve the optimal reactive power dispatch [42]. The hybrid method was developed by combining the fundamental differential evolution (DE) algorithm with variable scaling mutation and probabilistic state transition rules used in the ant system. The performance of the proposed method was verified by comparing with other optimisation based case studies. The investigations showed that the proposed approach obtained better results with lower active power transmission losses and better convergence performance than the existing methods.

In addition to the swarm algorithms the neural network has also played a significant role to optimise the RPD in this domain.

2.1.3.1.5 Neural Network based RPD Problem

A new methodology for ancillary services market dispatch using Neural Network was considered by Canizes et.al., [43]. The method was proposed on the basis of deterministic optimization. An Artificial Neural Network was used for day-ahead prediction of regulation-down, regulation-up, spin reserve and non-spin reserve requirements to illustrate the application of the proposed method. Two cases based on California Independent System Operator data concerning dispatch were studied in this work. Further an artificial neural network (ANN)-based approach for online monitoring of a voltage stability margin (VSM) in electric power systems was presented by Bahmanyar et.al., [44]. In this work, the Gram–Schmidt orthogonalization process along with an ANN-based sensitivity technique has utilised a few input variables required to approximate the VSM with sufficient accuracy and high execution speed. The efficiency of the proposed method was inspected on the dynamic models of the New England 39-bus and the southern/eastern (SE) Australian power systems. The investigations indicated that the proposed scheme provided a compact and efficient ANN model that has been working successfully and accurately to estimate the VSM.

Besides this, few advanced meta-heuristics are also applied to solve the proposed RPD which require extensive considerations.

2.1.3.2 Advanced Meta-heuristics based RPD

Aribia et.al., presented three problems of the electric networks likely the economic environmental dispatch (EED), the optimal reactive dispatch (RD) and the active, reactive and environmental dispatch (ARED) [45]. While solving the multi-objective problems an Improving Strength Pareto Evolutionary Algorithm (SPEA2) method was applied to the New-England Power System (39 buses, 10 thermal generators). The results proved the proficiency of the proposed approach to find Pareto optimal solution and to maintain a Pareto front in one single run. Mallipeddi et.al., [46] analysed the

performance of different constraint handling methods such as superiority of feasible solutions (SF), self-adaptive penalty (SP), ε-constraint (EC), stochastic ranking (SR), and the ensemble of constraint handling techniques (ECHT) on ORPD problem evaluation. The proposed methods were investigated on IEEE 30-bus, 57-bus, and 118-bus systems. Simulation results provided a clear evidence of employing an efficient constraint handling method for solving the ORPD problem effectively.

Besides the applications of different advanced meta-heuristics methods to solve the RPD problem, few advanced devices were considered to solve the proposed problem. Amongst these devices, energy storages played a vital role in the power sector.

2.1.4 Advanced Energy Storage System (ESS) for RPD

The ESS are widely applied in different sector of power grid including the power transmission and distribution domain due to their efficient performances.

2.1.4.1 Applications of ESS in the Different Power Sectors

However, the appropriate selection of the energy storage devices is a challenging task to the present deregulated transmission and distribution network with undefined daily and seasonal load demand. This issue was viewed by Luo et.al., [47] describing a state-of-the-art of the ESS devices based on their energy density, power density, specific energy and power, power rating and rated energy capacity. Further, to acquire stable, reliable and usable grid operation involving power factor corrections and renewable energy arbitrage, suitable ESS were considered by Pearre et.al., [48]. This work utilised a range of metric while incorporating the ESS. In this regards, Wu et.al., [49] utilised a simultaneous active and reactive power (P−Q) control scheme of a superconducting magnetic energy storage (SMES) unit. Here, a method for repressing the low frequency oscillation of a synchronous generator was considered. Moreover, the Eigen value analysis and digital simulation were also utilized to show the damping effect of the SMES unit over a wide range of loading conditions. Due to its effectiveness in this sector, SMES device further might be considered to be applied as *var* compensators in different cases of RPD analysis.

2.1.4.2 SMES as Var Compensator

In this regards, Shi et.al., incorporated SMES in wind farms for voltage stability [50]. This work integrated a doubly fed induction generator (DFIG) with SMES unit to the power grid. This helped to improve the voltage stability of the power system considerably using the SMES. Moreover, Kwan et.al., [51] has developed a 50 ampere 36 volt three-phase power converter using a SMES for

controlling the active and reactive power. The proposed SMES device had a 6.7 H superconducting coil for which the phase and modulation index were adjusted by the PWM method experimentally. Mean the while, as continuous var controller SMES device was applied to operate the converter in the buck-boost mode with a switched capacitor bank [52]. The investigation provided that this mode of control improved the overall performance of the power system in P-f and Q-V loops. This also allowed the use of any additional *var* compensator in the power area with the SMES unit satisfactorily. In this context, Mitani et.al., [53] proposed the experimental results of stabilization of a model power transmission system by incorporating a SMES. Here, this work demonstrated a significant contribution of the SMES device in the power system stabilizing sector by P-Q simultaneous control. Besides this, the combined operation of capacitor-SMES was considered for voltage profile improvement elsewhere [54]. This work represented a new algorithm to show voltage sag optimization issue by voltage source inverter operated *var* compensation using combined capacitor-SMES device.

Now advanced *var* compensations helped to improve reactive power loss minimisation which were widely considered for the transmission lines.

2.1.5 RPD through Transmission Lines (TL)

Reactive power compensations in transmission lines are major issues which should be illustrated thoroughly for better RPD.

2.1.5.1 Reactive Power Compensation in Transmission Lines

While discussing the *var* compensation in transmission lines Acha et.al., demonstrated the principles of transmission-system compensation [55]. The compensation schemes included the shunt and series compensation in a long transmission lines and cables. This work analysed the behaviour of distributed parameters with variable voltages and currents throughout the line. In this regards, El-Marsafawy [56] presented a mathematical model and an analytical procedure for determining the economics of series capacitor compensation. Results were determined considering a sample of 500 kV transmission line. The effects of different electrical parameters on the economical compensation were also observed. Now, in the view of *var* compensation in long transmission lines, Kumar et.al., [57] proposed a comparative assessment of the static *var* system (SVS) for improving the transient performance. Here, the application of the auxiliary controllers considerably improved the system damping. This further helped to stabilise the disturbances in the system modes. In this regards, the characteristics analysis for HV transmission lines was an important issue which requires special attention in connection to RPD.

2.1.5.2 Characteristics Analysis for HV Transmission Lines

Characteristics analysis of two-terminal HVDC transmission link is one of the most important elements for RPD for which Kiliç et.al., represented a simplified HVDC link for the optimal reactive power flow (ORPF) studies [58]. Here, the proposed problem was solved by genetic algorithm (GA) considering the modified IEEE 14-bus, the modified IEEE 30-bus and the modified new England 39-bus test systems. The efficiencies of the proposed method were determined by comparing the obtained results with that reported in literature. Further, an analytical approach showing the performance of a series capacitor placed both at the sending and the receiving end is justified elsewhere [59]. In this direction, a new method for calculating the maximum power transfer limit of high voltage compensated transmission lines was determined [60]. Two schemes i.e., series and shunt compensation were studied here. This helped to obtain the numerical results for maximum power transfer limits, critical angular separation and critical voltage. Besides these few important *var* compensations schemes were applied to solve the RPD issues efficiently.

2.1.5.3 Different Var Compensation Schemes in Transmission Lines

Variations in reactive power compensation in long transmission lines is an important aspects of existing power sector which had been discussed by Ramar et.al. [61]. This work proposed a generalized approach to manage reactive power for maximum power transfer constrained with voltage stability. Further, Singh et.al., placed the capacitors both at the sending and the receiving end to maintain constant voltage at these points with high levels of power transfer [62]. This work showed two different control criterions. In this context, the use of static *var* compensators in long distances AC transmission system was demonstrated [63]. The proposed device had been found to minimize the voltage fluctuations, small disturbance and transient stability. Moreover, few FACTS devices namely the static synchronous compensator (STATCOM), the static synchronous series compensator (SSSC), and the unified power flow controller (UPFC) were extensively utilized as *var* compensators [64]. Here, the proposed devices helped to improve the operational performances of an interline power flow and VSC-based high voltage DC systems.

Although the modern FACTs devices perform satisfactorily, but the harmonics distortion of the devices is a major concern.

2.1.5.4 Harmonic Analysis Considering Transmission Lines

In the domain of Harmonic, García et.al., analysed [65] the adverse impact of the thyristor-controlled series capacitor (TCSC) on transmission line.. This work solved different TCSC based operations for the total harmonic distortion, apparent power, active power, reactive power, distortion power and power losses. Encouraging observations were obtained. Now, the RPD study is extended to the distribution power network which is also a major sector of present power deregulation area.

2.1.6 Reactive Power Compensation in Distribution Networks

Reactive power compensation in distribution network is an important issue which requires closer observation.

2.1.6.1 Var Compensation in the Distribution Network

Reactive power compensation is one the prime aspects of solving the RPD which was considered by Bisanovic et.al. [66]. The work provided an efficient solution for reactive power control of capacitor bank by varying the reactance of connected reactor. This also helped to maintain the quality of supply. In this connection, again a PSO based active and reactive power compensation strategy of power distribution network was determined elsewhere [67]. While compensating the active and reactive power in the distribution sector, the optimal placement of distribution generation (DG) and capacitor unit was considered. The PSO based results have also been compared with the fast analytical approach to validate its efficiency. In this context, real time optimal *var* compensation has a great impact on the distribution network concerning RPD issues.

2.1.6.2 Real-time Optimal Reactive Power Control

An efficient algorithm for optimal reactive power and voltage control applicable to large distribution networks was proposed by Salama et.al. [68]. In this work, the proposed algorithm considered a partitioning and Kron's reduction technique as an optimisation tool. The proposed algorithm helped to maintain the voltage levels for all buses within permissible limits at all times. The results proved the algorithm to be efficient, fast, and reliable. Therefore, it can be implemented to optimize line loss reduction at distribution feeders. In this connection to different feeders, the radial distribution feeders were widely visible in real field which therefore required closer view in the RPD context.

2.1.6.3 Reactive Power Compensation in Radial Distribution Network

Das et.al., applied genetic algorithm (GA) to select the optimum values of fixed and switched shunt capacitors to solve RPD for varying load conditions [69]. The proposed method helped to minimize the energy loss while keeping the voltage at load buses within the specified limit by considering the cost factors of the capacitors. Based on the obtained results, a comparative performance was also presented. Again Ramalinga Raju et.al., [70] proposed a new algorithm to determine the optimal sizes and locations of capacitors in a radial distribution system. The approach helped to improve the voltage profile as well as the net savings. As a test case, standard 69 bus systems, 85 bus systems and practical 22 bus systems were chosen. The obtained results were compared with the results of the other methods which showed improved responses compared to the other optimisation techniques. However, to obtain more improved response, advanced optimisation was applied to solve the RPD in the radial distribution systems.

2.1.6.4 Advanced Optimisation for Radial Distribution Network

In this conjunction, a Clustering Based Optimization (CBO) was proposed elsewhere [71] for the optimal sitting and sizing problem of the shunt capacitors. This work minimized the costs of power losses as well as capacitor investment costs. While solving the issue, over-compensation and voltage constraints were also taken into consideration. As a test cases a 22-bus, 34-bus, 69-bus and 85-bus distribution systems were considered. The CBO based results were found quite encouraging compared to few established optimisation techniques. Besides the singular RPD analysis, the proposed problem as multi-objective function were extended by few researchers which needs to be discussed thoroughly.

2.1.7 Multi-objective RPD Formulation

The RPD problem comprising of real power loss minimisations and voltage limit crossover analysis can jointly be solved in terms of multi-objective optimisations. These are majorly solved by *var* compensation which help to generate a better and secured voltage profile in the network.

2.1.7.1 Voltage Security based Multi-objective RPD Analysis

In this regards, optimal reactive power dispatch considering voltage stability (ORPD-VS) was considered by a new hybrid fuzzy multi-objective evolutionary algorithm (HFMOEA) [72]. The HFMOEA based optimization results were compared with the elitist non-dominated sorting genetic algorithms such as NSGA-II and MNSGA-II. The simulation results provided proficiency of HFMOEA for generating improved Pareto-optimal fronts with improved convergence and diversity.

In this context, Roselyn et.al., [73] proposed multi objective differential evolution (MODE) algorithm to solve the voltage stability constrained reactive power planning (VSCRPP). While modelling the reactive power planning (RPP), total cost of energy loss and reactive power production cost of capacitors were minimized. In addition to this, the maximisation of the voltage stability margin was also considered. The simulation results including the optimised *var* compensators were found not only very promising, but it helped to maintain the diversity of the solutions. As a test cases, IEEE 30 bus and IEEE 57 bus systems were chosen. Nevertheless, though the specified *var* compensators helped to ascertain the improved results, but few advanced *var* compensators were integrated in the networks for sustainable multi-objective optimisations.

2.1.7.2 Multi-objective Optimisation by Advanced Var Compensators

In this context, Krichen et.al., [74], proposed a new approach to solve of multi-objective RPD problem formulation considering real time wind generators. Here, a capacitor and reactor banks were incorporated in the load nodes in addition to the wind generators. In this regards, Cheng et.al., [75] solved a Reactive Power Optimization in multi-objective mode (MORPO) considering distributed generation (DG). This is accomplished by Dynamically Adaptive Multi-objective Particle Swarm Optimization (DAMOPSO) algorithm. A detailed study was analysed to verify the feasibility and effectiveness of the proposed method considering IEEE 33-bus system. Besides the advanced *var*-compensations to solve the MORPO problem, few advanced meta-heuristics were also incorporated by few researchers which should be discussed a priory.

2.1.7.3 Advanced Meta-heuristics based Multi-objective RPD Formulation

Ghasemi et.al., [76] proposed a new multi objective Chaotic Parallel Vector evaluated Interactive Honey Bee Mating Optimization (CPVEIHBMO) to determine the feasible optimal solution of the Multi-objective Reactive Power Dispatch (MORPD). To achieve a good design with different solutions, Pareto dominance concept and fuzzy set theory were employed. The computational results showed improved convergence characteristics compared to other multi objective optimization algorithms. In this regards, Wang et.al., applied an innovative technique likely the fisher fishing optimization algorithm (SFOA) for solving the MORPO [77]. The simulation results were determined for IEEE-30 nodes and IEEE-57 nodes system. This showed that SFOA had global search performance and steady convergence compared to other methods. In the backdrop of advanced meta-heuristics, Wang et.al., [78] proposed a multi-objective fuzzy adaptive particle swarm algorithm to solve the proposed problem. Considering the system security and economics, a practical reactive power optimization model was configured here considering all the operational constraints. The results of the proposed method helped to achieve the global optimal solution by reducing the computational

complexity and improving the efficiency. Moreover, Pires et.al., [79] presented a multi-objective reactive power compensation model subjected to economical and operational evaluation aspects. Here, an Elitist Non-dominated Sorting Genetic Algorithm (NSGA II) was invoked to handle the local search. Further Lashkar Ara et.al., [80] proposed a multi-objective optimization methodology to solve the proposed problem by formulating a multi-objective mathematical programming (MMP). As a test case IEEE 14, 30, and 118 bus test systems were considered to optimize simultaneously the objective functions. These were likely the total fuel cost, the power losses and the system loadability. The obtained results evidenced the efficiency of the proposed algorithm for solving the reactive power planning. In this regards, MORPO in the distribution sector gained major attentions.

2.1.7.4 Multi-objective RPD Formulation in Distribution Sector

As a multi-objective RPO problem, Antunes et.al., proposed the sitting and sizing of capacitors in electrical radial distribution networks [81]. The performance of the capacitors in a distribution network was analysed in this work. Minimization of system losses and cost of the capacitor installation were explicitly optimized in this model.

Nevertheless, the reactive power optimisation was the prime objective of the RPD problem, but the economics issues were also considered as one of the governing aspects of the proposed problem. Hence, the total economics likely the fuel cost, the cost of the *var* compensators in the back drop of RPD problem are required to be discussed thoroughly.

2.1.8 Economics of the Var Compensators in RPD

Economics of the *var* compensation is connected to the minimisation of operational costs as well as fuel costs.

2.1.8.1 Minimization of Operational Costs

In conjunction to the economics of the RPD problem, the fuel cost minimization for the optimal power flow (OPF) was elaborated by the Teaching-Learning-Based Optimization technique elsewhere [82]. In this work, different objectives related to OPF issue were solved considering the standard IEEE 30-bus and IEEE 118-bus test systems. The comparative study indicated that the Teaching-Learning-Based Optimization technique provided an effective and robust solution by solving the proposed problem in different scenarios. In this context to solve the OPF problem, a DE algorithm was applied elsewhere [83]. As a test case standard IEEE 30-bus test system was considered to solve the OPF where the fuel cost was represented by a non-smooth piecewise quadratic costs function. The

results showed the effectiveness and robustness of the proposed approach while solving the OPF problem. Now, the influence of distributed generation (DG) on distribution losses in medium voltage (MV) distribution networks was considered because of economics [84]. The work focussed to minimize the losses and operation costs of the DG for reactive power compensation w.r.t voltage constraints. The obtained solutions evidenced the fast, simple and efficient performance of the proposed method with an acceptable level of accuracy. Besides this, few more advanced methods related to economic RPD problem are utilised in the present day power sectors.

2.1.8.2 Advanced Methods to Optimise Economic RPD Problem

Dong et. al., presented [85] an approach to solve for a Preventive Security Constrained Optimal Power Flow (PSCOPF) with two sample applications in power system planning and operation. Further, as the OPF problems with generators having either convex or non-convex fuel cost characteristics, a biogeography-based optimisation (BBO) algorithm was applied to solve it elsewhere [86]**.** Different operational constraints, such as generator capacity limits, power balance constraints, line flow and bus voltages limits were included to solve the proposed fitness function. The obtained solution focused the superiority of the BBO technique as an alternative approach of solving the OPF problems over other methods. In this context to the optimal reactive power planning, a new multi-level methodology was shown elsewhere [87]. The basis of the OPF solution was considered here to improve the voltage profile. The obtained simulation results showed the effectiveness of the proposed approach while minimising the system voltage deviation.

Due to different complexities, the RPD problem earned major focus in the deregulated power scenario which needs strategic *var* compensation which includes adequate reactive power planning.

2.2 Reactive Power Optimizations (RPO) for Restructured Power Transactions

Reactive power optimizations or reactive power compensations issue are extensively utilised in the deregulated power environment for the loss compensation. This further helps to derive monetary benefit to the network under observation. In such network, these *var* compensators are often acting as ancillary service (AS) providers to deal while maintaining the reliability of a power system. In this regards, the AS providers are allowed to provide service under certain contract based on payment and system security. In this connection, reactive power pricing is one of the important aspects of the electricity market. Therefore, the economic reactive power supply by the ancillary service providers is a vital part of the deregulated power environment. This majorly controls the transmission network

voltages which are hindered due unstable operations of the different security constraints of the network. To manage the crisis, a number of advanced analytical tools are incorporated in the network which helps to secure the power system reliability in a new dimension. This has a great effect on bid and contract markets where a number of participants are present. However, it may also result in opportunistic bidding strategies that seriously affect economic efficiency of the restructured power industry.

2.2.1 RPD Issue in Restructured Power Market

The RPD issue in restructured power market are often designed in terms of utilisation of various advanced reactive power supports,

2.2.1.1 Utilization of Various Reactive Power Supports

Restructured power markets are usually governed by economics which therefore needed various type of arrangements that could derive profit as easy as possible. In this regards, the optimum allocation of reactive power supports in the deregulated power market was proposed elsewhere [88]. In this work, a floating point genetic algorithm (FPGA) was utilised as optimisation methodology to allocate reactive power compensators in IEEE-14 bus system. The FPGA based results were found efficient in achieving optimal solutions under real time constraints and price based conditions. Further, a case study with Colombia system was shown elsewhere [89] to provide adequate voltage support in a regulatory framework. Additionally, this work handled the placements of the *var* compensators for both monopoly and market-based mechanisms.

2.2.1.2 Allocation of Advanced Var Compensating Devices

In the deregulatory power environment, Mithulananthan et.al., [90] presented a flexible AC transmission (FACTs) devices based congestion management ensuring the economic benefit of the power network. The proposed concept was analysed and validated on five-bus test system by incorporating thyristor controlled series capacitor (TCSC). The obtained results showed to relieve the congestion of the system and the investment cost recovery with benefit. In this regards, Porkar et.al., [91] proposed a mathematical optimization model to obtain the optimal sizing and sitting of the distributed generation (DG) units. The proposed model also optimized the location and sizing of the DG at the new market price as well. The DG based model accomplished the economical and electrical benefits with improved power quality to distribution system. This further helped to minimize its total planning cost by reducing its consumers' bills. Therefore, RPD issues might be treated by solving multi-objective optimisation problem for better practice.

2.2.1.3 Multi-objective System Planning Considering RPD Issue

Augugliaro et.al., [92] designed the reactive power optimization problem considering the new deregulated energy market. In this restructured market, reactive energy is considered as a purchasable entity using the MV grid operator. This helped to improve the efficiency of the transmission system in all its operating conditions with a strong movement of the reactive power compensation. In this context, Rabiee et.al., [93] proposed a multi-objective problem formulation on a day-ahead system based on reactive power optimisation. A multi-objective mathematical programming (MMP) formulation was utilised here to solve the proposed problem using a fuzzy approach. The validation of the proposed method was tested considering the IEEE 24-bus reliability test system (IEEE 24-bus RTS). It has been found that, economic load dispatch which is one of the singular function of the proposed problem played a major role in the multi-objective reactive power planning issue. Therefore, the optimal economic load dispatch was required to analyse restructured power sectors involving certain conditions.

2.2.1.4 Optimal Economic Load Dispatch in Restructured Power Scenario

Restructured power scenarios are frequently observed to have a number of power transactions either bilateral or multilateral. This has a vast impact on the loss allocation issues which were majorly discussed by Galiana et.al. [94]. The proposed problem of loss allocations were formulated involving bilateral power transactions. A number of test cases were solved here. In this direction, Raglend et.al., [95] solved the economic load dispatch (ELD) problem with bilateral and multilateral transactions by few optimization techniques. The obtained results were compared among the different optimisation technique with respect to solution time, production cost and convergence criteria considering IEEE 30-bus system. Amongst the different optimisation methods, the DE based solutions were proved to be quite encouraging and useful for the considered ELD environment. Moreover, Venkatesh et.al., utilised [96] Evolutionary Programming (EP) methods to solve the problem in case of three, six, and thirteen unit systems. To improve the speed of convergence, a nonlinear scaling factor was also incorporated to EP algorithm. The observations showed improved response in the economic load as well as emission environment. Now, pricing is the governing factor of the restructured power market. Therefore, the pricing of the combined economic emission dispatch (CEED) should be discussed a priory.

2.2.1.5 Transmission Pricing involving Economic Load Dispatch

In this context, a simulations-based ELD for a hybrid electricity market was demonstrated elsewhere [97]. The simulation results showed efficient performance of the proposed method for the hybrid-decentralized market. Further, Gnanadass et.al., [98] proposed an improved method for allocating embedded cost of power transmission to its users under deregulated power market. The effect of reactive power flow due to power transaction was taken into consideration to assign the embedded cost. The IEEE-30 bus and the Indian utility - 62 bus systems were considered to allocate the proposed embedded cost. The observations showed improved response for the test systems in a decentralized power market.

2.2.2 Decentralized Power Transactions

Decentralised power transactions are considered here in terms of strategic planning based coordinated multilateral trades.

2.2.2.1 Coordinated Multilateral Trades for Decentralized Power Networks

As stated earlier, the multilateral power transactions are one of the vital aspects of decentralised power sector which was presented by Wu et. al. elsewhere [99]. This showed a new operating paradigm to handle economics and reliability of system under observations. The proposed work was able to obtain maximised social welfare by coordinating private multilateral trades. It was found that the coordinated multilateral trading model could function well enough with the traditional model. It was also observed that the proposed multilateral trading model provided non-discriminatory service to both utility customers and direct-access customers. This was derived due to proper strategic planning as implied in the proposed transactions.

2.2.2.2 Strategic Planning for De-centralized Multilateral Power Transactions

In this regards, Liu et. al. [100] considered a decentralized model for DC load flow based on congestion management issue by optimal resource allocation (ORA) method. In the proposed model, each transaction utilized profit maximization under certain limits of transmission line capacities as directed by the individual system operator (ISO). The obtained results illustrated the effectiveness of proposed approach considering IEEE 30 bus systems. Further, Visalakshi et.al. presented AC load flow-based decentralized model to handle congestion management issue in elsewhere [101]. This work utilized the resource allocation technique. A covariance matrix adapted evolution strategy (CMAES) algorithm was applied to solve decentralized congestion management problem involving

multilateral transactions. The test systems were chosen as IEEE 30 bus, IEEE 118 bus and practical Indian utility 62 bus systems. The CMAES algorithm based simulation results showed better performance over the PSO and SQP. Moreover to assign the effectiveness of the improved decentralized model, the obtained results were also compared with centralized model. This also provided improved performance by the proposed model.

However, a number of successful researches were carried out for the optimal congestion management but the study involving transmission loss allocations with power transactions based congestion management required adequate solutions.

2.2.3 Transmission Loss Allocation based on Different Power Transactions

Transmission loss allocations are observed here for the different power transactions with different pricing mechanisms and advanced optimisations in competitive power domain.

2.2.3.1 Transmission Loss Allocation under Bilateral/Multilateral Contracts

A tuned approach to allocate transmission loss to bilateral/multilateral contracts considering a real time dispatch was observed by Daroj et.al. [102]. The problem formulation was developed on the basis of the speed increment methodology considering IEEE 6-bus and 30-bus system. The observations were found more promising than the pro-rata method. Meanwhile, an application of proportional sharing principle to transmission loss allocation for different power transactions were considered [103]. The proposed neural network based framework was proved to allocate the power losses efficiently in adjacent to power transactions. Further, an artificial neural network based transmission loss allocation method was shown [104]. The observations for both peak and off-peak hours were compared with those obtained using another technique for IEEE 24-bus test system. In this regards, Zhang et. al. proposed two methodologies to determine the optimal bilateral transaction while considering minimization of the total transmission loss [105]. Although certain assumptions were considered, the loss formula based approach provided better optimal results for the four test systems. Besides the optimal operations, the economics of the operation is one the guiding factor of the decentralised power scenario. Therefore, the pricing of the transmission loss allocation should be discussed a priory in the backdrop of power contracts.

2.2.3.2 Pricing for Transmission Loss Allocation under Decentralized Power Contracts

A suitable method to handle the power dispatch problem in a decentralised power environment including bilateral and multilateral transmission transactions were observed elsewhere [106]. This work developed a price-based operational framework considering the power transaction issue in the backdrop of optimal transmission dispatch. The case studies demonstrated that the proposed market arrangement and its operating mechanisms were appropriate with respect to the competitive power environment.

2.2.3.3 Advanced Techniques to Allocate Transmission Loss in Competitive Environment

In this direction, Gross et. al., proposed a new scheme to conduct different power transactions based on loss allocation [107]. In this work, rigorous numerical testing based on proposed schemes were experimented considering several test systems. Further, a new methodology on path-integrals for accurate bus-wise transmission loss allocation was developed by Kyung-Il [108]. Integral path determination was a vital part of this study which helped to obtain a unique and accurate solution to the loss allocation or the RPD issue in a competitive market place. Now, reactive power was represented as a purchasable commodity or ancillary service provider to allocate loss as well as to improve voltage instability issues. Hence, the significance of reactive power as ancillary service providers was required to justify.

2.2.4 Reactive Power as Ancillary Service Provider

The ancillary service providers are constrained and it has a great impact on worldwide competitive power scenario.

2.2.4.1 Constrained Ancillary Services

Reactive power is one of major commodity acted as ancillary service provider which was considered by Gomes et. al. [109]. This work proposed the two optimization models. One of the proposed models rigidly maintained its fixed voltage and branch flow limits. The second one controlled the voltage and branch flow limits using fuzzy set concepts while considering its flexible mode. Finally, the work described the application of these ancillary service models with a case study on a 55 node MV/LV network. In this connection, Madureira et.al., proposed a voltage control in multi-micro grid systems to control an ancillary service (AS) market framework [110]. This AS based reactive market proposal

for MV distribution systems could be formed by involving Distributed Generation (DG) units where micro-grids would act as an AS provider. In the open market, bidding of the each player was considered and the market settlement was performed satisfactorily. Moreover, Ongsakul et.al., proposed a constrained optimal power dispatch algorithm (COPD) including the auction based electricity and ancillary services [111]. This work solved both the maximization of social welfare and minimisation of real power losses simultaneously. The proposed COPD was tested on the modified IEEE 30 bus system. Here, the present six Gencos were bidding to sell the electricity and ancillary services. Considering the Thailand power pool, a lower average electricity price was calculated. In this regards, the spot price was also considered to final price involving the marginal electricity price and marginal ancillary services prices. Meanwhile, Costa et. al., demonstrated a dynamic optimal power flow (DOPF) approach to operate day-ahead markets considering both energy and spinning reserve [112]. In the restructured environment, the DOPF derived the optimal solutions for both energy dispatch and reserve allocation. The proposed approach was proved to be very powerful while achieving the final optimal solution as per generating limits and ramp rate restrictions. Moreover, the proposed framework allowed to conduct the multiple zones in the network for each time interval while assuring sufficient distribution of ancillary services in the competitive power scenario.

2.2.4.2 Ancillary Services at the Competitive Power Scenario

The requirement of ancillary services were an emerging issues in a deregulated power scenario which was considered elsewhere [113]. This work modulated the reactive power supply service into voltage regulation and reactive power spinning reserve. The proposed case study was demonstrated considering a simplified South-Eastern Mexican grid. In this regards, El-Araby et. al., [110 114] proposed a new market-based technique for obtaining var ancillary service in the electricity market. Here, as optimisation method to deal the *var* ancillary service problem, particle swarm optimization was approached with successive linear programming "SLP". The proposed method has been tested on the standard IEEE 57 bus-system and compared with other evolutionary methods to demonstrate its efficiency. Moreover, an ancillary service by power system stabilizers (PSSs) was shown elsewhere [115] to evaluate the small signal stability analysis in a competitive framework. This work applied NSGA-II to solve the resulting multi objective optimization problem which showed its effectiveness it the sector. It was evidenced that the ancillary services helped to maintain network stability efficiently in the competitive power market. Hence, its impact in worldwide power sector is required to justify a priory.

2.2.4.3 Impact of Worldwide Ancillary Service Usage to the Network

In this direction, the management of ancillary services in the Spanish power system were considered elsewhere [116]. This study demonstrated a detailed technical description of the services including its functions. Raineri et.al., [111, 117] presented a comparative study on technical and economic aspects of ancillary services on the markets of England and Wales, Nordic Countries, California, Argentina, Australia and Spain. The analysis showed that the ancillary service providers relied on the instruction of the system operators. The mandatory conditions of the services were provided by the different service providers based on the voltage control and primary frequency regulation. The mentioned constraints were to be maintained within security limit whatever prices were invested. Now, in the practice of ancillary service provider frequently arranged reactive power in terms of renewable energy. In this concern, distributed generation (DG) units had achieved major focus.

2.2.5 Major Focus of Distributed Generation (DG) in Connection to RPD

Distributed generating units have been playing a major role in the competitive power scenario.

2.2.5.1 Reactive Power Compensation by DG

Reactive power compensation based hysteresis controller and adaptive hysteresis controller was utilised elsewhere [118] for inverter interfaced DG to control the active and reactive power independently. The performance indices measured the total harmonic distortion (THD) of the grid current during steady state and transient conditions which evidenced the proficiency of the proposed method. Further, Mahmud et. al. proposed a reactive power compensation approach to control voltage of distribution networks with DG units [119]. This concept was utilized on a 15- bus Japanese distribution system where the test system was integrated with the distributed wind generators, photovoltaic, and synchronous generators. Now, the incorporation of the DG units was played a major role in the deregulated power scenario which further needs a detailed analysis.

2.2.5.2 Impact of DG Installation in Deregulated Power Scenario

In this context, Lin et.al., proposed an inductive reactive power optimization configuration method towards the 10kV distribution network with DGs [120]. The objectives of the proposed work were to minimize the power loss as well as the voltage deviation together as multi-objective formulation. Here the considered multi-objective problem was solved by particle swarm algorithm (PSO). The approach was not only had a good voltage regulation effect, but also had economically compensated the reactive power in a practical regional competitive market. Moreover, a static and dynamic *var* control

method with distributed wind generation was proposed [121]. This work was formulated on the reactive power margin for improving dynamic voltage stability in a distribution networks. Here, a new index, reactive power loadability (Q-loadability), was used to measure the critical point of the network due to voltage collapse. As a compensator, a cost-effective combination of shunt capacitor bank and distribution static compensator (D-STATCOM) was developed to use through static and dynamic analyses. The observations showed that the proposed approach would reduce the required sizes of compensating devices which, in turn, reduced the costs. In this direction, Singh et. al. proposed [122] a sensitivity method for allocating distributed generators (DGs) to consider congestion management and voltage security simultaneously. Here, the genetic algorithm (GA) was proposed to solve due its different strength in this sector. It had been observed that the method accomplished the both normal and contingency conditions in an efficient manner. The proficiency of the proposed method was obtained by measuring the available transfer capability (ATC), congestion cost and reliability risk indices of Loss of Load Expectation (LOLE). Alike this, few advanced applications with DG units were available in the literature.

2.2.5.3 Advanced Applications of DG

In the backdrop of advanced applications with DG units, Su et.al., proposed a new optimization model of reactive power compensation by DG unit [123]. In this proposed model, fuzzy dynamic programming was utilised. The scheme provided a satisfactory output with improved accuracy and increased convergence velocity. Meanwhile, a robust predictive dual-loop control strategy to control single-phase grid connected distributed generation (DG) system was proposed elsewhere [124]. The proposed control strategy was based on improved reactive current detection and robust predictive dual-loop control. The validity of the proposed strategy was verified based on simulation and experimental results. Further, the particle swarm optimization (PSO) based new methodology for the optimal placement of distributed generation (DG) units in the radial distribution systems was considered elsewhere [125]. As a test case 26-bus radial distribution system was considered which was further modified by the Provincial Electricity Authority (PEA) distribution system. The load flow analysis on distribution was conducted by forward-backward sweep methodology. The simulation results showed the effectiveness of the proposed approach.

In the competitive power market, a number of participants, ancillary service providers were involved to have various power transactions. This frequently caused few disturbances like congestion issues, threats to the isolations of security constraints etc. which therefore requires a major attention.

2.2.6 Reactive Power Services considering System Security

Reactive power services are available mainly based on the system security involving different constraints and cost optimisation models.

2.2.6.1 Security based Reactive Power Procurement Model

This paradigm of reactive power procurement study comprises of OPF issue over-viewing security and welfare analysis, security based reserve requirements.

2.2.6.1.1 OPF Issue Over-viewing Security and Welfare Analysis

In this regards, Samahy et.al., presented a two-level framework considering system security aspects in a competitive market using reactive power ancillary services [126]. Here, the proposed reactive power procurement model was formulated on the basis of a two-step optimization process. While running this, the system security was given priority where all transmission system constraints were considered. Alike this, Rabiee et.al., proposed a pay-at-MCP settlement mechanism on the basis of voltage stability and security issues for branch loading limits [127]. The investigations were considered a coupled configuration using the IEEE 24 bus system for a day ahead energy and reactive power market. Now, security aspects in terms of reserve requirement is also very important issues which needs proper care.

2.2.6.1.2 Security based Reserve Requirements

In this direction, Aghaei et.al., proposed a new stochastic configuration for providing the reserve requirements (spinning and non-spinning reserves) in the competitive power market domain [128]. This work simulated the energy auction in a day-ahead pool-based aggregated market. The fitness function of the proposed problem comprised of different cost functions. They are fundamental cost function (including both energy and reserves offer costs), lost opportunity cost (LOC) and expected interruption cost (EIC) which were solved separately. Each fitness functions were solved including AC power flow and security constraints of the power system. The proposed model was examined with the IEEE 24-bus Reliability Test System (IEEE 24-bus RTS). The obtained result validated the effectiveness of the proposed method.

Nevertheless, advanced optimisation methods involving reactive power procurement model helped to maintain the system security steadily. However the network constraints played a significant role in this sector which needs more analysis.

2.2.6.2 Network Constraints to System Security

In this direction, Raoofat et.al., proposed a voltage security based new algorithm to optimize reactive power procurement through commercial transactions [129]. With a major focus on voltage profile which was the most fundamental security constraints, were adjusted to handle the proposed problem. The proposed algorithm had been tested on IEEE-RTS test system. Moreover, Hsiao et.al., proposed a simulated annealing based computer package for multi-objective *var* planning in large scale power systems-SAMVAR [130]. This provided improved response while handling the load, contingency constraints. In this context, the optimal allocation of energy and spinning reserve by differential evolution algorithm was shown elsewhere [131]. The efficiency of the proposed method was observed by examining the IEEE 30-bus test system. A comparative study was also carried out to validate the proposed algorithm with analytical and evolutionary methods in various cases. Further, a new self-adaptive differential evolutionary (SADE) technique was formulated to detect the ceiling point (CP), weaker buses under practical security constraints etc. [132]. For both standard IEEE test systems and ill-conditioned systems, the performances of the proposed algorithm were checked and compared with the some established meta-heuristics techniques. Here, the FACTS devices were implemented on the weaker buses. The simulation results showed the robustness and efficiency of the proposed algorithm. Now, cost is one prime issue in everywhere of the deregulated power scenario. Therefore, in parallel with the security aspects, cost of the secured schemes is to be considered a priory.

2.2.6.2.1 Cost based System Security

In this connection, Li et.al., proposed an algorithm to procure reactive power pricing structure in the view of secured competitive power sector [133]. The proposed algorithm determined the reactive power capacity to provide adequate security as well as the production costs of the reactive power. Output on a sample test system was accomplished the feasibility and validity of the algorithm. Further, Chung et.al., proposed a cost-based reactive power pricing, which integrated the reactive power cost minimization and the voltage security in the backdrop of OPF problem [134]. While implementing this, sequential quadratic programming (SQP) was employed. The effectiveness of the proposed method was tested using a modified IEEE 14-bus system. Meanwhile, Amjady et,al., proposed a new security-constrained self-scheduling configuration [135]. In the proposed framework, the uncertainty of the market prices was considered in addition to the risk and profit trade off of a GENCO. The performance of the proposed schemes were validated using IEEE 30-bus and IEEE 118-bus test systems in day-ahead electricity markets. Nevertheless the cost of security based reactive power procurement model is a vital aspect of the deregulated power scenario; however the total economics of the *var* compensation is required an extensive analysis.

2.2.7 Economics of Reactive Power Compensation in Deregulated Power Environment

In deregulated power scenario, economics of the reactive power compensation are majorly dependent on the reactive power pricing, reactive power bidding, minimal of reactive power support etc.

2.2.7.1 Reactive Power Pricing

In such scenario, reactive power pricing issues are majorly discussed about the different cost components and criteria as;

2.2.7.1.1 Concepts of Reactive Power Pricing and Management

In this regards, Hao et.al., [136] focussed the reactive power pricing structures in an open-access environment considering the technical and economic issues. The work developed a framework for reactive power pricing and management by allocating several cost schemes. Further, an integrated framework to explore the issues of reactive power planning and reactive power pricing were proposed elsewhere [137]. The planning problem considered the optimal placement and sizing of capacitors to procure minimum costs of the devices. A modified iteration method based on cost-benefit analysis (CBA) scheme was chosen to solve a simple bus system. In this conjunction, Gil et,al., focussed the control activity on reactive power supply and voltage control services [138]. Here, a marginal pricing based theoretical approach was presented in order to explain the principles to accommodate the suppliers and the consumers of these services. A modified OPF model was utilized to analyse a real-time pricing policy of reactive power. Therefore, the pricing structure of reactive power indicated that the cost of the reactive power is a major sector of the competitive power scenario which needs detailed analysis.

2.2.7.1.2 Determination of Reactive Power Cost Components

In this regards, the production cost of reactive power as well as the investment cost of capacitor banks was included into the OPF problem formulation by Ketabi et.al., [139]. Marginal price theory was utilized here for calculating the cost of active and reactive power at each bus in deregulated power markets using Ant Colony Search Algorithm. The obtained result validated the effectiveness of the proposed method considering IEEE 14-bus system. In this context, peaking units at hydroelectric power plant in condenser mode operation were a major source of reactive power support which was considered elsewhere [140]. Here, Koyna Hydro Electric Power Plant (KHEPP) was considered to find the capability of the proposed methodology based on these components. The different issues like

reactive power requirements, voltage support and transmission losses were properly handled with an induction motor model. Besides this, few other pricing issues are there related to reactive power which also achieved major importance in the backdrop of deregulated power scenario.

2.2.7.1.3 Different Reactive Power Pricing Issues in Competitive Power Markets

In this regards, Meliopoulos et.al., showed the pricing structure for voltage and reactive power support with adequate simulation results [141]. This work was utilized to justify the long-term pricing agreements between the suppliers and customers. Meanwhile, Rider et.al., proposed a methodology for calculating active and reactive power marginal prices considering a competitive electric market [142]. Total cost of reactive power production (CRPP) was derived here considering the corresponding economic loss due to the opportunity cost. A modified sequential linear programming solve the OPF problem. As a test case, IEEE-30, 57, 118 bus systems and a modified configuration of the interconnected Brazilian system had been used to apply the proposed methodology. The obtained results showed the economic active and reactive power marginal price. In this direction, maximization of social welfare in the open power market by unified power flow controller (UPFC) devices were considered by Verma et.al., [143]. The installations of UPFC, considering an appropriate location selection and the settings of its control parameters were provided optimal congestion management solutions. These solutions were further utilized to determine nodal spot prices for both real and reactive powers calculation and the impact of UPFC on the spot pricing have been justified. As evidenced, the pricing of the reactive power was mostly influenced by the bidding of the market participants in the competitive power scenario which therefore requires a special attention.

2.2.7.2 Reactive Power Bidding

Reactive power bidding are procured based upon definite strategies, different constraints, impact of sustainable energy sources on it etc.

2.2.7.2.1 Bidding Strategies for Power Transactions

Competitive power scenarios were often engaged by power transactions by several participants with system operators. In this connection, Gomes et.al., [144] proposed two new active/reactive dispatch models to allocate reactive power considering bilateral contracts phenomena by involving all the market participants and system operators. This work formulated the proposed model based on a market approach ensuring operational transparency. Sequential Linear Programming (SLP) approach was applied to solve the problem for an IEEE 24 bus test system. In this context, optimal bidding strategies of generating companies were considered for a bilateral contracts elsewhere [145]. The

problem was decomposed with a bi-level optimization algorithm considering a risk management-based method including the impacts of the generator's bidding. IEEE 30-bus test system was used as a test case and the obtained results were validating the effectiveness of the proposed model. Further, Duan et.al., [146] proposed a transaction pricing method considering IEEE 30 bus test system. The observations showed that the proposed pricing method was effective in creating economic signals by operating an efficient and secure transmission system. However, the reliability in terms of efficient and secured transmission systems could be developed only due to proper maintenance of all the constraints.

2.2.7.2.2 Different Constraints of Bidding

Kim et.al., [147] proposed an innovative approach for market clearing considering voltage stability with system security in a decentralized power markets. The market-clearing algorithm was formulated for voltage stability constrained OPF (VSC-OPF) for the IEEE 14-bus system. The results showed that the proposed method was able to improve system security in terms of better market solutions and total transaction levels. Further, Dotoli et.al., [148] proposed a Nash equilibrium notion for the auction based day ahead electricity generation market simulation model. The proposed approach was evaluated for the Italian electricity market showing its effectiveness by varying the number and capacity of participating bidders in different scenarios. In this regards, Karthikeyan et.al., [149] proposed a comprehensive review on market power with various indices. By comparing with other relevant works, it was found that the proposed work facilitated few unattempted issues of competitive power market. Recently, Prabavathi et.al., surveyed a risk based energy bidding strategies [150]. This work analysed a comprehensive literature on the state of the art research of bidding strategies in restructured electric power market. Moreover, the work showed that the maximization of profit for power companies was highly associated with the bidding strategies. It had been observed that bidding strategies were often governed by the characteristics of the market participants however the impact of sustainable energy sources on bidding are required to be observed thoroughly.

2.2.7.2.3 Impact of Sustainable Energy Sources on Bidding

Nielsen et.al., presented a double auction theorty, to determine effective frame for large shares of free renewable energy sources (FRE) [151]. From the analysis, the marginal prices were found better for the FRE sources. Further, a quantitative analysis of TCSC on congestion management and spot pricing in deregulated electricity markets were presented [152]. The analysis discussed the behaviour of the market participants in a voluntary pool market by the study of bilateral contracts. Here, the electricity market was modelled based on optimal power flow framework with the maximization of

the social welfare. The observations were carried out with and without TCSC at peak and low loading conditions. Further the significance in compensation level on the spot prices due to bilateral loading conditions by TCSC was highlighted for a 5-bus test system. It is therefore evidenced that the reactive power compensation in any form was a vital aspect in a deregulated power scenario since it helped to improve the economic welfare of the system under consideration. In this concern, minimal reactive power support also played a major role to upgrade the economics.

2.2.7.3 Minimal Reactive Power Support

Minimal reactive power supports are mostly value based, meta-heuristics technique supported and transmission access oriented useful for restructured RPD.

2.2.7.3.1 Value based Reactive Power Support

In this context, an OPF based reactive power optimization model based on a power flow tracing method was presented by Wu et.al [153]. The methodology was applied on four test systems. Detailed analysis of the results of the 39-bus test system was shown in the article. Moreover, Li et.al., proposed an algorithm for procuring reactive power from reactive resources based on competitive reactive power pricing structure [154]. Feasibility and validity of the algorithm were tested on a sample test system. Besides the value based approaches, few advanced methods were utilised to handle the minimal reactive power support in the competitive power markets.

2.2.7.3.2 Metaheuristics Approach to Handle Reactive Power Support

As known, the reactive power support is necessary to transmit active power which was detailed elsewhere [155]. In this work, the concept of minimum *var* requirement (Q_{min}) for generators was accomplished in a small and medium-sized system. In this context, a population based differential evolution technique to control load bus voltages was proposed elsewhere [156]. Obtained results have been compared with other standard techniques to show its effectiveness. Moreover, Xu et.al., proposed PSO based approach for scheduling the reactive power control variables for voltage stability improvement [157]. Proposed algorithm had been tested on 6-bus, 7-line and 25-bus 35-line standard test systems. PSO based results have been compared and found better compared to other potential methods. However, as reactive power support is considered a commodity in the competitive power scenario, its operation considering transmission access is a matter must be discussed more clearly.

2.2.7.3.3 Transmission Access Oriented Reactive Power Support

In this ground, Xu et.al., demonstrated the progress and proposal of a new concepts and schemes for equitable reactive power support valuation [158]. The proposed work was inherently designed based on system security and stability due to reactive power support services. The proposed method was validated through sensitivity analysis. Further, the development of ideas and schemes for equitable reactive power support valuation were presented elsewhere [159]. This work utilized a simple system to frame the problem in deregulated power market. It proposed the concept of value curves considering a small case study. Now, the economic welfare estimation is the most fundamental objectives of the competitive power market which needs to be discussed a priory

2.2.7.4 Economic Welfare for Constrained RPD in Competitive Market

Economic welfare analysis due to RPD in the competitive power market are majorly based on optimal *var* compensation and ancillary service.

2.2.7.4.1 Optimal Var Compensation based Economic Welfare

The impact of compensation with other cost component, was discussed elsewhere [160]. Various pricing policies involving wheeling transactions and cost due to independent power producers were considered. Finally, the obtained results reflected the cost of incurred losses while satisfying the network security constraints for the IEEE 6- and 30-bus test systems. Meanwhile, Nabavi et.al., [161] presented a fuzzy-based genetic algorithm to maximize total system social welfare. Here, the sitting and sizing of TCSC and SSSC devices considering their investment cost was demonstrated in a double auction energy market. Simulation results were validated w.r.t. few established approaches for the modified IEEE 14-bus and IEEE 30-bus test systems. In this direction, ancillary services are able to influence the economic welfare of the system under observations.

2.2.7.4.2 Ancillary Service based Economic Welfare

Reactive power ancillary service management is a critical task to power system operators from both technical and economic perspectives which have been focussed elsewhere [162]. This work proposed a practical market-based reactive power ancillary service management scheme to tackle the real time challenges. The proposed scheme was investigated using a modified IEEE 14-bus system. Now, one of the greatest challenges of deregulated power industry involving power transaction is the congestion management. This generally occurs due to violations of the operating limits of the security constraints during the power transactions period which therefore needs closer observations.

2.3 Reactive Power Optimization based Congestion Management

One of the greatest challenges of deregulated power industry is the operation of the grid in a non-discriminatory and equitable manner. Congestion in these power networks is the resultant of such operations. Flexible AC transmission systems (FACTs) can be an alternative solution to reduce the congestion matter in the heavily loaded lines. In the deregulated power market, the independent system operator (ISO) plays an active role to manage the congestion. In this respect, another real time task of ISO is to utilize the available resources to maintain system security and reliability. This process is termed as Dynamic Congestion Management (DCM). In parallel to the DCM, the risk minimisation with dynamic voltage stability, loss minimisations are also the various important tasks of the ISO. Therefore, power system stability margins should be considered within the congestion management framework market. In such market, the participants try to maximize their profits with increasing global welfare. Therefore, secured profit based congestion management is the most vital working area in a competitive electricity market.

2.3.1 Reactive Power Compensation for Line Congestion

Congestion management by reactive power compensation are analysed in terms of different advanced method, Pareto optimality based multi-objective analysis etc.

2.3.1.1 ABC of Congestion Management

The congestion management is one of the vital tasks performed by system operators (SOs) ensuring the operation of transmission system within operating ranges. Therefore, in the restructured power scenario, the congestion management is gaining major attention since it is imposing a barrier to the electricity trading. In this connection, Kumar et. al., performed a review study on congestion management [163] while discussing the issues connected to it. In this context, Hussin et.al., proposed an assessment of transmission congestion management considering the deregulated electricity market [164]. Comparative studies amongst the existing methods in allocating the congestion charge to the participants were focused here considering a case study on a 3 bus system. Further, Singh et.al., studied dynamic security constrained congestion management in the deregulated and unbundled electric power system [165]. In this study, it was found profitable to operate the system dynamically secured after a fault by rescheduling the real power generation along with curtailment of real power loads/transactions. Besides this, few more advanced approaches were considered for congestion management.

2.3.1.2 Advanced Approach for Congestion Management

In this regards, Tang et.al., presented a new electrical dissecting method for assessing ancillary service of phase-shifter to manage congestion issue [166]. The test cases showed the effectiveness of the proposed method for different ancillary service providers by FACTs and phase-shifters. The Dynamic Congestion Management (DCM) models have been developed as a constrained nonlinear optimization problem elsewhere [167]. The proposed method solved the constrained nonlinear DCM model by Real Coded Genetic Algorithm (RCGA). The performance of the proposed method was successfully investigated on a 3-machine, 9-bus WSCC system. Muneender et.al., [168] considered a new approach to solve the congestion problem at lower cost in addition to the rescheduling of real power generation. The adaptive fuzzy particle swarm optimization based optimal power flow (AFPSO-OPF) was used to derive the multi-congestion management problem. The proposed method based results were validated considering a practical 75-bus Indian systems. The results were compared with the other conventional optimization algorithms based on OPFs. A bee colony optimization approach based congestion management problem was proposed elsewhere [169]. The study optimised the cost of generation in power system network within the available constraints for IEEE 30-bus system. The obtained solutions showed that the proposed bee algorithm was found to work better than the evolutionary programming technique. Due to its growing importance, the proposed congestion management issue was represented by multi-objective congestion management.

2.3.1.3 Multi-objective Congestion Management

The multi-objective congestion management provided not only flexibility but also more security. Esmaili et.al., proposed a multi-objective congestion management framework to optimize simultaneously different objective functions. This framework was based on congestion management cost, voltage security, and dynamic security [170]. Here, the proposed multi-objective framework was solved by modified augmented ε-constraint method hybridized by the weighting method. Results were determined considering the New-England test system and compared with few other established techniques in detail. This comparative study validated the proficiency of the proposed method. Further, a multi-objective framework for congestion management issue was simultaneously optimized by competing different objective functions. These were the cost of congestion management, voltage security, and dynamic security [171]. A fuzzy decision maker was utilized to determine the most efficient value among Pareto-optimal solutions of multi-objective mathematical programming problem. As a test case the New-England test system was considered to elaborate the efficiency of the proposed method. While, the Pareto optimal solutions were considered, the Pareto optimality had a great impact on it.

2.3.1.4 Pareto Optimality based Multi-objective Congestion Management

In this direction, Wang et.al., [172] used the multi-objective transmission expansion planning (MOTEP) approach to improve the transmission system capability. An improved strength Pareto evolutionary algorithm (SPEA) was resumed to formulate the proposed model. A ranking method based on Euclidean distance was implied to determine proper Pareto-optimal set. The effectiveness of both the improved SPEA and the proposed multi-objective planning approach have been validated on the 18-bus system and the 77-bus system. Present power sectors solved the congestion matters several ways. Amongst them the incorporation of the flexible AC transmission system (FACTS) devices played a major role in different scenarios.

2.3.2 FACTs for Congestion Management

FACTs devices are one of the major advanced *var* compensating devices for congestion management.

2.3.2.1 Loadability Enhancement

Preedavichit et.al., proposed the FACTS devices as additional control parameters in the ORPD formulation [173]. This work studied the impact of static *var* compensator (SVC), thyristor controlled series compensator (TCSC) and thyristor controlled phase angle regulator (TCPAR) on system loss minimization. The ORPDs have been solved on a practical power system network of electricity generating authority of Thailand (EGAT) including the FACTs devices with satisfactory output. Moreover, Abdullah et,al, [174] demonstrated a static voltage stability index (SVSI) for optimal placement of Thyristor Controlled Series Compensator (TCSC). To determine optimal sizing of TCSC under contingencies, Evolutionary Programming (EP) techniques were used. As a test case the IEEE 30-bus RTS for several loading conditions was considered. The simulations results were compared and proved its efficiency compared to other methods. In this context, Nagalakshmi et.al., [175] proposed comparative study on computational intelligence algorithms to determine the optimal location and control of three types of FACTs devices. This also helped to enhance the loadability in deregulated power system. In this work, PSO, DE and Composite Differential Evolution (CoDE) algorithms were comparatively analysed. Here, TCSC, SVC and Thyristor Controlled Phase Shifting Transformer (TCPST) were chosen as control variables for the proposed problem. Simulation results were tested on IEEE 118 bus system. In this direction, Edward et.al., proposed [176] Enhanced Bacterial Foraging algorithm (EBFA) to solve a bi-objective problem. These objectives were associated with the OPF for fuel cost minimization and optimal allocations of the FACTS devices in IEEE 30 bus system. In this work, the proposed method was found to reduce the required

computational time compared to earlier proposed algorithms. It was further observed that the inclusion of the FACTs devices as SVC and TCSC in the network reduced the generation cost along with the increased voltage stability limits. Therefore, in addition to the improved methods, the optimum allocations of the FACTs devices have an important role to handle the congestion issues.

2.3.2.2 Optimal Allocation Schemes for FACTs Devices

Besharat et.al., [177] proposed a method to determine the optimal location of the TCSC devices based on real power performance index with congestion management. To reduce congestion, Acharya et.al., proposed two new methodologies for the placement of series FACTS devices in deregulated electricity market [178]. The presented methodologies were based on the use of LMP differences and congestion rent respectively. To locate the TCSC, IEEE 14, IEEE 30 and IEEE 57-bus test systems were chosen and the obtained results were compared with other sensitivity methods based OPF solutions. The observations showed that the proposed methods were capable to minimize the total congestion rent while maximizing the social welfare. In this direction, Singh et.al., proposed a simple and efficient model for optimizing the size and the locations of FACTS devices to control the congestion management [179]. A 5-bus system was utilized to show the effectiveness of the proposed methods. Further, Rashed et.al., focussed the system security issue for the single contingencies by the optimal TCSC placement [180]. Two evolutionary optimization techniques namely, GA and PSO were applied in the work which were concerned about the optimal location and the optimal parameter setting of TCSC under single line contingency ($N-1$ Contingency). The proposed techniques were validated by testing an IEEE 6-bus power system and an IEEE 14-bus power system. The results proved the efficiency of the proposed optimisation techniques to find out the optimal location and the optimal parameter settings of TCSC. In this context, multi-type FACTs device placement also handled the congestion management issues efficiently.

2.3.2.3 Optimal Placement of Multi-type FACTs Devices

A hybrid tabu search and simulated annealing (TS/SA) approach was presented by Bhasaputra et.al., to optimize the generator fuel cost in optimal power flow (OPF) control [181]. The considered problem was solved here by incorporating two types of FACTS devices namely TCSC and TCPS. They were optimized by the Quadratic Programming (QP) in modified IEEE 30-bus system. The investigations showed to provide better solutions in less CPU times by the proposed hybrid TS/SA approach over the singular GA, SA, or TS methods. Further, Jordehi et.al., applied Evolution Strategies (ES) to determine optimal placement of FACTS devices in power systems [182]. The optimization was based on the choice of locations and sizing of the multi-type FACTS devices such as SVC, TCSC and UPFC. The obtained solutions were found to be promising and encouraging while implementing the same in the IEEE 30-bus test system as well as in real power sectors. So far the

studies on FACTs devices are concerned it showed to perform effectively. However, their size needs to be optimised by suitable meta-heuristics techniques.

2.3.2.4 Meta-heuristics based FACTs Incorporation

In this context, the optimal setting of power system variables, including FACTs devices were optimized by GA and DE along with Fuzzy Logic (FL) elsewhere [183]. In this work, two types of FACTS devices, TCSC and SVC were chosen to reduce the congestion in transmission lines. Optimal allocation of FACTS devices in the heavily loaded line helped to control the reactive power flow. Additionally, it helped to improve the voltage profile of the all nodes and reduced the transmission losses and the operating costs. The proposed technique was compared with other global optimization which showed the superiority of the proposed fuzzy based optimization approach over the other methods. Further, a hybrid tabu search and simulated annealing (TS/SA) approach was applied to find the optimal placement of multi-type FACTS devices elsewhere [184]. This work helped to minimize the total generator fuel costs at all loading levels. Here, four types of FACTS devices were utilized: TCSC, TCPS, UPFC, and SVC for a small test system of 6 buses. The results showed to perform better for the hybrid TS/SA approach compared to the sensitivity index approach. In this regards, Jumaat et.al., proposed PSO based optimal placement and sizing of FACTS devices to minimize transmission losses. This work also considered to maintain a stable voltage profile at optimum costs [185]. In this work, TCSC was chosen as the *var* compensation device for the IEEE 30-bus system. The simulation results were compared with those obtained from the Evolutionary Programming (EP) technique. This proved the effectiveness of the proposed approach. However, the FACTS devices handled the congestion management problem efficiently; few advanced technologies have been found to provide better optimisations.

2.3.3 Advanced Technologies for Congestion Management

To handle the congestion issues, a number of advanced technologies such as renewable energy sources etc or different strategies have been adopted in the power systems.

2.3.3.1 Renewable Energy Sources for Congestion Management

In this direction, Sood et.al., proposed an optimal model of congestion management with renewable energy sources (RES) in deregulated electricity market [186]. This work outlined a generalized optimal model of congestion management involving bilateral and multilateral contracts. The proposed model obtained the locational marginal pricing (LMP) based on marginal cost theory for an IEEE-30 bus test system with RES. The RES provided its power to load either by firm transactions or by using

power pool. Besides the RES, few strategic congestion management schemes were also considered for congestion management.

2.3.3.2 Strategic Congestion Management

Kumar et.al., considered an important aspect of transmission system congestion management in a pool electricity market [187]. Here, the voltage stability was considered as the loadability limit. To reduce the congestion effect, the impact of FACTs devices was surveyed including the optimal rescheduling of generators' outputs. This was followed by the cost determination for the congestion. As a test case IEEE 24 bus and IEEE 57 bus systems were explored. Meanwhile, a new method of fuzzy adaptive bacterial foraging (FABF) based congestion management (CM) for optimal rescheduling of active powers of generators was described elsewhere [188]. The proposed approach was based on the generator sensitivity. As test case IEEE 30-bus system and a Practical Indian 75-bus system was chosen. Here, the FABF algorithm was comparatively analysed while solving the proposed problem. The experimental results showed that the FABF effectively minimized the cost of generation while relieving the congestion in the transmission line. Further, a new congestion management framework was presented elsewhere [189] considering the dynamic voltage stability. While solving this, dynamic modelling of power system equipment including generators and loads were integrated into the proposed congestion management framework. The proposed congestion management framework was validated considering the New England 39-bus power system. System Security was found to be an important aspect in these studies. Therefore, congestion management as an alternative to maintain system security requires serious attention.

2.3.4 Congestion Management considering System Security

One of the major issues of the congestion management study is to provide voltage security to the power system under consideration. This is attempted by many research groups.

2.3.4.1 Voltage Security based Congestion Management

Balanced voltage profile is one of the most desiring criteria of the present competitive power sectors, which otherwise may cause to initiate the congestion problem. Esmaili et.al., presented a novel congestion management method based on the voltage stability margin sensitivities [190]. As a test case the New-England test system was considered to solve the proposed problem. The result indicated better voltage stability at a lower security cost. In this direction, Wang et.al., [191] utilised QV curve analysis to experiment the voltage instability performance of risk-based security-constrained optimal power flow (RB-SCOPF). Here, the QV curves helped to obtain the reactive power reserves for both

the RB-SCOPF and SCOPF models. Test results were considered for the IEEE 30-bus system. This showed improved voltage stability performance by the RB-SCOPF over the original SCOPF model. Further, Conejo et.al., presented the congestion management problem to address limit crossover while avoiding offline transmission capacity limits [192]. These results were described considering an illustrative case study based on the IEEE 24-bus reliability test system. A new stochastic method for optimal reactive power market clearing considering voltage limit crossover was analysed by Kargarian et.al. [193]. Here, the presented algorithm solved a multi-objective nonlinear problem where market payments were minimized in conjunction to the maximization of voltage security margin. These helped to schedule the stochastic reactive power market. As a test case IEEE 14-bus test system was considered. The proposed method provided satisfactory results while securing the network in terms of congestion management.

2.3.4.2 Advanced Stability Analysis for Secured Congestion Management

A new transient stability criterion was presented by Esmaili et.al., [194] using a novel congestion management method. The proposed method showed to retain the network in its transient security limit compared with earlier methods. As a test case the New-England test system was considered. The results of the proposed method proved the proficiency of the approach compared to the earlier ones. The comparisons were done from the viewpoint of providing a better transient stability margin at economic security cost. Meanwhile, Hsiao et.al., proposed a framework for quantitative risk and profit assessments of system protection schemes (SPS) [195]. The proposed schemes were able to obtain the benefits from the power market by reducing the customer interruption costs resulting from SPS operations compared to different alternatives. Numerical results were determined based on an actual event-based SPS example. In such direction, a new approach was developed considering a LMP scheme for congestion management using an optimization technique [196]. This scheme was successfully developed on a DC optimal power flow (DC-OPF) model. Again Wang et.al. proposed a model to obtain the optimal screening policy to maximize the network security aspects [197]. Analytical solutions were provided for the optimal non-discriminatory screening policy and numerical illustrations for both the discriminatory and non-discriminatory conditions. In parallel to the advanced solutions for secured congestion management, advanced energy sources were utilised to handle the proposed issues.

2.3.4.3 Different Energy Sources for Congestion Management

In this context, a sensitivity method for allocating distributed generators (DGs) to mitigate the congestion and voltage security issue was simultaneously proposed [198]. Here, GA fixed the objective to improve the system performance by minimizing the system losses. In addition to this, the

voltage profiles of the various buses were tried to be maintained nearly to their nominal value. It had been observed that the proposed method successfully reduced the problem of overloading of the lines. Both the normal and contingency conditions were considered here in an optimal manner. Moreover, Kumar et.al., [199] solved the congestion management issue considering the impact of constant impedance, current, and power (ZIP) load model. The proposed models were following a load variation pattern in a day-a-head hybrid electricity market. Here, the function of up and down rescheduling within the upper and lower limits was applied for congestion management. As a test case IEEE 24 bus system was considered. As evidenced, a number of potential methods were attempted to solve the congestion management issues in deregulated power scenarios considering security. Since economics was a prime issue in the present competitive power sector, it was also analysed in the backdrop of congestion management.

2.3.5 Economics considering Congestion Management

In deregulated power scenario, few economic terms such as spot pricing, merchandising surplus have been found to play an important role on economic welfare of the considered network. Many research groups have tried to understand their impact on the Congestion Management in deregulated environment.

2.3.5.1 Impact of Spot Pricing on Congestion Management

In a deregulated power market, the generation scheduling is dependent on suppliers' and consumers' bids which make the operation of such market complex in nature. Since a large number of transactions do occur in the power market, it is more likely that some transmission lines will face congestion. This situation could be improved by series compensation by TCSC. The TCSC helps to control the power flow directly to improve the operation of transmission networks. Shrestha et.al., considered a modified IEEE 14-bus system for TCSC placement to optimise congestion based optimal power flow (OPF) problem [200]. The effects of TCSC on the operation of a spot price power market were studied in this work besides the optimal sizing and pricing issues of TCSC. With this social benefit was determined by incorporating economic impact of the TCSC device. Meanwhile, Chattopadhyay et.al., proposed a spot pricing mechanism for reactive power to manage congestion issues and also supporting the reactive power ‘reserve’ for the system voltage stability [201]. This work solved an OPF based dispatch/pricing model which optimally allocated real and dynamic reactive reserve amongst the generators to meet a pre-specified voltage stability margin. The observations were considered for a reduced New Zealand North Island power system. Here, the impacts of the voltage stability constraint on real and reactive power prices were determined. In this context, Xie et.al.,

summarised the optimal pricing for real and reactive power in the backdrop of an extended optimal power flow problem [202]. This work also considered the spot pricing which were divided into different components reflecting various ancillary services. Now, amongst these ancillary services, ESS played a vital role as *var* compensators. Further, this also facilitated the efficiency of the transmission and distribution systems. However, the deployment of the devices will remain limited until they receive an attractive internal rate of return (IRR).

2.3.5.2 Energy Storage Systems for Economic Congestion Management

In the direction of economic congestion management, Bradbury et.al., analysed a comparative price arbitrage of different EES [203]. The work showed that the profit-maximizing size (i.e. hours of energy storage) of an ESS was primarily obtained by its technological characteristics. This also helped to increase IRR. Moreover, Zheng et.al., demonstrated a cost-effective building-based electricity storage system for providing a number of benefits to the residents under U.S. electricity systems [204]. The proposed building-based electricity storage helped to enable demand response (DR) without curtailing actual appliance usage and offered potential benefits of different aspects. These aspects were the lower electricity production cost, higher grid reliability, and more flexibility to integrate renewable energy sourced devices. This work included the economics of proving peak shaving demand response (DR) under a realistic tariff using a range of conventional and advanced ESS. Since, DR had been receiving a positive response to shield retailers against the financial risks, Ghazvini et.al., utilized the concept of short term incentive based DR in a liberalized retail market [205]. The work showed a non-dominated sorting genetic algorithm II based multi-objective optimization model. This model helped to enhance the profit of the retailers as well as to reduce peak demand. This model also helped to avoid the high capacity charges in form of grid tariffs or penalties. In this context to penalties, the impact of the merchandising surplus is needed to be discussed. The merchandising surplus is the cost due to power loss which is therefore required to be analysed thoroughly to improve economic welfare in terms of *var* compensation.

2.3.5.3 Merchandising Surplus for Improved Economics

Merchandising surplus is an important aspect in the deregulated environment. In this context, Mithulananthan et.al., [90] considered optimal allocations of TCSC to reduce the power losses due to congestion in a deregulated power scenario. In this scenario, bilateral power transactions were considered for a small test systems. However the investment cost of the proposed device was high, but the accumulated reduced merchandising surplus due to TCSC helped to enhance the net economic welfare of the considered system. Further, the maximisation of the economic welfare was considered elsewhere [152]. The study also incorporated the reduced congestion rent and spot pricing. This work

analysed different cases on load variations to improve the economics for a small five bus test systems. In this direction, Acharya et.al., elaborated two new methodologies for the placement of series FACTs devices in deregulated electricity market [178]. Here, the maximisation of economic welfare was ascertained by the use of LMP differences and congestion rent respectively. Therefore, it was evidenced that the reduced merchandising surplus or the congestion rent had a major impact to improve the economic welfare of the network.

2.3.5.4 Economic Welfare for Congestion Management

The meta-heuristics based social welfare maximization by multi type FACTs devices in pool electricity market have been elaborated elsewhere [206]. In this work, Balamurugan et.al., considered EP and DE based overloading and excess power flow of the small system. Here, the benefit maximization was majorly considered for pool electricity market. Here, the incorporated multi-type FACTS devices helped to maximize the benefit in accordance with minimizing the cost. Further, profit maximization based on demand side management (DSM) had been studied by several researchers, amongst them the investigations by Jiang et.al., were different. This work showed a comparative studies on the social welfare and the industrial load reduction considering a day-ahead competitive market [207]. This work discussed a comparative study on two popular types of DSM approaches in a day-ahead wholesale market.

Now, the above discussion presented an extensive study on the RPD problem by reactive power compensation in monopoly as well as deregulated power scenario. In addition to the technical analysis, the economics of the proposed problem has also been considered here. Addressing the presented study, few areas can be identified in this sector where the adequate solutions are sparse.

2.4 Scope for RPD in Deregulated Environment

So far, the reactive power optimisations have been observed to deal with different power loss minimisation, security and stability analysis issues. The studies also considered the voltage profile of the transmission lines as well as the distribution systems. The initial works majorly focused on the fundamentals of the RPD problem in a monopoly market without considering the economics as priority basis. Here, the capacitors are applied as most promising *var* compensators to solve the RPD issues.

The power scenarios of the advanced economic and most of the developing economic countries are reformed and restructured since 1980s; it is now very much essential to consider the RPD issue in view of the deregulated power sector. It is therefore a necessity to analyse it considering secured

decentralised power transactions, transmission loss allocation, procurement of economic reactive power as ancillary service, DG installations etc. in connection to the fundamental RPD issues. Deregulated power sectors no doubt ascertain a stability to power flow by improving the quality of service, reduced price etc., but the operational mechanisms become more complex. Further, due to enhancement of private participation by the number of market players in the power transactions more difficulties are introduced in the operation. With these, probabilities of the dynamic voltage limit crossover, network congestion in terms of the violation of security constraints increase which need proper attention.

To manage the situation, a number of advanced *var* compensators may be incorporated in the deregulated power network instead of singular capacitors. Moreover, some of their combinations likely capacitor [208-11] and SVC [212], STATCOM [213], SMES [214-15] may be applied to solve the congestion management problem. Moreover, these works many a times are solved in the RPD domain in the backdrop of deregulated power scenario without considering the total economics. The economics is comprised of the Pareto efficient global welfare [216], individual participant's benefit [216], economics of the *var* compensations, merchandising surplus [216], spot pricing [216] etc. In this context, double auction bidding plays an important role to achieve Pareto efficient global welfare of the system under considerations. Moreover, literature reviews in most of the cases tried small test systems. Therefore, major attentions are required to solve these issues for larger test systems like IEEE 57, 118 bus systems including the real time inter-regional grids.

Since, the RPD issue is a non-linear, non-differentiable, non-convex optimisation problem, it was found to be solved by a number of meta-heuristics techniques. Amongst them DE is one of the most proficient and sustainable evolutionary algorithms available to solve these types of problem very frequently. However, the DE technique often suffers from the poor convergence problem at global optima. To overcome the drawbacks of the fundamental DE, one way is to modify it with the incorporation of the tournament best vector. This may help to search the population space thoroughly to provide the global optimal solution. This modified DE technique is termed as Differential Evolution with Random Localization (DERL) which may be deemed fit for the problem formulations. Further, one swarm evolutionary based advanced meta-heuristics technique namely Cuckoo Search Algorithm (CSA) has been observed to solve successfully a number of combinatorial optimization problems of power system available now a days. Due to its large step length, the Lévy flight of the CSA has extensive search space exploration ability. Hence, this technique may be suitable to solve the reactive power dispatch involving different operational situations. Again different *var* compensators play active role in reactive power dispatches. Their operational features should be known properly before formulating the objective functions involving different situations. A short excursion is

therefore necessary to understand the *var* compensators thoroughly. Further from the above literature surveys it is evident that RPD analysis by newer soft computing techniques in the backdrop of deregulated environment including the economics and advanced *var* compensations is very much necessary for betterment of the power system.

Chapter 3

3 Var Compensators for Reactive Power Dispatch

Power systems are tussling with power loss and operating cost minimization issues since two decades. Even in the present Indian or global wide power scenario, the most predominant problem is identified as the real power loss for the transmission and distribution sector. These problems are of current focus for many utilities and it has been pointed out as one of the most essential tasks. In the middle of the nineteenth century these issues were treated as optimal power flow (OPF) problem [82-86]. The OPF majorly dealt with the minimisations of the fuel cost, generation cost, *var* investment cost and transmission power losses. To optimise the proposed issues, voltage control and *var* compensation were applied while satisfying physical and operating limits of the different variables. The OPF problem tried to enhance the benefit by maintaining the system stability and reliability. In fact the OPF solution depicted the optimal, economic active and reactive power dispatch solutions for a static power system loading condition. Hence the relevance showed that the OPF problem is the summation of a number of individual sub-problems. Whenever the OPF problem is tried to solve, cost minimization function always obtained the priority amongst the other sub functions. Hence the OPF solutions frequently received the final observation as cost prioritized solution over the other sub-functional solutions. Therefore, to achieve optimized solution of the each individual sub-function of the OPF issue, these were divided and solved into few separate individual optimization problem. In this context the real power loss minimization aspect nowdays is practiced separately from the OPF issue for better performance. The proposed aspect is addressed as reactive power dispatch (RPD). But obviously in real time situations these are accomplished by different types of *var* compensators. Analysis of RPD involving *var* compensators therefore demands extra attention in the restructured power system background.

3.1 Deregulated Reactive Power Dispatch (RPD) with Var Compensators

Reactive power dispatch (RPD) is one of the major areas of modern power management system. In power system, minimizations of the real power losses with reduction of the voltage deviation are referred to as reactive power dispatches (RPD) [15, 16]. The RPD optimizes power system losses with reduced voltage deviations by controlling the different reactive power sources. These may be exciter control for generator voltages, transformer tap-settings and capacitor banks while satisfying a number

of equality and inequality constraints. Apart from the static capacitive *var* compensators [208-209], the RPDs are solved by several dynamic *var* compensating devices like synchronous condensers [210-211], flexible AC transmission devices (FACTs) [212-213], energy storage systems [214-215] etc. These advanced *var* compensators provide better system voltage control, resulting in an improved voltage profile, system security, power transfer capability and overall system operation. However the issue is a mixed integer, nonlinear optimization problem which controls both the continuous and discrete variables.

Amongst the two major power components of power triangle, real power is considered as main traded commodity in electricity markets while the reactive power plays an important role for steady real power flow. In restructured power scenario, the real power generators as well as the ancillary service (AS) providers and system operators utilize the network from a commercial view point to maximize their profits. In such scenario, the reactive power support helps to provide requisite amount of voltage level along with the support for real power flow. Hence for the smooth and secured real power flow reactive power generation is necessary. Now if the generating companies are able to support real power flow within its marginal reactive power generation level and if required be able to support the other system, they will get reward from the system operator for the extra support that they made. On the other hand if the generating companies are unable to provide required amount of *var* support for smooth conduct of real power flow and have to take support from the other *var* sources via system operators, they have to be penalized in terms of money. Here, the entity who have supported and provided reactive power will get the benefit from the system operators. Hence the minimal reactive power generation aspect saves the economics of the generating companies which is a very vital issue of the deregulated power market. Therefore, the RPD issue these days is majorly connected to three main aspects of the present power scenarios. These are the minimisations of the real power loss, reduction of the voltage deviation and the economic reactive power generation. These are also dependent on few factors.

3.2 Factors affecting the RPD with Var Compensators in Deregulated Environment

Present power scenarios are influenced by the few issues like voltage security, real power losses, reactive power support etc. Bulk AC transmission of electrical power has two fundamental requirements; one is synchronism and another is stable voltage profile. All synchronous machines must maintain synchronism. Further, balanced voltage profile in the ac transmission is also another desirable aspect of the present power scenario. The overvoltage may cause the risks of flashover, insulation breakdown, and saturation of transformers etc. Similarly, the under voltage may also lead to

initiate the rise of high current, high temperature, speed variation of the machine etc. These further direct the network towards the loss of load, fluctuation of frequency, cascading failure and finally collapse of the power system. Hence voltage limit maintenance is an important criterion of power system planning and operation in terms of the reactive power compensation. Voltage crossover limit of a system is measured in terms of the network topology and settings of reactive power compensation devices. Therefore the transmission and distribution loss issues require proper compensation and adequate treatment. In this regards, *var* compensators are incorporated in the systems to tackle the RPD issues.

3.3 The Var Compensating Devices

A number of *var* compensators are incorporated in the network to enhance the power handling capability with improved voltage profile. Thereby, it helps to reduce real power losses. Amongst them few are more utilised. The devices namely capacitor bank, synchronous condenser, FACTs device, SMES as ESS play important role in reactive power dispatch.

3.3.1 Capacitor Bank

The capacitor [208-209] is the most popular fundamental source of reactive power compensation. A simple capacitor is comprised of two conducting plates which can accumulate charges having separated by any dielectric material. In a DC circuit a capacitor behaves like an open circuited one after a brief period of time. In an AC circuit, current flows through the capacitor continuously in alternating direction being proportional to the rate of change of electric filed. For a pure capacitor, current leads the voltages by 90 degree causing a positive phase shift towards the power factor improvement. Hence the device is utilized as *var* compensating device in the power system environment. Two types of compensation take place with the device; shunt and series compensation.

3.3.1.1 Shunt Compensation

Shunt compensation are extensively used in the practical power system to optimize active and reactive power loss ensuring satisfactory voltage compensation. Capacitive shunt compensators are usually incorporated throughout the transmission or distribution systems. Two type of shunt compensation can be considered; active and passive. Passive compensating devices are the shunt capacitor banks which are widely applied in the power network since 1930s. They can be operated in the network either by permanently placed or switched to improve voltage profile of the line. Developments of the new technology proposed the blend of power electronics devices to project the shunt active

compensators like static *var* compensator (SVC) or static compensator (STATCOM) to improve voltage profile of the network in faster and effective way. This devices help to improve line load ability by reducing stresses and losses of the overloaded lines. However, there is a certain drawback of the shunt compensation. If a fall of voltage at a particular node in a network occurs, the shunt reactive *var*s are also reduced. Similarly, at no load or light load conditions when shunt reactive *var*s are required in relatively small quantity, the capacitor output is high. Therefore, the applications of series capacitors are considered in the network as *var* compensator.

3.3.1.2 Series Compensation

By incorporating capacitor devices in series in the transmission and the distribution network series compensation are performed. The series compensation provides improved transfer capability of the power system by reducing net transfer reactance of the line. This helps to reduce reactive power loss. The series compensation also helps to keep a steady balance between the voltage and reactive power of the line. However, the series capacitors produce high overvoltage under short circuit conditions which causes a spark due to interaction between the current (twenty times higher than the full load current) of the network with capacitive reactance. Besides this, the capacitors have short service life (8-10 years). It may be damaged easily if voltage exceeds the rated value. Therefore, another device namely synchronous condensers which is able to provide step less control of power factor, is used as *var* compensator frequently.

3.3.2 Overexcited Synchronous Motor

Overexcited synchronous machines [210-211] are more familiar as synchronous condenser or synchronous capacitor or synchronous compensator. This device is connected to the electrical power grid to generate or absorb reactive power as needed to improve power factor of the network. This also helps to improve voltage profile of the power system. As the overexcited synchronous motor is operated with leading power factor this devices are utilized for the power factor correction of the loads. In a transmission network several induction motors and transformers are connected which draws heavy amount of reactive current causing the plant power factor to be very poor. Synchronous condenser helps to provide the excess current in terms of *var* supply making the power factor improved. Even asynchronous condenser can deliver up to 150% reactive power by providing step-less automatic power factor correction to the grid. The proposed synchronous motors neither generate any extra switching transients nor are influenced by any system generated harmonics. Therefore, the motors help to maintain balanced voltage profile without being influenced by the electrical resonances. However, due to the high rotating inertia of the synchronous condenser, it is able to

provide restricted voltage support during very short power drops. However they produce disturbance at variable load conditions. Moreover to obtain the starting torque, the synchronous motors need an auxiliary equipment. Therefore, the maintenance cost of the synchronous motor is high compared to other *var* compensators. In this context to ever increasing demand of electric power, expansion or enhancement of the power transfer capability the existing transmission network requires huge amount of finances and sometimes even faces technical difficulties. To handle the situation, a new technology called FACTs devices is employed in the network.

3.3.3 Flexible AC Transmission System (FACTs) Devices

In a deregulated environment, occurrence of several transactions can cause for a sudden increase in power demand resulting to overloading conditions. Sometimes the networks are also subjected to transient instability and cascading outages due to failure of protection relays. Increase in the loading and consumption of huge amount of reactive power may lead the system towards voltage collapse phenomena. This situation needs critical care in terms of *var* compensation which can be mitigated by adopting FACTs devices [212-213]. These devices consider the contingencies and load variations. Moreover, the FACTs devices enhance power transfer capability and maintain a controllability on the network. These devices are designed by incorporating power electronics and other static controllers to provide control of one or more AC transmission system parameters. FACTs devices are having certain benefits:

- System optimality is maintained by power loss reduction and improving voltage profile.
- Fast control mechanisms of the FACTs devices helps to enhance the operating margin with increasing power carrying capability of the lines.
- Systems are made more dynamically secured by increasing transient stability limit of the line.
- Auxiliary stabilizing controllers may be employed by the FACTs devices to damp low frequency oscillations which improve the steady state stability of the system.
- FACTs controllers namely TCSC can resolve the problem of sub-synchronous resonance (SSR).
- The dynamic overvoltage phenomena can be mitigated by the FACTs devices.

Depending upon the control mechanisms of the power electronic circuitry inside, FACTs controllers can be classified into two groups. First set is variable impedance type and second set is voltage source converter based.

3.3.3.1 Variable Impedance Type FACTs

The variable impedance types are majorly classified into static *var* compensator (SVC) and thyristor controlled series capacitor (TCSC).

3.3.3.1.1 Static Var Compensator (SVC)

The SVCs are solid state *var* compensating devices incorporated in the network to improve power system transmission and distribution performance in a number of ways. The SVCs increase the power transfer capability and dynamic stability of the grid while improving the voltage profile of the network and reducing the losses. The SVC can be operated by adopting several schemes by combining reactor, capacitor and thyristor. Amongst them the effective ones are thyristor controlled reactor and fixed capacitor (TCR/FC), thyristor switched capacitor (TSC), thyristor controlled reactor/ thyristor switched capacitor (TCR/TSC) etc. The TCR/FC provides continuous control with zero transients and harmonics are eliminated by tuning the FCs as a filter. The TSCs are categorized by stepped control with no transients, no harmonics, low losses, redundancy and flexible operations. The TCR/TSC is having continuous control with zero transients where harmonics can be filtered by TSR control. This operating mode signifies low losses, redundancy, flexible control and operation. However, SVC has several advantages over synchronous condenser though it injects current harmonics. This can be reduced by segmented TCR and operating one module in the TSR (Thyristor Switched Reactor) mode.

3.3.3.1.2 Thyristor Controlled Series Capacitor (TCSC)

The TCSC is an important FACTs device to improve post contingency stability with dynamic flow control. It helps to damp active power oscillations and eliminates sub synchronous resonance risks. Further this device can be installed in new as well as existing network. Controlled series compensation is a beneficial tool for optimizing power flow between varying load regions and grid. The TCSC based power flow control provides system loss minimization, reduction of loop flows, elimination of line overloading, optimal load sharing between parallel lines etc.

Although the variable impedance type performed effectively to enhance the loadability of the lines, the voltage source converter types are having several advantages over the variable impedance type.

For example, the size of a voltage source converter like STATCOM is much more compact than a SVC for similar rating and is technically superior. It can provide the desired reactive current even at low values of the voltage and can be designed to have in built short term overload capability. The two very frequently applied voltage source converter are described below.

3.3.3.2 The Voltage Source Converter (VSC) based FACTs Devices

The voltage source converter types are majorly divided into static synchronous compensator (STATCOM) and static synchronous series capacitor (SSSC).

3.3.3.2.1 Static Synchronous Compensator (STATCOM)

The STATCOM is a regulating device which provides reactive power to improve low power factor and voltage of a network. Physically the STATCOM is a voltage source inverter operated device which translates dc input voltage to ac output voltage in order to compensate the required reactive power in the network. In addition to voltage control, STATCOM handles damping of power system oscillation leading to improvement of the transmission capability. Further this device exploits significant performance in terms of dynamic load changes, grid voltage fluctuation and harmonic distortion.

The use of multi-pulse and/or multilevel converters eliminates the need for harmonic filters in the case of a STATCOM. However, the costs of the application increases not only due to the increased costs of magnetics and self-commutated devices (such as GTO thyristors), but also resulting from increased losses (The total losses can vary from 0.5 to 1.0%). The new developments in power semiconductor technology are expected to reduce the costs and losses.

3.3.3.2.2 Static Synchronous Series Capacitor (SSSC)

SSSC is one of the important series FACTs devices which are operated by a voltage source converter, transformer and an energy source. SSSC device is typically employed to revise the voltage during fault period in a power network. Further it can be utilized for the power factor correction through continuous voltage injection and in combination with a properly structured controller. Additionally SSSC device help to balance load in interconnected distribution networks. It also fulfills capacitive and reactive power demand with adequate power flow control and reduces harmonic distortion by active filtering.

However, the voltage source converter type performs even better than the variable impedance type FACTs controller; they have only drawback of requirement of self-commutation. Therefore different

self-commutating power semiconductor devices likely the Gate Turnoff (GTO) thyristors, Insulated Gate Bipolar Transistors (IGBT), Integrated Gate Commutated Thyristors (IGCT) are used to operate the voltage source converter. Therefore, the incorporation of the energy storage systems (ESS) is proposed to be an upcoming technology to have great potentials in meeting few confrontations of present complex power scenarios. Besides the *var* compensation, to improve voltage stability, like SVC and STATCOM, the ESS have its energy storage capability. It can store energy at a certain state and can convert the same into electrical energy when needed. This property is very much essential due to power quality/reliability, congestion handling, and reserve/spinning aspects in the present competitive power scenario.

3.3.4 Energy Storage Systems (ESS)

EES technology works on the basis of converting energy from one form (mainly electrical energy) to a storable form and reserving it in various mediums [214-215]. When needed, the stored energy can be converted back into electrical energy. Besides this, the EES perform a number of attractive value propositions (functions) to power network operation and load balancing, such as:

- It helps to meet peak electrical load demands
- It provides time varying energy management
- It alleviates the intermittence of renewable source power generation
- It improves power quality/reliability
- It satisfies remote and vehicle load needs
- It supports the realization of smart grids
- It helps to manage the distributed generation /standby power generation.
- It also reduces the electrical energy import during peak demand periods.

Now, there are a number of ESS technologies available now a days; Flow Battery Energy Storage (FBES), Capacitor and supercapacitor, Superconducting Magnetic Energy Storage (SMES), Flywheels etc are some important categories used for RPD issues.

Now, the choice of the ESS amongst these variants is a topic worth of consideration. It can be seen that SMES devices have high specific power but low specific energy due to their fast response time.

Therefore, they are more suitable for power quality applications for electric power (current) delivery. Moreover, the SMES can completely release their stored energy after a few hours or even shorter i.e., they have very high daily self-charge ratios, from 10% to 100%. Hence, they can be utilized for short-term storage durations (up to hours) based applications likely grid/network fluctuation suppression, spinning reserve, uninterrupted power supply, ramping and load following. The EES technologies used for maintaining power quality will need to have very fast response time (at the millisecond level) for which the SMES are well suited along with the voltage regulation and control.

3.3.4.1 Super-conducting Magnetic Energy Storage (SMES) Device

SMES device [214] is a system to store energy in the magnetic field which is developed by the flow of direct current in an inductive coil which has been cryogenically cooled to a temperature below its superconducting critical temperature. A superconducting wire is represented by a state of the material where the resistance of the material is zero. In this state the current in a coil can flow for infinite time imposed by certain constraints of superconductivity. The conductor has to be operated below a critical temperature which is achieved by providing cryogenically cooling mechanisms across the coil. This imposes the current to circulate indefinitely with almost zero loss. Therefore the energy remains stored as a magnetic field. The stored energy can be discharged back to a connected power system by converting the magnetic energy to electricity by discharging the coil.

A typical SMES device is comprised of three parts. They are superconducting coil and core, power conditioning system and cryogenically cooled refrigerator unit. Once the coil is charged, the current will flow indefinitely providing enormous magnetic energy release.

Overall the SMES device has few fundamental benefits over other devices. The points are listed below:

- As the energy density of the SMES device is high, it can deliver large amount of energy in a very short time resulting to a suitable energy storage solutions to compensate for fast power fluctuation.
- High efficiency
- Long lifetime
- Short response time
- Completely static construction

- SMES are not producing any harmful chemicals while operating

In this context the advanced *var* compensators therefore play a major role to solve the RPD based power transactions in a deregulated power scenario. In such scenario, the networks are found frequently suffering from the problem of dynamic voltage limit crossover issue. This further causes huge current flow leading to increasing power losses. Besides the minimisation of power losses, the incorporation of the *var* compensating devices in the restructured environment also helps to improve the global welfare of the system under consideration.

Chapter 4

4 Restructured Economic Reactive Power Dispatch

The restructured power scenarios are hindered by many unexpected events and therefore, many uncertainties are associated with the network security constraints. In this context, the reactive power dispatch (RPD) has been drawing a significant attention due to involvement of frequent power transactions in the deregulated power networks. The power transactions are a contract between the few numbers of power producers and power consumers to trade a certain amount of power for a certain period time. These transactions are conducted under the surveillance of the ISO to maintain the system security. The benefits of the transactions are distributed among the market players. In this regards, the ISO can charge penalty to the respective participant if any disorder such as power mismatch while violating the contract are observed. Now, during the power transactions, it has been found that the security constraints (load bus voltage) are oscillating nearly their boundary values. Even sometimes it violates the boundary limits. This causes dynamic voltage limit crossover which is also a major problem of power transactions in a restructured network. This dynamic voltage limit crossover issues further enhance line current flow leading to the enhanced power losses. In the context, advanced *var* compensations are required to solve the RPD issue in an efficient, reliable, and sustainable manner. Since the economics is one of the governing factors of the deregulated power scenario, the economics of the advanced *var* compensations are required to be considered while improving the global welfare of the present system. The economics of the advanced *var* compensators i.e., the net monetary benefit by the *var* compensators are considered as reduced merchandising surplus or congestion rent. These are controlled by the ISO to improve the global welfare. Additionally, the global welfare is also dependent on the planned biding of the participants of the double auction bilateral power transactions. In such transactions both the power suppliers and consumers submit their bid to the transaction authority. During the power transaction period, the Pareto efficient transactions provide the maximum benefits to the competent participants while satisfying the market equilibrium criteria [5, 6]. Therefore, the participants would expect to earn highest benefit in terms of Pareto efficient transaction. Moreover in parallel to the incentive facilities, penalties are also applied in the deregulated power scenarios due to violations of any norms as spot pricing. These will help to improve the quality of services with improved economic welfare. Therefore, the several issues of the deregulated power markets such as power transactions, optimal bidding, economics of the power transactions, Pareto efficiency, global welfare analysis, dynamic

voltage limit crossover and network congestion are needed be analysed in the deregulated power market.

4.1 Power Transaction

One of the major aspects of deregulated power market is power transaction. It is defined as the power transmission between two utility (buyer and seller) of the deregulated power market without violating any constraints regarding transmission facility. Power transaction may be accomplished by increasing generation in the supplying utility and by reducing the same amount in the receiving utility. This will cause a complete revision of the power flow pattern of the transmission system including the intermediate system if any. The impact of power transaction may be seen in terms of voltage deviation, voltage fluctuation, increase or even decrease in loss.

The power transaction is decomposed into three major categories. One of them is based on mode of transaction, other is dependent on number of participants (buyer-seller) and the third one is based on the bidding of participants. These are described here briefly.

4.1.1 Mode of Transaction

The category of power transactions are classified in four types:

4.1.1.1 Firm Transmission Transaction

The firm transactions takes place between the two utilities under certain terms and condition rather contractual agreement basis. Hence the transaction should be free of interruptions. Due to this reason the firm power transaction reserves few capacities on transmission facilities to fulfil transaction demands.

4.1.1.2 Non-Firm Transmission Transaction

These types of transaction generally occur in short term basis. These are economic. Moreover, these are operational when enormous transmission capacity are available in certain areas of the network for specific times.

4.1.1.3 Long-Term Transmission Transaction

These types of power transaction continue over a period of several years. During the long interval of this type of transactions, new transmission facilities are employed. These types of transmission

transactions are performed between the buyers and customers under certain specific rules and regulation in a contractual manner.

4.1.1.4 Short-Term Transmission Transaction

This type of power transaction may be as short as few hours. Therefore this type of transmission transactions are not associated with any transmission reinforcements. This may be imposed as part of pooling arrangement or may be served under bilateral contracts.

4.1.2 Power Transaction based on Number of Participants

In this category power transactions are based on the number of participants. These are addressed below:

4.1.2.1 Bilateral Transmission Transaction

The bilateral transmission transactions are one of the agreements between the willing buyer and the willing seller to exchange electricity by obeying certain rights to generating capacity for a specific period of time. Mathematically, each bilateral transaction between a seller at bus-*i* (P_{gi}) and power purchaser at bus-*j* (P_{di}) may be represented by the following power balance relationship. In this type of transaction operations, the number of buyer and seller are equal.

$$P_{gi} - P_{dj} = 0 \tag{1}$$

4.1.2.2 Multilateral Transmission Transaction

In the case of multilateral transaction, same sort of agreement alike the bilateral transaction are imposed between the willing parties to exchange the electricity. These transactions are co-ordinated under certain rights and mutually agreeable terms for specified period of time. Multilateral power transaction is generally conducted for a long period of more than a year. In this case summation of power injected in different buses (*i*) will be equal to the summation of load powers taken out at various buses (*j*).

$$\sum_{i} P_{gi}^{k} - \sum_{j} P_{dj}^{k} = 0 \tag{2}$$

where, P_{gi} and P_{dj} represent the power injection into the seller bus *i* and the power taken out at buyer bus *j*, *k* is the total number of transactions. In this case the number of buyers and the sellers are not equal in numbers.

4.1.3 Power Transaction based on Bidding of the Participants

This paradigm of power transactions is distributed in to two major categories which are illustrated as:

4.1.3.1 Single Auction Power Transaction

Whenever, only Gencos submit their bids for power transactions, this is termed as single-auction power transactions. These arrangements usually are found in UK.

4.1.3.2 Double Auction Power Transaction

Whenever both the power producers and consumers freely bid for power transactions, these are called as double-auction power transactions. These arrangements are widely used in the power pools of New Zealand, California and NordPool markets.

Therefore, bidding is one of the prime factors of any power transactions which need proper planning to make the deal profitable.

4.2 Optimal Bidding

The basis of a restructured power market is competitiveness amongst the market players to achieve maximum economic welfare while maintaining the desired quality. The competitions are invoked in a deregulated power scenario by procuring suitable the bidding strategies. These bidding strategies are required for the market players to survive in the competitive power market [9, 11, 216]. The strategic bidding formulation is one of the essential criteria for the market participants to run their company at the most profitable way. Several factors are affecting the strategic bidding procedure amongst them its own bid, the bids placed by the other participants, energy demand at that time etc are very much important. Strategic bidding is placed based on two important factors to improve economic welfare of the respective participants. Firstly, the bidder should have a very good knowledge of the market situation where the bid is to be placed and a clear understanding of the market and a precise price forecasting known a priory. Secondly, the bidding will be placed on the basis of a good knowledge of generation cost and the probable way to optimize them. Thus, the strategic bidding has a great impact on the economics of the market participants.

4.2.1 Economics of the Market Participants

Based on the planned bidding, the benefits of the market participants are determined. The producer's profit is addressed as the difference between the producer's revenue and the expense of electricity

production. Now the producer's revenue is expressed as the product of the total traded quantity and the market price. In this context, the surplus or consumer's surplus are defined as the difference between the gross consumer's surplus and the expense of purchasing the electricity. Now the concept of surplus is dependent on the inverse demand function of the consumers. If the market price for a commodity is increasing, the consumption level decreases which further reduces the net surplus of the consumers and vice-versa.

Finally, by combining the aggregate of the net profit of the power suppliers ($\sum_{k=1}^{ns} S\_Profit_k$) and surplus of the power consumers ($\sum_{k=1}^{nc} C\_Surplus_k$), the economic benefit is determined. The economic benefit is termed as the global welfare of the system [216]. Here, the fundamental global welfare (*GW*) are given by (3) as

$$\sum_{k=1}^{nc} C\_Surplus_k + \sum_{k=1}^{ns} S\_Profit_k \quad \$/\text{ h} \tag{3}$$

Here, *nc* and *ns* are the number of consumers and suppliers. The global welfare is inherently dependent on the market equilibrium point (MEP) [11]. The market equilibrium point (MEP) or the market clearing point is identified by the crossing point of the supplier's aggregated curve and the consumer's aggregated curve. This point is also referred as market clearing in terms of price and volume. These are termed as market clearing price (MCP) and the market clearing volume (MCV). The MEP indicates the quantity that the suppliers are willing to provide is equal to the quantity that the consumers wish to obtain. The economic performances of the participants in MEP can be further extended with the realisation of the Pareto efficiency in the deregulated power scenario.

4.2.2 Pareto Efficiency

When a system is under control of more than one organisation or dependent on the interplay of various organisations with diverging interests, the conventional optimisation is not applicable and must be replaced by Pareto efficiency. An economic state of market model is Pareto efficient if the benefit achieved by any of the parties can be increased only by dipping the benefit enjoyed by one of the other parties. This can only be possible to occur at MEP. In this regards, the power transaction which are traded far from the MEP, are not viewed as Pareto efficient transactions, thereby the economic welfare of such transactions have low contribution to the total economics [11]. However, if the power transactions are traded very close to the MEP, their economic returns are also found extremely high. Therefore, the theoretical analysis showed that the global welfare will be maximum

for the Pareto efficient transactions and would be very close to the maximum value for the non-Pareto efficient transactions nearing MEP. This gap in exact transaction point and the MEP is called the deadweight losses. These are originated due to the reduction in the amount transacted caused by the price distortion. Hence, the global welfare is the key entity to justify the economic RPD while ascertaining the significance of the Pareto efficient power transactions over the non-Pareto efficient one in the backdrop of deregulated power scenario.

Now, the global welfare is further influenced by the spot pricing which is one of the prime economic issues of the restructured power scenario [11].

4.2.3 Impact of Spot Pricing on Global Welfare

Spot pricing may influence the global welfare when there is a power mismatch in the network during the power transactions. The power mismatch during the power transactions is a common issue due to various reasons such as faulty load forecasting, fault in generator operations etc. Therefore, the power mismatch among the market participants will cause to have spot pricing by the transaction authority [11, 216]. In such scenario, if the suppliers are unable to produce the required amount of contracted power, the spot price in terms of balancing cost will be charged from its profit for the mismatched power amount. Similarly, if the consumers consume excess power beyond the contracted power from the transaction network, the spot price in the form of balancing cost will be added to the supplier's profit. Considering power mismatch of ΔP_{MPT} MW and *SP* as spot price set by the transaction authority, the balancing cost (*BC*) can be determined by (4).

$$BC = \Delta P_{MPT} \times SP \quad \$/h \tag{4}$$

When generators are unable to fulfil the demand, the *BC* will be subtracted from the supplier's profit as (5)

$$\sum_{k=1}^{ns} S\_Profit_k = \sum_{k=1}^{ns} S\_Profit_k^{'} - BC \quad \$/\mathrm{h} \tag{5}$$

Here, $\sum_{k=1}^{ns} S\_Profit_k^{'}$ is the initial profit without considering the spot pricing.

Similarly, when the consumers draw more power compared to its schedule value, the *BC* is added favourably to the supplier's profit as (6)

$$\sum_{k=1}^{ns} S\_Profit_k = \sum_{k=1}^{ns} S\_Profit_k^{'} + BC \quad \$/\text{h} \tag{6}$$

Finally, by cumulating the net profit of the suppliers and consumers, the global welfare will be obtained here. Now, the global welfare characterised by the spot pricing issues can be improved by incorporating the economics of the *var* compensators.

4.2.4 Impact of Var Compensation to Global Welfare

The integration of the *var* compensators has a positive economic impact in the form of reduced merchandising surplus [216]. The reduced merchandising surplus is represented here as the economics of the *var* compensation. This is considered as the difference between the net incentive returns due to loss minimization and the operational pricing of the proposed *var* compensator. This further cumulated to the fundamental global welfare which helped to strengthen the total economics while enhancing the net benefits of the participants of the system under observation. Here the economics of the *var* compensators such as singular capacitor, synchronous condensers (SC), TCSC, SMES, combined capacitor-SC, combined capacitor-SMES are discussed thoroughly.

4.2.4.1 Economics of the Capacitor

Now, the incentive benefit returns from the transaction authority for minimizing power loss are well expressed by the expression (7) as

$$(P_{LOSS\_bVCP} - P_{LOSS\_aVCP}) \times Inc \quad \$/\text{h} \tag{7}$$

The investment cost of the capacitive *var* compensator is represented by the expression (8) as

$$HIC_{Capacitor} \quad \$/\text{h} \tag{8}$$

Thus, by combining these two expressions, the net monetary benefit ($NMB_{Capacitor}$) due to shunt capacitor placement is calculated by (9) as

$$NMB_{Capacitor} = (P_{LOSS\_bVCP} - P_{LOSS\_aVCP}) \times Inc - HIC_{Capacitor} \quad \$/\text{h} \tag{9}$$

where *Inc* indicates the incentive return due to power loss compensation in \$/ MWh. P_{LOSS_bVCP} and P_{LOSS_aVCP} are the power loss occurred before and after respective *var* compensators placement respectively in MW. Now, the $HIC_{Capacitor}$ [217] is determined by (10) as

$$HIC_{Capacitor} = Unit\ Size \times Cost \quad \$ \tag{10}$$

where *Unit size* defines the size of the capacitor in kVar and *cost* is represented by yearly price of each unit capacitor in $/ kVar.

For obtaining better performances, the synchronous condensers are connected to the network in place of capacitors.

4.2.4.2 Economics of the Synchronous Condenser (SC)

The net monetary benefit (NMB_{SC}) due to placement of SC is obtained by (11) as

$$NMB_{SC} = (P_{LOSS\_bVCP} - P_{LOSS\_aVCP}) \times Inc - HIC_{SC} \quad \$/h \tag{11}$$

Where HIC_{SC} is the installation and operating cost of the SC device in $ /h [218] which is calculated by (12) as

$$HIC_{SC} = Unit\ Size \times Cost \quad \$ \tag{12}$$

where *Unit size* represents the size of the integrated SC in kVar and *cost* is given by yearly price of each unit SC in $/ kVar.

To achieve loadability with improved performances, TCSC is incorporated further in the network.

4.2.4.3 Economics of the TCSC

The economics *viz* the net monetary benefit of the TCSC device (NMB_{TCSC}) is determined by (13) as:

$$NMB_{TCSC} = (P_{LOSS\_bVCP} - P_{LOSS\_aVCP}) \times Inc - HIC_{TCSC} \quad \$/h \tag{13}$$

Here, HIC_{TCSC} is the installation and operating cost of the TCSC in $ / h which is determined as follows:

According to [219], the investment cost of TCSC is given by (14) as

$$C_{TCSC} = 0.0015 S_{TCSC}^2 - 0.7130 S_{TCSC} + 153.75 \quad \$/\text{kVar} \tag{14}$$

Where C_{TCSC} is the cost of TCSC in $ /kVar and S_{TCSC} is the operating point of TCSC in MVar. Overall investment cost (IC_{TCSC}) in $ is calculated by (15) as follows

$$IC_{TCSC} = (C_{TCSC} \times S_{TCSC} \times 1000) \quad \$ \tag{15}$$

With these, the annual investment cost (AIC_{TCSC}) in $/ year can be calculated by (16) given in [219]:

$$AIC_{TCSC} = IC_{TCSC} \frac{ir(1+ir)^{LT}}{(1+ir)^{LT}-1} \$/\text{year} \quad (16)$$

Where *ir* is the rate of interest and *LT* is the life time of the device. In this work, it is considered as *ir* = 0.05 and *LT* = 5 years.

From the above cost, the hourly investment cost for TCSC (HIC_{TCSC}) is calculated by (17).

$$HIC_{TCSC} = [\frac{AIC_{TCSC}}{8760}] \$/\text{h} \quad (17)$$

To determine sustainable as well as improved response, SMES is integrated in the network for which necessary economics is required to be determined for further calculations.

4.2.4.4 Economics of the SMES

The net monetary benefit (NMB_{SMES}) due to integration of the SMES device is determined by (18) as

$$NMB_{SMES} = (P_{LOSS\_bVCP} - P_{LOSS\_aVCP}) \times Inc - HIC_{SMES} \quad \$/\text{h} \quad (18)$$

The HIC_{SMES} which is the operating cost of the SMES device is comprised of three parts. The first part represents the cost due to SMES coil including containment, leads and bus and external support. The cost of cryogenic system including refrigerator and vacuum vessel is further denoted as second part. The third part considers the price for the power conversation system.

Incorporating the costs of the above mentioned three parts, the total cost of the SMES (C_{SMES}) is represented by (19) [220].

$$C_{SMES} = f_1(\text{E}) + f_2(\text{E}) + K_3 * Q_{SMES} \quad \$ \quad (19)$$

where the first and second part of the cost equation are given by (20) and (21) which are dependent on energy (*E*) of the coil and core of the respective SMES at certain temperature [221].

$$f_1(E) = 0.2 * E * K_1 \quad (20)$$

$$f_2(E) = 0.2 * E * K_2 \tag{21}$$

where K_1 and K_2 are the respective constants in \$/ MJ [220]. In the third part of the cost equation (19), K_3 [220] is the constant required to handle the proposed power conversation in \$/ kVar.

To determine the yearly investment cost of the SMES (AC_{SMES}), a life span (LT) of 30 years and 5% rate of interest (ir) is assumed. The AC_{SMES} is presented here by equation (22).

$$AC_{SMES} = C_{SMES} \frac{ir(1+ir)^{LT}}{(1+ir)^{LT} - 1} \quad \$ / \text{year} \tag{22}$$

Finally the hourly investment cost of the SMES device (HIC_{SMES}) is determined by (23)

$$HIC_{SMES} = \left[\frac{AC_{SMES}}{8760} \right] \quad \$ / \text{h} \tag{23}$$

To obtain the economic performances, combined *var* compensation in the form of capacitor-Synchronous condensers are incorporated in the network.

4.2.4.5 Economics of the Combined Capacitor-SC

The net monetary benefit ($NMB_{Capacitor+SC}$) due to combined integration of the shunt capacitor and SC is calculated by (24) as

$$NMB_{Capacitor+SC} = (P_{LOSS\_bVCP} - P_{LOSS\_aVCP}) \times Inc - HIC_{Capacitor} - HIC_{SC} \quad \$ / \text{h} \tag{24}$$

Further, to accomplish sustainable as well as economic performances, combined *var* compensation in the form of capacitor-SMES devices are integrated in the network.

4.2.4.6 Economics of the Combined Capacitor-SMES

The net monetary benefit ($NMB_{Capacitor+SMES}$) due to combined incorporation of the shunt capacitors and SMES device is given by (25) as

$$NMB_{Capacitor+SMES} = (P_{LOSS\_bVCP} - P_{LOSS\_aVCP}) \times Inc - HIC_{Capacitor} - HIC_{SMES} \quad \$ / \text{h} \tag{25}$$

The economics due to *var* compensation help to reduce merchandising surplus controlled by the transaction authority [11]. This will further enhance the global welfare involving the profit surplus of

the power producers and consumers of the proposed power transactions. Therefore, the economic RPD in the view of improved global welfare should be identified a priori.

4.2.4.7 Global Welfare including the Economics of the Var Compensator

The improved global welfare with considering the economics of the *var* compensations for the six cases stated above are comprehended in (26-31) as

Case 1: $$\sum_{k=1}^{nc} C\_Profit_k + \sum_{k=1}^{ns} S\_Profit_k + NMB_{Capacitor} \quad \$ / h \tag{26}$$

Case 2: $$\sum_{k=1}^{nc} C\_Profit_k + \sum_{k=1}^{ns} S\_Profit_k + NMB_{SC} \quad \$ / h \tag{27}$$

Case 3: $$\sum_{k=1}^{nc} C\_Profit_k + \sum_{k=1}^{ns} S\_Profit_k + NMB_{TCSC} \quad \$ / h \tag{28}$$

Case 4: $$\sum_{k=1}^{nc} C\_Profit_k + \sum_{k=1}^{ns} S\_Profit_k + NMB_{SMES} \quad \$ / h \tag{29}$$

Case 5: $$\sum_{k=1}^{nc} C\_Profit_k + \sum_{k=1}^{ns} S\_Profit_k + NMB_{Capacitor+SC} \quad \$ / h \tag{30}$$

Case 6: $$\sum_{k=1}^{nc} C\_Profit_k + \sum_{k=1}^{ns} S\_Profit_k + NMB_{Capacitor+SMES} \quad \$ / h \tag{31}$$

Here, *C_Profit*, *S_Profit* are denoted as the individual consumer's profit, the individual supplier's profit during the power transactions. As shown, these improvements in global welfare expressions are observed due to the economics of the *var* compensations. These are thereby distributed among all the participants of the power transactions. Thus, the participants are found economically benefitted.

Technically, these *var* compensations enormously helped to reduce network congestion which is generated due to dynamic voltage limit crossover problem. This problem is the resultant of frequent power transactions. The proposed problem of dynamic voltage limit crossover causes huge voltage drop which also generates enhanced current leading to line congestion. Therefore, the network congestion in the backdrop of power transactions are needed to be discussed beforehand for better understanding.

4.3 Dynamic Voltage Limit Crossover leading to Network Congestion

Network congestion is the major concern of the deregulated power environment which may rise due to various reasons. When the transmission network is unable to accommodate all the desired

transaction due to violation of any operational constraints majorly the security constraints such as voltage profile, congestion may occur. In the restructured power scenario, congestion hits the network frequently due to the occurrence of a number of power transactions and thereby the limit violations of the bus voltages at different operating points i.e., the dynamic voltage limit crossover issues occur. In this work, the dynamic voltage limit crossover in the form of congestion is expressed by two factors namely the current enhancement factor (CEF_{ij}) and power loss enhancement factors ($PLEF_{ij}$). These are quantified by the enhanced bus voltages to affect the other connected buses of the network in terms of enhanced line current flow and power losses. Assuming the constant impedance between the two buses (say *i* and *j*), the CEF_{ij} and $PLEF_{ij}$ are determined by (32) and (33) respectively as,

$$CEF_{ij} = \left(\frac{V_{i\_enhanced} - V_j}{V_{i\_nominal} - V_j} \right) \tag{32}$$

$$PLEF_{ij} = \left(\frac{V_{i\_enhanced} - V_j}{V_{i\_nominal} - V_j} \right)^2 \tag{33}$$

where $V_{i\_enhanced}$ is the enhanced line voltage of bus *i* (violating the nominal value of 0.95 pu to 1.10 pu), $V_{i\_nominal}$ is the nominal voltage and V_j is the voltage of j^{th} bus connecting to the i^{th} one. It may further be noted that for CEF_{ij} and $PLEF_{ij}$ values greater than one, the lines will be considered as congested lines. These increased line voltages are generally brought to nominal values by *var* compensations.

4.3.1 Congestion Management Schemes

The problem of congestion may be solved by several means like real and reactive power generation and distribution rescheduling, topological changes or restructuring of the network or by incorporating power flow and voltage controlled devices like Flexible AC Transmission systems (FACTs) or SMES. In solution to this Congestion Management (CM) problem the topological changes may result in reduction of stability margin and risk of grid failure or blackouts. Even the real and reactive power rescheduling is also very difficult to be managed in the deregulated environment due to presence of multi constraints. In this situation the incorporation of the FACTs devices [212-13] and ESS [214-15] in the existing system may be the most feasible solution to handle the CM problem without making the system stressed. While integrating the proposed devices load-ability of the existing system enhance resulting in to improved tackling of dynamic voltage limit crossover issue. As a result real power loss will reduce.

Therefore the RPD issues involving power transaction which induce congestion problem are needed to be handled technically as well as economically in deregulated power sector. Initially this can be done by considering appropriate mathematical problem formulations.

Chapter 5

5 Mathematical Modelling of the Reactive Power Dispatch

Reactive power dispatch (RPD) is an important aspect of present power scenario which is already discussed in chapter 3 as well as in chapter 4. The RPD problem minimizes power system losses frequently by controlling the generator bus voltages, transformer tap-settings and other sources of reactive power such as capacitor banks while satisfying a number of equality and inequality constraints. In this context, while power transactions occur, the security constraints likely the bus voltages are fluctuating around their boundary values causing to the dynamic voltage limit crossover issues. Even few buses are violating their prefixed operating limit which causes current and power loss enhancement leading to network congestion. Now, it has been found that in such restructured power scenario, the capacitive *var* compensators are not found to provide desired economic results due to its static operations. Hence, to manage the different uncertainties of restructured RPD, a number of dynamic *var* compensating devices like synchronous condensers, FACTs devices, ESS and some of their combinations with capacitors are incorporated in the network. Their performances can be visualised by suitable problem formulations.

5.1 Problem Formulation

Here, the fundamental RPD is considered initially including the voltage limiting issues. Besides this, RPD involving the double auction bilateral and multilateral power transactions are considered in the backdrop of restructured environment.

5.1.1 Fundamental RPD Formulation

The proposed objective function of the fundamental RPD is represented by (34, 35) which is being constrained by few equality and inequality issues. Here, loss is minimized with respect to a fixed amount of load.

The RPD problem can be expressed as [222, 7-8]:

$$min\ P_{Loss} = \sum_{k=1}^{nbus} G_k \left[(t_k V_i)^2 + V_j^2 - 2 t_k V_i V_j cos(\delta_i - \delta_j) \right] \tag{34}$$

It is tuned into the following expression as given by (35):

$$min\ P_{Loss} = \sum_{i=1}^{NG} P_{GEN} - \sum_{\substack{i=1, \\ i \neq slack\ bus}}^{NL} P_{LOAD} \tag{35}$$

where, P_{Loss} is the power loss in the network. G_k is the conductance of the k^{th} bus, t_k is the transformer tap ratio, V_i, V_j is the bus voltages of the i^{th} and j^{th} buses respectively, δ_i and δ_j is the voltage angle of bus i and j respectively. The P_{GEN} and P_{LOAD} is the generated power from central generating station, real power generated via distributed generation and the total load power connected to the given system. The *NG*, *NL* are the number of generator buses, number of load buses respectively and *nbus* are the total buses in the network. In this work, P_{GEN} and P_{LOAD} is solved with load flow analysis using Newton Raphson method [222].

In conjunction with the real power loss minimization problem, the voltage security issues are also considered to be formulated. Here, the voltage security of the network is measured by cumulating the load bus-voltage deviation (V_{dev}). It is expressed as

$$min\ V_{dev} = \sum_{\substack{i=1, \\ i \neq slack\ bus, NG}}^{nbus} (V_i - V_{ref}) \tag{36}$$

Here, V_i is the i^{th} bus voltage and V_{ref} is the reference bus voltage which is considered as 1.00 p.u. Further, the total reactive power generation (Q_{Gen}) minimization aspect as a sub function of the RPD problem is also considered to be solved in the view of RPD analysis. The expression is given by equation (37)

$$min\ Q_{Gen} = \sum_{i=1}^{NG} Q_i \tag{37}$$

Here, Q_i represents the net generated reactive power across the connected generator buses.

The proposed functions such as (35-37) are handled by two sets of decision variables. One is termed as state variable (x) and other is called as control variable (u). Now the proposed objective functions i.e. (35) and (37) are sometimes connected together and solved as multi-objective RPD formulations which may have same sets of variables.

The state variable (x) can be expressed as:

$$x^T = [P_{G1}, Q_{G1} \dots \dots \dots Q_{GNG}, V_{L1} \dots \dots \dots V_{LNL}, \theta_1 \dots \dots \dots \theta_{nbus}] \quad (38)$$

where, P_{G1} is the generator real power output at slack bus, Q_G is the generator reactive power output, V_L is the Load bus voltage, and θ is the bus voltage angle. These variables are dependent on the objective function.

The fundamental RPD can be controlled by different parameters. They are generator bus voltages, transformer tap settings, capacitors, SMES etc. The control variable (u) can be expressed as:

$$u^T = \begin{bmatrix} V_{G1} \dots V_{DG} \dots \dots V_{GNG}, \; t_1 \dots \dots \dots t_{NT}, \; Q_{C1} \dots \dots \dots Q_{CNC}, \\ Q_{SMES1} \dots\dots\dots Q_{SMESNC} \end{bmatrix} \quad (39)$$

where, V_G is generator bus voltages, t are the transformer taps setting, Q_C is shunt capacitors, Q_{SMES} are the reactive power injection by the superconducting magnetic energy storage (SMES) device, V_{DG} is the voltages of the buses where distributed generation are taken place. Moreover, the *NT*, *NC*, and *NS* are the number of the regulating transformers, number of shunt, and SMES *var* compensators respectively.

The optimization of the above objective functions (35, 36, 37) are subjected to a number of equality and inequality constraints.

5.1.1.1 Equality Constraint for RPD

Equality Constraints are represented by typical load flow equations [222]:

$$P_{Gi} - P_{Di} - V_i \sum_{j=1}^{nbus} V_j \left[G_{ij} cos\left(\delta_i - \delta_j\right) + B_{ij} sin\left(\delta_i - \delta_j\right) \right] = 0 \quad (40)$$

$$Q_{Gi} - Q_{Di} - V_i \sum_{j=1}^{nbus} V_j \left[G_{ij} sin\left(\delta_i - \delta_j\right) - B_{ij} cos\left(\delta_i - \delta_j\right) \right] = 0 \quad (41)$$

where P_G is the real power generation from central generating station, Q_G is the reactive power generation from central generating station, P_D is the active load demand, Q_D is the reactive load demand, and G_{ij} and B_{ij} are the conductance and the susceptance between bus i and j respectively.

5.1.1.2 Inequality Constraint for RPD

Inequality Constraints are expressed for different parameters such as:

Generation Constraints: Generator bus voltages, reactive power outputs are having by their lower and upper limits as:

$$V_{Gi}^{\min} \le V_{Gi} \le V_{Gi}^{\max}, \qquad i = 1,\ldots,NG \tag{42}$$

$$Q_{Gi}^{min} \le Q_{Gi} \le Q_{Gi}^{max}, \qquad i = 1,\ldots, NG \tag{43}$$

Transformer Constraints: Transformer tap settings are bounded by their minimum and maximum limits as:

$$t_i^{min} \le t_i \le t_i^{max}, \qquad i = 1,\ldots, NT \tag{44}$$

Security Constraints: This includes the load bus voltage to be limited within their lower and upper limits as:

$$V_{Li}^{min} \le V_{Li} \le V_{Li}^{max}, \qquad i = 1,\ldots, NL \tag{45}$$

Shunt var Constraints: Shunt *var* compensators are maintained by their minimum and maximum limits as:

$$Q_{Ci}^{min} \le Q_{Ci} \le Q_{Ci}^{max}, \qquad i = 1,\ldots, NC \tag{46}$$

SMES var Constraints: SMES *var* compensators are bounded by their lower and upper limits as:

$$Q_{SMESi}^{min} \le Q_{SMESi} \le Q_{SMESi}^{max}, \qquad i = 1,\ldots, NS \tag{47}$$

In this context, the SMES device is a purely inductive device which is generally expressed by its coil energy (E), the rated active and reactive power (P_{SMES}, Q_{SMES}) output by the following equations (48-51)

$$E = \frac{1}{2} L I_{Coil}^{2}(t) \tag{48}$$

$$P_{SMES}(t) = \frac{dE(t)}{dt} = L I_{Coil}(t) \frac{dI_{Coil}(t)}{dt} \tag{49}$$

$$Q_{SMES} = \sqrt{S_{SMES}^2 - P_{SMES}^2} \tag{50}$$

$$P_{SMES} = S_{SMES} \cos\phi \tag{51}$$

While determining the P_{SMES} and Q_{SMES} the following inequality constraint given by (52) is to be maintained.

$$\sqrt{P_{SMES}^2 + Q_{SMES}^2} \leq V_{Coil}.I_{Coil}(t) \tag{52}$$

Now, most of the developing economic power sectors are already restructured in addition to the advanced economy, where a number of power transactions frequently occur. It has been found that, during the bilateral and multilateral power transactions, the losses are increased due to dynamic voltage limit crossover issues. Therefore, the restructured RPD problem is required to be handled by suitable advanced *var* compensating devices.

5.1.2 RPD Problem with Bilateral Power Transactions

Now, according to the principles of the bilateral power transactions by equation (1), the said transaction can be developed as,

$$\sum_{k=1}^{ns} P_{S\_BiLat_k} - \sum_{k'=1}^{nc} P_{C\_BiLat_{k'}} = 0 \tag{53}$$

Here, the power mismatch is considered to be zero.

Now, by involving the equation (53), the restructured RPD characterised by bilateral power transactions can be represented as,

$$min\, P_{BiLatLoss} = \sum_{i=1}^{NG} P_{GEN} + \sum_{k=1}^{ns} P_{S\_BiLat_k} - \sum_{i=1}^{NL} P_{LOAD} - \sum_{k'=1}^{nc} P_{C\_BiLat_{k'}} \tag{54}$$

Here, $P_{BiLatLoss}$, P_{S_BiLat} and P_{C_BiLat} are shown as the bilateral transactions based real power loss, transacted power from supplier and power provided to consumer considering the network under consideration. The number of suppliers and consumers are *ns* and *nc* respectively.

Here, the presented problem is initially optimized by controlling generator bus voltages and transformer tap settings as case 1. To tackle the drawbacks of the case 1 likely the dynamic voltage limit crossover problem, the proposed problem is re-optimized by shunt capacitors placement in

addition to the other control variables as case 2. To achieve better and economic performances in the view of the deregulated power scenario, the advanced *var* compensators are applied to solve the proposed problem. In this work, the synchronous condenser (SC), the combination of capacitors and SC, the SMES, and the combination of capacitors and SMES in place of single shunt capacitive compensators are utilized by maintaining other constraints of case 1 unaltered. The RPD problem characterised by bilateral power transactions are optimised by subjecting it to a number of equality and inequality constraints which need to be elaborated for better optimization and understanding purpose.

5.1.2.1 Equality Constraints for Bilateral Transactions based RPD

Here equality constraints for real power is given by (55). The equation (55) is representing the modified form of the real power equality constraints of the fundamental RPD. It showed the incorporation of the traded power by the different participants of the bilateral power transactions.

Case 1-6 $$P_{Gi} + P_{S\_BiLat_k} - P_{Di} - P_{C\_BiLat_k'} - V_i \sum_{j=1}^{nbus} V_j \left[G_{ij} cos\left(\delta_i - \delta_j\right) + B_{ij} sin\left(\delta_i - \delta_j\right)\right] = 0 \quad (55)$$

Similarly, the equality constraints for the reactive power are shown by (56-61) respectively which are also the revised version of the reactive power equality constraints of the fundamental RPD. It showed the incorporation of the traded power by the different participants of the bilateral power transactions with/without the reactive power handled by the different *var* compensators. These are represented as,

Case 1 $$Q_{Gi} + Q_{S\_BiLat_k} - Q_{Di} - Q_{C\_BiLat_k'} - V_i \sum_{j=1}^{nbus} V_j \left[G_{ij} \sin(\delta_i - \delta_j) - B_{ij} \cos(\delta_i - \delta_j)\right] = 0 \quad (56)$$

Case 2 $$Q_{Gi} + Q_{S\_BiLat_k} + \sum_{k=1}^{Nc} Q_{Ck} - Q_{Di} - Q_{C\_BiLat_k'} - V_i \sum_{j=1}^{nbus} V_j \left[G_{ij} \sin(\delta_i - \delta_j) - B_{ij} \cos(\delta_i - \delta_j)\right] = 0 \quad (57)$$

Case 3 $$Q_{Gi} + Q_{S\_BiLat_k} + \sum_{k=1}^{Nsc} Q_{SCk} - Q_{Di} - Q_{C\_BiLat_k'} - V_i \sum_{j=1}^{nbus} V_j \left[G_{ij} \sin(\delta_i - \delta_j) - B_{ij} \cos(\delta_i - \delta_j)\right] = 0 \quad (58)$$

Case 4 $$Q_{Gi} + Q_{S\_BiLat_k} + \sum_{k=1}^{Nc} Q_{Ck} + \sum_{k=1}^{Nsc} Q_{SCk} - Q_{Di} - Q_{C\_BiLat_k'} - V_i \sum_{j=1}^{nbus} V_j \left[G_{ij} \sin(\delta_i - \delta_j) - B_{ij} \cos(\delta_i - \delta_j)\right] = 0 \quad (59)$$

Case 5 $$Q_{Gi} + Q_{S\_BiLat_k} + \sum_{k=1}^{Ns} Q_{SMESk} - Q_{Di} - Q_{C\_BiLat_k'} - V_i \sum_{j=1}^{nbus} V_j \left[G_{ij} \sin(\delta_i - \delta_j) - B_{ij} \cos(\delta_i - \delta_j)\right] = 0 \quad (60)$$

Case 6 $$Q_{Gi} + Q_{S\_BiLat_k} + \sum_{k=1}^{Nc} Q_{C_k} + \sum_{k=1}^{Ns} Q_{SMES_k} - Q_{Di} - Q_{C\_BiLat_k} - V_i \sum_{j=1}^{nbus} V_j \left[G_{ij} \sin(\delta_i - \delta_j) - B_{ij} \cos(\delta_i - \delta_j) \right] = 0 \quad (61)$$

During the bilateral transaction, reactive power for supplier and consumer are represented by Q_{S_BiLat} and Q_{C_BiLat} respectively. Here, the reactive power handled by the generator, load buses are Q_G , Q_D respectively. The reactive power output of the proposed SMES, SC and capacitors are given by Q_{SMES}, Q_{SC} and Q_C which are positioned at the bus numbers N_S, N_{SC} and N_C respectively.

5.1.2.2 Inequality Constraints for Bilateral Transactions based RPD

While considering the RPD formulation, the required inequality constraints are generator constraints, transformer constraints, security constraints, *var* constraints.

Generation Constraints: Generator bus voltages including market participants (V_G , $V_{P_{P\_BiLat_K}}$), reactive power outputs including market participants (Q_G, $Q_{P_{P\_BiLat_K}}$) are maintaining their boundary limits as:

$$V_{G_i}^{\min} \le V_{G_i} \le V_{G_i}^{\max}, \qquad i = 1,\ldots,ng \quad (62)$$

$$V_{P_{G\_BiLat_k}}^{\min} \le V_{P_{G\_BiLat_k}} \le V_{P_{G\_BiLat_k}}^{\max} \quad (63)$$

$$Q_{G_i}^{min} \le Q_{G_i} \le Q_{G_i}^{max}, \qquad i = 1,\ldots,ng \quad (64)$$

$$Q_{P_{G\_BiLat_k}}^{\min} \le Q_{P_{G\_BiLat_k}} \le Q_{P_{G\_BiLat_k}}^{\max} \quad (65)$$

Transformer Constraints: Transformer tap settings (t) are maintaining their lower and upper limits as:

$$t_i^{min} \le t_i \le t_i^{max}, \qquad i = 1,\ldots,NT \quad (66)$$

where NT are the t connected lines.

Security Constraints: The load bus voltages (V_L) are represented as security constraints which are the key entity for measuring the dynamic voltage limit crossover. These constraints are operated within their lower and upper limit as:

$$V_{L_i}^{min} \le V_{L_i} \le V_{L_i}^{max}, \qquad i = 1,\ldots,nbus \quad (67)$$

Capacitor var constraints: Capacitor *var* compensators are following their lower and upper limits as:

$$Q_{C_i}^{min} \le Q_{C_i} \le Q_{C_i}^{max}, \qquad i = 1,\dots, N_C \tag{68}$$

Synchronous Condenser var Constraint: Synchronous condenser *var* compensators are balancing their lower and upper limits as:

$$Q_{SC_i}^{min} \le Q_{SC_i} \le Q_{SC_i}^{max}, \qquad i = 1,\dots, N_{SC} \tag{69}$$

SMES var Constraint: SMES *var* compensators are operating within their lower and upper limits as:

$$Q_{SMES_i}^{min} \le Q_{SMES_i} \le Q_{SMES_i}^{max}, \qquad i = 1,\dots, N_S \tag{70}$$

The bilateral power transactions frequently occur in the power network. However due to the increasing number of uneven participant (where the number of power producers are not equal with number of power consumers) in the advanced economy or in major developing economic inter-regional markets, this model can further be utilized in the next phase of study considering multilateral power transactions.

5.1.3 RPD Problem Formulation with Multilateral Power Transactions

As described earlier in equation (2), the power balance equation for the traded power by the different participants of the multilateral power transaction can be developed as,

$$\sum_{k=1}^{ns} P_{S\_MultiLat_k} - \sum_{k'=1}^{nc} P_{C\_\text{Multi}\,Lat_{k'}} = 0 \tag{71}$$

By considering the above equation, the restructured RPD problem involving the multilateral power transaction can be written as,

$$min\, P_{MultiLatLoss} = \sum_{i=1}^{NG} P_{GEN} + \sum_{k=1}^{ns} P_{S\_MultiLat_k} - \sum_{\substack{i=1, \\ i \neq slack\ bus}}^{nbus} P_{LOAD} - \sum_{k'=1}^{nc} P_{C\_\text{Multi}\,Lat_{k'}} \tag{72}$$

Here, $P_{MultiLatLoss}$, $P_{S\_MultiLat}$ and $P_{C\_MultiLat}$ are represented as the multilateral transactions based real power loss, transacted power from supplier and power provided to consumer ($ns \neq nc$) respectively.

Here, the proposed problem of multilateral transactions is optimized initially by controlling generator bus voltages and transformer tap settings. To reduce the drawbacks of the case 1 likely the dynamic

voltage limit crossover as well as the congestion issue, the proposed problem is revisited by shunt capacitors placement, TCSC incorporation, integration of the SMES and some of their combinations with capacitor with the other constraints of the network. The RPD problem formulations involving multilateral power transactions are subjected to a number of equality and inequality constraints enumerated below;

5.1.3.1 Equality Constraints for Multilateral Transactions based RPD

Here equality constraints in terms of real power are given by (73-74). Both the equations (73-74) are the revised form of the real power equality constraints of the fundamental RPD. The equation (73) represents the real power balance incorporating the traded power by the different participants of the multilateral power transactions with/without *var* compensators that placed at different load buses such as capacitors, synchronous condensers, SMES.

Case 1, 2, 4, 5:
$$P_{Gi} + P_{S\_MultiLat_k} - P_{Di} - P_{C\_MultiLat_k}, - V_i \sum_{j=1}^{nbus} V_j \left[G_{ij} cos\left(\delta_i - \delta_j\right) + B_{ij} sin\left(\delta_i - \delta_j\right) \right] = 0 \quad (73)$$

Similarly, the real power equality constraints including the effect of TCSC is represented by equation (74) where traded power by the different participants of the multilateral power transactions are also included.

Case 3:
$$\begin{aligned} & P_{Gi} + P_{S\_MultiLat_k} - P_{Di} - P_{C\_MultiLat_k}, \\ & -V_i \sum_{j=1}^{nbus} V_j \left[\left(\frac{r_{ij}}{r_{ij}^2 + (x_{ij} - X_{TCSC})^2} \right) Cos(\delta_i - \delta_j) + \left(-\frac{x_{ij} - X_{TCSC}}{r_{ij}^2 + (x_{ij} - X_{TCSC})^2} \right) Sin(\delta_i - \delta_j) \right] = 0 \end{aligned} \quad (74)$$

where, the injected reactance from the TCSC is X_{TCSC}. Moreover, the line resistance and reactance of the i^{th} and j^{th} line is r_{ij} and x_{ij} respectively.

Further, the equality constraints for the reactive power including the traded power by different participants of the multilateral power transactions for different case studies with/without the *var* compensators are shown by (75-79):

Case 1:
$$Q_{Gi} + Q_{S\_MultiLat_k} - Q_{Di} - Q_{C\_MultiLat_k}, - V_i \sum_{j=1}^{nbus} V_j \left[G_{ij} \sin(\delta_i - \delta_j) - B_{ij} \cos(\delta_i - \delta_j) \right] = 0 \quad (75)$$

Case 2:
$$Q_{Gi} + Q_{S\_MultiLat_k} + \sum_{k=1}^{Nc} Q_{Ck} - Q_{Di} - Q_{C\_MultiLat_k}, - V_i \sum_{j=1}^{nbus} V_j \left[G_{ij} \sin(\delta_i - \delta_j) - B_{ij} \cos(\delta_i - \delta_j) \right] = 0 \quad (76)$$

Case 3:
$$Q_{Gi} + Q_{S\_MultiLat_k} - Q_{Di} - Q_{C\_MultiLat_k'} - V_i \sum_{j=1}^{nbus} V_j \left[\left(\frac{r_{ij}}{r_{ij}^2 + (x_{ij} - X_{TCSC})^2} \right) \sin(\delta_i - \delta_j) - \left(-\frac{x_{ij} - X_{TCSC}}{r_{ij}^2 + (x_{ij} - X_{TCSC})^2} \right) \cos(\delta_i - \delta_j) \right] = 0 \quad (77)$$

Case 4:
$$Q_{Gi} + Q_{S\_MultiLat_k} + \sum_{k=1}^{Ns} Q_{SMES_k} - Q_{Di} - Q_{C\_MultiLat_k'} - V_i \sum_{j=1}^{nbus} V_j \left[G_{ij} \sin(\delta_i - \delta_j) - B_{ij} \cos(\delta_i - \delta_j) \right] = 0 \quad (78)$$

Case 5:
$$Q_{Gi} + Q_{S\_MultiLat_k} + \sum_{k=1}^{Nc} Q_{C_k} + \sum_{k=1}^{Ns} Q_{SMES_k} - Q_{Di} - Q_{C\_MultiLat_k'} - V_i \sum_{j=1}^{nbus} V_j \left[G_{ij} \sin(\delta_i - \delta_j) - B_{ij} \cos(\delta_i - \delta_j) \right] = 0 \quad (79)$$

5.1.3.2 Inequality Constraints for Multilateral Transactions based RPD

The inequality constraints are given below as:

Generation Constraints: Generator bus voltages including market participants (V_G, $V_{P_{G\_MultiLat_K}}$), reactive power outputs including market participants (Q_G, $Q_{P_{G\_MultiLat_K}}$) are following their boundary limits as:

$$V_{Gi}^{\min} \le V_{Gi} \le V_{Gi}^{\max}, \qquad i = 1, \ldots, NG \quad (80)$$

$$V_{P_{G\_MultiLatk}}^{\min} \le V_{P_{G\_MultiLatk}} \le V_{P_{G\_MultiLatk}}^{\max}, \quad (81)$$

$$Q_{Gi}^{min} \le Q_{Gi} \le Q_{Gi}^{max}, \qquad i = 1, \ldots, NG \quad (82)$$

$$Q_{P_{G\_MultiLatk}}^{\min} \le Q_{P_{G\_MultiLatk}} \le Q_{P_{G\_MultiLatk}}^{\max}, \quad (83)$$

Transformer Constraints: Transformer tap settings (t) are maintained by their lower and upper limits as:

$$t_i^{min} \le t_i \le t_i^{max}, \qquad i = 1, \ldots, NT \quad (84)$$

where NT are the t connected lines.

Security Constraints: This includes the constraints of voltage at load buses (V_L) as:

$$V_{Li}^{min} \le V_{Li} \le V_{Li}^{max}, \qquad i = 1, \ldots, nbus \quad (85)$$

Capacitor var Constraints: Capacitor *var* compensators are having by their lower and upper limits as:

$$Q_{Ci}^{min} \le Q_{Ci} \le Q_{Ci}^{max}, \qquad i = 1,\dots, Nc \tag{86}$$

TCSC var Constraints: TCSC *var* compensators are limited by their lower and upper limits as:

$$x_{TCSCi}^{min} \le x_{TCSCi} \le x_{TCSCi}^{max}, \qquad i = 1,\dots, NTC \tag{87}$$

SMES var Constraint: SMES *var* compensators are operated by their lower and upper limits as:

$$Q_{SMESi}^{min} \le Q_{SMESi} \le Q_{SMESi}^{max}, \qquad i = 1,\dots, Ns \tag{88}$$

Now, from the above RPD formulations, it can be observed that that the proposed problems are nonlinear, non-differentiable, non-convex and combinatorial multi-constraints types in nature. Hence attempts were made to solve them by different meta-heuristics and advanced optimization techniques for various reasons.

Chapter 6

6 Solution Methodology for RPD: Soft-computing Techniques

Optimizations are the act of generating most sensible solution to a particular problem under certain circumstances. Therefore the optimization can be defined as the process of achieving the conditions that give maximum or minimum value of a function where the function itself expresses the desired benefit. Any critical problem in science and engineering may be formulated as optimization problem. There are several classical and advanced clever algorithms available to solve the optimization problems. The application of classical methods to solve discontinuous and non-differentiable problem are limited. The classical methods usually handle single variable functions, multivariable functions with no constraints and multivariable functions with both equality and inequality constraints. The equality constraint based functions are generally solved by Lagrange multiplier method and Kuhn-Tucker conditions which may be applied to address the inequality constraint based functions. The complexities in the practical problems lead to certain difficulty to solve by the classical methods [223]. Hence several advanced optimization methods are approached to explore the problem solutions. Some of them are Linear Programming, Integer Programming, Quadratic Programming, Nonlinear Programming, Stochastic Programming, Dynamic Programming, Combinatorial Optimization Programming, Infinite-dimensional Optimization Programming etc [223-24]. These techniques are computationally fast but easily converge at the local optimum point. In practical engineering field most of the optimization problems are local and global optima based. Hence the accurate solution is difficult to find by these methods. To solve this difficulty, soft-computing techniques in terms of computational intelligence, meta-heuristics and clever algorithms are extensively utilized in the field of optimization problem [225]. Soft-computing techniques are efficient, robust and fast tool for knowledge discovery.

The soft-computing techniques are represented as different grouping of paradigms which are divided into computational intelligence and probabilistic methods.

6.1 Advancement of Soft-computing Techniques with Different Aspects

The principle constituents of the soft-computing techniques are represented by natural computation, computational intelligence, meta-heuristics and clever algorithms. These different paradigms are introduced in the soft-computational domain due to their requirement at different stages.

6.1.1 Natural Computation

Natural computation is an interdisciplinary field concerned with the relationship between the biology to computation. In this study, biologically inspired computations are utilized to solve the engineering or science optimization problems using the events of natural world. Moreover, few computational procedures are considered to replicate the behaviour of biological entities. Some advanced application considering computations with biology are the molecular or DNA computing and quantum computing.

However, natural computations are very much suitable for a wide range of real time applications, but are bounded by some limitations for complex real world problem. In these situations, the computation intelligence based methods are preferred.

6.1.2 Computational Intelligence

The computational intelligence methods which are based on strategy and outcome to solve the complex real world problem are comprised of six primary fields namely: Physical Algorithms, Evolutionary Computation, Swarm Intelligence, Fuzzy Systems, Artificial Immune Systems and Artificial Neural Network.

- Physical Algorithm

These algorithms are inspired by the physical and social state of a system. The inspiring physical systems may belong to metallurgy, the interplay between culture and evolution, music etc. These include Simulated Annealing, Cultural Algorithm, Harmony Search which are generally stochastic optimisation algorithms with a combination of local and global search techniques. In this context to global optimisations, Swarm Intelligence techniques have also drawn major attentions to this optimisation domain.

- Swarm Intelligence

This prototype considers collective intelligence as behaviour emerging through the interfacing and assistance of a large numbers of lesser intelligent agents. The paradigm is divided into few dominant sub-prototypes such as Ant Colony Optimization, Particle Swarm Optimization and Cuckoo Search Algorithms etc. The Swarm Intelligence based methods also obey adaptive strategy in searching the optimization domain. In this regards, the Evolutionary Computation (EC) has played a very vital role to solve different constraints based optimisation problem.

- Evolutionary Computation

Evolutionary Computation (EC) is based on the principle of the neo-Darwinian theory of evolution by means of natural selection. This methodology utilizes an adaptive strategy to solve continuous and combinatorial problems. Evolutionary Computation includes popular evolutionary algorithms like Genetic Algorithm, Evolutionary Strategy, Genetic and Evolutionary Programming and Differential Evolution. Besides the EC, the Artificial Neural Networks (ANN) are also utilised to solve the optimisation problems successfully.

- Artificial Neural Network

This paradigm of computational intelligence is worked out on the basis of investigation of architectures and learning strategies inspired by the modelling of neurons in the human brain. Learning strategies are divided into supervised and unsupervised domains which critically absorbs environmental feedback in different ways. Neural network learning process is approached via adaptive learning methodology. The Function Approximation and the Pattern Recognitions are the typical applied domain of the artificial neural network. In addition to this, Fuzzy Intelligence methods are also frequently applied tool to solve multi-variable, multi-objective optimisation problems.

- Fuzzy Intelligence

This paradigm is typically operated by the fuzzy logic which is formulated on the basis of approximate truth, or degree of truth represented by several functional forms. Fuzzy logic followed by fuzzy systems is proposed by a reasoning strategy. The typical applied domains of the fuzzy intelligent systems are expert system and control system domain. In this direction, Artificial Immune Systems played a vital role in the field of optimisation problems.

- Artificial Immune Systems

The artificial immune systems are inspired to address by the structure and function of the acquired immune system of vertebrates. Alike the evolutionary computation and artificial neural network this paradigm follows the adaptive process with variable strategy in its applied domain. They are typically utilized for optimization and pattern recognition domains. Some common approaches in the domain are namely Clonal Selection, Negative Selection, Dendritic Cell Algorithm and Immune Network Algorithm.

In this regards, to achieve even better optimisation for solving a wide range of complex real world problem, these technologies are modified in terms of upper-level strategy *viz* the meta-heuristics.

6.1.3 Metaheuristics Methods

In the field of soft-computational methods, the meta-heuristics are one of popular approximate iteration based optimization techniques. It can provide an acceptable solution in a reasonable time while solving hard, complex, combinatorial problem in the real valued search space. Like the heuristics methods, meta-heuristics techniques are capable to solve an optimization problem with precision, quality and accuracy in favour of computational effort with relative few modifications by using upper-level strategy. Unlike the exact optimization algorithms the meta-heuristics do not define the optimality of the obtained solution or how close it is (solution) from the optimal ones. Some of the popular meta-heuristics are iterated Local Search, Tabu Search, Genetic Algorithm, Differential Evolutionary Technique, Ant Colony Optimization, Simulated Annealing etc. Few important characteristics of the meta-heuristics are given below:

- A strategic guidance to control search space to obtain near optimal solutions.

- The meta-heuristics algorithms cover a simple local search to typical machine learning methodology by exploring the search space.

- They are approximate and non-deterministic.

- They incorporate strategy to avoid to be trapped into the local search space.

However, the meta-heuristics are providing the global convergence efficiently. But the solution methodology needs to be revised covering the field of biologically inspired computation, computational intelligence and meta-heuristics to satisfy the present requirement of different real

world complex combinatorial problems. Therefore, as a collective set of the above three mentioned aspects are combined to formulate the clever algorithms.

6.1.4 Clever Algorithms

These sets of algorithms are the sub fields of artificial intelligence systems but not limited to the field of biologically inspired computation techniques, computational intelligence or the meta-heuristics methodologies. The clever algorithms may be considered as collective set of interesting and useful computational tools under a consistent and accessible manner. These algorithms are organized considering historic and newly developed method. The clever algorithms are formulated to provide a rich and interesting coverage to the field of biologically inspired computation, computational intelligence techniques and meta-heuristics such as Physical Algorithms, Swarm Intelligence Algorithms and Evolutionary Algorithms. Few frequently applied clever algorithms are Simulated Annealing, Harmony Search, Cultural Algorithm, Particle Swarm Optimization, Ant Colony System, Cuckoo Search Algorithm, Differential Evolution, Evolutionary Programming etc.

6.2 Choice of the Appropriate Soft-computing Techniques

By observing the total characteristics of the soft-computing techniques, it has been found that the biologically inspired natural computations are the successful techniques to solve the optimization problems of specified zone. Moreover, the computational intelligence techniques which are covering a wide range of applications are suitable for complex real world problems. In this direction, the upper level strategies based computational intelligence or as meta-heuristics are found to work satisfactorily to solve the hard, complex, combinatorial problems. Recent studies observed that a combination of biologically inspired natural computations, computation intelligence, and meta-heuristics methods as clever algorithms are proved to be successful to solve the proposed optimization problems. Hence, the choice of appropriate optimisation techniques to solve the proposed problem is a work worth of investigation.

Initially the fundamental RPD was considered to be solved in this work. This problem was further characterized by power transactions which induced a rapid dynamic voltage limit crossover leading to huge power losses *viz* network congestion. This situation required critical care in terms of appropriate clever algorithm based optimizations. Therefore, the first attempt was taken to solve the proposed problem by the Physical Algorithms. There are a number of such algorithms in this paradigms however the Simulated Annealing (SA) method was found to work efficiently as presented elsewhere [36, 37]. Although the proposed method obtained the global optimum results, it was limited by few

constraints. The major disadvantage of the fundamental SA method is that it has no population space therefore probabilities of generating new solutions are quite less here. In this context, Swarm Intelligence which has been frequently applied to solve the fundamental RPD, was applied to solve the proposed problem [17, 20, 40, 78, 125]. Amongst the different Swarm Intelligence methods, the Particle Swarm Optimization (PSO) has been found to optimize the proposed problem significantly but sometimes converged at local optima or has faced immature convergence problem. This issue was handled to some extent by incorporating constriction factor. However further modifications are required to achieve desired results for solving the restructured RPD. In this regards, one of the Evolutionary Computation technique namely Differential Evolution (DE) was considered to solve the proposed problem due to its proficient and sustainable applications in the power sector [23, 32, 34, 226-230] available now a days. However, the DE techniques often suffer from the poor convergence problem at global optima [231]. To overcome the drawbacks of the fundamental DE, Kaelo et.al., proposed two modifications namely Differential Evolution with Localisation around the Best Vectors (DELB) and Differential Evolution with Random Localization (DERL) elsewhere [232]. It has been generally found that DE as well as modified DE algorithm provided optimum results at higher population which therefore consumed higher computational time. To overcome this problem, one optimisations technique based on Swarm Intelligence but advanced Meta-heuristics namely Cuckoo Search Algorithm (CSA) has been applied to derive desired results with less computational time for a fixed parameters. A number of CSA based applications while solving different optimisation problems are available elsewhere [233-237]. These optimizations techniques implemented RPD issues are elaborated one by one.

6.3 Proposed Optimization Techniques and their Implementation to the RPD Problem

Initially, Simulated Annealing (SA) algorithm was considered to solve the fundamental RPD problem.

6.3.1 Simulated Annealing

Simulated Annealing (SA) which belongs to the family of meta-heuristics is inspired by the process of annealing in metallurgy. In 1983, SA was introduced by Kirkpatrick, Gelatt, and Vecchi [238]. The annealing property, there is a scope to improve the strength and durability of the material. Utilizing the said mechanism, SA technique is focused to locate the optimum configuration in the search space. Each pattern of a solution in the search space is represented by the different internal energy of the system. As the system is cooled, the acceptance criteria of samples are narrowed to converge towards the optimum solutions. Once the system has cooled, the arrangement will represent a sample at or

close to a global optimum. This probabilistic decision is fixed on the basis of the Metropolis-Hastings algorithm for a thermodynamic system [239].

6.3.1.1 Working Principles of Simulated Annealing (SA) Technique

The operating steps of the SA method are explained as:

Step 1: The initial variables (x) are generated with the help of probability distribution function;

$$x_j^{(0)} = x_j^{\min} + \sigma_j (x_j^{\max} - x_j^{\min}) \tag{89}$$

where $j \in [1,....D]$, D is the dimension of the system. The initial solution vector (x) is utilised to determine the fitness function $f(x)$.

Step 2: Initial temperature (T_i) and final temperature (T_f) is fixed depending upon requirement of cooling schedule. The proposed work considered the geometric cooling schedule to settle the temperature variation. This is realized as: $T = T_i$ and $T = \alpha * T$, where running temperature is denoted by T and the multiplying factor α is varied from 0.5 to 1. This way T will change to crystallize or freeze till the final temperature reaches.

Step 3: The annealing process is started by generating a new set of solution as given by (90) as

$$x_{n+1} = x_n + randn \tag{90}$$

Here, x_n is the initial solution, x_{n+1} is the new set of solution and '*randn'* is the random number generation command used in MATLAB 7.1. With x_{n+1} a new set of objective function $f(x_{(n+1)})$ is determined. Therefore the difference in energy level i.e., $\delta f = f(x_{(n+1)}) - f(x_n)$ has been calculated which further helped to proceed through the annealing schedule.

Step 4: Acceptance Criteria:

If the new solution is found better, it would replace the old one; otherwise a random number r will be generated. According to Metropolis criteria [240] new solution might be accepted while satisfying (91).

$$P = exp[-\delta f/kT] > r \tag{91}$$

where k is the Boltzmann's constant.

Step 5: The iterative loop would continue until the terminating condition is reached. Terminating condition might be set as reaching to the final temperature i.e., final iteration *N (= n: 1: N)* or reaching to the optimal value or even attaining the certain number of repetitive results.

After the detailed understanding of the SA technique, the SA was used and applied to the RPD problem.

6.3.1.2 SA Implemented RPD Problem

By following the above mentioned steps, SA based RPD was formulated as:

Step 1: Initially a solution vector (x) was generated by probability distribution function as given in (89). Here, the control variables of the proposed problem i.e., V_G, t and Q_C were expressed by solution vector (x) in (92) for which fitness function ($P_{LOSS}(x)$) was determined.

$$x^{(0)} = \left[V_{G_D}, t_D, Q_{C_D} \right] \tag{92}$$

Step 2: Cooling schedule was fixed after considering T_i, T_f and α.

Step 3: Then new solution vector was generated by (90) and subsequently new fitness function ($f(x_{n+1})$) was calculated with the new solution vector.

$$f(x_{n+1}) = P_{LOSS}(x^{(0)}) \tag{93}$$

Step 4: Further δf was calculated to proceed through the annealing schedule.

Step 5: If the new solution was found to be better it will be assigned, otherwise a random number r would be generated and Metropolis criteria by (91) will be verified.

Step 6: The operating cycle would be continued till the terminating condition has attained. This thesis fixed the terminating condition either to reaching to the final temperature point or to exceeding the pre-set maximum number of repetitive solutions.

Due to the limitations of single solution based approach of SA method, the Swarm Intelligence based meta-heuristics technique namely Particle Swarm Optimization (PSO) was applied to solve the RPD.

6.3.2 Particle Swarm Optimization (PSO)

PSO is a population based random number generation optimization technique. Eberhart and Kennedy [240, 241] introduced the concept of particle swarm optimization as a stochastic global optimization

method for continuous functions in 1995. Particle swarm optimization (PSO) belongs to the field of swarm intelligence and collective intelligence which is developed by the inspiration of the social foraging behaviour of some animals such as flocking of birds and the schooling of fish. The objective of the algorithm is to have all the particles find the optima in a multi-dimensional space. This is accomplished by assigning initial random positions and velocities to all particles in the space. The algorithm is simulated by advancing the position of each particle in turn based on its velocity as local optima followed by best position and velocity in the problem space as global optima to a particle. The objective function is updated by comparing each position update till the iteration counter runs. In this regards, the conventional PSO method was found frequently suffering from the problem of premature convergence. To prevent this problem, inclusion of the constriction factor by Clerc [242] has been utilised here to achieve better result.

6.3.2.1 Working Principle for PSO

The operating strategies of the constriction factor based PSO technique are demonstrated bellow:

Step 1: Initially population space of *n* number of particles with *D* dimension was considered. Here the initial velocity (V_i^k) and position (X_i^k) of i^{th} particle at the k^{th} iteration (initially iteration counter is set to be zero) were generated by equation (94), (95). These are developed using random probability distribution function given by equation (89).

$$V_i^k = (v_{i1}^k, v_{i2}^k, \dots, v_{iD}^k) \tag{94}$$

$$X_i^k = (x_{i1}^k, x_{i2}^k, \dots, x_{iD}^k) \tag{95}$$

With the initialized velocity and positions of each particle, the fitness function was solved. For *n* number of particles *n* numbered local best value was obtained i.e., (*pbest*, $P_{best_i}^k$). Amongst them best solution providing particle was known as global best position (*gbest*, g_{best}^k).

Step 2: In the second step particles were changing their velocity and position based on their cognitive and social components. These are given by (96) and (97).

$$V_i^{k+1} = \phi * \left((w \times V_i^k + C_1 \times rand_1() \times (P_{best_i}^k - x_i^k) + C_2 \times rand_2() \times (g_{best}^k - x_i^k) \right) \tag{96}$$

$$X_i^{k+1} = x_i^k + V_i^{k+1} \tag{97}$$

The updated velocity (V_i^{k+1}) as shown in (96) was divided into three parts. Here the first part represented the inertia weight based previous velocity which provided the required momentum to the particles. The second part was regarded as cognitive component which encouraged the particles to move towards their own best positions found so far. The third component was referred to as social component which always dragged the particles toward the global best position found so far. Here, the updated position is X_i^{k+1}, w was inertia weight parameter which kept a balance between global and local exploration, $rand_1$ and $rand_2$ were separately generated uniformly distributed random numbers in the range [0, 1]. The acceleration constant were denoted by c_1 and c_2 and φ was represented as the constriction factor which was a function of c_1 and c_2. Moreover, w and φ were given by eqn. (98) and (99).

$$w = w_{max} - \frac{w_{max} - w_{min}}{iter_{max}} \times iter_i \tag{98}$$

$$\varphi = \frac{2}{\left|2 - c - \sqrt{c^2 - 4c}\right|} \tag{99}$$

where w_{max} and w_{min} were the maximum and minimum value of w respectively, *iter* was the number of iteration, $iter_{max}$ was the maximum number of iteration, $c = c_1 + c_2$ and $c > 4$.

Step 3: With the updated velocity and position, fitness function was calculated. In each iteration, the obtained fitness value was compared with the previous result. If a particle found a better position than it obtained before, the *pbest* would be replaced by the position. The best *pbest* position amongst all the particles was termed as the *gbest* which would replace the previous position. This way PSO ran until the terminating condition was reached. Terminating condition may be taken as reaching to the maximum iteration number ($iter_{max}$) or obtaining the prefixed value.

Once the operational strategy of the PSO technique is understood, its implementation to the proposed RPD was made and analysed.

6.3.2.2 PSO Implementation to RPD

In this section, PSO implementation to solve the RPD problem is briefly explained.

Step 1: Initially the control variables of the RPD problem such as V_G, t and Q_C were randomly generated within its maximum and minimum limit as shown by solution vector (x) in (100). Now x is

dependent on number of particle and their initialized velocity and position. Here the velocity and positions of i^{th} particle at the k^{th} iteration is shown by (101-102).

$$x^{(0)} = \left[V_{G_D}, t_D, Q_{C_D}\right] \tag{100}$$

$$V_i^{k=0} = (V_{Gi_1}^{k=0}, tap_{i_1}^{k=0}, \ldots, Q_{Ci_1}^{k=0}) \tag{101}$$

$$X_i^{k=0} = (V_{Gi_1}^{k=0}, tap_{i_1}^{k=0}, \ldots, Q_{Ci_1}^{k=0}) \tag{102}$$

Using the initialized velocity and positions, fitness function ($P_{LOSS}(x)$) was determined. Moreover, a number of local best solutions by the whole population space were termed as *pbest* and amongst them the best solution providing vector was called the *gbest* solution.

Step 2: Iteration counter was initialized to operate till maximum iteration number ($iter_{max}$) was reached. At each iteration the particles were made to change their position as well as velocity as shown in (96) - (97). With the updated velocity and position new fitness values were obtained.

Step 3: After comparing the new fitness value with the previous one, it would substitute the old fitness function only if the new one was found to be improved compared to previous one. This would also revised the *pbest* and *gbest* with updated value. This way PSO technique would carry on till the terminating condition reached.

Step 4: At the terminating point, the final solution with respective *gbest*, was declared as final optimum value and corresponding vector was called solution vector.

Although PSO has several merits over SA technique, but the poor convergence problem remained unattempted in the method. In this context, one of the well-known evolutionary algorithm namely differential evolutions (DE) has been considered to solve the proposed problem.

6.3.3 Differential Evolution (DE) Technique

Among many meta-heuristic techniques applicable to resolve non-linear, non-differentiable, non-convex, multi-objective, multi-constraint function, differential evolution (DE) showed very commendable result. The differential evolution (DE) technique was first proposed by Storn and Price in a technical report [243] considering continuous function optimization problems. The DE is a stochastic direct search and global optimization algorithm which is comprised of four steps; Initialization, mutation, crossover, selection. Initially a set of vectors in terms of target vector is

evolved by using the uniform probability distribution function and then stored in a population space. In the mutation step the mutant vector is framed as the summation of the base vector and weighted difference of the two randomly chosen vectors from the entire population pool. In the crossover stage new offspring or trial vector is generated from target vector and mutant vector depending upon the crossover factor. Finally best fitness value providing vector among the target and trial vector is selected as parent vector for the next generation. The loop continues this way till the terminating condition is met.

Though DE proficiently solves several optimisation problems it frequently suffers from the problem of slow convergence at the global minima region. As remedy to this problem, Kaelo et.al., proposed few modifications to the fundamental DE method [232]. This work showed two approaches of modified differential evolution (MDE). They are new differential evolution algorithm with localizations around the best vector (DELB) and new differential evolution algorithm with random localizations (DERL) which are considered in this work. Before going to the simulation of these methods, the working principles of these MDEs are detailed out here.

6.3.3.1 A New Differential Evolution Algorithm with Localizations around the Best Vector (DELB)

Alike the fundamental DE algorithm, DELB method comprised of basic four steps like initialization, mutation, crossover and selection. The encouraging features of the DELB technique was its extensive searching procedure for better solution compared to generated trial vector or target vector solution. At the selection stage of the DELB technique a fine tuning was introduced by generating two more hybrid vector sets and a comparative review of their corresponding fitness value. The hybrid vectors were formulated by combining trial vector and target vector set. However, this new modification to the fundamental DE technique might slow down the processor speed though the probability of obtaining good result increased. At the selection of the DELB method searching process got emphasized which caused its name as localization around the best vector or DELB algorithm.

6.3.3.1.1 The Working Principle for DELB

The operating strategy of the DELB method was designed in the following steps:

Step 1: Initialization: Alike the other optimisation techniques including DE, a set of target vector (x_{ij}) was generated by the uniform probability distribution function as shown in (89).

Step 2: Mutation: Alike the DE, here in the mutation step three perturbation vectors were randomly chosen from the population pool. With these randomly chosen vectors, mutant vector (v_{ij}) was formed which is given by the equation (103).

$$v_{i,j}(t+1) = x_{r1,j}(t) + fm(x_{r2,j}(t) - x_{r3,j}(t)) \tag{103}$$

where r_1, r_2, r_3 were the random numbers and $r_1 \neq r_2 \neq r_3$, $i \in [1,....N_p]$, $j \in [1,....D]$, N_p and D was the number of population and dimension of the required target vector respectively, Here f_m was the scaling factor or mutation factor ($f_m \in (0,1)$) and t was the generation counter.

Step 3: Crossover: Alike the fundamental DE, in the crossover stage new offspring or trial vectors (y_{ij}) which were produced depending upon the crossover factor ($C_R \in \text{rand}$), is given here as:

$$y_{i,j}(t) = \begin{cases} v_{i,j}(t) \; if \; rand(0,1) < C_R \\ x_{i,j}(t) \; \text{else} \end{cases} \tag{104}$$

Step 4: Selection: This was the most fundamental part of the DELB technique which made it superior to DE. Here, tuned selection was conducted where instead of choosing the final solution between trial vector and target vector two more hybrid vector sets were generated. Fitness values of the new vectors were compared on the basis of few conditions that are discussed in detail in the following steps (step-4.(i) to step-4.(iv)). For every generation better fitness value providing vector will be considered as the fit solution. The terminating condition was fixed as reaching to final generation (Gen_{max}) and corresponding value was regarded as final solution vector.

- Tuned Selection are expressed as

Step 4.(i): Fitness value due to trial and mutant vector was calculated. If mutant vector provided better result it would be considered as final solution at the specified generation and step-4.(i) would be repeated for the next generation. Otherwise if $R^i < w$ and if the fitness value of the target vector (x) was greater than the fitness value of trial vector (y), a new set of vector r_i was formulated. It is given as:

$$r_i = x_b - (y_i - x_b) \tag{105}$$

where R^i is a random number between 0 to 1, w is a constant = 0.5, x_b is the current best target vector.

Step 4.(ii): In this step, utilizing both r_i set and y_i set fitness value was obtained. If r_i set gave better result, v_i would be replaced by r_i hybrid vector set and process would be revisited from step 4.(i) else step 4.(iii) would be continued where a new set of vector c_i would be framed and it is expressed here as:

$$c_i = v_b + 0.5(y_i - v_b) \tag{106}$$

where v_b is the mutant vector set.

Step 4.(iii): In this step, fitness function was determined by putting c_i set and the result was compared with fitness value by the trial vector set. If c_i set provided better result, c_i would replace v_i and process would be again started from step 4(i) else step 4(iv) would be carried on.

Step 4.(iv): Here v_i would be replaced by y_i and process would be revisited from step 4.(i) for the next generation. Thus final v_i would be declared as fitness vector for the said problem. Until the final generation is achieved the searching process would be continued.

Once the operational strategy for the DELB technique is described clearly, it was implemented to the RPD scenarios.

6.3.3.1.2 DELB Implementation to the RPD Problem

Step 1: The Target vector ($x_i^{(0)}$) comprising all the control variables are given by (107).

$$x_i^{(0)} = \left[V_{g_1}^i, ..., V_{g_d}^i, t_1^i, ..., t_d^i, Q_{C1}^i, ..., Q_{Cd}^i \right]_{i=N_p} \tag{107}$$

Step 2: As described in (104), the DELB based mutant vector was shown in (108).

$$V_i^{(0)} = \begin{bmatrix} V_{g_{r3}} \\ t_{r3} \\ Q_{C_{r3}} \end{bmatrix} + f_m \left(\begin{bmatrix} V_{g_{r1}} \\ t_{r1} \\ Q_{C_{r1}} \end{bmatrix} - \begin{bmatrix} V_{g_{r2}} \\ t_{r2} \\ Q_{C_{r2}} \end{bmatrix} \right) \tag{108}$$

Step 3: In this step trial vector (y_i) was determined by (100) as demonstrated earlier.

Step 4: In the selection step, to get best vector around the local position, tuned-selection was composed as stated earlier. While performing this, hybrid vectors (r_i) and (c_i) were generated by (109-110).

$$r_i = \begin{bmatrix} V_{g\,best_i} \\ t_{best_i} \\ Q_{C\,best_i} \end{bmatrix} - \left(y \begin{bmatrix} V_{g_i} \\ t_i \\ Q_{C_i} \end{bmatrix} - \begin{bmatrix} V_{g\,best_i} \\ t_{best_i} \\ Q_{C\,best_i} \end{bmatrix} \right) \tag{109}$$

$$c_i = V \begin{bmatrix} V_{g_i} \\ t_i \\ Q_{C_i} \end{bmatrix} - 0.5 * \left(y \begin{bmatrix} V_{g_i} \\ t_i \\ Q_{C_i} \end{bmatrix} - V \begin{bmatrix} V_{g_i} \\ t_i \\ Q_{C_i} \end{bmatrix} \right) \tag{110}$$

Final solution would be received by following the steps of the tuned-selection as stated earlier (Step 4(iii)-(iv). The DELB based solutions would terminate while reaching to the maximum generation number (Gen_{max}) and the obtained solution at that point was considered as final optimum value.

Although DELB technique searched the population space extensively and obtained optimal solutions, it consumed huge computational time. Therefore, this technique has limited applications such as for small network based applications. Then another modified differential evolutionary algorithm as proposed in [233] namely differential evolutions with random localizations (DERL) was attempted to solve the proposed problem.

6.3.3.2 A New Differential Evolution Algorithm with Random Localizations (DERL) Technique

Alike the DELB method, the DERL technique has been formulated by incorporating few improvements or modifications in the fundamental DE technique. DERL technique comprised of five steps i.e. initialization, tournament best value selection, mutation, crossover and selection which are described as:

6.3.3.2.1 The Working Principle for DERL

Step 1: Initialization: In this step, a set of target vector (x_{ij}) was generated using the uniform probability distribution function as given by (89).

Step 2: Tournament best value selection: In the second step fitness function was determined for each vector of the entire population pool. Among them the best fitness value providing vector was

considered as tournament best vector (x_{tb}) and this was finally considered as base vector for the mutation process. This approach made the DERL technique faster as well as proficient among the other meta-heuristics.

Step 3: Mutation: The mutant vector (v_{ij}) was formulated as the summation of the base vector and weighted difference of the two randomly chosen vectors from the entire population pool alike the fundamental DE. In the proposed DERL method, f_m was proposed by random number generation ($f_m \in \text{rand}(0,1)$). The mutant vector presented by (111) where $x_{ij}(r_2)$ and $x_{ij}(r_3)$ were the randomly chosen vectors and r_2, r_3 were the unequal random numbers.

$$v_{i,j}(t+1) = x_{tb}(t) + f_m\left(x_{r2,j}(t) - x_{r3,j}(t)\right) \tag{111}$$

Step 4- Crossover: In this step trial vector or offspring was derived from either target vector or mutant vector depending upon the value of crossover factor ($C_R \in \text{rand}$). Trial Vector (y_{ij}) formulation was expressed by (112).

$$y_{i,j}(t) = \begin{cases} v_{i,j}(t) \; if \; rand(0,1) < C_R \\ x_{i,j}(t) \; \text{else} \end{cases} \tag{112}$$

Step 5- Selection: In this final step DERL provided the efficient offspring among the target vector and the trial vector depending upon the fitness value. The better solution providing vector amongst the two was chosen as fit vector. It was passed to the next generation as parent vector. This way the DERL technique worked until the terminating condition was reached. The terminating condition may be settled as setting of a pre-optimum value or attaining the maximum generation number. At the terminating point, obtained solution (offspring) was declared as the final solution.

Once the working steps of the DERL technique was fixed, it was implemented to solve the proposed RPD.

6.3.3.2.2 DERL Implementation to the RPD Problem

Step 1: A set of target vector (x_{ij}) was initialized using (89) by the proposed DERL technique. Here, a number of control variables such as V_G, t, Q_C , x_{TCSC}, Q_{SMES} in the form of target vectors were represented by (113) as:

$$x_i^{(0)} = \left[V_{g_1}^i, ..., V_{g_d}^i, t_1^i, ..., t_d^i, Q_{C_1}^i, ..., Q_{C_d}^i, x_{TCSC_1}^i, ..., x_{TCSC_d}^i, Q_{SMES_1}^i, ..., Q_{SMES_d}^i \right]_{i=N_p} \tag{113}$$

where *d* was the dimension of the vector and N_P was the population size.

Step 2: In this step, the tournament best vector ($x^t_{tbest_i}$) was determined. Here, the P_{LOSS} was the proposed fitness function, which was solved here by the Newton Raphson method [224].

$$F(x^t_{tbest_i}) = min(P_{LOSS}) \tag{114}$$

Step 3: After determining $x^t_{tbest_i}$, the mutant vector (v_i) was generated by adding the base vector $x^t_{tbest_i}$ and multiplication of mutant factor (f_m) and the weighted difference of the two randomly chosen vectors from the entire population pool. According to the DERL method, f_m was selected by random number generation ($f_m \in \text{rand}(0,1)$). The mutant vector was given by equation (115).

$$V_i^{(0)} = \begin{bmatrix} V_{g\,tbest_i} \\ t_{tbest_i} \\ Q_{C\,tbest_i} \\ x_{TCSC\,tbest_i} \\ Q_{SMES\,tbest_i} \end{bmatrix} + f_m \left(\begin{bmatrix} V_{g_{r1}} \\ t_{r1} \\ Q_{C_{r1}} \\ x_{TCSC_{r1}} \\ Q_{SMES_{r1}} \end{bmatrix} - \begin{bmatrix} V_{g_{r2}} \\ t_{r2} \\ Q_{C_{r2}} \\ x_{TCSC_{r2}} \\ Q_{SMES_{r2}} \end{bmatrix} \right) \tag{115}$$

Step 4: In this step trial vectors or off springs were produced by comparing either the target vector or mutant vector depending upon the value of crossover factor ($C_R \in \text{rand}$). Trial Vector (y_i) was demonstrated by equation (116).

$$y_i(t) = \begin{cases} v_i(t) \; if \;\; rand(0,1) < C_R \\ \qquad x_i(t) \; \text{else} \end{cases} \tag{116}$$

Step 5: In the selection step, both the target vectors, trial vectors based fitness functions (power loss) were determined by equation (117-118) and compared to obtain better offspring and fitness value.

$$F(x_i^{t+1}) = P_{Loss}(x_i^{t+1}) \;\; . \tag{117}$$

$$F(y_i^{t+1}) = P_{Loss}(y_i^{t+1}) \tag{118}$$

After comparisons, if the target vector based solution was found to be better, it was considered and forwarded to the next generation as parent vector otherwise the trial vector based solution was accepted for the next generation. This way DERL based operating cycle was continued hitherto until

the terminating condition was reached. Here, the terminating condition was set as to reach at the maximum generation number (Gen_{max}). At the terminating point, the obtained solution was declared as final optimum value and corresponding vector was called solution vector.

However, although DERL technique solved the proposed problem with different case studies satisfactorily it required higher population sizes to provide optimum results. In this context, a Swarm Intelligence based advanced Meta-heuristics technique namely Cuckoo Search Algorithm (CSA) was implemented to solve the proposed problem for different scenarios.

6.3.4 Cuckoo Search Algorithm (CSA)

Cuckoo search algorithm belongs to the family of Computational Intelligence and Meta-heuristics. Being inspired by the obligate brood parasitism of some cuckoo species, Yang and Deb proposed an advanced optimization technique namely, cuckoo search algorithm (CSA) in 2009 [244]. This algorithm utilises the obligate brood parasitism of some cuckoo species while laying their eggs in the nests of other host birds. Some host birds can throw these alien eggs away or simply abandon its nest and build a new nest elsewhere if it discovers the eggs are not their own.

With these considerations, the algorithm is formulated on the basis of three idealized rules:

- Each cuckoo will lay one egg at a time, and keep its egg in a randomly chosen nest.
- High quality of eggs is addressed as the best nests that will carry over to the next generation.
- The numbers of available host nests are constant. A probability factor is to be considered based on that the host bird will check the egg laid by a cuckoo. Checked solutions will be discarded from further calculations.

6.3.4.1 Working Process of CSA

The operating strategies of the CSA technique are illustrated bellow:

Step 1: Parameter Initialization: In this step, different parameters of the CSA algorithm like the number of host nests (n), iteration counter ($iter$), probability (p_a) for the worst nests were initialized. The initialized vectors of the proposed problem $x_i^{(0)}$ were generated initialized randomly by (89). With this, the fitness function was derived for which x_{best_i} and G_{best} were obtained. The nest corresponding to best fitness value was termed as G_{best}.

Step 2: Generation of Cuckoo: In the second step, new cuckoo was generated by Lévy flight [244]. Generally at each generation it was assumed that one egg will be laid by a cuckoo. The new vectors x_i^{new} are shown by (119).

$$x_i^{(t+1)} = x_i^{(t)} + \alpha \oplus Le'vy(\lambda) \tag{119}$$

where α>0 is the revised step size. $Le'vy(\lambda)$ was expressed by (120) where *rand* is a normally distributed stochastic variable

$$Le'vy(\lambda) = rand \times \Delta x_i^{new} \tag{120}$$

Now, Δx_i^{new} was calculated using (121).

$$\Delta x_i^{new} = v \times \frac{sigma_1(\beta)}{sigma_2(\beta)} \times (\mathrm{x}_{best_i} - Gbest) \tag{121}$$

where, $v = \dfrac{rand_1}{|rand_2|^{\left(1/\beta\right)}}$ and $rand_1$, $rand_2$ are normally distributed stochastic variables. The standard deviation functions of the variables are $sigma_1(\beta)$ and $sigma_2(\beta)$ which were determined using (122) and (123).

$$sigma_1(\beta) = \left[\Gamma(1+\beta) \times \sin\left(\frac{\pi\beta}{2}\right) / \Gamma\left(\frac{(1+\beta)}{2}\right) \times \beta \times 2^{\left(\frac{\beta-1}{2}\right)} \right]^{1/\beta} \tag{122}$$

$$sigma_2(\beta) = 1 \tag{123}$$

where β is the distribution factor having a value of $0.3 \le \beta \le 1.99$ and $\Gamma(\cdot)$ is the distribution function.

With the new vectors, the fitness function (*f*) was determined.

Step 3: Replacement: In this step, a nest was selected randomly from the initialized set. To achieve better solution a comparison took place between the fitness values of the randomly selected nest and the newly generated cuckoo egg solution. The better solution was accepted for the next iteration.

Step 4: Generation of New Nest: The worse nests were abandoned by the host bird based on the probability (p_a) for which new solution (x_d^{dis}) were generated by (124).

$$x_d^{dis} = x_{best_d} + K \times \Delta x_d^{dis} \tag{124}$$

Now, K was the revised coefficient set which could be obtained by (125).

$$K = \begin{cases} 1 & if\ rand < p_a \\ 0 & otherwise \end{cases} \tag{125}$$

Here, the Δx_d^{dis} was obtained using (126).

$$\Delta x_d^{dis} = rand \times \left[randp_1(x_{best_d}) - randp_2(x_{best_d}) \right] \tag{126}$$

where $randp_1(x_{best_d})$ and $randp_2(x_{best_d})$ were the random perturbations for positions of the nests in x_{best_d} . With the discovered vectors, the fitness function (power loss) was re-determined for the three cases and selected depending upon the fitness value.

Step 5: Termination: The operating cycles of the CSA would be continued until the stopping criterion has been reached by fulfilling the upper and lower constraint limit. In this work, the terminating condition was set as reaching to the maximum iteration number.

Once the working strategies of CSA technique were fixed, it could be implemented to solve the proposed RPD problem.

6.3.4.2 CSA Implementation to the RPD Problem

In this section, CSA technique was implemented to formulate different RPD. The generalised steps were given here:

Step 1: In the initialisation step, the initial vector (x_0) which was generated by the uniform probability distribution function by (89), was given by (127)

$$x_i^{(0)} = \left[V_{g_1}^i, ..., V_{g_d}^i, t_1^i, ..., t_d^i, Q_{C_1}^i, ..., Q_{C_d}^i, Q_{SC_1}^i, ..., Q_{SC_d}^i, Q_{SMES_1}^i, ..., Q_{SMES_d}^i \right]_{i=n} \tag{127}$$

As discussed, with the initial vector, the fitness function was determined generating x_{best_i} and G_{best}.

Step 2: Generation of Cuckoo: In the second step cuckoo was generated by Lévy flight [245]. Generally at each generation it was assumed that one egg will be laid by a cuckoo. The new vectors x_i^{new} were shown by (128).

$$x_i^{new} = \begin{bmatrix} V_{g\ bset_i} + \alpha \oplus Le'vy(\lambda) \\ t_{best_i} + \alpha \oplus Le'vy(\lambda) \\ Q_{C\ best_i} + \alpha \oplus Le'vy(\lambda) \\ Q_{SC\ best_i} + \alpha \oplus Le'vy(\lambda) \\ Q_{SMES\ best_i} + \alpha \oplus Le'vy(\lambda) \end{bmatrix} \tag{128}$$

While solving this, (120-123) were further utilised. With the new vector, the fitness function (F) was determined for the different cases. Here, the fitness function was given (129).

$$F(iter) = P_{Loss}(x_i^{new}) \tag{129}$$

Step 3: Replacement: In this step, a nest was selected randomly from the initialized set. To achieve better solution a comparison was made between the fitness values of the randomly selected nest and the newly generated cuckoo egg solution. The better solution was accepted for the next iteration.

Step 4: Generation of New Nest: The worse nests were abandoned by the host bird based on the probability (p_a) for which new solutions were obtained by equations (124 - 126). With the discovered vectors, the fitness function (power loss) was re-determined for the three cases and selected depending upon the fitness value.

Step 5: Termination: Until the stopping criterion was fulfilled, the cycles of the CSA would be continued to receive the optimum solution satisfied by upper and lower constraint limit. In this work the terminating condition was set as reaching to the maximum iteration number.

Once, the different meta-heuristics techniques based proposed problem formulations are developed, the results were simulated and analysed to justify the significance of the work in terms of technical and economical view point of restructured RPD.

Chapter 7

7 Simulation Result & Discussion

Here, the RPD formulation considering different cases are accomplished by utilizing MATLAB 7.1 programming platform. In this thesis, IEEE 14, 30, 57 and 118 bus-systems are considered as test cases. In addition to this, one real Indian scenario of 62 bus system has been considered to analyze the RPD issues.

7.1 Different Test Systems

The test systems are briefly described as;

7.1.1 Test System 1

Initially, the RPD problem is solved considering IEEE 14-bus network [245] as test system 1. This network is comprising of fourteen number of buses amongst them bus 1 is considered as slack bus. In this test system the 2nd, 3rd, 6th and 8th number buses are generator buses and remaining nine are load buses.

7.1.2 Test System 2

The IEEE 30-bus network [245] is considered here as test system 2 to solve the proposed RPD. This system is consisting of thirty numbers of buses amongst them bus 1 is considered as slack bus. In the same system 2nd, 5th, 8th, 11th and 13th number buses are represented as generator buses where voltages are to be control (V_{g2}, V_{g5}, V_{g8}, V_{g11} and V_{g13}). The remaining twenty four buses are the load buses. In the network four tap changing transformers are placed at the lines (11th, 12th, 15th and 36th). Based on the requirement of *var* compensation, few case studies are considered. In first case 10th and 24th buses are chosen for shunt compensation (Q_{C10}, Q_{C24}) [32]. In the second case 6th, 17th, 18th and 27th buses are preferred for shunt compensation (Q_{C6}, Q_{C17}, Q_{C17}, *and* Q_{C27}) [40]. In the third case nine buses i.e., (Q_{C10}, $Q_{C12,}$ Q_{C15}, $Q_{C17,}$ Q_{C20}, Q_{C21}, Q_{C23}, $Q_{C24,}$ Q_{C20}) are selected for shunt compensation [33]. Moreover, a DG unit of 35MW is allocated in the 11th bus of the IEEE 30-bus system while considering multilateral power transactions in a deregulated power scenario [246].

7.1.3 Test System 3

A medium network i.e., IEEE 57-bus network [245] is considered as test system 3. This network is comprising of fifty-seven number of buses amongst them bus 1 is assigned as slack bus. In the IEEE 57-bus network 2^{nd}, 3^{rd}, 6^{th}, 8^{th}, 9^{th} and 12^{th} number buses are considered as the generator buses for which voltages are controlled (V_{g2}, V_{g3}, V_{g6}, $V_{g8,}$ V_{g9} and V_{g12}). In the network fifteen tap changing transformers are placed at several lines. Generally, 18^{th}, 25^{th} and 53^{rd} buses are chosen for shunt capacitor placement (Q_{C18}, Q_{C25}, and Q_{C53}) for *var* compensation. Moreover, as an alternative and sustainable source of reactive power, SMES device is integrated in the IEEE 57-bus system. The locations of SMES devices are optimally chosen using meta-heuristics technique. Further, to achieve an economic as well as sustainable solution, a combination of capacitor and SMES are integrated in the network while considering the restructured RPD.

7.1.4 Test System 4

In this direction, a larger network such as IEEE 118-bus system network [245] is considered as test system 4. This network is being comprised by hundred and eighteen numbers of buses among them 69^{th} bus is considered as slack bus. In this network total fifty four numbers of generator buses are present for which the bus voltages are to be controlled. Remaining sixty three buses are load buses among them twelve buses are frequently selected for shunt capacitor placement to minimize active power loss. Apart from this, nine tap changing transformers are assigned in various positions of the network for the RPD problem solving issue. Alike the IEEE 57-bus system, a SMES based case study is considered here to solve the RPD issue. Further, the synchronous condensers, SMES and their suitable combinations with capacitors are considered to solve the RPD involving power transactions in the backdrop of deregulated power scenario.

7.1.5 Test System 5

Finally, an Indian power network of 62-bus system [98] is further considered here as test system 5 to solve the RPD considering an inter-regional power grid. This network has eighteen generator buses, one slack bus and forty three load buses. Additionally eleven tap changing transformers are placed in the network.

Now, considering these test systems the simulation studies in terms of the proposed RPD is developed.

7.2 Simulation Studies

In the thesis, RPD problem formulation in different scenarios are considered.

- Initially, the fundamental RPD issue including the voltage security and reactive power generation minimisation is considered to be solved as case study 1. The proposed problems are handled by controlling generator bus voltages, transformer tap settings and shunt capacitor placement. To obtain improved response, the fundamental RPD problem is further revisited and solved by integrating different advance *var* compensating devices such as FACTs, SMES into it.

- In the next phase of study, the restructured RPD problem with bilateral power transactions is solved as case study 2. It has been noticed that during the power transactions the security constraints of the network are fluctuating near the boundary value which caused dynamic voltage limit crossover. Therefore, the proposed problem is analyzed here by incorporating different *var* compensators. These *var* compensators are made of capacitors, synchronous condensers (SC), FACTs, SMES and some of their combinations with capacitors. Moreover, the economics of the *var* compensations are determined. With this, the improved global welfare is obtained. To derive the Pareto efficient power transactions for maximum economic efficiency, planned bidding are implemented in this phase.

- Further, the restructured RPD problem is solved by considering multilateral power transactions. Besides the power loss optimizations, the studies also solved the dynamic voltage limit crossover with power mismatches during the power transactions. As *var* compensators, capacitors, TCSC, SMES and hybrid capacitor-SMES are comparatively utilized here. In addition to the economics of the advanced *var* compensations and global welfare improvement, the impact of spot pricing on global welfare is also considered. Moreover, the planned bidding is also accomplished here to derive Pareto efficient power transactions for maximum global welfare. Suitable solution methodologies of meta-heuristics techniques are applied to obtain optimal size and locations of the *var* compensators.

7.3 Solution Techniques

In this work, four meta-heuristics techniques from the different paradigm of clever algorithms are applied to solve the proposed problem. They are Simulated Annealing (SA) method, Constriction-factor based Particle Swarm Optimization (Cf-PSO) technique, Differential Evolution Localisation around the Best Vectors (DELB), Differential Evolution with Random Localization (DERL) and Cuckoo Search Algorithm (CSA). Based on the technical advantages over other algorithms, two amongst them likely the DERL and CSA are further considered to solve the restructured RPD issues.

Once the meta-heuristics based problem formulations are developed, simulations are made to obtain results.

7.4 Simulation Result

In this section different simulation studies are analysed for complete understanding starting from the fundamental situation.

7.4.1 Fundamental Reactive Power Dispatch and Voltage Security Analysis

In this work, the fundamental RPD problem was solved by controlling different control variables such as V_g, T and Q_c. In few cases, Q_{SMES} was also used as control variable. The operating ranges of the control variables were given in Appendix Table A.1, Table A.2 and Appendix B.2. Here, the proposed problem were solved by SA, PSO, DELB, DERL and CSA technique respectively.

7.4.1.1 SA based RPD Problem

Initially SA technique was applied to solve the RPD problem for IEEE 14-bus system.

7.4.1.1.1 Result Analysis for Test System 1

In this work, the different optimization parameters of SA algorithm were set as: T_i = 1, T_f = 10^{-20}, α = 0.9 and k = 1 after 100 trial runs of the proposed fitness function for the IEEE 14-bus system. By controlling the V_g, t and Q_c, the minimum power loss (P_{LOSS}) was derived as 13.0722 MW. Amongst the 80 trial runs, the average and the worst results in the form of power loss (P_{LOSS}) were obtained as 13.1309 MW and 13.1702 MW respectively. Moreover, according to the SA based optimization as shown in Figure 1, the best P_{LOSS} was found to converge at the 105th iteration with 14.33 sec where the iteration counter stopped at 250 determined by the set conditions of termination. Here, the average loss was obtained by determining the average P_{LOSS} for the eighty sets of data as shown in Figure 2. The curve was considered to have closest findings near by the average P_{LOSS} value. However, according to Figure 2 the average and the worst P_{LOSS} were found to converge nearly at 150th iterations with 26.78 sec where the iteration counter continued till 400 as set in the algorithm. From the figures, it could be observed that, there were few local minima points where the optimal solution might be struck but the efficient strategy of the SA method finally helped to converge the final solution at the global optima. Here, all the control variables were found within the stable operating margin for all the three cases. The final P_{LOSS} and % P_{LOSS} were given in Table 1 where a comparative study was shown

to justify the betterment of SA for the proposed work. The comparative study showed reduction of maximum % P_{LOSS} to 3.097 and a minimum value of 1.260 from the other methods.

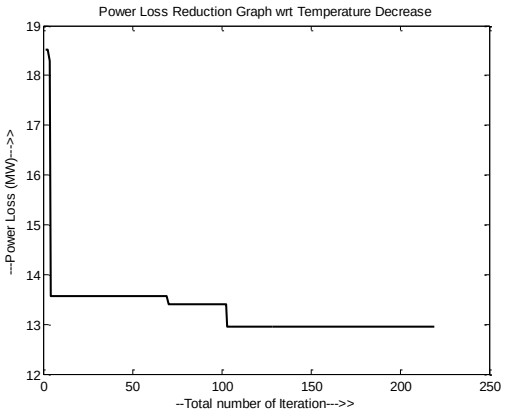

Figure 1. Simulated Annealing (SA) based power loss minimization solution for IEEE-14 bus network (best case)

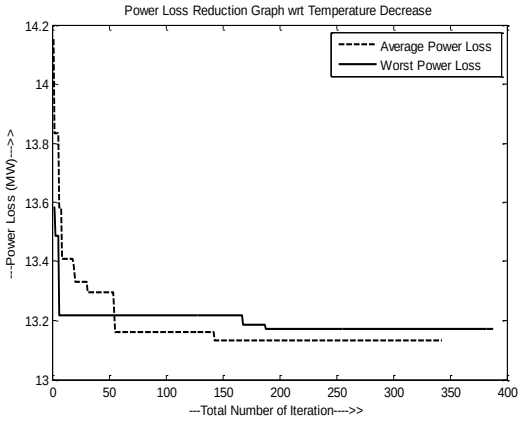

Figure 2. Power loss minimization by SA for IEEE-14 bus network (average and worst case)

Table 1. Comparative study on SA based power loss optimization result for IEEE 14-bus system

	Base case by Newton Raphson Method [247]	PSO [247]	DE [32]	SARGA [33]	Proposed SA based solution
P_{LOSS} (MW)	13.49	13.32	13.239	13.0722	13.0722
% P_{LOSS} reduction w.r.t proposed SA	3.097	2.002794	1.860	1.260	-

With the effective response to solve the proposed problem in a small test system, SA was further applied to solve the fundamental RPD problem in IEEE 57-bus system.

7.4.1.1.2 Result Analysis for Test System 3

In this work, a SA based parametric variation studies were conducted to check their effect on the proposed problem. The parametric variation studies are usually performed to achieve appropriate parameters for the optimization procedure particularly when the test system is not very small. Here, two important parameters of the cooling schedule of the SA were varied. They are final temperature (T_f) and the multiplying factor *(α)*. By varying these parameters, three sets were found for the proposed problem for the IEEE 57-bus system which were shown in Table 2.

Table 2. Parametric variation study for SA considering IEEE 57-bus system

	SA Study 1	SA Study 2	SA Study 3
SA technique based Parameters	T_i = 1,T_f = 10^{-5}, Maximum repetition of result = 150, α = 0.9	T_i = 1,T_f = 10^{-8}, Maximum repetition of result = 150, α = 0.8	T_i = 1,T_f = 10^{-10}, Maximum repetition of result = 150, α =0.7

According to the parametric variation SA Study 1, the P_{LOSS} was obtained as 20.8088 MW. In this case, the average and the worst value were determined as 21.8843 MW and 22.319 MW respectively, considering fifty trial runs. Similarly, considering the set parameters of the SA Study 2, the P_{LOSS} was found as 25.859 MW. In this case, the average and the worst values were determined as 26.001 MW and 26.571 MW respectively after fifty trial runs. Finally the set parameters of the SA Study 3 provided the best value of P_{LOSS} as 25.564 MW. In this case the average and the worst value were determined as 25.712 MW and 26.157 MW respectively after fifty trial runs. The best, average and the worst values for the three cases were summarized into Table 3. Here, the losses were optimised by controlling the V_g, t and Q_c. In this regards, one point is to be mentioned that all the control variables as obtained by SA were found within the stable operating margin.

Table 3. Best, average and worst power loss optimization results by SA for IEEE 57 bus system

Considered cases	Best Value (MW)	Average Value (MW)	Worst Value (MW)
SA Study 1	20.8088	21.8843	22.319
SA Study 2	25.859	26.001	26.571
SA Study 3	25.564	25.712	26.157

Further, the SA Study 1, 2, 3 based optimizations were also graphically demonstrated in Figure 3, 4 and 5 respectively. From these figures, one similar point was noted. It indicated that there were several local optimal points where the fitness functions were found to converge. However, the strategic acceptance criteria of the SA method prevented the local convergence and helped to converge at the global optima. According to the Figure 3, the best value of the optimization process converged at the earlier iteration count of SA study 1. However the average and the worst values were found to converge at later iteration count of SA study 1. Here, the iteration count is considered in terms of temperature variation.

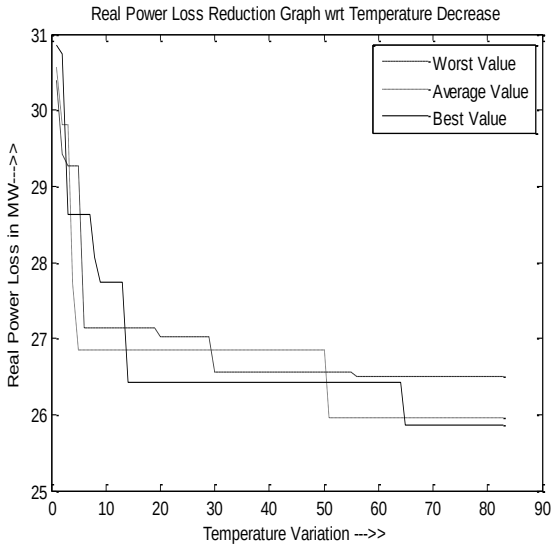

Figure 3. SA Study 1 based power loss optimizations for IEEE 57-bus network

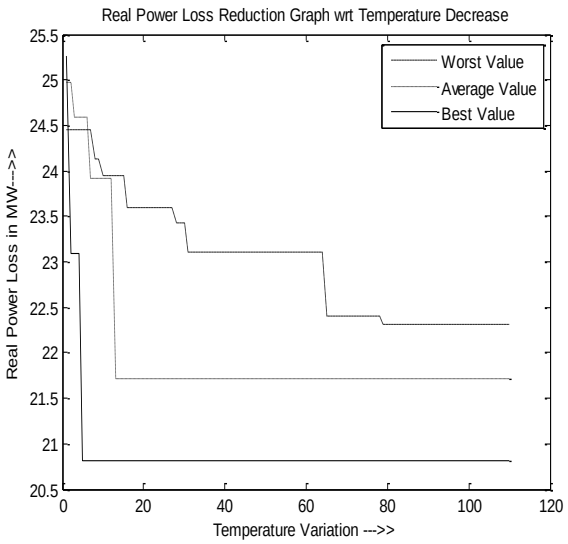

Figure 4. Power lows optimizations for SA Study 2 in IEEE 57-bus network

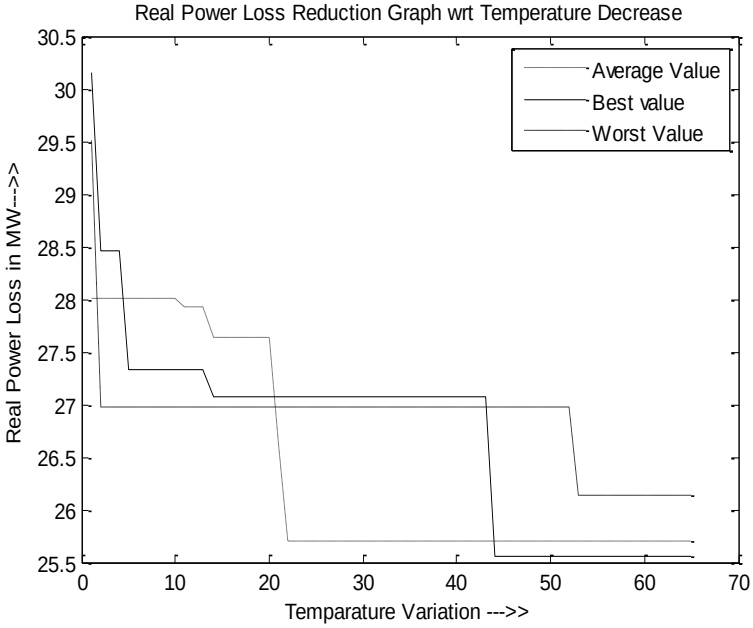

Figure 5. SA Study 3 based power loss optimizations for IEEE 57-bus system

After analysing the parametric variation based case studies, it could be remarked that the SA Study 1 provided not only the best solution, the average and the worst values of the SA Study 1 were even better than the best values of the other two cases. Since, the iteration counter were variable and was generated with the influence of T_f and α, the variation in result has occurred. Hence the SA Study 1 based results were considered as the proposed result for the IEEE 57-bus system. Further, to validate the improved performance of the proposed SA based results, a comparative study was shown here in Table 4. The comparative study showed a steady progress of the minimized P_{LOSS} by the SA method to minimize power losses for a medium sized network. Therefore, the SA technique has been further utilized to solve the proposed problem in a large operating network of IEEE 118-bus system.

Table 4. Comparative study for SA on power loss optimizations for IEEE 57-bus system

	L-SACP-DE [230]	CGA [35]	DE [23]	SPPSO-07 [248]	Proposed SA based solution
P_{LOSS} (MW)	27.91553	25.24411	25.0475	24.43043	24.43043
% P_{LOSS} reduction w.r.t proposed SA	25.46	17.57	16.92	14.82	-

7.4.1.1.3 Result Analysis for Test System 4 utilising SA

SA technique was further applied to solve the RPD issue for the larger network of IEEE 118-bus system. Here the optimising parameters of the proposed technique was chosen as T_i = 1, T_f = 10^{-8}, Maximum repetition of result = 150, α = 0.9 after considering fifty trial runs of the proposed fitness function for the considered network. By controlling the V_g, t and Q_c, the P_{LOSS} was reduced to 128.735 MW and the % P_{LOSS} was found decreased by 2.10266% from the value obtained by Newton Raphson based solution. In this work, the average and the worst values were obtained as 130.173 MW and 131.405 MW respectively after fifty trial runs. While analysing the results, one important point was to be mentioned that all the results maintained the dynamic voltage limit of the network under considerations.

Moreover, to determine the efficiency and precision of the SA technique, standard deviation (S_N) of the obtained results (P_{LOSS}) were observed. The standard deviation (S_N) of the P_{LOSS} was determined by (130) considering fifty trial runs.

$$S_N = \sqrt{\frac{1}{N}\sum_{i=1}^{N}(x_i - \bar{x})^2} \tag{130}$$

where (x_1, x_2, …, x_N) were the observed value of the sample items and $\bar{x}$ is the mean value of the observation and N stands for the number of sample collected (50 in this case). Here, the standard deviation of the solution was obtained as 0.868405. Mean the while, the best, average and worst

responses were plotted in Figure 6. From the Figure 6, it had been found that the optimal values efficiently escaped the local minima at several times and converged to the global optima providing desired solutions. In this regards, to validate the efficiency of the proposed method, a comparative study was co-ordinated involving different meta-heuristics methods based results in Table 5.

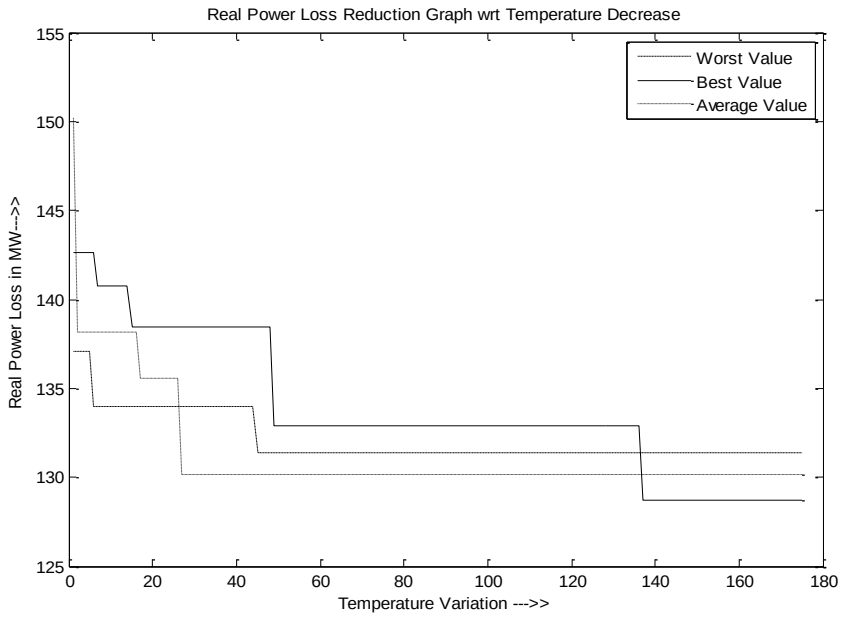

Figure 6. SA based power loss
optimizations for IEEE 118-bus system

Table 5. SA based comparative study on power loss optimizations for IEEE 118-bus system

	L-SACP-DE [230]	CGA [35]	SPPSO-07 [248]	DE [23]	Proposed SA based solution
P_{LOSS} (MW)	141.79864	139.41498	139.27522	128.318	128.235
% P_{LOSS} reduction w.r.t proposed SA	9.56	8.0192	7.867	0.064	-

Technically, SA showed improved performances while solving the fundamental RPD problem. However, the lack of adequate population space, made the operating region of the SA small. Therefore, another attractive population based swarm intelligence method called PSO has been adopted here to solve the considered problem.

7.4.1.2 PSO based Simulation analysis

Alike the SA, PSO method was applied to solve the RPD issues. Now, besides the real power loss minimisation aspects, reactive power generation minimisation is another major issues related to the RPD aspects. This thereby needs to be discussed a priory.

7.4.1.2.1 Reactive Power Generation Minimisation (RPGM) Analysis by PSO

Here, the Test System 1 (IEEE 14-bus system) was considered for the proposed problem using PSO. Initially, a parametric variation study on RPGM aspects was conducted to obtain most efficient sets of optimization parameter for the PSO. At the beginning of the parametric variation study, by keeping N_p = 20, w_{max} and w_{min} was varied to determine the fitness function for $c_1 = c_2 = 2.05$ and $iter_{max}$ = 40. By considering fifty trial runs, it was observed that optimum value was found at $w_{max} = 0.9$, $w_{min} = 0.4$. Now, considering $w_{max} = 0.9$, $w_{min} = 0.4$ with $c_1 = c_2 = 2.05$ and $iter_{max}$ = 40, N_p was varied in between 30 and 40. Finally, the optimum value was obtained at N_p = 40 with $w_{max} = 0.9$, $w_{min} = 0.4$ for $c_1 = c_2 = 2.05$ and $iter_{max}$ = 40 considering fifty trial runs. Once, the parameters were fixed, PSO was applied to sole the RPGM problem by controlling the V_g, t and Q_c. In this work, the minimum generated reactive power (Q_{Gmin}) was obtained at 3.500 MVar when N_p = 40, $w_{max} = 0.9$, $w_{min} = 0.4$, $c_1 = c_2 = 2.05$ and $iter_{max}$ = 40 by considering fifty trial runs. The optimization characteristic for the best case was drawn in Figure 7 where the global convergence of optimum value occurred at the 9th iteration which was very close to the local optima. In this regards, one point must be mentioned that all the control variables were converged within the stable operating margin of the population space. For the three sets of populations V_g for the four generator buses are compared in Table 6. The comparative study showed that the V_g, values are almost equal for the 2nd and 6th buses for the three populations. For the third bus, the V_g has got 1.0192 p.u. in case of N_p = 40 where the average value of the third bus voltage at N_p = 20, 30 was 0.9705 p.u. Similarly, the average bus voltage of the 8th bus was found 1.0705 p.u. for the N_p = 20, 30 where it was obtained as 0.9893 p.u. for N_p = 40. Now, the combinations of generator as well as load bus voltages for N_p = 40 were being able to derive optimum results. However, the dynamic voltage limits of the network remained secured for all the simulation studies.

Table 6. PSO based statistical analysis on RPGM problem considering IEEE 14-bus system

Population Size	w_{max}	w_{min}	Q_{Gmin}	Bus Voltage
$N_p = 20$	0.9000	0.4000	3.50281	$V_{g2} = 1.0823$, $V_{g3} = 0.9687$ $V_{g6} = 1.10$, $V_{g8} = 1.0759$
$N_p = 30$			3.50127	$V_{g2} = 1.0810$, $V_{g3} = 0.9723$ $V_{g6} = 1.10$, $V_{g8} = 1.0651$
$N_p = 40$			3.5000	$V_{g2} = 1.0715$, $V_{g3} = 1.0192$ $V_{g6} = 1.10$, $V_{g8} = 0.9893$

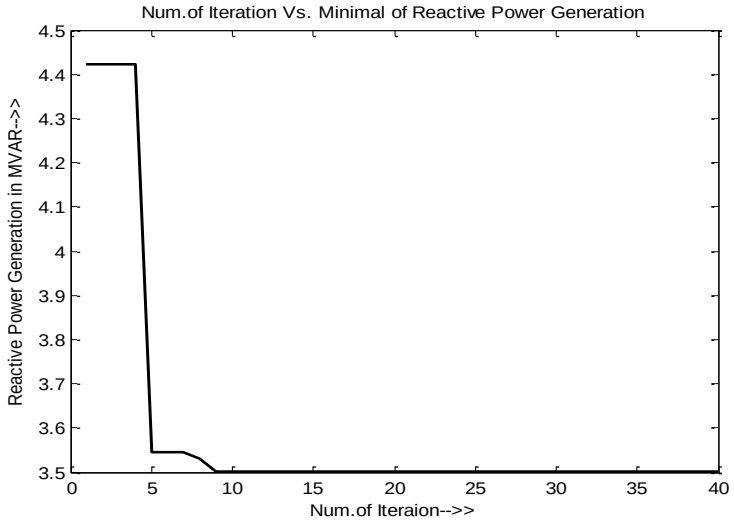

Figure 7. Reactive power generation minimizations based RPD analysis by PSO for IEEE 14-bus system

However, though PSO worked satisfactorily to solve the fundamental RPD problem, it frequently suffered the problem of poor convergence for a simple optimization problem. This therefore needed modifications. The incorporation of the constriction factor is one of the effective solution to the poor convergence problem of PSO. Therefore, the RPD based simulations were further continued with the constriction factor based PSO (Cf-PSO).

7.4.1.2.2 Constriction Factor-PSO based Simulation Analysis

Now, the test systems were attempted by the constriction factor based PSO (Cf-PSO) for solving the proposed problem.

7.4.1.2.2.1 Result Analysis for Test System 1 based on Cf-PSO

Alike the SA method Cf-PSO was considered to solve the RPD loss optimisation problem for IEEE 14-bus system. Initially, a Cf-PSO based parametric variation was considered to solve the fitness functions. It was found that the population size (N_p) = 42, maximum number of iterations ($iter_{max}$) = 40, $c_1 = c_2 = 2.05$, $w_{max} = 0.9$ and $w_{min} = 0.4$ provided most optimized results. Here, the proposed Cf-PSO based P_{LOSS} has been optimized to 12.7812 MW which was found much better compared to the base case loss value of 13.49 MW [247]. The control variables namely V_g, t and Q_c were found to remain within the operating boundary limit. The optimization was graphically shown in Figure 8 which inferred that the P_{LOSS} had converged at the 13th iteration generation. The figure also elaborated that there were few local optima for convergence; however the Constriction Factor based PSO provided global optimal convergence.

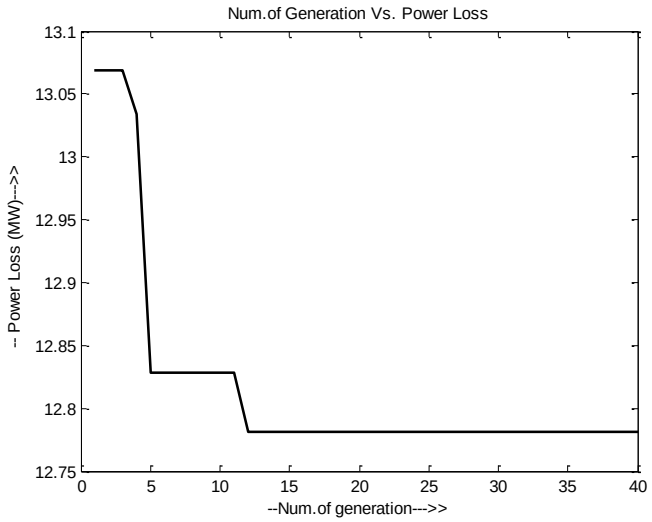

Figure 8. Cf-PSO based RPD problem optimizations for IEEE 14-bus system

Moreover, to validate the steady performance of the proposed method, a comparative study was considered in Table 7. From the comparative study, it can be concluded that Constriction Factor based PSO provided much improved results for the IEEE 14-bus system. Here, the integration of the constriction factor in the algorithm played a vital role to generate such response.

Table 7. Comparative study on Cf-PSO based power loss optimizations for IEEE 14-bus system

	Base case by Newton Raphson Method [247]	PSO [247]	DE [32]	SARGA [33]	Proposed PSO based solution
P_{LOSS} (MW)	13.49	13.32	13.239	13.2164	12.7812
% P_{LOSS} reduction w.r.t proposed SA	5.25426	4.045	3.457	3.2928	-

Since the proposed method works satisfactorily, it has been further utilized to solve RPD issue for a IEEE 57-bus network.

7.4.1.2.2.2 Result Analysis for Test System 3 by Cf-PSO

Here, the optimal parameters for the PSO technique were chosen as N_p = 20, w_{max} = 0.9, w_{min} = 0.4, c_1 = c_2 = 2.05 and $iter_{max}$ = 100 by considering fifty trial runs. By controlling V_g, t and Q_c the minimum P_{LOSS} was obtained as 20.2454 MW and % P_{LOSS} reduces by 2.2546% with respect to the base value (Newton Raphson method based solution without shunt capacitor). The average and the worst values were found as 20.487 MW, 20.7974 MW respectively after considering fifty trial runs with the computational time approximately 321.080 sec. Here, the obtained results in terms of decision variables were found within system stable margin to maintain dynamic voltage limit. The P_{LOSS} convergence curve w.r.t. to iteration count is shown in Figure 9. From the Figure 9, it can be marked that the there are several local optimum points to converge, but the strategic PSO finally converged at the global optima at the 75th iteration. Therefore, the problem of premature convergence was removed here by the incorporated constriction factor. Hence the proposed PSO method based multidimensional solution vectors searches the population space thoroughly while solving the RPD problem. Overall the results are satisfactory and all the obtained variables maintain the system operating limits.

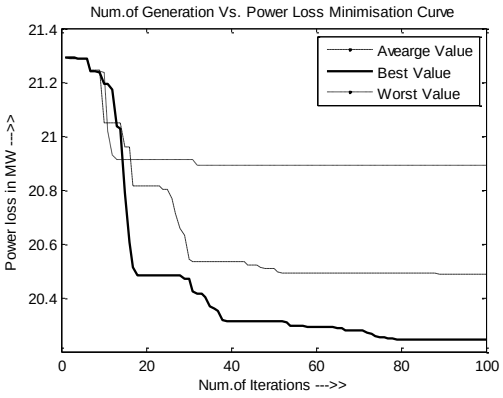

Figure 9. Power loss optimization results by Cf-PSO for IEEE 57-bus system

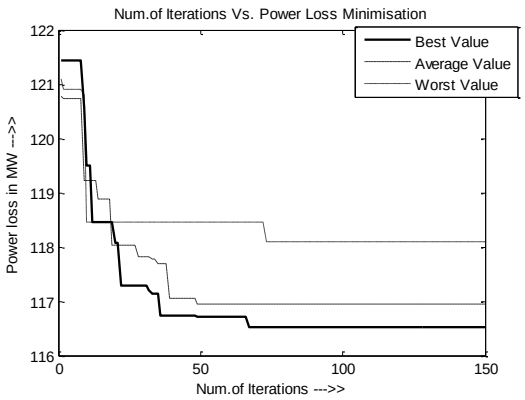

Figure 10. Cf-PSO Technique based power loss optimization for IEEE 118-bus system

Further to validate the performances of the proposed method, a comparative study was considered here with other optimisation techniques shown in Table 8. The proposed Cf-PSO method based observations showed better results over other methods.

Table 8. Cf-PSO based comparative study on power loss optimisations for IEEE 57-bus system

	L-SACP-DE [230]	CGA [35]	SPPSO-07 [247]	DE [23]	AGA [35]	Proposed PSO based solution
P_{LOSS} (MW)	27.91553	25.24411	24.43043	25.0475	24.56484	20.2454
% P_{LOSS} reduction w.r.t proposed SA	27.4762113	19.8014903	17.1303984	19.1719733	17.583831	-

After observing effective performances of the proposed method, it was considered to be applied to a larger network such as IEEE 118-bus network.

7.4.1.2.2.3 Result Analysis for Test System 4 by Cf-PSO

Considering the same set of optimal parameters and control variables alike the previous case, the minimum P_{LOSS} was obtained as 116.523 MW. Considering fifty trial runs the average and the worst values were achieved as 116.938 MW and 118.104 MW respectively. The control variables of the optimisation was found to be within standard operating limit which therefore helped to maintain system dynamic voltage limit. The convergence characteristics were drawn in Figure 10 which demonstrated several local optima points. However, the final result converged at the global optima at the 70th iteration. Hence, the constriction factors played a major role here to generate global optimal solution. Further, to validate the improved performances of the proposed method, it was compared with few meta-heuristics based solutions shown in Table 9. The comparative study showed the

proficient performances of the proposed method over the other techniques while solving the RPD issues.

Table 9. Comparative study on Cf-PSO based power loss optimizations for IEEE 118-bus system

	L-SACP-DE [230]	CGA [35]	SPPSO-07 [248]	DE [23]	Proposed PSO based solution
P_{LOSS} (MW)	141.79864	139.41498	139.27522	128.318	116.523
% P_{LOSS} reduction w.r.t proposed SA	17.8250229	16.4200289	16.336158	9.19200736	-

Although, Cf-PSO worked satisfactorily in comparison to fundamental PSO, it could not tackle the problem of premature convergence for all cases. This thereby needed major modifications. In this context, the strategic evolutionary computational optimization tools were observed to work satisfactorily to solve fitness functions characterised by few complexities in terms of multi-constraints having static and dynamic behaviour. Therefore, instead of continuing with the Constriction Factor based PSO, Evolutionary Computational techniques were considered for solving the proposed problem.

7.4.1.3 DELB Technique based Result Analysis

As stated earlier, in this work two type of modified Differential Evolutionary techniques were applied to solve the proposed problem. Amongst them Differential Evolution with Localisations around the Best Vectors (DELB) is elaborated first with simulation results. Since the optimization technique based results depend on the proper choice of the optimisation parameters, here a parametric variation study was initially conducted to fix the different parameters of DELB such as N_p, f_m and C_R. Here, the mutant factor was selected randomly ($f_m \in (0,1)$), therefore the choice of the rest parameters was very crucial for the result. The terminating condition was chosen as reaching to the maximum generation number (Gen_{max} = 50).

7.4.1.3.1 Result Analysis for Test System 1 by DELB

In this work, initially N_p was kept constant and C_R was varying as 0.2, 0.5, 0.6, 0.7, 0.8 and 0.9. Six sets of result were obtained in this context. By increasing N_p, more six sets of results were taken. This way total twenty four sets (4×6) of result (N_p = 20, 30, 40 and 60) were obtained among them the best, average and worst value for each population with respective C_R was kept aside. Amongst the four best results for different N_p (= 20, 30, 40 and 60), the optimum one was considered as the final value

which was shown in Table 10. Corresponding N_p and C_R was chosen as best parameter set for the proposed method. Further, the best value providing parameters (N_p, C_R) were selected as the final parameters for higher test cases (IEEE 30-bus system).

According to Table 10, the minimum P_{LOSS} value was obtained as 13.0928 MW for N_p = 20 with C_R = 0.7 by controlling the V_g, t and Q_c. The proposed DELB method subsequently reduced the P_{LOSS} to 13.0829 MW, 13.0696 MW and 13.0532 MW with N_p = 30, 40 and 60 and C_R = 0.9, 0.6 and 0.7 respectively. From the Table 10, it can be further implied that medium C_R and the higher N_p provided better results.

Table 10. DELB method based variation of population size (*Np*) and crossover factor (*Cr*) for power loss optimization

P_{LOSS} in MW	C_R =0.2	C_R=0.5	C_R =0.6	C_R =0.7	C_R =0.8	C_R =0.9
N_p = 20	13.1011	13.1274	13.1231	13.0928*	13.1439	13.0956
N_p = 30	13.0874	13.1018	13.0794	13.1132	13.1017	13.0829*
N_p = 40	13.0882	13.1031	13.0696*	13.0926	13.0817	13.0724
N_p = 60	13.0755	13.0908	13.0816	13.0532*	13.0996	13.0869

*Best value for the population considered

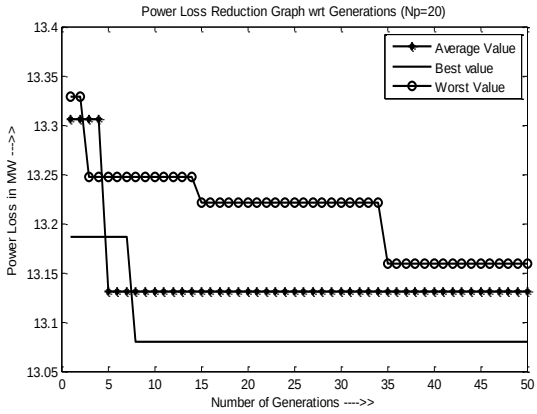

Figure 11.(i) $N_p = 40$

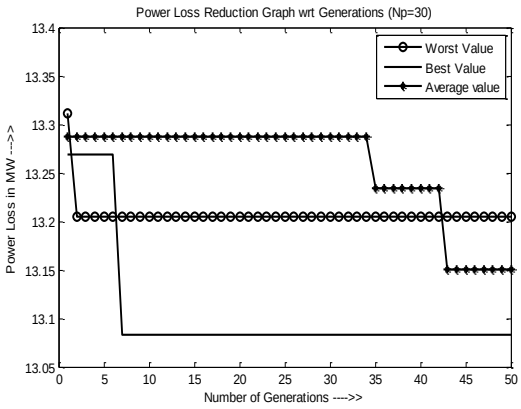

Figure 11. (ii) $N_p = 60$

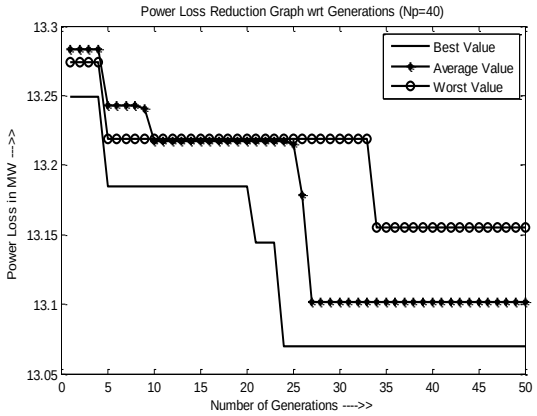

Figure 11.(iii) $N_p = 40$

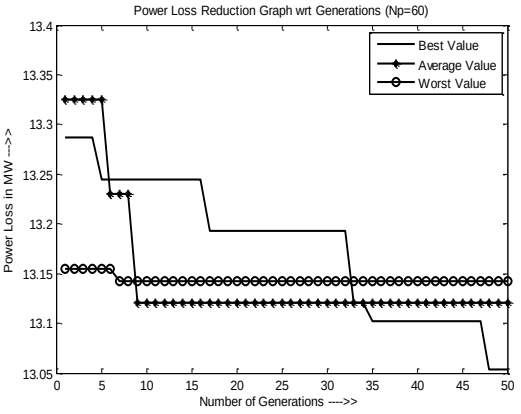

Figure 11. (iv) $N_p = 60$

Figure 11. DELB based power loss optimization for IEEE 14-bus system (i)-(iv)

The power loss optimisations w.r.t the number of generations were characterised in Figure 11 (i-iv) for the given populations (N_p = 20, 30, 40 and 60) considering the best, average and the worst cases. From these figures, it can be remarked that there were several local optimal converging points throughout the generations. However, the final solution converged at the global optima efficiently. The Figure 11. (i) and (ii) showed that the power loss curves converged early but Figure 11. (iii) and (iv) provided the convergence at 24^{th} generation and 48^{th} generation respectively. Regarding the observations, one point may be stated that all the control variables were found converging within the boundary value to maintain system dynamic voltage limit with 210.0908 sec CPU operating time.

Moreover, to justify the efficiency of the proposed DELB method, the observations were compared with previously applied techniques to solve the RPD having same configurations shown in Table 11. The comparison proves the effectivity of the proposed method.

Table 11. Comparative study on DELB based power loss optimisations for IEEE 14-bus system

	Base case by Newton Raphson Method [247]	PSO [246]	DE [32]	SARGA [33]	Proposed DELB based solution
P_{LOSS} (MW)	13.49	13.32	13.239	13.2164	13.0532
% P_{LOSS} reduction w.r.t proposed SA	3.237954	2.003003	1.40342926	1.23482945	-

Although, the DELB method took more times to search the global solutions at the selection steps, it worked satisfactorily to solve the RPD issue for small test systems. Therefore, it can be further applied to solve RPD for the IEEE 30-bus system.

7.4.1.3.2 Test System 2 based Result Analysis by DELB

As stated earlier, here the DELB based best optimisation parameter sets for the IEEE 14-bus system were considered for the RPD issue for IEEE 30 bus system. In this work, RPD was solved by controlling V_g, t in addition to the varying positions of the shunt capacitor in three ways [32, 7, 8]. Initially, DELB method was applied to solve the above mentioned cases using different N_p (= 20, 30, 40 and 60) with C_R = 0.7, 0.9, 0.6 and 0.7 respectively. Due to implementation of the said parameters sixteen sets (4×4) of result were obtained for the specified three cases. Amongst them, (one set contains best, average and worst value) only the best values are shown in Table 12. In this regards, the optimisation characteristics curves for the best values of each cases were drawn and shown in Figure 12 (i-iii). From Figure 12 (i), it can be observed that the case 1 based optimum value (4.8797 MW) was obtained after convergence at nearly 40th generation. Here, both the average and the worst values were obtained above 5 MW which were obtained after 30th generation. In case of Figure 12 (ii) and (iii), the final convergence occurred after 40th and 30th generation respectively for case 2 and case 3. Here, the case 2 based best, average and the worst value were determined as 4.60636MW, 4.70571MW and 4.73765MW respectively. Similarly, for the case 3 the best value was obtained as 4.50089MW with the average and worst value at 4.70571 MW and 4.73383 MW respectively. According to the optimization principle of DELB method, data searching process did get emphasis here at the selection stage. Therefore, this method took longer time although it provided global convergence by avoiding successfully the local optimal solutions.

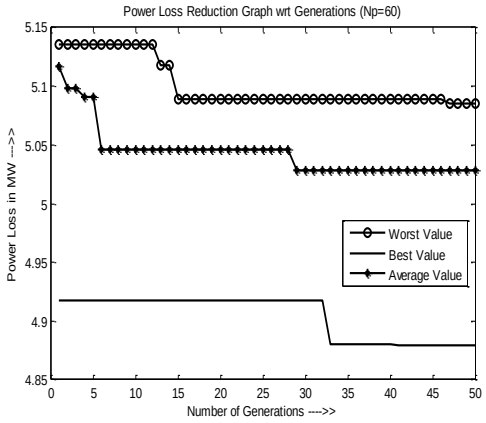

Figure 12. (i) Case 1

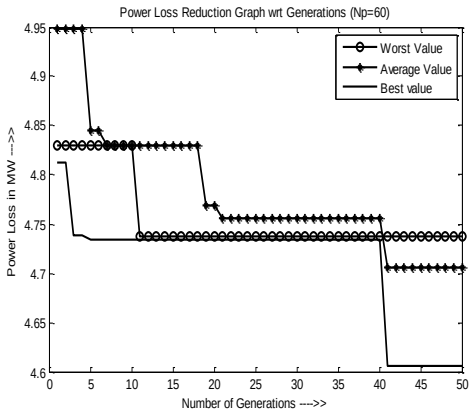

Figure 12. (ii) Case 2

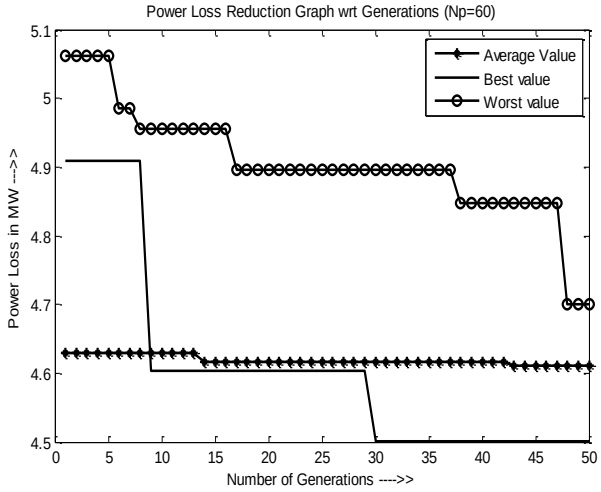

Figure 12. (iii) Case 3

Figure 12. DELB based RPD loss optimizations for IEEE 30-bus system for different cases

Table 12. Power loss optimizations amongst DELB based three cases with different populations for IEEE 30-bus system

	Case1 (P_{LOSS} (MW))	Case2 (P_{LOSS} (MW))	Case3(P_{LOSS} (MW))
N_p = 20, C_R = 0.7	4.91962	4.71728	4.58955
N_p = 30, C_R = 0.9	4.90072	4.70172	4.56152
N_p = 40, C_R = 0.6	4.89288	4.63539	4.50546
N_p = 60, C_R = 0.7	4.8797*	4.60636*	4.50089*

*Best value for the considered cases

According to the obtained result, one thing is to be mentioned that all the control variables were found within stable operating range to maintain steady dynamic voltage limit with 402.7452 sce as average CPU operating time. To validate the performance of the proposed DELB method to solve the RPD issue, the results on three cases were compared with previous works on evolutionary technique for validation. Here, Table 13 (i) provides a comparative study for case 1, Table 13 (ii) shows comparative study on case 2 and Table 13 (iii) finally demonstrates the comparative study on case 3.

Table 13. Comparative study on DELB based power loss optimizations for IEEE 30-bus system for case 1-3

Table 13. (i) Case 1

	Base case by Newton Raphson Method [32]	PSO [32]	DE [32]	Proposed DELB based solution
P_{LOSS} (MW)	5.66	5.116	5.011	4.8797
% P_{LOSS} reduction w.r.t proposed SA	13.7862191	4.61884285	2.62023548	-

Table 13. (ii) Case 2

	Base case by Newton Raphson Method [7]	PSO [40]	CLPSO [40]	SARGA [33]	Proposed DELB based solution
P_{LOSS} (MW)	5.988	4.8136	4.7208	4.6135 (N_p=15) 4.5913 (N_p=36)	4.60636
% P_{LOSS} reduction w.r.t proposed SA	23.0734803	4.30530165	2.4241654	0.1547632 -0.32801167	-

Table 13. (iii) Case 3

	Base case by Newton Raphson Method [8]	PSO [40]	CLPSO [40]	SARGA [33]	Proposed DELB based solution
P_{LOSS}	5.8120	4.6282	4.5615	4.57401	4.50089
% P_{LOSS} reduction w.r.t proposed SA	22.5586717	2.75074543	1.32872958	1.59859729	-

From the three sets of comparative study it can be observed that the obtained results showed significant improvements from the base case. Moreover, the DELB based observations were found to obtain improved results compared to few recent optimization techniques likely CLPSO, SARGA etc.

Although, DELB method was found to work satisfactorily to solve the proposed problem for the small networks, it takes huge CPU operating time due to its thorough searching procedure in the selection stage. Moreover, the optimization process generated the desired solutions at higher population, therefore more time was required to satisfy terminating condition. Therefore, another modified differential evolution technique namely the Differential Evolution with Random Localizations (DERL) was further considered for the proposed problem.

7.4.1.4 DERL Technique based Result Analysis

Alike the DELB method, to obtain best optimal parameter sets, a parametric variation study was conducted for DERL method while solving the RPD considering the IEEE 14-bus system.

7.4.1.4.1 Result Analysis for Test System 1 by DERL

In this work, initially C_R was varied as 0.2, 0.5, 0.6, 0.7, 0.8 and 0.9 by keeping the N_p constant. At a particular population, six sets of result in the form of P_{LOSS} were obtained by controlling V_g, t and Q_c. Now, by varying N_p with variable C_R six more sets of results were determined by solving the fitness function (P_{LOSS}). This way total twenty four (N_p =4 and C_R =6, 4×6) sets of P_{LOSS} were obtained from which the best value is shown in Table 14 considering thirty trial runs. Table 14 showed that for N_p = 20, the minimum P_{LOSS} was obtained as 13.0068MW with C_R = 0.7. While population increases to N_p=30, 40 and 60, P_{LOSS} has been found to reduce gradually to 13.0058 MW, 12.9878 MW and 12.9792 MW with respective C_R =0.9, 0.2 and 0.9. Amongst the four results, the best P_{LOSS} was observed as 12.9792 MW for N_p = 60 with C_R = 0.9. From the Table 14, it can be concluded that large population number and higher C_R provided best result. One point may further be reported that all the control variables were found to operate within the stable operating limit. Here, the generator bus

voltages were observed to vary within 1.03 p.u. to 1.09 p.u. Therefore the dynamic voltage limit of the network remained unhampered.

Table 14. DERL method based variation of population size and crossover factor for power loss optimisation

P_{LOSS} in MW	Cr = 0.2	Cr = 0.5	Cr = 0.6	Cr = 0.7	Cr = 0.8	Cr = 0.9
N_p = 20	13.0338	13.0274	13.0084	13.0068*	13.0419	13.0483
N_p = 30	13.043	13.0118	13.044	13.0185	13.0149	13.0058*
N_p = 40	12.9878*	13.0077	12.993	13.0185	13.0107	13.0457
N_p = 60	13.0171	12.9945	13.0123	13.0072	13.0252	12.9792*

*Best value for the considered cases

Here, the proposed algorithm based convergence characteristics are shown in Figure 13 (i-iv) for different population sizes (N_p = 20, 30, 40 and 60). According to the fast converging principle of the DERL technique, all the figures apart from the Figure 13 (iii) showed the early but global convergence. Here, the Figure 13 (i-ii, iv) converged at 25th, 17th and 36th generation respectively by avoiding the trap of the several local optima. In this regards, the average and worst values of the four cases were found converged at the earlier generations with global converging solutions. Here, the best result i.e. 12.9792 MW was found to complete the generation cycle within 110.1264 sec. Therefore, it can inferred that the modified DE in the form of DERL performed efficiently compared to another modified DE namely DELB in terms of the magnitude as well as operational time.

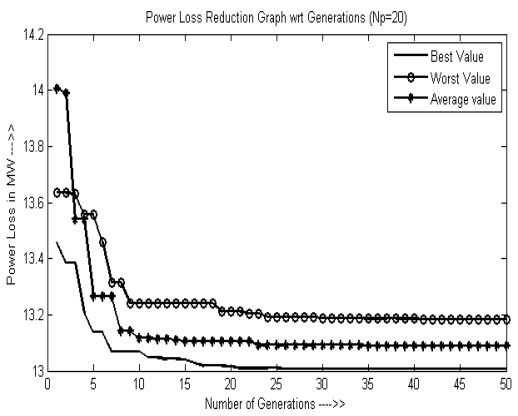

Figure 13. (i) N_p= 20

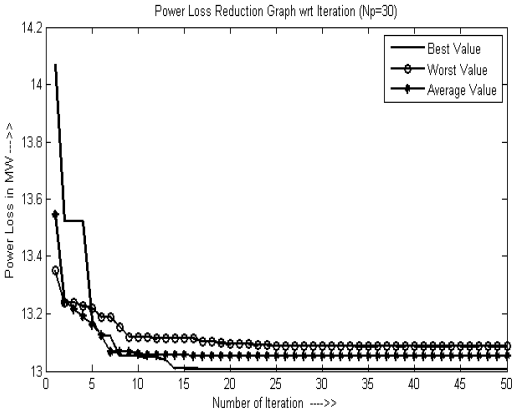

Figure 13.(ii) N_p= 30

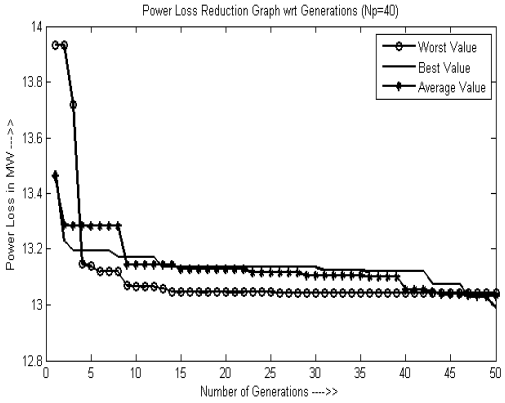

Figure 13. (iii) N_p= 40

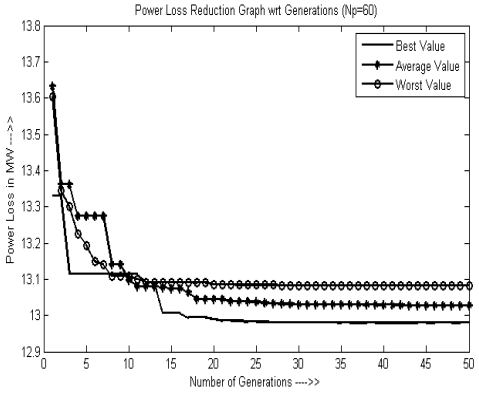

Figure 13. (iv) N_p= 60

Figure 13. DERL based power loss optimization for IEEE 14-bus system (i)-(iv)

Moreover, to validate the proficiency of the proposed methodology, the DERL method was compared with previously applied techniques to solve the RPD in same context as shown in Table 15. The comparisons as shown in Table 15, provided a steady improvement in optimal results while comparing with recent methodologies. Therefore, the DERL method further was further applied to solve IEEE 30-bus system with different case studies.

Table 15. Comparative study on DERL based power loss optimisation for IEEE 14-bus system

	Base case by Newton Raphson Method [247]	PSO [247]	DE [32]	SARGA [33]	Proposed DERL based solution
P_{LOSS} (MW)	13.49	13.32	13.239	13.2164	12.9792
% P_{LOSS} reduction w.r.t proposed SA	3.7865085	2.55855856	1.96238387	1.79473987	-

7.4.1.4.2 Result Analysis for Test System 2 by DERL

Since, the parametric variation study on DERL already generated a suitable C_R, here RPD issue was solved only by varying N_p for the IEEE 30-bus system. In this work, three set of shunt placements for reactive power compensation were considered along with the other control variables i.e. V_g and *t*. For the first sets of control variables the minimum P_{LOSS} was obtained as 4.83682 MW at N_p=20 which were gradually reduced to 4.78644 MW with the increase in N_p. In the second case, P_{LOSS} was determined as 4.56961MW at N_p=20. By increasing N_p, P_{LOSS} has been found to reduce till 4.51175MW for N_p=60. In the third case, P_{LOSS} reduced to 4.42649 MW at N_p=60 starting from 4.46017 MW at N_p=20. Alike the previous bus system, few points are to be noticed that for all the three cases improved results were achieved for the higher N_p (60) with all the control variables found within the stable operating limits. Thus the dynamic voltage limit of the system remains incessant. The three cases based P_{LOSS} are given in the Table 16.

Table 16. Best power loss optimisation values amongst DERL based three cases with different populations for IEEE 30-bus system

	Case1 (P_{LOSS} (MW))	Case2 (P_{LOSS} (MW))	Case3(P_{LOSS} (MW))
N_p=20, C_R=0.7	4.83682	4.56961	4.46017
N_p=30, C_R=0.9	4.81965	4.55677	4.45153
N_p=40, C_R=0.2	4.81535	4.53794	4.43708
N_p=60, C_R=0.9	4.78644*	4.51175*	4.42649*

*Best value for respective *Np* and C_R

Now, the optimisation characteristics of the optimal values of the three cases are further drawn in Figure 15 (i-iii) to analyse the convergence characteristics of the proposed DERL method. Here, the Figure 15 (i) provided the case 1 based best, average and the worst responses. These graphs showed to converge with the best results within the 20th generation where the average and the worst response curves were also converging within 20th generation. The average and the worst value are 4.86251 MW and 4.90031 MW respectively in this case 1 which are quite close to the best value. In the case 2, the average and the worst P_{LOSS} value has been obtained as 4.59471 MW and 4.6408 MW respectively. Like the earlier case these values are quite close to each other which are graphically plotted in Figure 15 (ii) with the best value. According to the Figure 15 (ii), the best value converged at 19th generation where the average and the worst values did converge even earlier than the best value. Lastly the Figure 15 (iii) analyzing the case 3 demonstrated convergence of all the P_{LOSS} (best, average and

worst) response curves within 15th generation. In this case, the average and the worst values are found as 4.47405 MW and 4.50531 MW respectively. In this context, one point is to be mentioned that, all the convergences were being able to avoid the local convergence. The total execution times for the three cases were found as 228.957 sec, 230.0747 sec and 230.2747 sec respectively which were found far less compared to the DELB method as stated earlier. Therefore, the fundamental principle of the fast convergence of the DERL method has been established with this attempt.

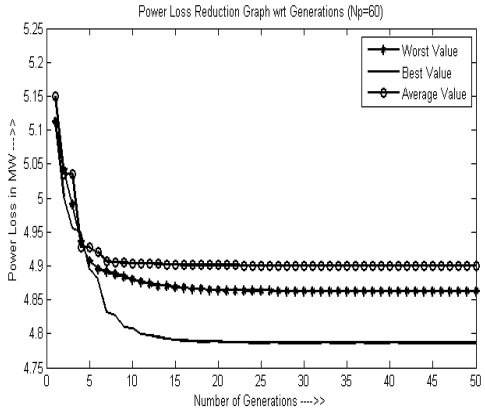

Figure 14. (i) Case 1

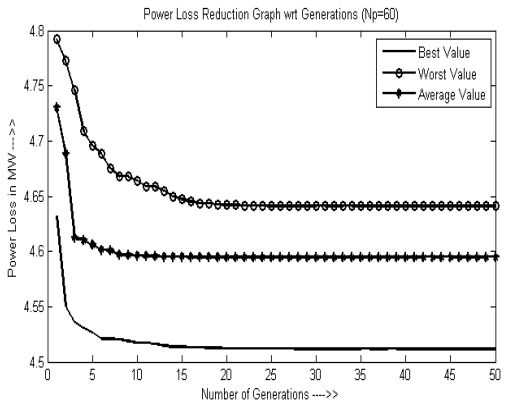

Figure 14. (ii) Case 2

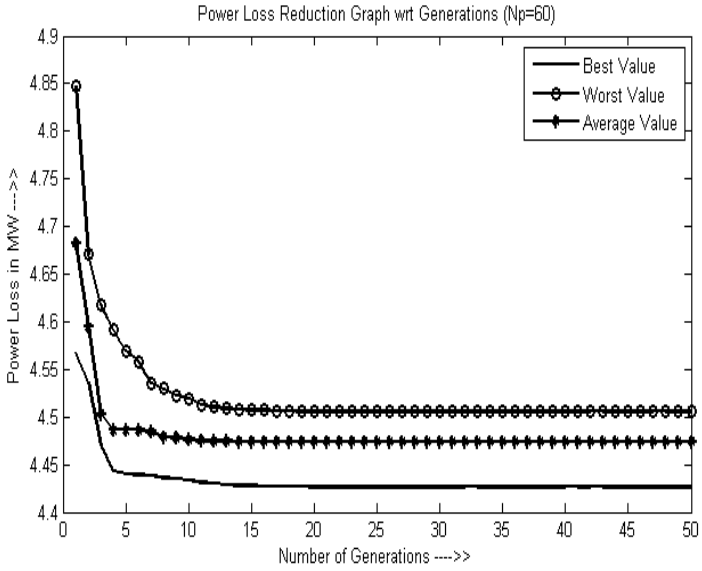

Figure 14. (iii) Case 3

Figure 14. Power loss optimization by DERL for IEEE 30-bus system (i) Case 1, (ii) Case 2, (iii) Case 3

Finally, to validate the proficiency of the proposed method, a comparative study was coordinated considering previous evolutionary techniques applied to solve the RPD problem with same constraints and configurations. The result of such is shown in Table 17 (i-iii).

Table 17. Comparative study on DERL based power loss optimisation results for IEEE 30-bus system (i) Case 1 (ii) Case 2 (iii) Case 3

Table 17. (i) Case 1

	Base case by Newton Raphson Method [32]	PSO [32]	DE [32]	Proposed DERL based solution
P_{LOSS} (MW)	5.66	5.116	5.011	4.78644
% P_{LOSS} reduction w.r.t proposed SA	15.433922	6.4417514	4.481341	-

Table 17. (ii) Case 2

	Base case by Newton Raphson Method [7]	PSO [40]	CLPSO [40]	SARGA [33]	Proposed DERL based solution
P_{LOSS} (MW)	5.988	4.8136	4.7208	4.6135 (Np=15) 4.5913 (Np=36)	4.51175
% P_{LOSS} reduction w.r.t proposed SA	24.653474	6.2707745	4.4282749	2.20548391 1.73262475	-

Table 17. (iii) Case 3

	Base case by Newton Raphson Method [8]	PSO [40]	CLPSO [40]	SARGA [23]	Proposed DERL based solution
P_{LOSS} (MW)	5.8120	4.6282	4.5615	4.57401	4.42649
% P_{LOSS} reduction w.r.t proposed SA	23.838782	4.3582818	2.959772	3.22517878	-

From the comparative study considering the three cases, it can be inferred that the proposed method not only generated improved solutions, it reduced the CPU operating time as well as the number of generations compared to the other evolutionary methods including DELB technique. Therefore, due to its successful applications, the DERL technique further was applied to solve the RPD having multi-objective considerations.

7.4.1.4.3 Test System 2 based Multi-objective RPD (MORPD) by DERL

In this work, the two important sub-functions of the RPD are proposed as multi-objective part for the optimization of the IEEE 30 bus system. Here, the two functions of the RPD problem are chosen as P_{LOSS} and Q_{Gen} which are solved together by controlling V_g and t with the optimal placement of one of the advanced *var* compensators likely the Thyristor controlled series capacitors (TCSC). The optimal location of the TCSC device has been chosen by considering line based sensitivity factor analysis [177] which provided 20th and 29th lines to be most positive sensitive ones for the placement. The size of the TCSC was settled by DERL method by controlling the given inequality as (131)

$$-0.5 \times x_L \le x_{TCSC} \le 0.5 \times x_L \ , \tag{131}$$

where x_L is the inductance of the congested line of the network where TCSC is supposed to be placed [177].

Since, the proposed problem was considered as multi-objective optimisation problem, the DERL based solution vectors are generated on a trade-off mode of the two functions of P_{LOSS} and Q_{Gen}. These solutions are dominant solution for function 1 (P_{LOSS}) w.r.t function 2 (Q_{Gen}) and Pareto optimal solution of function 1 (P_{LOSS}) w.r.t function 2 (Q_{Gen}). Here, the optimal parameters of the DERL method were fixed as N_p = 60, $f_m \in \text{rand}(0,1)$, C_R = 0.8, Gen_{max} = 50 considering fifty trial runs. The obtained results in terms of the optimal TCSC variables and the functional values are given in Table 18. The dominant solution for the prioritized function (P_{LOSS} minimization) has been found as 17.209 MW and other function (Q_{Gen} minimization) was found as 17.7676 MVar. The DERL optimisation characteristics for both the functions, individually and jointly, are presented in Figure 15, 16 and 17.

Table 18. DERL based real power loss minimisations representing multi-objective RPD for IEEE 30-bus system

Control variables x_{TCSC} (p.u.)	Dominant solution for function 1 (P_{LOSS}) w.r.t function 2 (Q_{Gen})	Pareto optimal solution for function 1 (P_{LOSS}) w.r.t function 2 (Q_{Gen}) from Figure 26
x_{TCSC20} = (+) 0.0128	P_{LOSS} = 17.2109 MW	P_{LOSS} = 17.216 MW
x_{TCSC29} = (-) 0.0012	Q_{Gen} = 17.7676 MVar	Q_{Gen} = 17.74 MVar

From the Figure 15 and 16, it can be observed that both the objective functions converged globally within the10th generations being untrapped into the local minima. Moreover, the Figure 17 showed to converge both the functions under a trade-off while maintaining the concept of Dominance and

Pareto-Optimality [249]. Now the level of trade-off is dependent on the priority of the objectives in the practical field. In this work, the minimization of P_{LOSS} was considered to prioritize over the Q_{Gen} minimization aspect. According to the DERL strategy, the solution ($x^{(1)}$) dominates the solution ($x^{(2)}$) if both the following conditions are satisfied.

First condition stated that the solution ($x^{(1)}$) would be no worse than the solution ($x^{(2)}$) for all fitness functions. The second condition has explained that the solution ($x^{(1)}$) would be strictly better than ($x^{(2)}$) for at least one fitness functions [249]. Here, these two conditions are strictly followed to organise the multi-objective RPD. The Figure 17 showed the Pareto optimal curve as generated by the optimisations of both the functions which provided the Pareto optimal solutions as P_{LOSS} = 17.216 MW and Q_{Gen} = 17.74 MVar respectively.

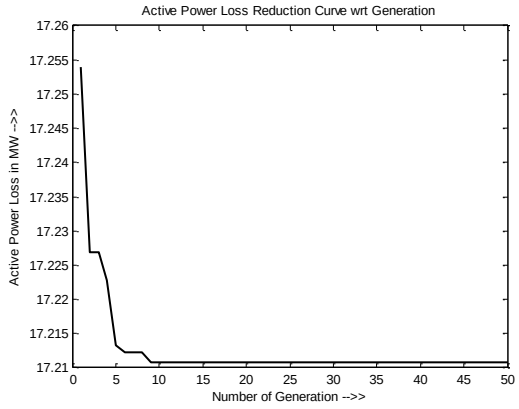

Figure 15. DERL based real power loss minimizations representing the multi-objective RPD for IEEE 30-bus system

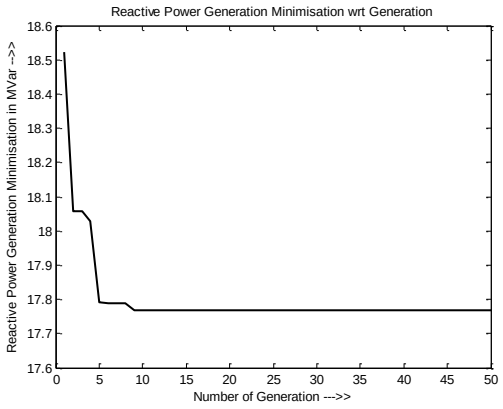

Figure 16. Reactive power generation minimizations representing the multi-objective RPD by DERL for IEEE 30-bus system

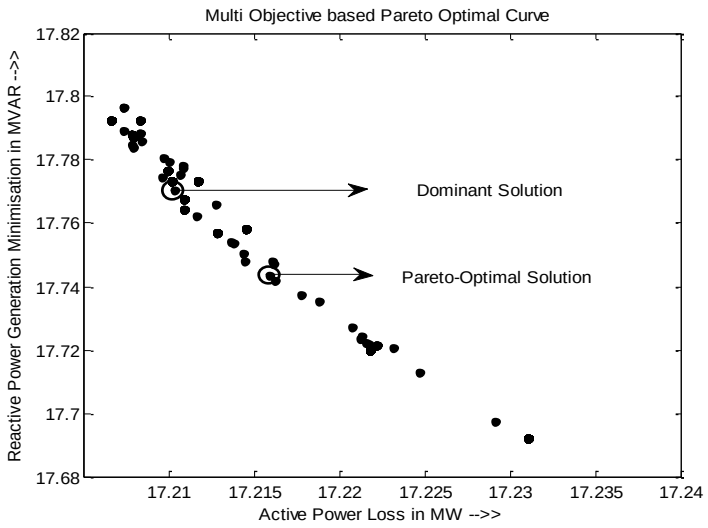

Figure 17. Multi-objective RPD based Pareto optimal curve for real power loss and reactive power generation minimization (min-min)

Overall, one point must be mentioned that all the DERL based control variables were found within the system stable operating limits. Therefore, the dynamic voltage limit of the system remained secured and therefore DERL method was further applied to a IEEE 57 bus network for solving the RPD issues with different scenarios.

7.4.1.4.4 Result Analysis for Test System 3 by DERL

Here, the DERL technique was initially applied to solve the RPD problem by controlling V_g, t and Q_C for the IEEE 57-bus network. The optimal parameters of the DERL method were considered as N_p = 30, $f_m \in \text{rand}(0,1)$, C_R = 0.8, Gen_{max}=100 after 100 trial runs. Here, the capacitor based *var* compensation provided P_{LOSS} as 22.1137 MW as best value. Moreover, the average and the worst values were observed as 22.9537 MW and 23.79 MW respectively. In this context, the control variables were found within the stable operating limit to maintain the dynamic voltage limit as desired.

Now, all the advanced economic countries as well as majority of the developing countries operate within the ambit of deregulated power scenarios. Sometimes a number of unexpected events like voltage limit crossover, line congestion initiation etc occur in the system. It has been observed that sometimes inefficient performance has been provided by the capacitors to handle these unexpected or uncertain events. Therefore, these uncertainties associated with the restructured power system needs considerations in the form of advanced *var* compensation which may help to achieve reliability and economy in the restructured power market. As stated earlier, amongst these different advanced *var*

compensators, here Superconducting Magnetic Energy Storage (SMES) device has been considered to provide reactive power (Q_{SMES}) in addition to other control variable as V_g, and t.

In this work, two case studies were accomplished for the SMES placement. Here two buses were randomly chosen for the SMES devices and minimisation of P_{LOSS} was obtained for each cases. The results involving singular Q_{SMES} for the two studies were found as 20.9173 MW and 20.8891 MW as shown in Table 19.

Further, to obtain sustainability, a combination of capacitor and SMES was also applied as control variable along with the V_g, t to solve the RPD. This provided 20.4514 MW of P_{LOSS} by the proposed DERL method which is also shown in Table 19.

Table 19. DERL based RPD with different *var* compensators for IEEE 57-bus system

	RPD with Q_C	RPD with Q_{SMES} (Case study 1)	RPD with Q_{SMES} (Case study 2)	RPD with combination of Q_C and Q_{SMES}
Control Variable	Q_{c18} = 0.1345, Q_{c25} = 0.1372, Q_{c53} = 0.0726.	Q_{SMES18} = 0.0158, Q_{SMES25} = 0.0233	Q_{SMES18} = 0.034, Q_{SMES53} = 0.042	Q_{c18} = 0.1170, Q_{c25} = 0.0950, Q_{SMES51} = 0.0353, Q_{SMES54} = 0.0200
P_{LOSS} (MW)	22.1137	20.9173	20.8891	20.4514

In this context, the DERL based optimisation characteristics were drawn as Figure 18 comprising all the P_{LOSS} optimisations for IEEE 57-bus system. From the Figure, it can be inferred that all the solutions including the optimal one showed global convergence while avoiding several local minima. Moreover, the convergence occurred earlier i.e., within the 30th generations for all the test cases.

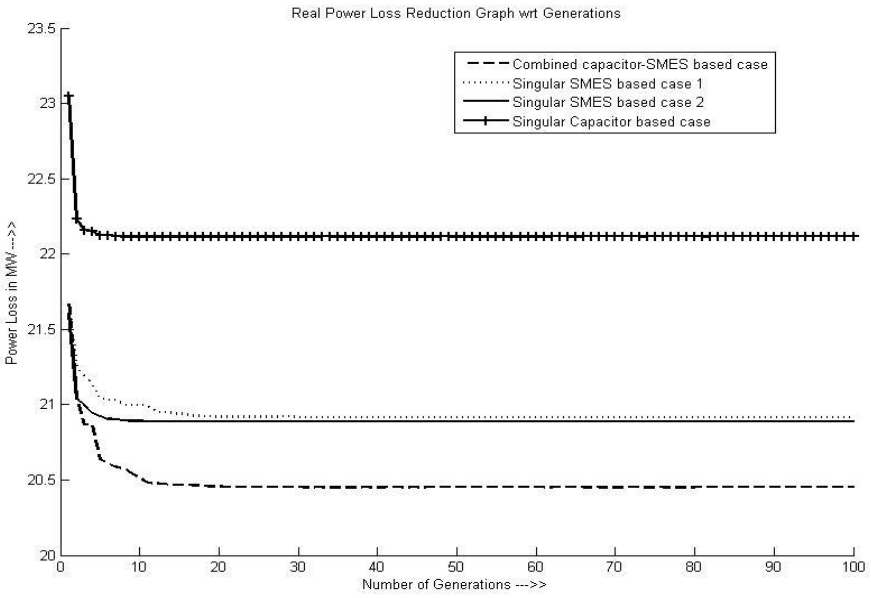

Figure 18. DERL based power loss optimization characteristics for IEEE 57-bus system

Moreover, to validate the performances of the proposed methods, the results were further compared with the few other meta-heuristics methods considering the same technological context as shown in Table 20. The comparisons shows reduced 8.80% P_{LOSS} by DERL technique compared to others methods obtained by optimal capacitive *var* compensations. In this context, the singular SMES helped to minimise 13.801% of P_{LOSS} which showed much improvement than the singular capacitor placement. Finally the combined capacitor-SMES *var* compensators were found to provide even better P_{LOSS} with 15.66% P_{LOSS} reduction w.r.t other meta-heuristics techniques. In this regards, it should be mentioned that the control variables were found within the stable operating limits while satisfying the all the equality and inequality constraints. This indicated the proficiency of the applied DERL method as well as the advanced *var* compensations for RPD as compared to others. Therefore, the DERL technique was further applied to solve the RPD problem for higher bus systems.

Table 20: Comparative study on meta-heuristics based fundamental RPD for IEEE 57-bus system

	DE [23]	CLPSO [40]	L-SaDE [250]	ICA [251]	IWO [251]	MICA-IWO [251]	Proposed DERL technique
Control Variables	V_g, t, Q_C						i. V_g, t, Q_C ii. V_g, t, Q_{SMES} iii. V_g, t, Q_C , Q_{SMES}
P_{LOSS} (MW)	25.0475	24.515	24.267	24.47	24.59	24.25	i. 22.1137 ii. 20.9032 iii.20.4514
% P_{LOSS} reduction	i. 11.713 ii. 16.546 iii. 18.350	i. 9.7952 ii.14.7330 iii. 16.576	i. 8.8734 ii. 13.861 iii. 15.723	i. 9.6293 ii. 14.576 iii. 16.423	i.10.070 ii.14.993 iii.16.830	i.8.809 ii.13.801 iii.15.664	-

7.4.1.4.5 DERL based Result Analysis for IEEE 118-Bus System (Test system 4)

Alike the previous case, DERL technique was applied to solve the RPD problem for the IEEE 118-bus system by controlling V_g, t and Q_C. Here, twelve buses were selected for shunt compensation to minimize active power loss. The optimal parameters for the proposed method were determined as N_p = 20, Gen_{max} = 40, C_R = 0.9 and $f_m \in (0,1)$ by considering 50 trial runs. Here, the minimum P_{LOSS} was reduced to 125.544 MW with the average and the worst results found as 125.825 MW and 126.5405 MW respectively. The capacitive *var* compensation based P_{LOSS} optimisation characteristics are further drawn in Figure 19 showing the best, average and the worst responses w.r.t the generation number. The Figure 19 showed the best value curve to converge at the optimal solution of 15th generation where the other two (worst and average) even found early convergences (nearly 10th generation). In this direction, one point to be noted that the operational strategy of the proposed DERL method helped to avoided several local convergence point successfully. Further, the DERL method provided fast global optimal convergence for all the cases. Moreover, to observe the precision as well as the accuracy of the DERL method, standard deviation of the 50 trial solutions such as P_{LOSS} was calculated by (126). This provided 0.464154 as the required standard deviation which indicated the proficiency of the proposed technique.

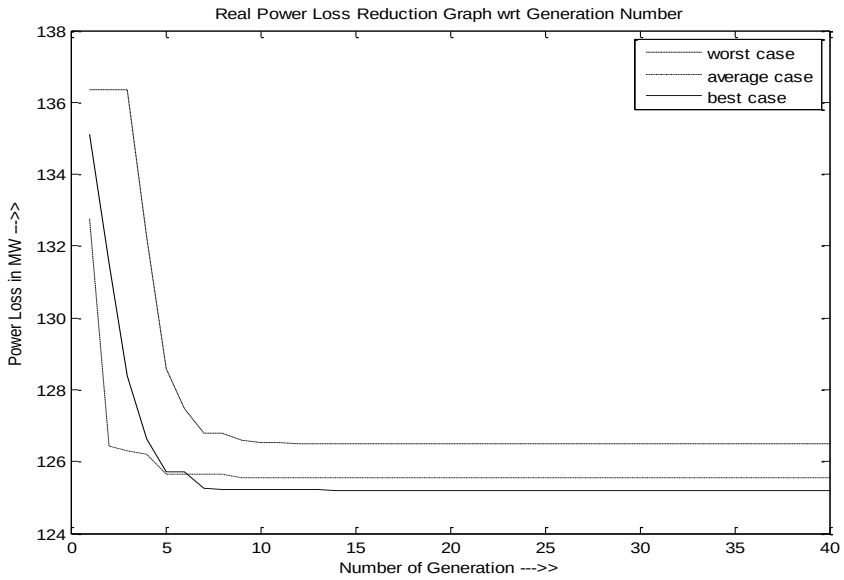

Figure 19. Power loss minimization by DERL for IEEE 118-bus system

Since, the restructured RPD issue is a major research area of the present power scenario, advanced *var* compensation was also considered here besides the capacitive *var* compensations. In this work, three different locations of singular SMES were integrated in the network as study 1 to study 3 to solve the fundamental RPD by DERL for the test system 4. Moreover, a combinations of capacitor-SMES were also considered as study 4 to solve the proposed problem.

Here, the control variables are considered to be V_g, t, Q_C and Q_{SMES}. The observations are shown in Table 21 which clearly indicated that all the control variables are maintained within the system operating limits [Appendix B2]. Therefore, the dynamic voltage profile of the system remain uninterrupted with reduced losses compared to capacitive *var* compensations. In this context, the power loss optimisations by advanced *var* compensations are also graphically plotted in Figure 20. Alike the other cases, the DERL based convergence characteristics as shown in Figure 20 provided the global convergence at the earlier generations (within 20^{th}) without being trapped into the local minima.

Table 21. DERL based fundamental RPD analysis by advanced *var* compensations in IEEE 118-bus network

	Study 1	Study 2	Study 3	Study 4
Control variables	Q_{SMES34} = 0.0332, Q_{SMES45} = 0.0454, Q_{SMES46} = 0.0569, Q_{SMES74} = 0.0196, $Q_{SMES107}$ = 0.0630, $Q_{SMES110}$ = 0.0529.	Q_{SMES34} = 0.0102, Q_{SMES44} = 0.0353, Q_{SMES48} = 0.0409, Q_{SMES79} = 0.0235, Q_{SMES82} = 0.0329, $Q_{SMES110}$ = 0.0446.	Q_{SMES34} = 0.0198, Q_{SMES46} = 0.0252, Q_{SMES74} = 0.0206, Q_{SMES83} = 0.0204, $Q_{SMES105}$ = 0.0288, $Q_{SMES110}$ = 0.0299.	Q_{C44} = 4.6538, Q_{C45} = 6.4261, Q_{C48} = 9.5934, Q_{C83} = 1.3446, Q_{C105} = 5.3987, Q_{C107} = 2.5255, Q_{SMES34} = 0.0198, Q_{SMES46} = 0.0252, Q_{SMES74} = 0.0206, $Q_{SMES110}$ = 0.0299.
P_{LOSS} (MW)	125.11	124.601	124.272	123.591

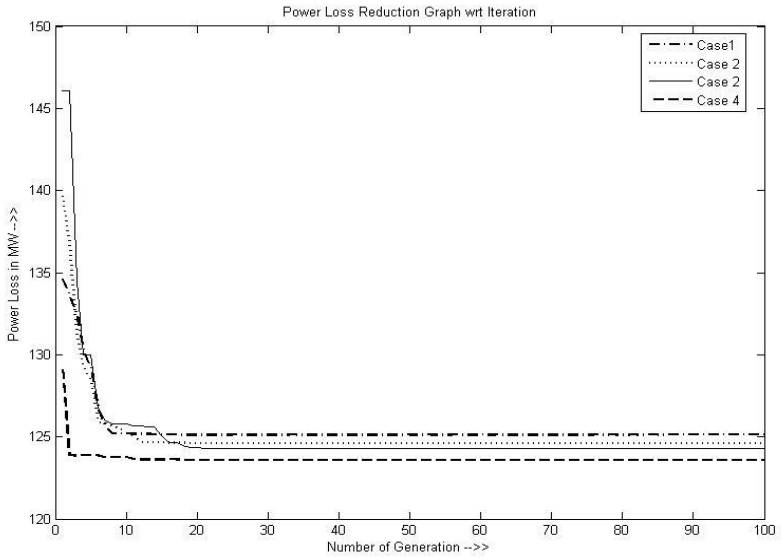

Figure 20. Power loss optimization by DERL based advanced *var* compensation in IEEE 118-bus system

Finally, to validate the proficiency of the proposed optimisation method, its performances were compared with other few meta-heuristics methods considering same network configuration of the proposed problem shown in the Table 22. The comparisons demonstrated to reduce minimum 1.94% P_{LOSS} by DERL technique compared to others methods for optimal capacitive *var* compensations (Study 1). In this context, both of the singular SMES based studies (Study 2 and Study 3) provided better responses over Study 1. Amongst them, Study 3 derived 3.15 % of P_{LOSS} which showed much improved response than the singular capacitor placement (Study 3). Finally the combined capacitor-SMES *var* compensators (Study 4) accomplished even better P_{LOSS} with minimum 3.68% P_{LOSS} reduction w.r.t other meta-heuristics techniques. From the Table 22, it can be concluded that proposed

results has been showing a steady improvement starting from capacitive *var* compensation to var compensation based on combination of capacitor-SMES. In this regards, the control variables of the proposed problem were found within the stable operating limits such that it maintained dynamic voltage limit within the network.

Table 22. Comparative study in the view of DERL on power loss optimizations for IEEE 118-bus system

	L-SACP-DE [232]	CGA [35]	SPPSO-07 [247]	DE [23]	Proposed DERL based solution i. Singular Q_C ii. Singular Q_{SMES} iii. Combined Q_C and Q_{SMES}
P_{LOSS} (MW)	141.79864	139.41498	139.27522	128.318	i. 125.825 ii. 124.272 iii. 123.591
% P_{LOSS} reduction w.r.t proposed method	i. 11.2650164 ii. 12.3602314 iii.12.8404899	i.9.7478621 ii.10.8618027 iii.11.3502724	i.9.65729582 ii.10.7723542 iii.11.2613141	i.1.94282953 ii.3.15310401 iii.3.68381677	-

Meanwhile, it has been noticed that the DERL technique has been proved to be very efficient; however the optimal parameters particularly the N_p are required to be higher which therefore consumes more computational time. To avoid this crisis, one advanced swarm intelligence based clever algorithm namely Cuckoo Search Algorithm (CSA) was considered to be applied to these cases. It has been evidenced [244] that by a moderate operational ranged parameters, CSA can generate optimal solutions for problems of different dimension.

7.4.1.5 CSA Technique based Result Analysis

Initially, the CSA technique was applied to solve the RPD problem for IEEE 14-bus system.

7.4.1.5.1 Result Analysis for Test System 1 by CSA

In this work, CSA was finally applied to solve RPD by controlling V_g, t and Q_C considering a small test system likely the IEEE 14-bus system. Here, by varying n from 10, 15 and 20 three sets of data were obtained. Amongst them the optimal solution providing parameters were considered for the optimisation process. Here, the parameters were found as n = 20, *No. of iterations* = 150 and p_a =

0.25. In this work, the RPD was investigated by two ways. Initially, P_{LOSS} was minimized and the corresponding voltage deviation (V_{dev}) was observed and vice-versa. Therefore, the initial observations optimised the P_{LOSS} to 12.9575 MW when V_{dev} was found 0.2460 V. In the second approach, V_{dev} has been minimized and corresponding P_{LOSS} was measured as 13.3641 MW at 0.1052 V. Now, comparing these two approaches, it has been observed that the case 1 provided significant loss reduction with reduced voltage deviation. The case 2 optimised the V_{dev} to large extent but the reduction in P_{LOSS} was not up to the expectations. Therefore, the first one will be considered as the final optimal solution to the RPD. However, the control variables were obtained within their standard operating limits therefore the proposed method was able to maintain system dynamic voltage limit for both the cases. Now, the optimisation characteristics of P_{LOSS} and V_{dev} are drawn in Figure 21 (i-ii) respectively.

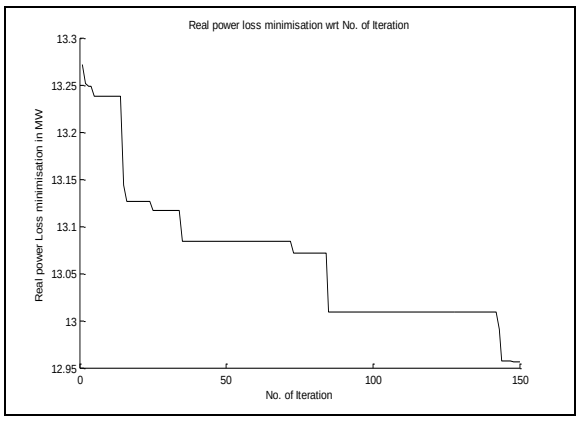

Figure 21. (i) Power loss

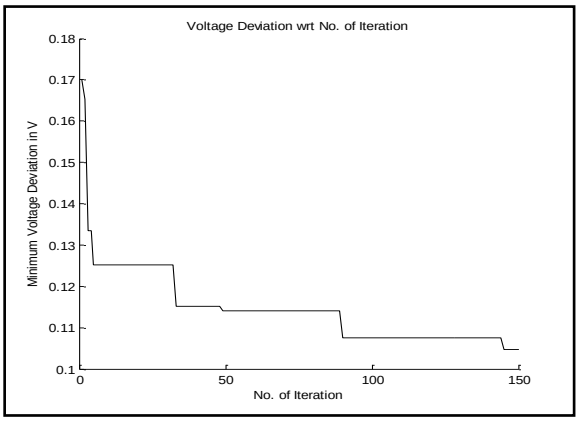

Figure 21. (ii) Voltage deviation

Figure 21. CSA based optimizations for IEEE 14-bus system (i) & (ii)

The convergence characteristics of both the fitness function demonstrated that the applied Lévy flight of the proposed CSA helped to avoid local traps of the several local optima rather to converge at the global optima at the end of the set iteration count.

Finally, to justify the efficiency of the proposed method, a comparative study has been conducted considering few meta-heuristics technique applied to solve the RPD with same configuration shown in Table 23. The comparative study concluded that the proposed method of CSA generated much improved results compared to other methods.

Table 23. CSA based comparative study on power loss optimization for IEEE 14-bus system

	PSO [247]	SQP [32]	DE [32]	SARGA [33]	Proposed Method CSA	
					Case 1	Case 2
P_{LOSS} (MW)	13.32	13.246	13.239	13.21643	P_{LOSS} = 12.9575 MW, V_{dev} = 0.2460 V	V_{dev}=0.1052 V, P_{LOSS} =13.3641 MW
% reduction in P_{LOSS} w.r.t CSA	2.72	2.19	2.13	1.96	-	-

Since, the CSA method has been found to work successfully to solve the proposed problem, it has been considered further to solve the RPD with different case studies for another larger IEEE network of 118 bus system.

7.4.1.5.2 CSA based Result Analysis for Test System 4

With reference to its proficient performances, the CSA technique was further applied to solve the RPD issue for a large network of IEEE 118-bus system. Here, Here, the optimal parameters of the proposed method were found as n = 20, *No. of iterations* = 150 and p_a = 0.25 after considering 100 trial runs. In this work, the RPD was investigated by three ways. Initially the P_{LOSS} has been optimised to 124.982 MW by controlling V_g, t, Q_C as case 1. Further to obtain more reliable and improved output in the view of restructured power scenario, the CSA based RPD was optimised by controlling Q_{SMES} in place of Q_C as case 2. Here, the other network parameters remained unchanged w.r.t case 1. This provided P_{LOSS} to be equal to 122.512 MW for case 2. Moreover, to ascertain more economic and sustainable output, a combination of capacitors-SMES were applied to solve the proposed problem as case 3 in addition to the control of V_g, t. This approach provided the P_{LOSS} as 119.52 MW. In this regards, the control variables were found to be within system operating margin which further helped to maintain system dynamic voltage limit. The optimal size and the locations of the *var* compensators for case 1 to case 3 are shown in Table 24. Moreover, the optimisation characteristics are also observed in Figure 22 which showed the global convergence of the optimal solutions while avoiding several local minima points.

Table 24. Case studies on sizing and allocation of different *var* compensators by CSA for IEEE 118 bus system

Cases	Size and locations of *var* compensators (p.u.)
Case 1	Q_{C34} = 4.3621, Q_{C44} = 9.5728, Q_{C45} = 10.00, Q_{C46} = 10.0, Q_{C48} = 3.0941, Q_{C74} = 6.4426, Q_{C79} = 20.00, Q_{C82} = 14.3202, Q_{C83} = 6.3565, Q_{C105} = 20.00, Q_{C110} = 3.5479
Case 2	Q_{SMES09} = 0.0420, Q_{SMES34} = 0.0106, Q_{SMES44} = 0.0261, Q_{SMES45} = 0.042, Q_{SMES46} = 0.042, Q_{SMES48} = 0.0188, Q_{SMES83} = 0.0188, $Q_{SMES110}$ = 0.0261
Case 3	Q_{C34} = 3.1515, Q_{C45} = 3.7210, Q_{C46} = 1.7620, Q_{C48} = 5.5240, Q_{C79} = 6.6369, Q_{C82} = 4.5105, Q_{C83} = 1.1151, Q_{SMES7} = 0.0200, Q_{SMES33} = 0.0300, Q_{SMES96} = 0.0100, Q_{SMES97} = 0.0200, $Q_{SMES114}$ = 0.0200

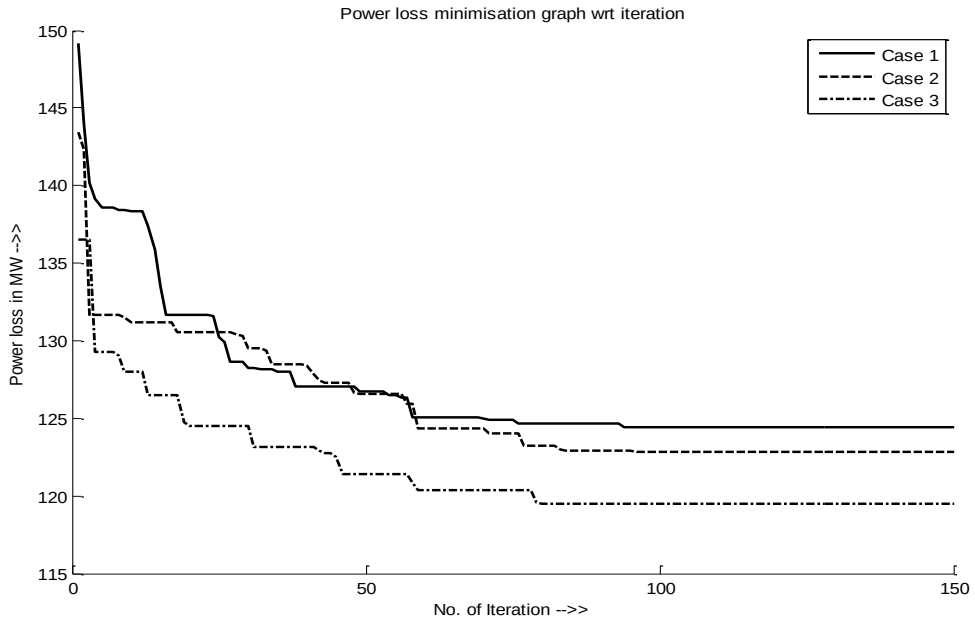

Figure 22. Power loss optimizations by CSA for IEEE 118-bus system

To validate the proposed method, the obtained result was compared with other meta-heuristics techniques based solutions which were determined considering the identical system characterised by similar equality and inequality constraints as shown in Table 25. The comparisons showed to reduce 3.03% P_{LOSS} by DERL technique compared to others methods for optimal capacitive *var* compensations. In this direction, the singular SMES generated 4.25% of P_{LOSS} which is better than the singular capacitor placement. Finally the combined capacitor-SMES *var* compensators provided much improved P_{LOSS} with minimum 6.85% P_{LOSS} reduction w.r.t other meta-heuristics techniques.

Moreover the SMES and combined SMES placement achieved 1.24% and 3.93% more P_{LOSS} reduction compared to capacitor based solutions. The observations proved the proficiency of the proposed CSA technique compared to others in the applied domain of *var* compensations.

Table 25. Comparative study on different cases for RPD by CSA for IEEE 118-bus system

	IPM [31]	PSO [11]	CLPSO [11]	DE [2]	Proposed CSA
Control variables used	V_g, t, Q_c				i. V_g, t, Q_c ii. V_g, t, Q_{SMES} iii. V_g, t, Q_C and Q_{SMES}
P_{LOSS} (MW)	132.110	131.99	130.96	128.318	i. 124.4131 ii. 122.8597 iii. 119.5200
% P_{LOSS} reduction	i. 5.82612974 ii. 7.00196806 iii. 9.52993717	i. 5.74051064 ii. 6.91741799 iii. 9.44768543	i. 4.99916005 ii. 6.18532376 iii. 8.73549175	i.3.04314282 ii. 4.25372902 iii. 6.85640362	-

The above result analyses are based only on the technical aspects of the fundamental RPD issues without considering the complexities of the deregulated power scenarios. As stated earlier, all advanced economic countries and few of the developing economic countries nowadays have restructured power market where double auction power transactions frequently occur. Amongst these transactions, bilateral ones are very common in an inter-regional network which require special attention in the view of the restructured RPD.

7.4.2 Restructured Reactive Power Dispatch with Bilateral Power Transactions in Double Auction Mode

To emphasize the impact of bilateral power transactions on economic RPD, two case studies are considered here. The first study investigates the RPD solutions for a fixed double auction bilateral power transaction by a comparable *var* compensator. This study also determines the economics of the *var* compensators in the form of reduced congestion rent which further helped to improve the fundamental global welfare of the market participants.

In the second study, RPD characterised by 12-h variable double auction bilateral power transactions is investigated considering some technical and economic aspects. Technically the loss minimisation aspects and dynamic voltage limit crossover analysis by suitable advanced *var* compensation are considered first. In the economics part, the Pareto efficient power transactions and its economic impact on the global welfare are involved. In this context, planned bidding of the participants is also required. Moreover, economics of the *var* compensators in the form of reduced merchandising surplus are accommodated to the fundamental global welfare to find its improvement in the restructured scenario.

7.4.2.1 Economic Reactive Power Dispatch and Dynamic Voltage Crossover Limit Analysis

In this work, the RPD based optimisations for different case studies involving bilateral power transaction (BPT) were considered by Cuckoo Search Algorithm (CSA). Initially, the proposed problem was optimised by controlling V_g and t without incorporating any *var* compensators. This generated dynamic voltage limit crossover issues which was then attempted to be mitigated by integrating adequate *var* compensations. Therefore, the proposed problem was revisited one by one by different *var* compensators such as shunt capacitors, synchronous condensers (Q_{SC}), SMES (Q_{SMES}) and some of their combinations with other control variables of V_g and t.

Here, IEEE 118-bus system was considered as test system 4 where 546 MW of power was traded by bilateral power transactions [252]. The optimal parameters for the proposed CSA technique was chosen as n = 25, maximum number of iteration = 150 and p_a = 0.25 considering 100 runs. The upper and lower boundary limit of the variables such as V_g, t, Q_c were considered from Appendix Table A1, Q_{SC} from Appendix B1 and Q_{SMES} from Appendix B2. The participant buses of the bilateral power transactions are available elsewhere [252] whereas the amount of individual transacted power by each bus is shown in Table 26. These traded powers by each bus were optimally settled by such a way that the participants could acquire higher economic benefit through the bidding. This is discussed in detail in section 7.4.2.1.3.

Table 26. Schedule of bilateral power transaction in case of IEEE 118-bus system

No. of Bilateral Transaction	Buses as power supplier	Power injections in MW	Buses as power consumer	Power consumption in MW
T_1	76	110	75	200
T_2	1	186	07	280
T_3	6	250	07	66

7.4.2.1.1 RPD Analysis for Bilateral Power Transactions

As stated, the RPD problem is technically analysed initially without *var* compensators. Then shunt capacitors and different combinations are tried for BPT analysis.

- **Case 1: RPD with BPT Analysis without Var Compensators**

Here, the CSA based RPD issue characterised by BPTs was initially solved by optimizing V_g and t without considering any *var* compensating devices. This reduced the power loss (P_{LOSS}) to 137.4398 MW after fifty trial runs. The optimal convergence of the P_{LOSS} is given in Figure 23. It showed that during the 150 iterations, there were several local optimum points till the 90th iteration where the P_{LOSS} might have converged. But the presence of Lévy flight due to its heavy step length distribution prevented the local convergence by exploring the search space extensively. This further helped P_{LOSS} to converge at the global minima. In this conjunction, the control variable were obtained within the standard operating ranges however the security constraints (load bus voltages) of the network was found to fluctuate near the boundary value. Even in the three buses (($j\_enhanced^{th}$) namely 9th, 30th and 37th, the voltages were observed to violate the boundary value of 0.95p.u. to 1.10 p.u. This therefore influenced the other associated buses (j) negatively. Since, the voltage difference between the affected and associated buses were increased compared to the normal conditions, this situation caused the dynamic voltage limit crossover. Here, the voltages of the affected buses ($V_{i\_enhanced}$) are shown in Table 27 which also included the associated bus voltages (V_j). In the Table 27, out of the thirteen buses, two buses namely 9th and 30th are marked as critically overshooted voltage buses which fixed themselves at 1.1168 p.u. and 1.1146 p.u. during the power transactions. This invited dynamic voltage limit crossover issue majorly in terms of enhanced line current flow and power losses for the eleven lines. In this direction, the range of the factors CEF_{ij} and $PLEF_{ij}$ (as described in section 4.3.6) are shown in Table 28 including the most critically violated line ($CEF_{26\text{-}30}$ and $PLEF_{26\text{-}30}$). These factors are also plotted in Figure 24 and Figure 25 respectively to indicate that out of eleven lines,

eight lines based CEF_{ij} and $PLEF_{ij}$ are found between the 1.08 to 1.52 and 1.18 to 2.32 respectively. Amongst all the voltage deviated lines, the 30th - 26th line showed highest dynamic voltage limit crossover in terms of CEF_{ij} and $PLEF_{ij}$ as 1.52 and 2.32 respectively. This was caused due to the higher voltage deviation of the 30th bus. This caused the sudden rise to these factors at the specified sector. Therefore, the dynamic voltage limit crossover needs critical attentions in terms of *var* compensations.

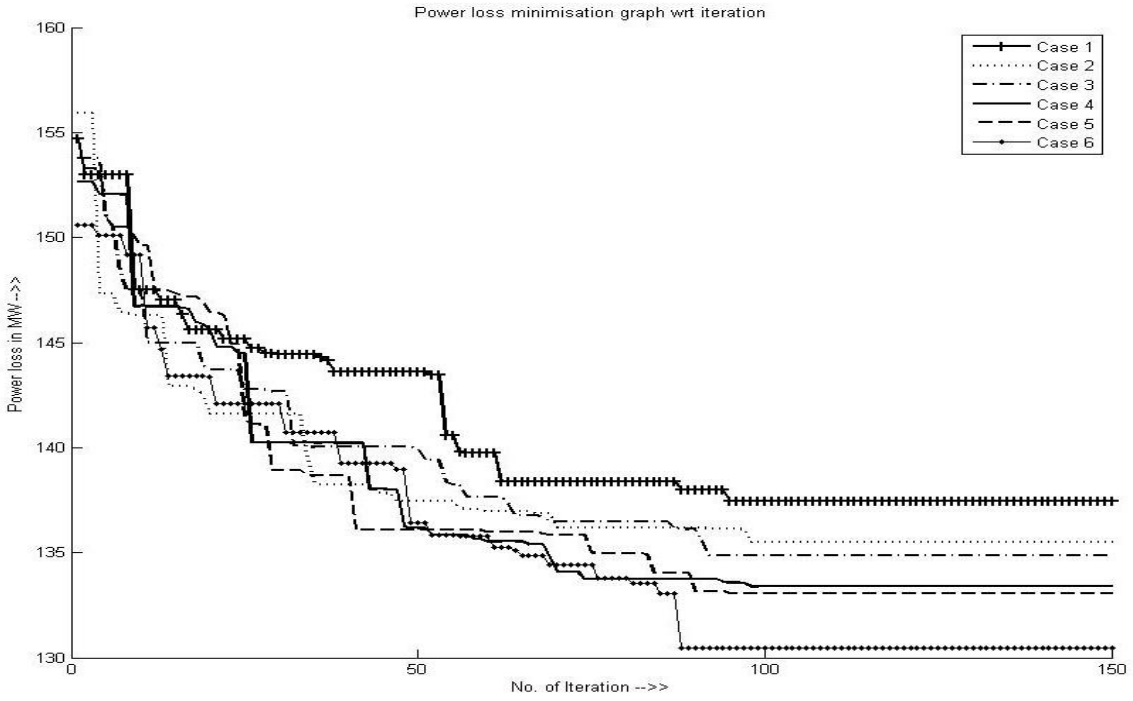

Figure 23. Power loss optimization curves involving bilateral power transactions by CSA for the case 1- case 6

Table 27. Bus voltage profile (*V*) of the distinguished buses during the bilateral power transaction

Representation of $j\_enhanced^{th}$ and j^{th} bus	*V* in p.u. for bilateral power transaction					
	Case 1	Case 2	Case 3	Case 4	Case 5	Case 6
8	1.10	1.0427	1. 0958	1.0999	1.0925	1.0907
9	1.1168	1.0694	1.10	1.10	1.10	1.10
10	1.10	1.0324	1.0805	1.10	1.0635	1.0839
17	1.0375	1.0549	1.0677	1.0692	1.0674	1.0576
26	1.0722	1.0904	1.0578	1.0914	1.10	1.0766
30	1.1146	1.0781	1.10	1.0904	1.10	1.0793
33	1.0216	1.0402	1.0388	1.0348	1.0383	1.0309
34	1.0300	1.05	1.03	1.05	1.030	1.0300
35	1.0250	1.05	1.0368	1.0443	1.0193	1.0317
37	1.1068	1.0657	1.0478	1.0628	1.0447	1.0444
38	1.0542	1.0684	1.10	1.0958	1.10	1.0611
39	1.0698	1.0584	1.0452	1.0661	1.0548	1.0140
40	1.0618	1.0638	1.0536	1.0756	1.0703	1.0067

Table 28 Dynamic voltage limit crossover analysis for different *var* compensators

	Case 1	Case 2	Case 3	Case 4	Case 5	Case 6
Range of *CEFij*	1.08 to 1.52	0.05 to 0.514	0.028 to 1.00	0.00 to 0.6880	0.00 to 1.00	0.0213 to 0.51179
$CEF_{26\text{-}30}$	1.52	0.08761	0.3915	0.007	0	0.02133
Range of *PLEFij*	1.18 to 2.32	0.0027 to 0.264	0.00083 to 1.0	0.00 to 0.473	0.00 to 1.0	0.00045 to 0.261
$PLEF_{26\text{-}30}$	2.32	0.00767	0.15325	5×10-5	0	4.5×10-4

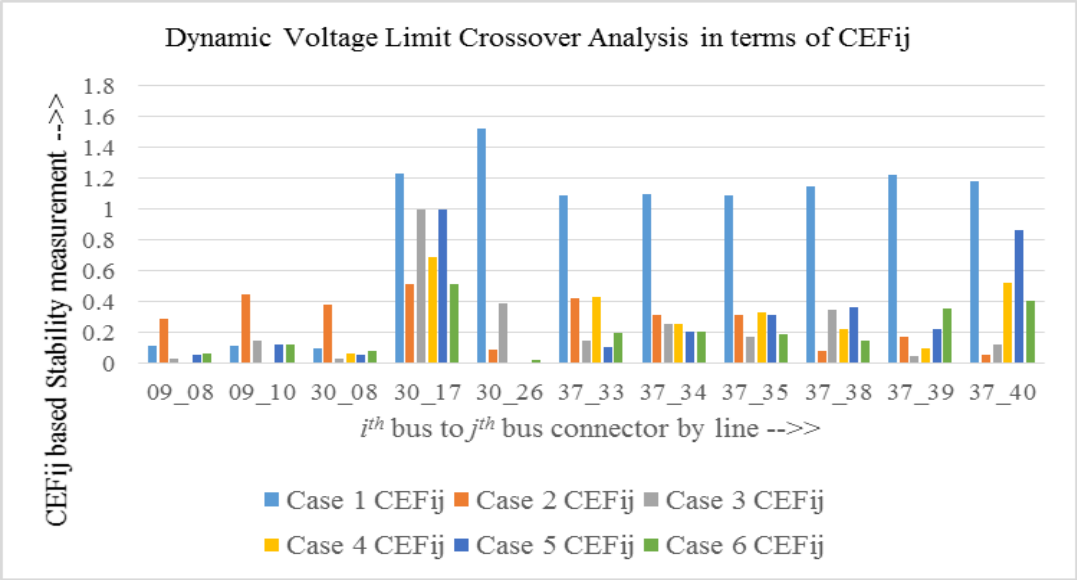

Figure 24. Dynamic voltage limit crossover analysis during the bilateral power transactions in terms of CEF_{ij} for the case 1- case 6

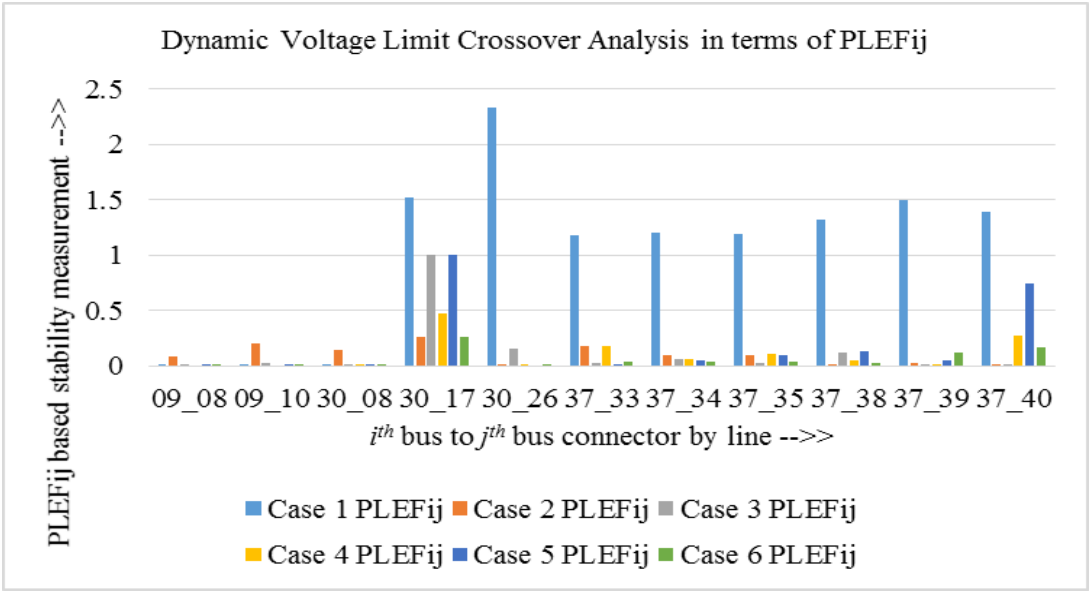

Figure 25. Bilateral power transactions oriented dynamic voltage limit crossover analysis in terms of $PLEF_{ij}$ for the case 1- case 6

- **Case 2: BPT based RPD Analysis by Shunt Capacitors**

To handle the dynamic voltage limit crossover as generated in case 1, Q_C placements in twelve buses were considered in addition to the control of V_g and t. This is considered as case 2 here. P_{LOSS} was found minimized to 135.4977 MW by conducting fifty trial runs which was also less compared to the case 1. The characteristics curve of the P_{LOSS} optimization are shown in Figure 23 which showed that there were a number of local convergence points where P_{LOSS} were supposed to trap till the 100^{th} iterations. But the CSA involved Lévy flights searched the population space thoroughly and finally provided the global convergence. Further, all the control variables were obtained here within the stable operating limits amongst them the optimal values of the Q_C is given in Table 29 (i).

Table 29. Var compensators as control variable at different buses (i) Case 2 based Q_c (ii) Case 3 based QSC (iii) Case 4 based Q_C (iv) Case 4 based Q_{SC} (v) Case 5 based Q_{SMES} (vi) Case 6 based Q_C (vii) Case 6 based Q_{SMES}

Table 29. (i) Case 2 based Q_c as control variable at different buses

Bus Numbers	34	44	45	46	48	74	79	82	83	107	110
Value in p.u.	1.6940	9.6243	6.4094	10.0	0.9330	3.6458	10.3351	14.5382	0.2630	3.8433	2.2275

Apart from the P_{LOSS} study, the dynamic voltage limit crossover issue which was raised in case 1 was also observed here. The investigations showed that the identified buses ($j\_enhanced^{th}$) of the previous case remained within the prefixed boundary value. The case 2 based bus voltages ($V_{j\_enhanced}$ and V_j) as shown in Table 27 lied between 1.0324 p.u. -1.0904 p.u. This also helped to solve the problem of dynamic voltage limit crossover in terms of reducing CEF_{ij} and $PLEF_{ij}$. These are plotted in Figure 24 and Figure 25 respectively. Moreover, the operating ranges of the CEF_{ij} and $PLEF_{ij}$ including the case 1 based most disturbed line based data is presented in Table 28. This showed that all the eleven lines based CEF_{ij} are obtained within 0.052 p.u. to 0.514 p.u. In this regards the $PLEF_{ij}$ are found to be within 0.0027 p.u. to 0.264 p.u. Here the operating ranges of CEF_{ij} and $PLEF_{ij}$ and exact value of the most congested line of case 1 are found as 0.08761 p.u. and 0.00767 p.u. respectively. Hence the case 2 based statistics indicated a steady management of the dynamic voltage limit crossover issue with higher losses. The reason for obtaining such a low value might be due to the closeness of the voltages of the specified lines as 1.0781 p.u. and 1.0904 p.u. To obtain better performance, the proposed problem is revisited by the synchronous condenser in place of capacitors.

➢ **Case 3: RPD characterized by BPT involving Synchronous Condenser (SC)**

Here, three buses were optimally chosen by the CSA to place the Q_{SC} in addition to the control of V_g and t in the chosen network to handle the proposed problem. This minimized the P_{LOSS} to 134.1473 MW considering fifty trial runs. The convergence characteristic is given in Figure 33 which showed that P_{LOSS} was supposed to trap in few local convergence points at the initial iterations. But the extensive searching by the incorporated Lévy flight helped to converge P_{LOSS} at the global minima. In this connection, all the control variables were obtained within the desired margin amongst which the optimal values of the Q_{SC} with bus locations are given in Table 29 (ii).

Table 29. (ii) Case 3 based Q_{SC} as control variable at different buses

Bus numbers of Q_{SC}	30	38	64
Value in p.u.	0.0587	0.2385	0.0659

In addition to the P_{LOSS} minimization, the voltage profile improvement of the disturbed bus voltages of the case 1 were observed to be improved by the Q_{SC} placement. Here the case 3 based voltage profile in terms of $V_{j\_enhanced}$ and V_j are shown in Table 27 which is found to be within 1.03 p.u. -1.10 p.u. This gives reduced value of CEF_{ij} and $PLEF_{ij}$ which are plotted in Figure 24 and Figure 25 respectively. Both the Figure 24 and Figure 25 show that the CEF_{ij} and $PLEF_{ij}$ are obtained between 0.028 p.u. to 1.0 p.u. and 0.00083 p.u. to 1.0 p.u. respectively for the considered eleven lines. Amongst them the most congested line based CEF_{ij} and $PLEF_{ij}$ as identified in the case 1, are found as 0.39147 p.u. and 0.15325 p.u. respectively as shown in Table 28. These are found better compared to the case 1. Hence the case 3 provided dynamic voltage crossover limiting with higher losses by the singular Q_{SC} placement. Further to obtain reliable output, a combination of Q_C and Q_{SC} were integrated to the network.

➢ **Case 4: BPT oriented RPD by the combinations of Capacitor and Synchronous Condenser**

Here, two buses for Q_{SC} and seven buses for Q_C were optimally chosen by CSA technique to solve the proposed problem in addition to the control of V_g and t. The combined *var* compensators reduced the P_{LOSS} to 133.3838 MW considering fifty trial runs. The convergence characteristic is plotted in Figure 34 which inferred that although there are several local optimum solutions where P_{LOSS} could easily be

confined. But the potential involvement of the Lévy flight helped to prevent the trapping to local convergence rather to provide global optimum solution. The optimal values of the Q_C and Q_{SC} with bus locations are given in Table 29 (iii) and (iv) respectively. Further the case 4 based % P_{LOSS} reduction compared to case 1, case 2 and case 3 are obtained as 2.95, 1.56 and 0.569 respectively. Though the improvement is low, but it has been derived by the combined *var* compensators as described in this case 4.

Table 29. (iii) Case 4 based Q_C as one of the control variable of combined *var* compensators at different buses

Bus numbers of Q_C	34	44	46	48	74	83	105
Value in p.u.	3.5856	0.4778	4.2847	2.6340	2.1653	5.0571	0.7527

Table 29. (iv) Case 4 based Q_{SC} as another control variable of combined *var* compensators at different buses

Bus numbers of Q_{SC}	59	63
Value in p.u.	0.2448	0.1432

In accordance to the P_{LOSS} minimization, the case 4 based voltage profile improvements in the disturbed buses of the case 1 are shown in Table 31 in terms of $V_{j\_enhanced}$ and V_j. These were found within 1.0348 p.u. -1.10 p.u. The reduced voltage profile influenced the network positively in terms of reduced CEF_{ij} and $PLEF_{ij}$ which are plotted in Figure 24 and Figure 25 respectively. Both the Figure 24 and Figure 25 demonostrate that the CEF_{ij} and $PLEF_{ij}$ are obtained in between 0.0 to 0.688 and 0.0 to 0.473 respectively for the considered eleven lines. Amongst them the CEF_{ij} and $PLEF_{ij}$ of the utmost congested line of case 1 are found here as 0.007 and 5×10^{-5} respectively indicating very positive results in terms of dynamic voltage limit crossover issue. Receiving very close voltage value between the connecting buses as 1.0904 p.u. and 1.0914 p.u. for the specified line was the major cause of obtaining such improved results by the combined Q_C and Q_{SC} placement. These result including the operating ranges of the CEF_{ij} and $PLEF_{ij}$ are shown in Table 28. Here, the case 4 solved the dynamic voltage limit crossover problem to some extent but power loss minimisation needs to be improved more. Therefore, to obtain improved results in the backdrop of modern restructured scenario, SMES device was incorporated in the chosen network.

➢ **Case 5: RPD with BPT with intregated SMES**

Here, ten buses were chosen optimally by CSA to handle the congestion as well as the RPD issue in addition to the control of V_g and t which reduced the P_{LOSS} to 133.06 MW while conducting fifty trial runs. The convergence characteristic is given in Figure 23 which showed that the P_{LOSS} has got several local optima until the 90th iteration. However instead of trapping into it, the P_{LOSS} finally converged at the global optima with the involvement of Lévy flight by extensive searching of the population space. Alike the other previous cases, the control variables were obtained here within the stable operating margins. Amongst them the optimal values of the Q_{SMES} with bus locations are given in Table 29 (v).

Table 29. (v) Case 5 based Q_{SMES} as control variable at different buses

Bus numbers of Q_{SMES}	09	34	44	45	46	48	74	83	105	110
Value in p.u.	0.0108	0.0362	0.0420	0.0420	0.0420	0.0420	0.0188	0.0420	0.0188	0.0420

In this conjunction to P_{LOSS} minimization, the voltage profiles of the disturbed buses of the case 1 were observed to be improving by the Q_{SMES} placement. Here the case 5 based voltage profile in terms of $V_{j\_enhanced}$ and V_j are obtained within 1.03 p.u. -1.10 p.u. as shown in Table 27. This indicated dynamic voltage limit issues in terms of reduced CEF_{ij} and $PLEF_{ij}$ as plotted in Figure 24 and Figure 25 respectively. The figures showed that out of the eleven lines the CEF_{ij} and $PLEF_{ij}$ values of most congested line (30th-26th) of the case 1 is found here as 0.0 due to equal magnitude of the voltage of the connecting buses of the specific lines as 1.10 p.u.. Besides this, the CEF_{ij} and $PLEF_{ij}$ of the other ten congested lines were found within 0.0 to 1.0. Therefore, an improved solution to the dynamic voltage limit crossover with lesser loss reduction was derived here by the optimal Q_{SMES} placement. Hence, to obtain more sustainable output in the backdrop of modern advanced deregulated power environment, a combination of capacitor and SMES device was tried for the chosen network.

➢ **Case 6: BPT involved RPD by the Combination of Capacitor and SMES**

In these investigations, a combination of seven capacitors and five SMES devices were optimally proposed by CSA in the network in addition to the control of V_g and t to manage the congestion of the restructure RPD. Here, the P_{LOSS} was reduced to 130.473 MW after considering fifty trial runs. This result was also found lowest amongst all the considered cases. The convergence characteristic is given in Figure 23 which illustrated two major aspects. Firstly, the curve showed a number of local converging points where the P_{LOSS} was supposed to dip but the heavy step length of the Lévy flight made it possible to avoid these local optimas. Secondly it had been observed that P_{LOSS} finally

converged at the global optima where the extensive searching by the Lévy flight played a very vital role. Here, the case 6 based percent P_{LOSS} reduction w.r.t case 1, case 2, case 3, case 4 and case 5 were found as 5.07, 3.70, 3.23, 2.18 and 1.95 respectively. This indicated an improved P_{LOSS} management by the combined Q_C and Q_{SMES} devices compared to other *var* compensators. In this regards, all the control variables were found converged within the operating limits. The optimal values of the Q_C and Q_{SMES} with bus locations are given in Table 29 (vi and vii) respectively.

Table 29. (vi) Case 6 based Q_C as one of the control variable of combined *var* compensators at different buses

Bus numbers of Q_C	44	45	46	79	82	83	105
Value in p.u.	0.8206	5.2083	3.6817	9.0706	10.0	9.7235	8.0345

Table 29. (vii) Case 6 based Q_{SMES} as another control variable of combined *var* compensators at different buses

Bus numbers of Q_{SMES}	41	44	94	106	114
Value in p.u.	0.0203	0.0381	0.0408	0.0318	0.0403

In conjunction to the P_{LOSS} minimization, the voltage profiles of the identified buses of the case 1 were observed to improve in case 6 which are shown in Table 27 in terms of V_i and V_j. Here the voltage profile of the V_i and V_j were maintained within 1.0067 p.u. -1.10 p.u. which was also reflected in terms of reduced network congestion indicated by CEF_{ij} and $PLEF_{ij}$. The proposed factors are projected in Figure 24 and Figure 25 respectively for the considered eleven lines. Both the Figure 24 and Figure 25 showed that the CEF_{ij} and $PLEF_{ij}$ were obtained between 0.0213 to 0.51179 and 0.00045 to 0.261 which was found to be minimum amongst the six cases. Amongst them for the most congested line of case 1 the CEF_{ij} and $PLEF_{ij}$ were found here as 0.02133 and 4.5×10^{-4} respectively. This is because the specified line voltages comprising of V_{30} and V_{26} were found here as 1.0793 p.u. and 1.0766 p.u. respectively which were very close to each other. It therefore, provided the CEF_{ij} and $PLEF_{ij}$ to such nominal value as shown in Table 28. Hence it could be concluded that the combined Q_C and Q_{SMES} placement were able to solve the dynamic voltage limit crossover issues with reduced power losses.

Since, all the *var* compensators were able to maintain dynamic voltage limit satisfactorily, investigations were summarized comparatively based on reduced P_{LOSS} and % P_{LOSS} reduction w.r.t case 1. This is shown in Table 30. Amongst all the *var* compensations based study, the case 6 showed

the maximum reduction in P_{LOSS} as well as % P_{LOSS} reduction w.r.t the case 1. In this regards case 3, case 4 and case 5 were found to have reduced P_{LOSS} as well as % P_{LOSS} reduction noticeably. However case 2 showed minimum percent of P_{LOSS} reduction in the considered study. In this regards, the Table 30 comprehended that the case 2 and case 3 based P_{LOSS} were nearly equal and case 4 and case 5 based P_{LOSS} were very close to each other. This inferred that amongst case 2, 3 and case 4, 5 either any of the *var* compensators might be opted for RPD involving the BPT issue depending upon its technical aspects although the case 6 based solutions was always be appreciated to be adopted where it would be fitted suitably.

Table 30. Case studies on power loss and percent of power loss reduction during the bilateral power transaction

	Case 1	Case 2	Case 3	Case 4	Case 5	Case 6
P_{LOSS} (MW)	137.4398	135.4977	134.8399	133.3838	133.0665	130.4713
% P_{LOSS} reduction w.r.t. Case 1	-	1.4130	1.8916	2.9511	3.1819	5.0702

Besides the reactive power handling of the restructured RPD, the economics of such is another governing factor of the deregulated power scenario which thereby needs closer observations.

7.4.2.1.2 Economics of Var Compensation with Global Welfare Analysis

Here, the economics part was distributed into two major categories as stated in section 5 which are elaborated in the following sections:

7.4.2.1.2.1 Economics of the Var Compensators

As evidenced from the Table 30, it is clear that *var* compensators were successfully reducing the P_{LOSS} in a significant amount in comparison to case 1. It therefore derived incentive returns in terms of monetary benefit. Considering 100 $/ MWh as the incentive return for loss minimization, the net incentive returns as benefit due to P_{LOSS} optimization were obtained elsewhere [177]. The net incentive returns benefit and the operating costs of the proposed devices for the respective cases are shown in Table 31. Finally the net monetary benefits due to *var* compensation for the case 2 to case 6 are given in Table 31.

Table 31. Economics of the *var* compensators as involved to solve RPD with bilateral power transaction

	Case 2	Case 3	Case 4	Case 5	Case 6
Net Incentive return as benefit $/ h	194.21	259.99	405.6	437.33	696.85
Investment cost $/ h	5.80	52.35	57.67	79.80	44.10
Net Monetary benefit $/ h	188.41	207.64	347.93	357.53	652.75

From the Table 31, it could be found that $HIC_{Capacitor}$ was much low compared to other cases. However, the incentive returns for case 3 - case 6 were determined further and found improved than the capacitors placement situations. Here, the HIC_{SC} was found 9 times higher than the $HIC_{Capacitor}$, although the case 3 based incentive returns are found 1.34 times better compared to the case 2. This showed the $NMB_{Capacitor}$ and NMB_{SC} to be close to each other as shown in Table 31. In this regards, the case 4 based $HIC_{Capacitor+SC}$ was observed 10 times more than the $HIC_{Capacitor.}$ However the $NMB_{Capacitor+SC}$ was found 1.67 times better compared to the case 2 based operations. Here, the incentive returns for case 4 was found almost 2.088 times more than the case 2. In this direction, after analyzing the case 4 and case 5 based economics of the *var* compensations, it could be inferred that $HIC_{Capacitor+SC}$ and HIC_{SMES} as well as the incentive return of the case 4 and case 5 were relatively closed to each other. This further provided nearly equal monetary benefit for the case 4 and case 5. Finally, case 6 based investment cost ($HIC_{Capacitor+SMES}$) of the capacitor-SMES combinations was determined. This cost is certainly 7.60 times more than the $HIC_{Capacitor}$ but 1.19, 1.30 and 1.80 times less compared to HIC_{SC}, $HIC_{Capacitor+SC}$ and HIC_{SMES} respectively. Here, the case 6 based incentive return was found much higher compared to all the cases. This thereby provided improved monetary benefit with a distinct margin from the other cases. Here, the $NMB_{Capacitor+SMES}$ was found 3.464, 3.143, 1.876 and 1.825 times better than the case 2, case 3, case 4, and case 5 based cases respectively as shown in Table 31.

To express the comparative study on economics of the different *var* compensators more clearly, the results are plotted in Figure 26-28 w.r.t the compensator's performances in percentage. In this regards, Figure 26 shows that the combined capacitor-SMES based net incentive return benefit was obtained 35% amongst all the other *var* compensators. However, the Figure 27 demonstrates that the $HIC_{Capacitor}$ obtained least cost for its developed percentage i.e., 3%. Finally, from Figure 28, it can be

inferred that $NMB_{Capacitor+SMES}$ was found highest as 37% for the combined capacitor-SMES amongst all the *var* compensators.

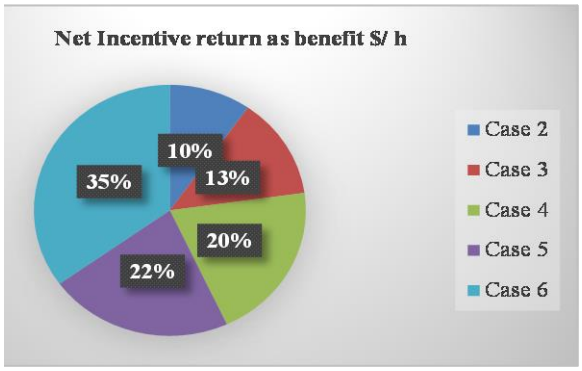

Figure 26. Net incentive return as economic benefit by the different *var* compensators in percent scale for case 2- case 6

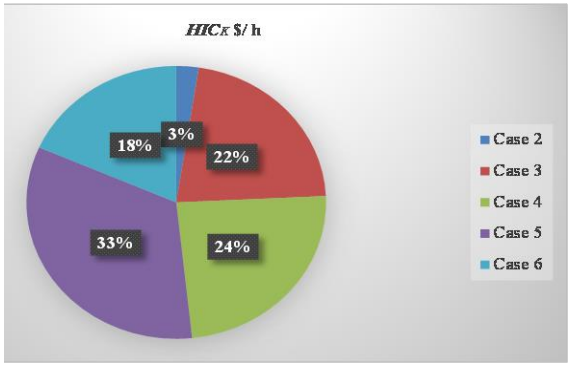

Figure 27. The investment and operating costs (HIC_K) by the different *var* compensator in percent scale for case 2- 6

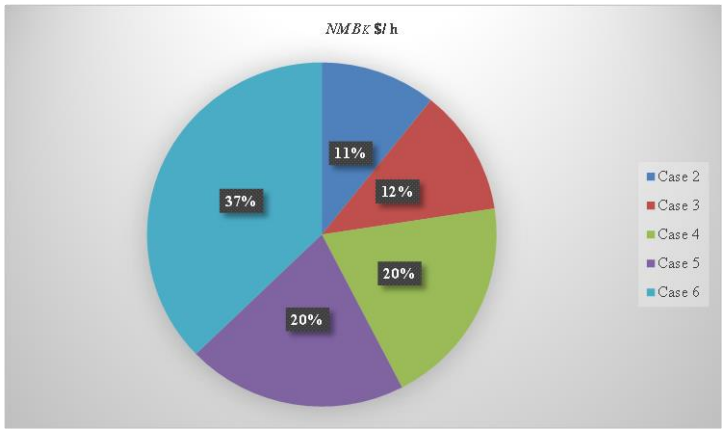

Figure 28. Net monetary benefit (NMB_K) by the different *var* compensator in percent scale for case 2- case 6

Now in the background of deregulated power scenario, the net monetary benefit due to *var* compensators helped to reduce congestion rent as generally tackled by the power transaction authority. This benefit is further distributed amongst the competing players. This helped to enhance the global welfare by improving the net benefit of the competing players. Hence the knowledge of participant's benefits in terms of improved global welfare is required for better economic understanding.

7.4.2.1.2.2 Global Welfare Analysis of the Bilateral Power Transactions

In this work, bilateral power transactions were conducted involving six participants who offered their bid prices based on their cost coefficients. The final bid prices of the suppliers and consumers are shown in Table 32. The cost coefficients of the participants are shown in Appendix Table C1. Here, the bidding of the participants was considered same for all the test cases. Based on the bid prices of the different market participants [150], the suppliers and consumers aggregated curves are plotted in Figure 29.

Table 32. The final bids of market participants during bilateral power transaction

Supplier's Bid ($/ MW h)	G1 (MW)	G2 (MW)	G3 (MW)	Total (MW)	Consumer's Bid ($/ MW h)	L1 (MW)	L2 (MW)	L3 (MW)
2563	110	-	-	546	3927	-	280	-
3025	-	-	250		3407	200	-	-
3051	-	186	-		3153	-	-	66

The matching point of the curves as shown in Figure 29, provided Market Clearing Price (MCP) as 3100 $/ MW h and respective Market Clearing Volume (MCV) as 600 MW. For case 1, the net profit of the suppliers, the net surplus of the consumers and the fundamental global welfare of the system were obtained as 822285 $/ h, 620110 $/ h and 1442395 $/h respectively which is shown in Table 33. Now, the contribution of *var* compensation which was referred to as reduced congestion rent are summed up to the fundamental global welfare. This further helped to improve fundamental global welfare. The fundamental and the improved global welfare were obtained by equations (3, 27-28, 30-32) given in Chapter 4. In this connection the individual profit and surplus of the competing players were also determined for all the cases including the base case. Here, the reduced congestion rent for each cases was equally distributed among the six market players. The individual profit and surplus of the market participants are given in Table 34.

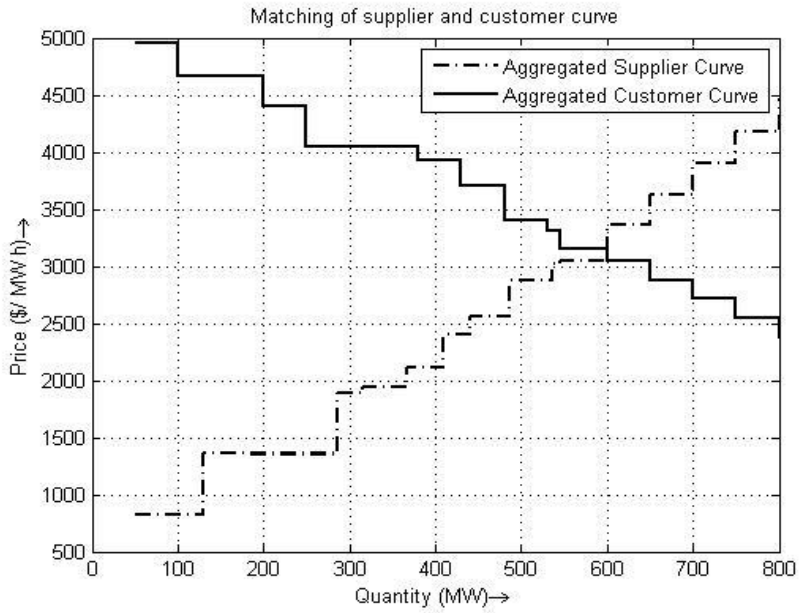

Figure 29. Matching of supplier and customer aggregated curve as market clearing

Further the percent sharing of net benefit i.e., the global welfare of the competing players were individually determined here. This provided that four participants among the six were having equal or more than 17% benefits. Moreover 2nd, 3rd suppliers and 3rd consumer were obtaining 20 % each and 29 % benefits out of the global welfare respectively due to their planned bidding. These is shown in Figure 30.

Table 33. The net profit or surplus, global welfare of the market players

Case studies	Net profit of the suppliers ($/h)	Net surplus of the consumers ($/h)	Global Welfare ($/h)
Case 1	822285	620110	1442395
Case 2	822379	620205	1442584
Case 3	822389	620214	1442603
Case 4	822459	620284	1442743
Case 5	822464	620289	1442753
Case 6	822611	620437	1443048

The total observations showed that the improved global welfare for case 2 and case 3 were found close to each other. This is generated due to their values being close to the net monetary benefits as explained in the 7.4.2.1.2.1. Here, the percent global welfare for case 2 and case 3 have improved 0.013 % and 0.0143 % respectively compared to the case 1. Similarly the global welfare of the case 4 and case 5 were obtained nearly close to each other as described in section 7.4.2.1.2.1. The observations on global welfare for case 4 and case 5 have been obtained as 0.0241% and 0.0246% improved respectively compared to case 1. In this regards, the global welfare as well as the benefits of the participants for case 6 have showed maximum improvement of 0.0452 % compared to case 1. This was due to the highest contribution in terms of net monetary benefit by combined *var* compensation in case 6 as described in section 7.4.2.1.2.1.

Table 34. The individual profit and surplus of the market players

Case studies	Profit of the suppliers ($/h)			Surplus of the consumers ($/h)		
	Supplier 1	Supplier 2	Supplier 3	Consumer 1	Consumer 2	Consumer 3
Case 1	243953	290403	287928	80309	122646	417155
Case 2	243985	290434	287959	80340	122677	417187
Case 3	243988	290437	287963	80343	122681	417190
Case 4	244011	290461	287986	80367	122704	417213
Case 5	244013	290462	287987	80368	122706	417215
Case 6	244062	290511	288037	80417	122755	417264

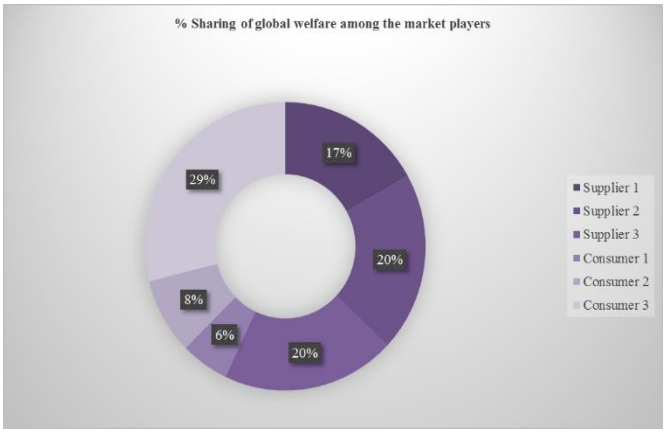

Figure 30. Percent of welfare sharing by the suppliers and consumers of the bilateral power transactions

In this conjunction, the market clearing rather MCV did not found to be matched with the transacted amount of power (546 MW). Hence the proposed bilateral transaction could not be termed as the Pareto efficient transaction because of the dead weight losses of 5400 $/ h. Now, in comparison to the obtained global welfare, the respective dead weight losses were sufficiently small. Therefore it could be remarked that the proposed transactions occurred very close to the Pareto efficient transaction which indicated most economically profitable situation of the power market.

In this context, the importance of Pareto efficient transactions on global welfare considering variable bilateral double auction power transactions was discussed.

7.4.2.2 Pareto Efficient Double Auction Bilateral Power Transactions for Economic Reactive Power Dispatch

In this work, the economic RPD issue in an inter-regional deregulated power scenario considering the IEEE 57-bus system was solved in MATLAB 7.10 programming platform. The economic welfare analysis was done using Microsoft Excel 2010. The operating ranges of the control variables as V_g, t and Q_c were considered elsewhere (Appendix Table A1) and the Q_{SMES} was found from the appendix (Appendix B2).

It has been already observed that amongst the different clever algorithms, the DERL provided satisfactorily global and fast converging solutions in many a cases. Thereby, in this study DERL was considered to be utilised as the clever algorithm for the optimisation process. Here, the optimal parameters of the DERL method was found as $N_p = 30$, $f_m \in \text{rand}(0,1)$, $C_R = 0.8$, $Gen_{max} = 100$ after 100 trial runs. The inter-regional 12-h variable double auction bilateral power transaction data was available elsewhere [11]. Here, the participant buses of the proposed transactions were optimally

chosen such a way that the total power losses are minimum. Further, the amounts of power by each participant was decided by planned biding to achieve higher economic benefit which has been elaborated in section 7.4.2.2.5. Here, the 8th and 9th buses were considered as the power producers while 12th and 8th buses were found as power consumers. The transacted amounts of power sharing by the four players is shown in Figure 31 where zero power mismatches was assumed during the power trading. Therefore, before analysing the simulation results considering 12-h variable power transactions, a brief discussion on the off peak and peak hour based transactions are required to be discussed a priory.

7.4.2.2.1 Off Peak and Peak Hour Operations

Off-peak hours for electrical networks are usually referred to lower, discounted electricity price based durations. These times are generally when the residential and industrial load requirements are found lesser like the night and /or weekends. Hourwise these are varied in between 8h-12h depending upon location and the nature of load. Now the peak hours of electrical networks are the time periods when the load demand is significantly higher than the average demand. This can occur on daily, monthly, seasonal and yearly cycles. For an interconnected network, the actual point of peak demand is a hourly period representing the highest point of load demand. Hence, the line loadability as well as security constraints of the peak hour based operations remains nearly at their marginal stability point compared to off-peak hour based operations. Thereby, loss minimizations with dynamic voltage limit crossover issues for any operations likely 12-h variable power transactions are majorly dependent on the off-peak and peak hour operations of the considered grid.

7.4.2.2.2 Power Loss Optimizations considering Power Transactions

Here, DERL algorithm based investigations were conducted considering IEEE 57-bus network as an inter-regional peak hour based deregulated market. In this work, the RPD problem involving 12-h variable bilateral power transactions has been optimised by controlling V_g and t as case 1. As a result, the hour wise variable P_{LOSS} was determined as shown in Table 36. From the Table 36 it could be stated that the P_{LOSS} were increasing with the increase in transacted amount of power and minimised according to the decreasing power transactions. Since, the 12-h variable traded power were following a non-linearity, the variations of P_{LOSS} was maintaining a non-linear asymmetry during the 12-h of variable power transactions. A comprehensive explanation of such P_{LOSS} characteristics could be generated by comparing 3rd and 12th, 4th and 11th, 5th and 10th, 7th and 9th hour based data (P_{LOSS}) in Table 36 as well as Figure 32. It has been observed that as the transacted amounts of power were very close in these specified groups of hours, the non-linear asymmetry in the losses were invoked. It was

found that after attaining the 8th hour based highest amount of power transaction, the P_{LOSS} started to reduce with asymmetric behaviour. In this regards, at the 3rd hour with 254 MW transacted power (P_{BiLat}), the P_{LOSS} was obtained as 26.42 MW where at the 12th hour with 256 MW P_{BiLat}, the P_{LOSS} was determined as 25.98 MW. Moreover, at the 4th hour with 318 MW P_{BiLat}, the P_{LOSS} was found to be 26.72 MW where at the 11th hour with 305 MW P_{BiLat}, the P_{LOSS} was obtained as 26.52 MW. Further, at the 5th hour with 358 MW P_{BiLat}, the P_{LOSS} was achieved at 27.43 MW where at the 10th hour with 345 MW P_{BiLat}, the P_{LOSS} was found to be 27.54 MW. Similarly, at the 7th hour with 390 MW P_{BiLat}, the P_{LOSS} was determined as 28.93 MW where at the 9th hour with 382 MW P_{BiLat}, the P_{LOSS} was accomplished at 29.05 MW. In this regards the P_{LOSS} was obtained highest as 29.55 MW at the 8th hour where the 410 MW power were traded. Similarly at the 2nd hour, the P_{LOSS} was also observed lowest as 24.83 MW where the P_{BiLat} was minimum with a value of 219 MW.

To obtain better response in terms of P_{LOSS} minimization, the proposed problem was further optimized by incorporating shunt capacitors at 18th, 25th and 53rd buses as case 2 by remaining the other constraints and control variables of the case 1 unchanged [11]. Here, the 12-h variable bilateral transactions based losses were found reduced compared to case 1 shown in Table 36 and Figure 32 due to capacitor placement. The optimal values of the capacitors are shown in Table 35 which was obtained within the secured margin as considered. Alike the case 1, case 2 based P_{LOSS} was also showed the non-linear asymmetry characteristics which were required to be explained concisely. Instead of explaining all the cases on non-linear asymmetry the 3rd and 12th, 5th and 10th hour based P_{LOSS} characteristics were explained in this section. Here, at the 3rd hour with 254 MW and at the 12th hour with 256 MW of power transactions, the P_{LOSS} was obtained as 24.57 MW and 24.46 MW respectively. Further, at the 5th hour with 358 MW and at the 10th hour with 345 MW of power transaction, the P_{LOSS} was determined as 25.88 MW and 25.90 MW respectively. Therefore, a clear non-linear asymmetry has been concluded from the variable bilateral power transactions. Here the minimum P_{LOSS} was found at the 2nd hour as 23.76 MW and the maximum P_{LOSS} was determined to be 28.03 MW at the 8th hour. The case 2 based P_{LOSS} minimizations by DERL method are shown in the Figure 33 and 34. In this regards the DERL algorithm proficiently brought the optimal parameters of the proposed RPD problem for the considered 12 hours within the stable operating limits. It was observed that although the P_{LOSS} was supposed to converge locally, but the incorporation of the tournament best vector with other two small perturbation vectors helped to explore the search space efficiently. This finally made the P_{LOSS} to converge at the global optima.

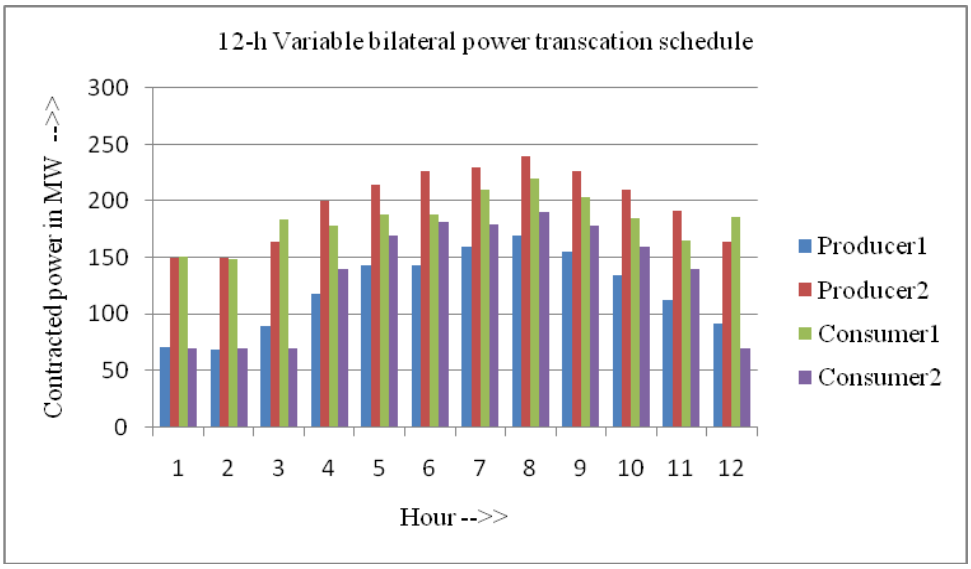

Figure 31. Variable bilateral power transactions schedule

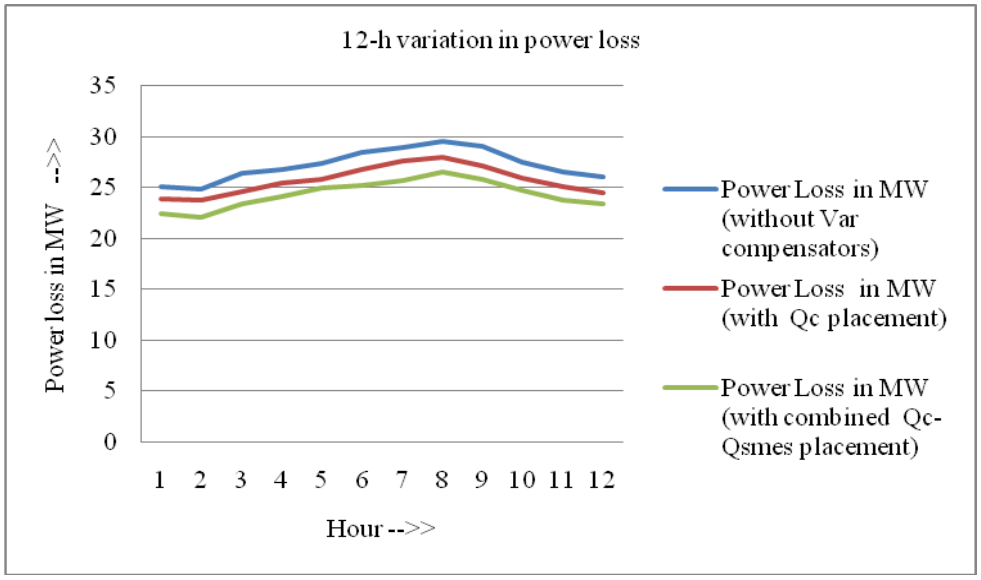

Figure 32. Variation of power loss optimization for 12-h variable bilateral power transactions

Table 35. Case 2 based Capacitor data in p.u.

Hour	1st	2nd	3rd	4th	5th	6th	7th	8th	9th	10th	11th	12th
Q_{C18}	0.1096	0.1149	0.1779	0.107	0.1773	0.0612	0.1776	0.0758	0.1187	0.0785	0.1473	0.1432
Q_{C25}	0.1579	0.1398	0.1474	0.06	0.1676	0.1286	0.1449	0.0829	0.1524	0.1108	0.1588	0.1148
Q_{C53}	0.141	0.1186	0.1219	0.0619	0.1065	0.0939	0.1506	0.0921	0.0842	0.1666	0.1217	0.1635

Further to achieve economic, reliable, and sustainable solutions in the context of deregulated power scenario a combination of capacitor with SMES were integrated to solve the proposed problem by keeping the other constraints of case 1 unaltered. Here the bus locations such as two buses, each for the Q_C and Q_{SMES} were optimally fixed by DERL method to derive optimum P_{LOSS}. By controlling the different optimization parameters including the combination of Q_C and Q_{SMES}, 12-h variable P_{LOSS} were determined and presented in the Table 36 as well as Figure 32. The case 3 based control variables were found converged within the secured limit amongst which the Q_C and Q_{SMES} were shown in Table 37. Here, the case 3 based observations in the form of P_{LOSS} showed non-linear asymmetry characteristics like the other cases. This could be explained by comparing the investigations comprising 3rd and 12th, 7th and 9th hour amongst all the statistics. Here, the P_{LOSS} at the 3rd hour with 254 MW of power transaction was found at 23.447 MW where at the 12th hour with 256 MW transacted power the P_{LOSS} was obtained as 23.36 MW. In this context, 7th hour based power transactions with 390 MW of power invoked 25.60 MW P_{LOSS} where the 9th hour with 382 MW of transacted power provided 25.76 MW of P_{LOSS}. Here, the minimum P_{LOSS} was obtained as 22.09 MW at the 2nd hour and the maximum P_{LOSS} was determined as 26.47 MW at the 8th hour. This inferred the best solutions by the advanced *var* compensation of combined capacitor-SMES over the singular capacitor or no-*var* compensator based results. In this context, the P_{LOSS} minimization curves for the considered case 3 are presented in the Figure 33 and 34 with adjacent to case 2. According to the Figure 33 and 34, the case 3 based convergence characteristics showed a number of local optimum solutions as P_{LOSS} in the solution space. However, the tournament best vector with other two small perturbation vectors of the proposed DERL method helped to converge the final P_{LOSS} at the global optima. This further showed the proficiency of the DERL algorithm with faster convergence.

Further the case 3 based percent P_{LOSS} reduction w.r.t the case 2 are shown in Table 36. This provided that the minimum % P_{LOSS} was obtained as 3.43 at 5th hour where the maximum % P_{LOSS} was found as 7.41 at 7th hour.

Table 36. Power loss optimisations for 12-h variable double auction bilateral power transaction by DERL

Hour	1st	2nd	3rd	4th	5th	6th	7th	8th	9th	10th	11th	12th
Transacted power in MW	221	219	254	318	358	370	390	410	382	345	305	256
P_{LOSS} in MW (without Var compensators)	25.07	24.83	26.42	26.72	27.43	28.42	28.93	29.55	29.05	27.54	26.52	25.98
P_{LOSS} in MW (with *Qc* placement)	23.84	23.76	24.57	25.45	25.88	26.79	27.65	28.03	27.17	25.9	25.15	24.46
P_{LOSS} in MW (with combined *Qc-Qsmes* placement)	22.43	22.09	23.447	24.16	24.89	25.117	25.6	26.47	25.76	24.7	23.8	23.36
% P_{LOSS} reduction by Case 3 w.r.t Case 2	5.91	7.03	4.57	5.07	3.83	6.24	7.41	5.57	5.19	4.63	5.37	4.50

Table 37. Case 3 based combined capacitor-SMES data in p.u.

Hour	1st	2nd	3rd	4th	5th	6th	7th	8th	9th	10th	11th	12th
Q_{C18}	0.111	0.0726	0.1171	0.1133	0.1222	0.1173	0.0907	0.1906	0.1289	0.1259	0.1392	0.0695
Q_{C53}	0.1462	0.0865	0.1494	0.1374	0.1377	0.1547	0.0749	0.1284	0.112	0.1375	0.12	0.0975
Bus number for Q_{SMES1}	47	56	4	27	4	27	52	22	51	4	5	38
Q_{SMES1} in p.u.	0.0417	0.0314	0.0242	0.0409	0.0237	0.0416	0.0367	0.0346	0.0318	0.025	0.0408	0.0245
Bus number for Q_{SMES2}	7	57	20	20	20	20	10	29	54	20	41	52
Q_{SMES2} in p.u.	0.0269	0.0343	0.0342	0.0387	0.0339	0.0415	0.0239	0.0402	0.0205	0.034	0.0282	0.0278

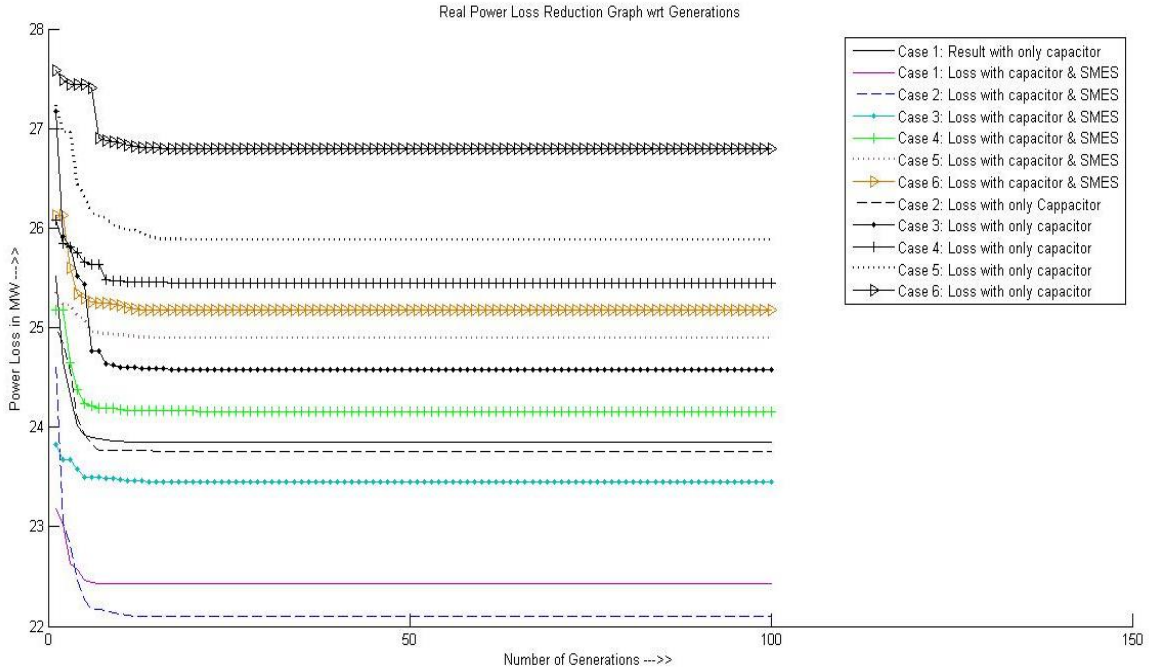

Figure 33. Power loss minimization curve for 1st -6th hour involving bilateral power transaction

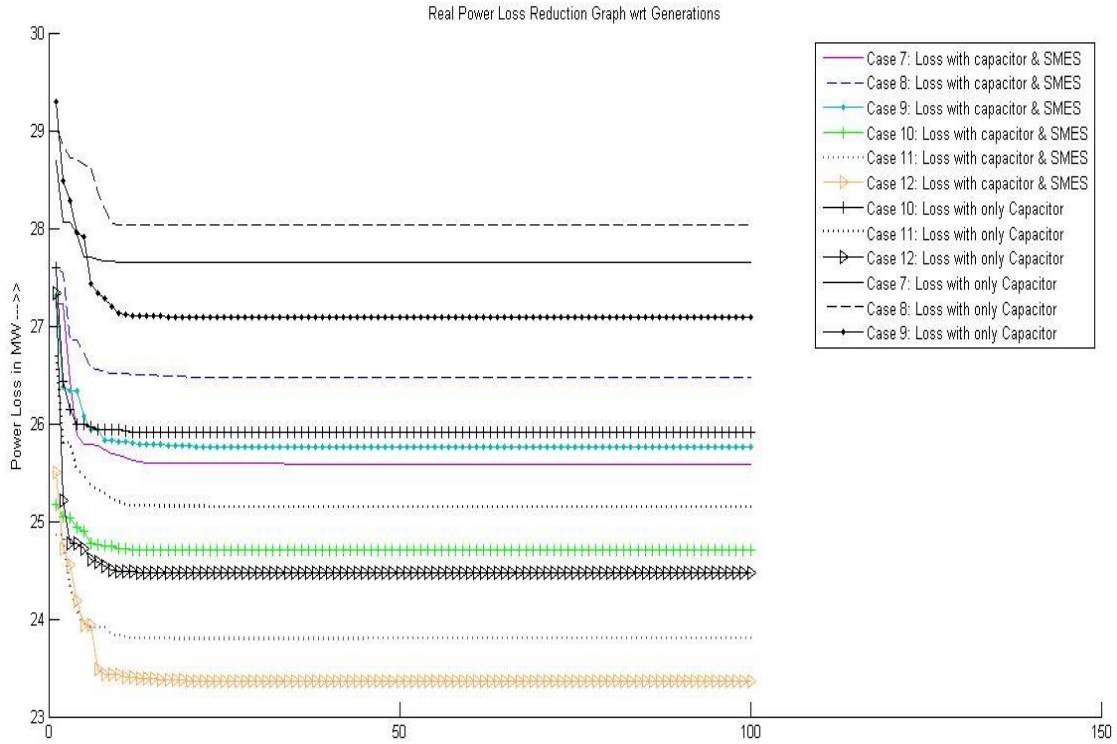

Figure 34. Bilateral power transaction oriented power loss minimization curve for 7th -12th hour

It is not viable to dispatch reactive power without security analysis on the dynamic voltage limit in a power network. Therefore, besides the minimizations of power loss, the improved dynamic voltage limit crossover needs major attention.

7.4.2.2.3 Dynamic Voltage Limit Crossover Analysis

Here, a case study on dynamic voltage limit crossover [23, 32] was also considered in the view of RPD problem characterized by power transactions. When there was no *var* compensators, the security constraints like load bus voltage of the chosen network were observed to fluctuate nearby to their bound values (0.95-1.10 p.u.). Even, some of them as shown in Table 38 had violated the boundary value in certain buses and stayed in between 0.95 p.u. 1.1199 p.u.. This caused increasing voltage drops which further increased the line current flow followed by huge power losses. According to the observations in Table 38, three buses likely 25^{th}, 30^{th} and 31^{st} were found to be disturbed at almost every hour of power tradings. The maximum violated voltage for every hour with corresponding bus numbers were specified in Table 38. According to Table 38, the hourly average critical voltage was obtained 1.11895 p.u. which required closer observations for security reasons.

This situation of voltage limit crossover was initially handled by incorporating shunt capacitors as *var* compensators. This helped to operate the network voltage profile within stable operating ranges likely (0.95 -1.10 p.u.) with reduced losses as described earlier. Here, the case 2 based bus voltages which generated maximum voltage limit violations in case 1, were found to have nominal value within the standard operating range likely 0.9624-1.0956 p.u. in Table 38. The case 2 based *var* compensation maintained the average hourly voltage of the maximum violated buses as 1.0237p.u. This result is stable in terms of boundary value satisfaction however the value showed fluctuation if compared with hourly individual values. Moreover, the operating range of dynamic voltage profile is also bulky here with higher losses.

In this context to realize dynamic voltage limit crossover issue at reduced loss with reduced operational margin, the RPD issue was solved by incorporating a combination of capacitor and SMES devices. This case 3 based combined *var* compensators provided better response in terms of improved dynamic voltage limit crossover as well as the reduced losses. Here, the bus voltage profile of the whole network was remained within 0.975-1.095 p.u. for case 3. This work also showed to maintain the case 3 based bus voltages within 0.9907 p.u. to 1.0836 p.u. in Table 38 which were found to be disturbed (1.1160 - 1.1199 p.u.) for case 1. This indicated a reduced operational margin while favouring the dynamic voltage limit crossover improvement. Moreover, the hourly average voltage for the maximum voltage violated buses was received as 1.03355 p.u. After comparing with each hour

results, this average bus voltage data further showed the steadiness towards the improvement of dynamic voltage limit crossover compared case 1, 2 in addition to the lower power losses as discussed in section 7.4.2.2.2.

Table 38. Dynamic voltage profile (p.u.) for 12-h variable double auction bilateral power transactions

	Hour											
	1st	2nd	3rd	4th	5th	6th	7th	8th	9th	10th	11th	12th
Voltage deviated buses	25, 30, 31	25, 26, 30-36, 40, 52-54, 56, 57	22-26,30-37, 39,40	19, 20, 31, 41-43, 56, 57	21-26, 30-40, 50	19,20, 25, 29, 30, 34, 41-43, 56, 57	21-25, 30-40, 44, 46-51	25, 30-33	18-20	21-26, 30-40	25, 30-33, 56, 57	25, 30-31, 34, 35, 43
Bus for maximum voltage violation	25	33	35	31	36	30	37	32	18	33	32	43
Maximum violated voltage value (p.u.)	1.1194	1.1199	1.1189	1.1193	1.1198	1.1192	1.1195	1.1181	1.1160	1.1195	1.1186	1.1192
Case 2 based voltage value (p.u.) for the buses at 4th row	0.9945	1.0042	0.9649	1.0915	1.0282	0.9624	1.0943	1.0827	1.0956	1.0392	0.9654	0.9625
Case 3 based voltage value (p.u.) for the buses at 4th row	1.0597	1.0192	1.0178	1.0053	0.9985	1.0682	1.0759	1.0114	1.0107	0.9907	1.0836	1.0616

Although, the power loss minimization as well as dynamic voltage limit crossover by *var* compensators were the governing part of the restructured RPD issue, but the economics behind such solutions should be discussed a priory in the context of deregulated power scenario.

7.4.2.2.4 Economics due to Var Compensation

In conjunction to the technical analysis of the RPD problem involving 12-h variable bilateral power transaction, the economics of the *var* compensation by capacitor and combination of capacitor-SMES were accomplished here by equations (7) and (23) respectively as available in Chapter 4. The results of economics due to *var* compensation were presented in Table 39 and Table 40 respectively. Here the incentive return for loss minimization (*Inc*) was used as 100 $/ MW h available elsewhere [178] for both the case 2 and 3. Table 39 provided case 2 based economics due to capacitive *var* compensation which demonstrated non-homogeneity between the results for the 12-h variable bilateral power

transaction. In this regards, 12-h variable total operating costs of the three capacitors ($HIC_{Capacitor}$) were determined to vary within 0.0209 to 0.0412 $/ h. These indicated nearly equal operating costs of the capacitors for the 12-h transaction. Now, the incentive returns were found to vary between 107 $/h to 188 $/h with persistence of non-homogeneity. Therefore, the 12-h variable $NMB_{Capacitor}$ were also obtained to fluctuate non-homogeneously. For better analysis, 7th and 9th hour transactions which were very close to each other were explained here to justify the non-homogeneity of the pricing. In the 7th hour transaction the difference in P_{LOSS} between case 1 and case 2 were 1.28 MW which provided 128.0 $/ h as incentive return. In this regards, the 9th hour based transaction generated the difference in P_{LOSS} between case 1 and case 2 as 1.88 MW which helped to get back 188.0 $/ h as incentive return. Now the $HIC_{Capacitor}$ for 7th hour and 9th hour transaction were calculated as 0.0432 $/ h and 0.0324 $/ h respectively and found very close to each other. As a result the $NMB_{Capacitor}$ for the 7th and 9th hour based transactions were determined as 127.957 $/h and 187.9676 $/ h respectively showing the non- homogeneity among them though the transacted power was nearly equal. Similarly the 3rd and 12th, 4th and 11th, 5th and 10th hour based transactions could be compared w.r.t economics to validate the non- homogeneity of the observation. Here the minimum $NMB_{Capacitor}$ was determined as 100.6 $/ h at the 2nd hour where the maximum $NMB_{Capacitor}$ was obtained as 187.97 $/ h at 9th hour.

In this regards the case 3 based economics due to combined Q_C-Q_{SMES} involving 12-h variable bilateral power transaction were also discussed. Here, the total operating costs of the two capacitors ($HIC_{Capacitor}$), total operating costs of the 1st SMES (HIC_{SMES1}) and total operating costs of the 2nd SMES (HIC_{SMES2}) were found to be within 0.0145 to 0.0291 $/ h, 5.405 to 9.587 $/ h, and 4.676 to 9.465 $/ h respectively. These inferred very adjacent value for the 12-h variable transactions. In this connection, the $NMB_{Capacitor+SMES}$ were found to vary non-homogeneously with minimum 1.5 times profit enhancement compared to case 2 as shown in Table 40. The reason for the non-homogeneity has been already elaborated for case 2. However, for better understanding, the 3rd and 12th hour based economics due to *var* compensation were analyzed here to justify the non-homogeneity in pricing. In the 3rd hour transaction the difference in P_{LOSS} between case 1 and case 3 were obtained 2.973 MW which helped to receive the incentive return as 297.3 $/ h. In this regards, the 9th hour based transaction got 262.0 $/ h as incentive return by minimising 2.62 MW P_{LOSS} in case 3 from case 1. In this connection, the total investment cost of combined *var* compensators for the 3rd and 12th hour transaction were determined as 13.3446 $/ h and 11.944 $/ h respectively which were close to each other. Therefore the $NMB_{Capacitor+SMES}$ for the 3rd and 12th hour based transactions were finally calculated as 283.955 $/h and 250.06 $/ h respectively which showed non-homogeneity however the transacted power amount of 3rd and 12th hour were almost same. Correspondingly the 4th and 11th, 5th and 10th, 7th and 9th hour based transactions would also be compared w.r.t economics to justify the

non-homogeneity of the investigations. In this regards, the $NMB_{Capacitor+SMES}$ was determined to be minimum to 237.88 $/ h at 4th hour and was found 319.163 $/ h as maximum at 7th hour.

Table 39. Economics of the capacitive *var* compensators

Hour	1st	2nd	3rd	4th	5th	6th	7th	8th	9th	10th	11th	12th
$HIC_{Capacitor}$ ($/h)	0.0373	0.0341	0.0408	0.0209	0.0412	0.0259	0.0432	0.0229	0.0324	0.0325	0.0390	0.03 84
$(P_{LOSS\_bVCP} - P_{LOSS\_aVCP}) \times Inc$ $/ h	123	107	185	127	155	163	128	152	188	164	137	152
$NMB_{Capacitor}$ ($/h)	122.96	106 .97	184 .96	126 .98	154 .96	162 .97	127 .96	151 .98	187 .97	163 .97	136 .96	151. 96

Table 40. Study on economics of the capacitor-SMES based *var* compensation

Hour	1st	2nd	3rd	4th	5th	6th	7th	8th	9th	10th	11th	12th
$HIC_{Capacitor}$ ($/h)	0.0235	0.0145	0.0243	0.0228	0.0237	0.0248	0.0151	0.0291	0.022	0.024	0.0237	0.0 153
HIC_{SMES1}($/h)	9.587	7.162	5.520	9.328	5.405	9.488	8.370	7.892	7.252	5.702	9.305	5.5 88
HIC_{SMES2} ($/h)	6.211	7.837	7.801	8.827	7.731	9.465	5.451	9.169	4.676	7.755	6.432	6.3 41
$(P_{LOSS\_bVCP} - P_{LOSS\_aVCP}) \times Inc$ $/ h	264	274	297. 3	256	254	330. 3	333	308	329	284	272	262
$NMB_{Capacitor+SMES}$ ($/h)	248.179	258. 987	283. 955	237. 822	240. 839	311. 322	319. 163	290. 911	317. 0450	270. 519	256. 2389	250 .05 6

As evidenced from Table 39 and Table 40, it was cleared that case 3 based *var* compensation provided better economic response over case 2. For more clear understanding, the ratio of the net monetary benefit between case 3 and case 2 involving 12-h variable bilateral transactions were presented in Figure 35. The Figure 35 demonstrated that out of twelve transactions, the 2nd and 7th hour transactions based monetary benefit ratio were found nearly 2.5. Amongst them the 7th hour transaction showed the highest benefit ratio of 2.49 which indicated to have maximum monetary benefit by the combined capacitor-SMES over singular capacitor to solve the proposed problem. Further it was found that 1st, 4th, 6th, 8th and 11th hour based benefit ratio were nearly 2 which also demonstrated the improved performance of the combined capacitor-SMES over singular capacitor.

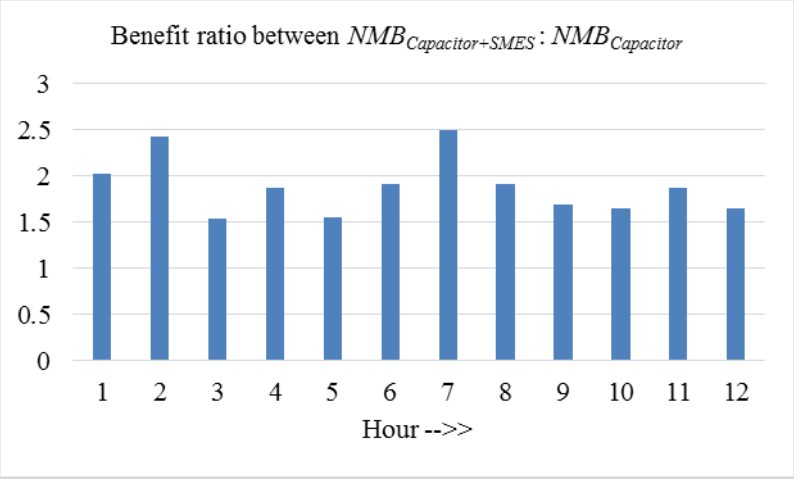

Figure 35. Economic analysis in terms of net monetary benefit ratio between $NMB_{Capacitor+SMES}$ to $NMB_{Capacitor}$ for bilateral power transactions

As stated earlier, the economics of *var* compensations have a major impact on the global welfare of system under observations in the form of reduced merchandising surplus. This will also help to improve the net monetary benefit of the market participants. Therefore, the knowledge of the participant's benefit in the backdrop of Pareto efficient global welfare of the considered network is to be discussed a priory.

7.4.2.2.5 Pareto Efficient Global Welfare Analysis

While accomplishing the Pareto efficient global welfare including the economics of the *var* compensation, the fundamental global welfare were required to obtain first. In this direction, the bidding of the market players of the double auction bilateral transactions was played a major role to obtain the fundamental global welfare. Here, the bids of the participants for the 12-h variable power transactions were determined by solving their respective cost equations [9]. The cost coefficients of the market participants are presented in Appendix Table C2. The final hour-wise offer prices of the participants are shown in Table 41. Here, the bid prices for a particular hour were considered same for all the three cases. The hour wise participants' bid characteristics were drawn as aggregated producer curve and aggregated consumer curve which is shown in Figure 36 (i-vi) to Figure 37 (vii-xii). Here, G_1, G_2, L_1 and L_2 are indexed as the generations and consumptions of two power producers and consumers respectively.

Table 41. Final Bids of the market participants for 12-h variable bilateral power transactions for different cases

Hour	*Producer's offer price* ($/ MW h)	G_1 (MW)	G_2 (MW)	Total (MW)	Total (MW)	*Consumer's offer price* ($/ MW h)	L_1 (MW)	L_2 (MW)	Total (MW)	Δ*price* ($/ MW h)
1	3650	-	150	150	221	4740	-	70	70	720
	3690	71	-	71		4410	151	-	151	
2	3650	-	150	150	219	4740	-	70	70	730
	3690	69	-	69		4420	149	-	149	
3	3730	-	164	164	254	4740	-	70	70	420
	3780	90	-	90		4200	184	-	184	
4	3920	-	200	200	318	4300	-	140	140	320
		118	-	118		4240	178	-	178	
5	4070	-	215	215	358	4180	188	-	188	60
		143	-	143		4130	-	170	170	
6	4070	143	-	143	370	4180	188	-	188	80
	4150	-	227	227		4070	-	182	182	
7	4180	-	230	230	390	4080	-	180	180	120
		160	-	160		4060	210	-	210	
8	4250	-	240	240	410	4020	-	190	190	250
		170	-	170		4060	220	-	220	
9	4150	155	227	382	382	4090	204	178	382	60
10	4020	135	-	135	345	4200	185	-	185	150
	4030	-	210	210		4180	-	160	160	
11	3900	-	113	113	305	4320	165	-	165	400
		192	-	192		4300	-	140	140	
12	3730	-	164	164	256	4740	-	70	70	250
	3790	92	-	92		4040	186	-	186	

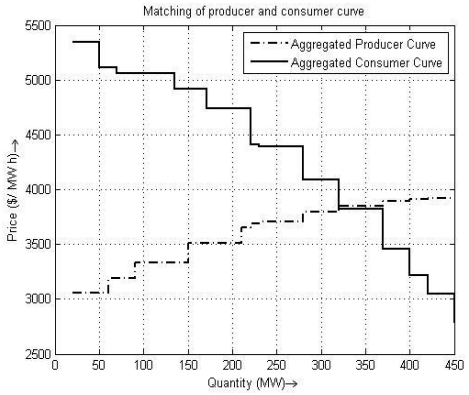

(i) 1st hour

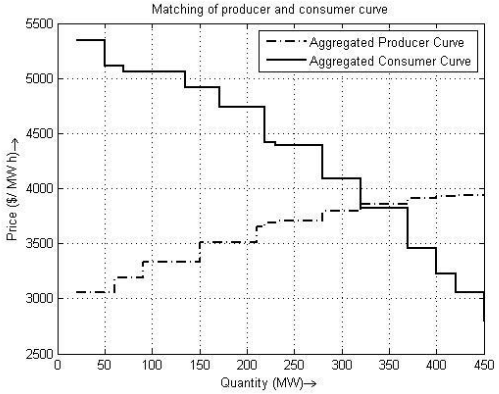

(ii) 2nd hour

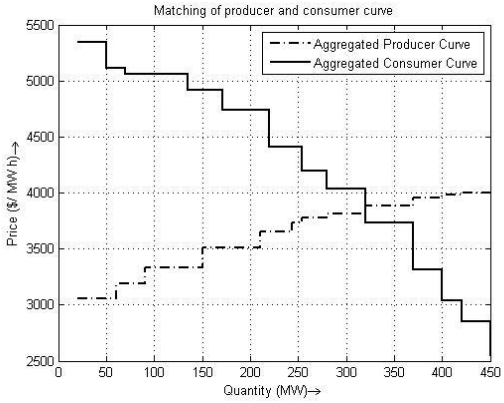

(iii) 3rd hour

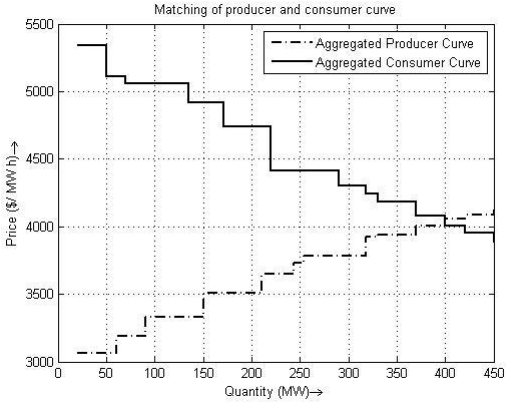

(iv) 4th hour

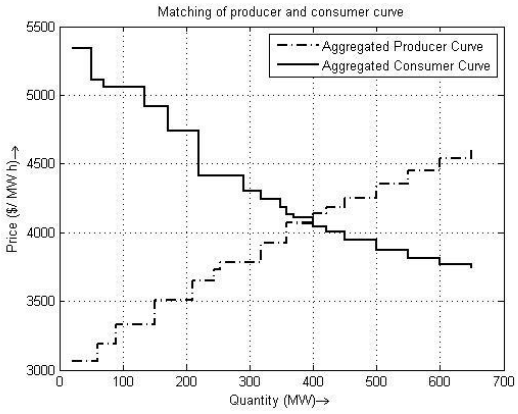

(v) 5th hour

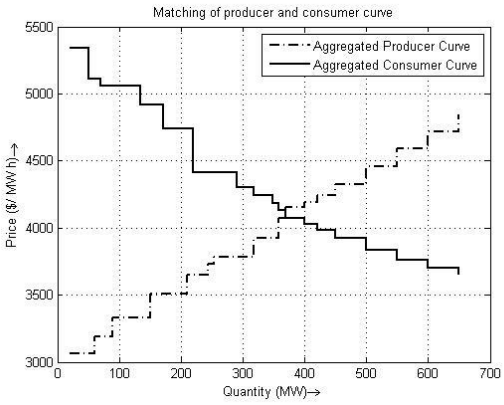

(vi) 6th hour

Figure 36. Market clearing at 1st -6th hour in (i-vi)

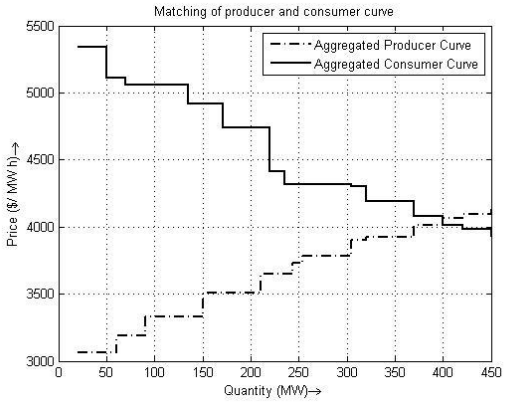

(vii) 7th hour

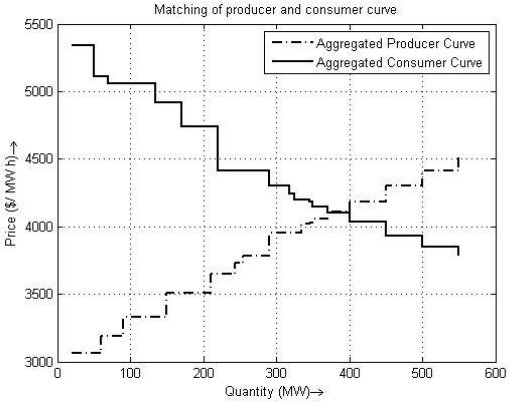

(viii) 8th hour

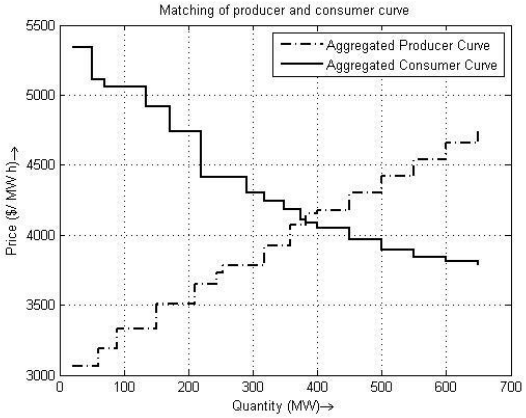

(ix) 9th hour

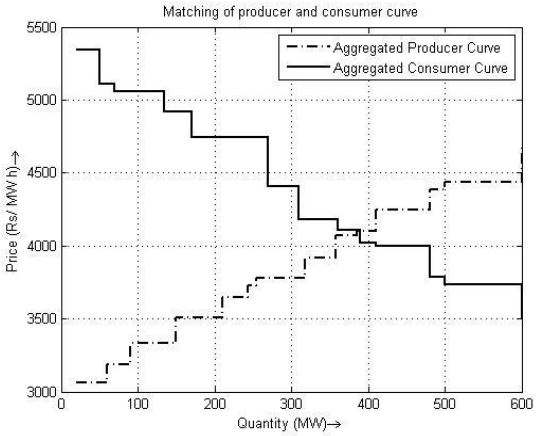

(x) 10th hour

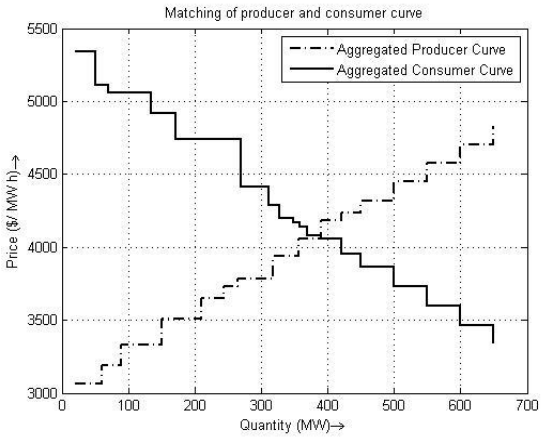

(xi) 11th hour

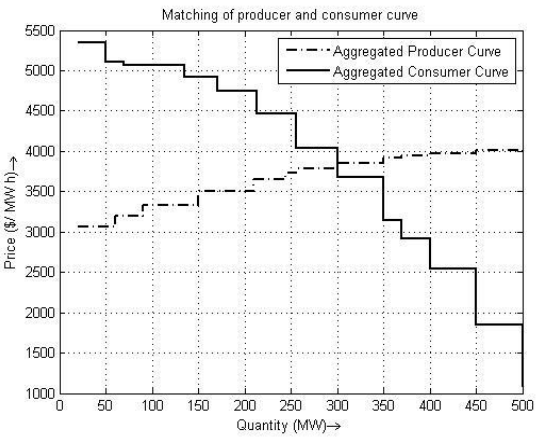

(xii) 12th hour

Figure 37. Market clearing at 7th – 12th hour in (vii-xii)

From the Table 41, the impact of bidding on Pareto efficient transactions can be comprehended clearly. According to the Table 41, the market equilibrium point (MEP) was moving towards the Pareto efficiency of the power market when the Δ*price* were reducing. Here, the first four hours and 11^{th} to 12^{th} hour demonstrated a large value of the Δ*price*. In this context, the 5^{th}-10^{th} hour except the 8^{th} hour has been generated a small Δ*price* compared to the other hours. Therefore, the hours where the Δ*price* is very small, are mostly found as the Pareto efficient transactions. Analysing the bid characteristics as well as the market clearing curves, it has been observed that out of the 12-h variable transactions, three transactions satisfied the Pareto efficient criteria as shown in Figure 38 [6]. After comparing the MCV with the traded power quantity, the Figure 38 inferred that the power transactions at 1^{st}-4^{th} hours and 11^{th} to 12^{th} hours were below the MEP. In this regards, the power transactions at the 5^{th} and 10^{th} hour were also found below but very close to the MEP. Moreover, the power transaction at the 8^{th} hour was observed beyond the MEP. Meanwhile, it could be found that the power transactions at the 6^{th}, 7^{th} and 9^{th} hour had reconciled exactly at the MEP which indicated to have the Pareto efficiency at the specified hours. The variable MCP and respective MCV were given in Table 42.

Table 42. Representations of hour wise market clearing

Hour	1^{st}	2^{nd}	3^{rd}	4^{th}	5^{th}	6^{th}	7^{th}	8^{th}	9^{th}	10^{th}	11^{th}	12^{th}
MCP ($ / MW h)	3835	3840	3850	4040	4100	4100	4070	4100	4100	4100	4040	3810
MCV in MW	320	320	320	400	400	370	390	390	382	370	400	300

With respect to the MEP, net benefit of the producers and of the consumers were determined for the considered 12-h variable power transactions [11] which would be equal for all the three cases. Now, the economic contribution of the *var* compensations as determined in the section 7.4.2.2.4 by case 2 and 3 would be added simultaneously to the case 1 based net benefit to improve the economic welfare of the participants. Here, the total economics due to *var* compensations were equally distributed among all the market players for both case 2 and case 3. The case 1, case 2 and case 3 based net surplus and profit of the market participants were shown in Table 43. From the each hour observations w.r.t the three cases, it could be shown that the difference between the $\sum_{k=1}^{nc} C\_Surplus_k$ and $\sum_{k=1}^{ns} P\_Profit_k$ were high enough when the considered transactions were far from the MEP likely the 1^{st}-4^{th} hour and the 11^{th} -12^{th} hour. As the transactions were converging towards the MEP, the

difference between the $\sum_{k=1}^{nc} C\_Surplus_k$ and $\sum_{k=1}^{ns} P\_Profit_k$ were also minimised likely the 5th, 8th and 10th hour operation. In this context, it should be remarked that the Pareto efficient power transactions (6th, 9th hour) showed a balanced margin between the profit and the surplus for the market players. However, one exception has been observed at the 7th hour based Pareto efficient transaction for maintaining a higher difference between the $\sum_{k=1}^{nc} C\_Surplus_k$ and $\sum_{k=1}^{ns} P\_Profit_k$ compared to few other cases. Since, the 7th hour based $\sum_{k=1}^{nc} C\_Surplus_k$ had increased remarkably compared to other cases, this high margined difference occurred. Moreover, it was to be noticed that $\Delta price$ has a great impact on net benefit of the market players.

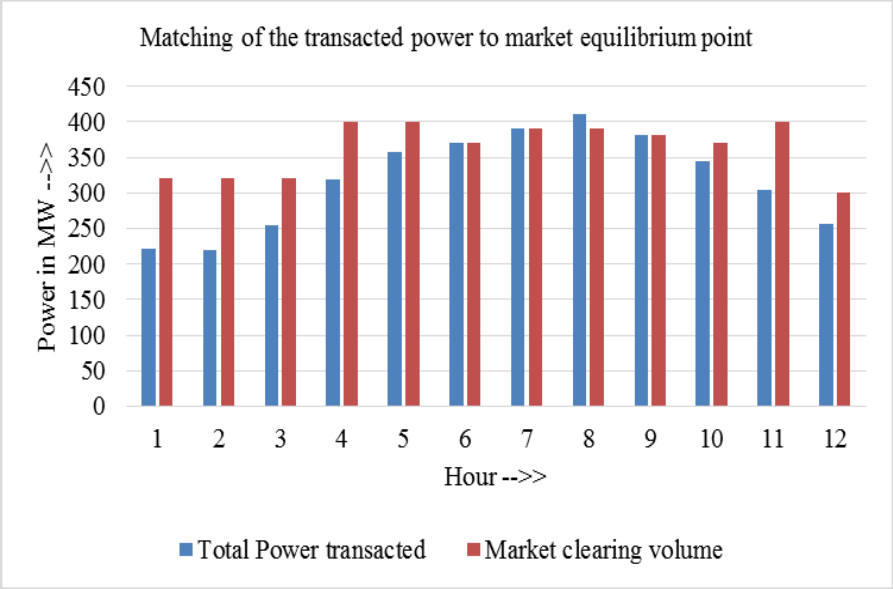

Figure 38. Market equilibrium analysis for 12-h variable bilateral power transactions w.r.t MCV

Table 43. Case1, case 2 and case 3 based net surplus and profit of the market players

Hour		1st	2nd	3rd	4th	5th	6th	7th	8th	9th	10th	11th	12th
Case 1	$\sum_{k=1}^{nc} C\_Surplus_k$ $/h	264685	261780	279520	251860	237780	238140	268020	252530	239140	235760	243830	290880
	$\sum_{k=1}^{ns} P\_Profit_k$ $/h	117685	118410	126800	191700	217980	218340	207190	218790	218700	209370	191560	116800
Case 2	$\sum_{k=1}^{nc} C\_Surplus_k + NMB_{Capacitor}/2$ $/h	264746	261834	279613	251924	237858	238222	268084	252606	239234	235842	243899	290956
	$\sum_{k=1}^{ns} P\_Profit_k + NMB_{Capacitor}/2$ $/h	117746	118464	126893	191764	218058	218422	207254	218866	218794	209452	191629	116876
Case 3	$\sum_{k=1}^{nc} C\_Surplus_k + NMB_{Capacitor+SMES}/2$ $/h	264809	261910	279662	251979	237900	238296	268180	252676	239299	235895	243958	291005
	$\sum_{k=1}^{ns} P\_Profit_k + NMB_{Capacitor+SMES}/2$ $/h	117809	118540	126942	191819	218100	218496	207350	218936	218859	209505	191688	116925

Besides, the investigations of the consumer's surplus and producer's profit, the fundamental global welfare were determined. Here the global welfare for the three cases were estimated by (3, 24, 28) which were given in Table 44 and drawn in Figure 39. Further, the improved economics in terms of enhanced global welfare were obtained by adding the case 2 and case 3 based reduced merchandising surplus to the case 1 based fundamental global welfare. In the context, the case 3 based global welfare provided maximum economic welfare due to significant economic contribution by the combined capacitor-SMES placement. In this direction, the maximum percent of global welfare improvement for case 3 compared to case 1 was observed in 9^{th} hour as 0.069. Moreover, the case 3 based maximum percent of global welfare improvement compared to case 2 was obtained in 7^{th} hour as 0.040. From the Figure 39 as well as Table 44 it could be remarked that the highest global welfare was achieved at the 7^{th} hour trading which was assigned as Pareto efficient transaction. Further the 8^{th}, 9^{th}, 6^{th} and 5^{th} hour based tradings were also found to generate sufficiently good global welfare. Amongst them 9^{th} and 6^{th} hour based transactions were found to be Pareto efficient. These specified transactions were shown either zero dead weight losses or very nomial valued dead weight losses which helped to accomplish such larger global welfare to the network. The dead weight losses were presented in Table 45 as well as Figure 40.

Table 44. Global welfare analysis for case 1, case 2 and case 3

Hour	1^{st}	2^{nd}	3^{rd}	4^{th}	5^{th}	6^{th}	7^{th}	8^{th}	9^{th}	10^{th}	11^{th}	12^{th}
Case 1 based Global welfare	382370	380190	406320	443560	455760	456480	475210	471320	457840	445130	435390	407680
Case 2 based Global welfare	382493	380297	406505	443687	455915	456643	475338	471472	458028	445294	435527	407832
Case 3 based Global welfare	382618	380449	406604	443798	456001	456791	475529	471611	458157	445401	435646	407930

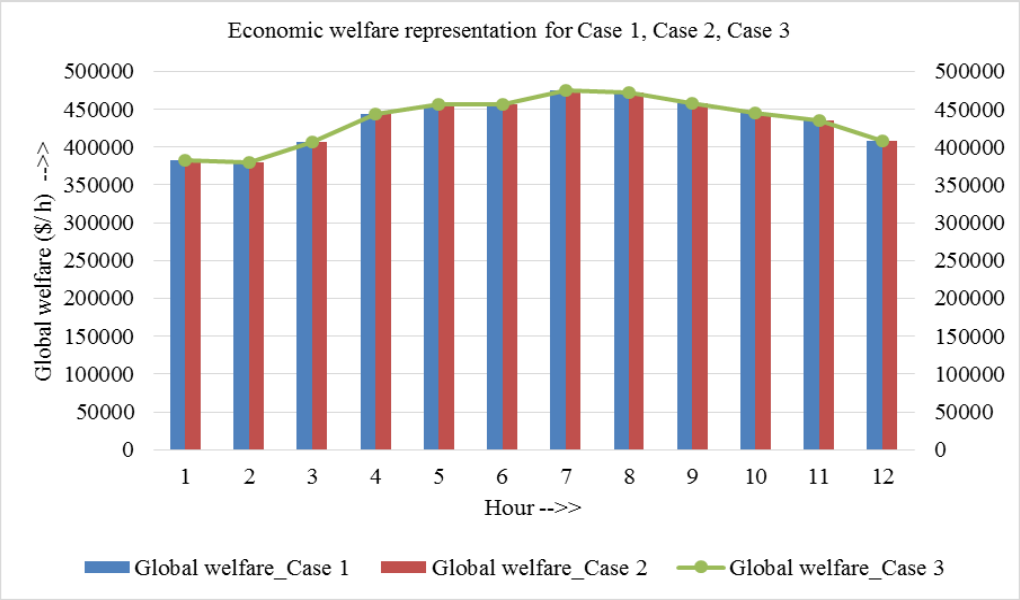

Figure 39. Study of global welfare for case 1-case 3

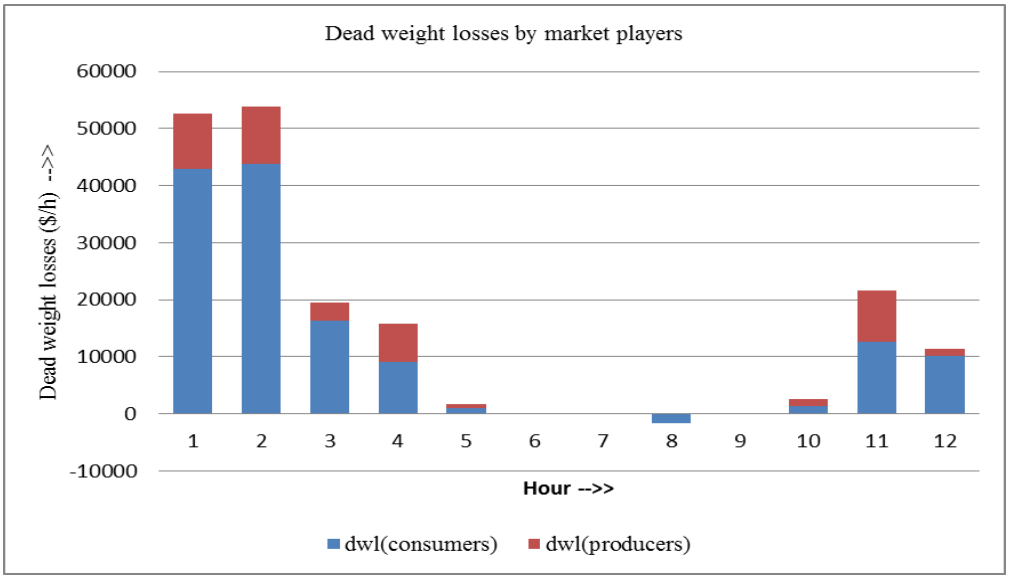

Figure 40. Hour wise variable dead weight losses

In this connection, 1st and 2nd hour transactions were providing poor global welfare compared to the 5th-9th hour based transactions. This probable reason due to their distant operation from the MEP, might be having very large dead weight losses as shown in Table 45 as well as in Figure 40. However the 3rd - 4th, and 10th -12th hour transactions were showing nominal global welfare compared to the 5th-

9th hour based transcations. Since, these transactions were quite clsoe to the MEP and thereby were generating small dead weight losses. This caused to have such a distinguished global welfare at these hours. However, this could be improved by considering suitable biding strategy.

Table 45. Hour wise deadweight losses

Hour	1st	2nd	3rd	4th	5th	6th	7th	8th	9th	10th	11th	12th
DWL_C \$/ h	43025	43880	16300	9170	960	0	0	-1600	0	1300	12700	10120
DWL_P \$/ h	9605	10000	3220	6630	780	0	0	0	0	1250	8850	1320

From the aforementioned analysis considering an inter-regional network with advanced *var* compensation based bilateral power transaction data, the global welfare in the view of Pareto efficiency can be summarised as:

1. The Pareto efficient transactions were every time generated significant economic contribution to the network under considerations.

2. The transactions which were very close to the Pareto efficient point were many a times able to provide significant global welfare.

3. The transactions which were distant from the Pareto efficient point, would be unable to generate expected global welfare with balanced benefits to the market participants.

Although, the initial investment cost of the advanced *var* compensators as proposed in case 3 were high, but net benefit as obtained by the compensations were sufficiently acceptable. Therefore, the advanced economy as well as few developing economic countries might adopt these *var* compensators as suitable option for restructured RPD solution in such inter-regional power network. Further, the planned bidding as proposed in this work helped to decide the economic operating point of the optimum power transactions in competitive power scenarios.

Now, these models are required to be utilized in the next phase of study while considering multilateral power transactions where the number of participants are more. The main reason for the model improvement is due to the increasing number of uneven participants (where the number of power producers are not equal with number of power consumers) in the advanced economy and few developing economic inter-regional markets.

7.4.3 Restructured Reactive Power Dispatch with Double Auction Multilateral Power Transactions (MPT)

In this work, two case studies were considered to solve the restructured RPD problem by multilateral power transactions (MPTs). Initially a small test system was considered to solve the proposed problem by advanced *var* compensators however the economics of the compensations towards the global welfare improvement are not considered here. In the second study, the MPTs oriented RPD problem was solved technically as well as economically for a real power scenario. Now, so far the power transactions are considered, it evidenced the zero power mismatches. However, power mismatch during the power transactions is an important issue which is considered in the next phase of study. In this work, the RPD problem with hourly power mismatches during the multilateral power transactions has been considered for a day ahead Indian real time scenario of 62-bus system as second case. Besides the technical analysis, the economics considering the spot pricing issues are therefore incorporated to observe the variations in global welfare. Moreover, the hourly variations in profit of the producers involving economics of the *var* compensators are also observed here. The case studies are illustrated in detail in the following sections

7.4.3.1 MPT based Reactive Power Dispatch and Congestion Analysis

In this work, the RPD problem characterised by MPTs was solved by controlling V_g and t with unconstrained security constraints for the IEEE 30 bus system as case 1. This generated dynamic voltage limit crossover issues causing to voltage drops leading to enhanced current flow as well as increasing power losses. Therefore, the situation was revisited by incorporating different *var* compensators such as shunt capacitors and SMES (Q_{SMES}) as case 2 and case 3 with other control variables as V_g and t with constrained security constraints one by one. Here, the DERL algorithm was considered here as an optimisation technique to settle the control variables. The optimal parameters of the method was chosen here as N_p = 30, C_R = 0.8 and Gen_{max} = 100 after 100 trial runs. The operating ranges of the control variables are shown in Appendix A.2 and B.2.

The schedule for multilateral power transactions is given in Table 46. Moreover, a 35 MW DG unit is placed in the 11th bus to bring the effect of deregulation more prominent in the chosen network [246].

Table 46. Schedule of multilateral transaction in case of IEEE 30-bus system

No. of Multilateral Transactions	Buses as power supplier	Power injections in MW	Buses as power consumer	Power consumption in MW
T_1	18	14	6	10
T_2	21	12	12	10
T_3	3	08	27	04
T_4	-	-	30	10

- **Case 1: RPD with MPT Analysis without Var Compensators**

Initially, the P_{LOSS} was minimized here to 14.8027 MW by controlling V_G and t considering multi-lateral power transactions in the DG based IEEE 30 bus network. The average and the worst P_{LOSS} values by DERL method were obtained as 14.8128 MW and 14.889 MW respectively considering 50 trial runs. Moreover, the convergence characteristics the terms of best P_{LOSS} w.r.t. the generation number are plotted in Figure 41. The Figure shows the global convergence of the optimal value within the 20th generation. Therefore, the proposed DERL method was being able to maintain its fast converging property by avoiding local trap.

Besides the loss minimisations aspect of the RPD problem, the voltage profiles of all the buses during the multilateral transactions were observed. It has been found that all the buses were fluctuating nearby their boundary value. Amongst them, 29th and 30th buses went below the allowable limits (0.95-1.10 p.u.) as shown in Table 47. This fall in voltage caused the dynamic voltage limit crossover problem in the network which further raised the line to line current flow as well as power losses with respect to the standard value. This situation leads the network towards the congestion. To analyse the situation more clearly CEF_{ij} and $PLEF_{ij}$ were determined and obtained 1.2981 times and 1.6851 in the line 27 to 29. Moreover, for the line 27 to 30, CEF_{ij} and $PLEF_{ij}$ were found 2.3540 and 5.5414 where they were derived as 3.5416 and 12.5434 in the line 29 to 30. The network congestion was presented in Figure 42 which needs proper management..

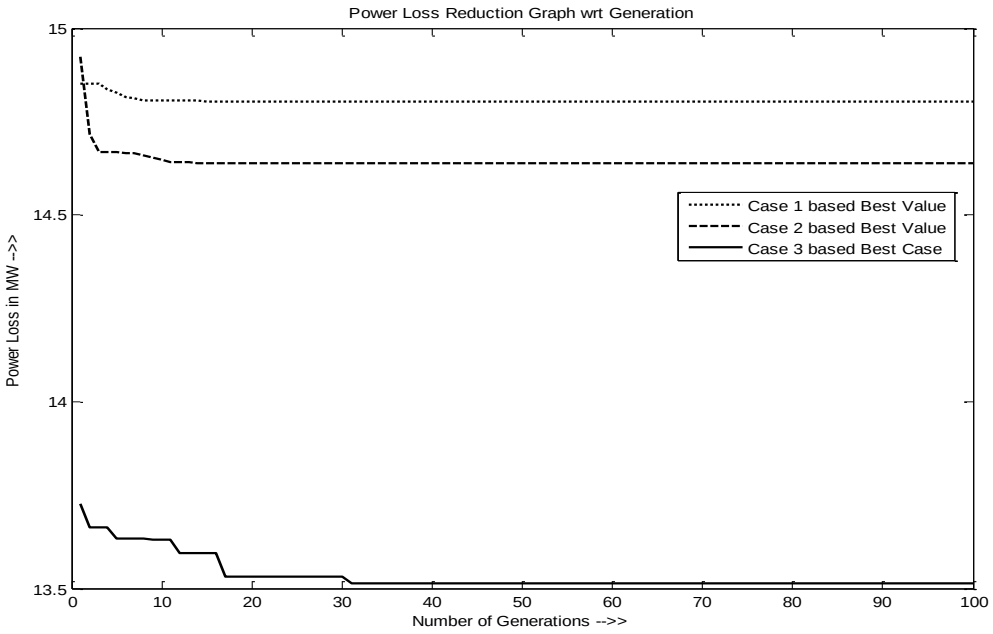

Figure 41. Restructured power loss optimizations for IEEE 30-bus system involving multilateral power transactions (MPT)

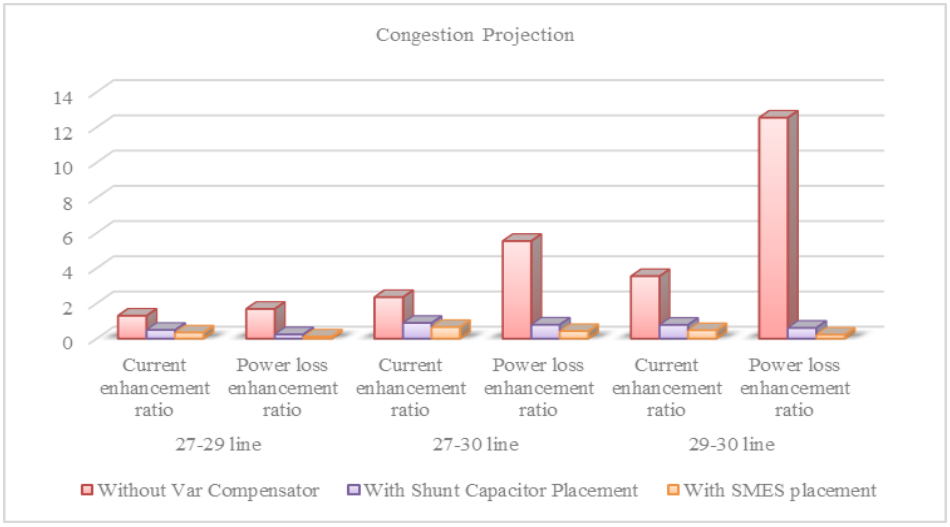

Figure 42. Congestion due to restructured RPD for IEEE 30-bus system

Table 47. Voltage profile of the affected buses during the multilateral power transactions based on RPD analysis

Bus No.	Bus voltage profile (p.u.)		
	Case 1	Case 2	Case 3
27	0.9822	1.0305	1.05
29	0.9404	0.9910	1.0158
30	0.9064	0.9590	0.9847

- **Case 2: RPD with MPT Analysis by the Capacitive Var Compensator**

In the case 2, the proposed problem was revisited by incorporating the shunt capacitors in addition with other control variables like V_G and t to optimize the RPD problem. By incorporating the capacitor bank, the P_{LOSS} was reduced to 14.6375 MW here. Simultaneously the average and the worst values were obtained as 14.7866 MW and 14.8214 MW after considering 50 trial runs. The convergence characteristic of the best value is presented in Figure 41. The Figure 41 showed that at alike the previous case, the best value was converging within the 20th generation. The Figure 41 also demonstrated that there were a number of local optima in the convergence path however the final value was reached at the global optima at the earlier generations. Therefore the working principle of the DERL method was found satisfactorily working here.

In addition to the P_{LOSS} optimisations, the voltage profiles of the network including the 29th and 30th buses were observed to provide a stable voltage profile throughout the network. The voltage profile of the 27th and 29th, 30th buses for the case 2 are shown in Table 47. In this case, the CEF_{ij} and $PLEF_{ij}$ in line 27 to 29 were observed as 0.4906 and 0.24077 where CEF_{ij} and $PLEF_{ij}$ for the line 27 to 30 were obtained as 0.8881 and 0.7888 respectively. In this connection, CEF_{ij} and $PLEF_{ij}$ for the line 29 to 30 were determined as 0.7804 and 0.6091 respectively. Therefore, in comparison to the case 1, case 2 based CEF_{ij} and $PLEF_{ij}$ were found to be improving with higher losses shown in Figure 42. Therefore, the proposed problem was further investigated for improved response with one of the advanced *var* compensator namely the SMES.

- **Case 3: RPD with MPT Analysis by the SMES**

Here in case 3 SMES was integrated to solve the RPD problem characterised by the multilateral power transactions. The two units of the proposed devices were optimally incorporated in the 24th bus in conjunction with the control of V_G and t. In this case P_{LOSS} was reduced to 13.5126 MW. In addition to this, the average and the worst P_{LOSS} value were obtained as 13.5498 MW and 13.5679 MW respectively considering fifty (50) trial runs. Finally the convergence characteristics curve of the best value is plotted in Figure 41. This figure showed the stable convergence of the optimal P_{LOSS} value at the global optima while avoiding several local optimal solutions.

In addition to the P_{LOSS} minimization, the voltage profile of the network including the 29th and the 30th buses were observed to be within the standard voltage limit of 0.95 p.u. to 1.05 p.u. Therefore, this also helped to maintain dynamic voltage profile within stable operating limit in the network while reducing the congestion in terms of reduced CEF_{ij} and $PLEF_{ij}$ as shown in Figure 42. Here, CEF_{ij} and $PLEF_{ij}$ in the 27th to 29th lines were determined to be 0.342 and 0.1169 respectively where CEF_{ij} and $PLEF_{ij}$ were obtained as 0.653 and 0.4264 respectively in the 27th to 30th line. Meanwhile, CEF_{ij} and $PLEF_{ij}$ in the 29th to 30th line were found as 0.4726 and 0.2233 respectively. Hence, the dynamic voltage limit crossover aspect in the form of CEF_{ij} and $PLEF_{ij}$ has been observed to improve here with significant loss reduction compared to case 1 and 2. Therefore, it can be concluded that the proposed advanced *var* compensation based analysis showed its efficiency over the other methods.

In this study, a small test system is analysed technically without any economic considerations. Since, economics is a governing issue of the deregulated power scenario; it is required to be considered in such back drop. Moreover, in real power scenario, the power mismatch either in the generation or consumer sides are frequently observed. Due to power mismatch, the global welfares are also affected in terms of spot pricing. Therefore, these issues are considered here as the second case study on MPTs for a real Indian power scenario.

7.4.3.2 Efficient Double Auction Multilateral Power Transactions for a Day Ahead Economic Reactive Power Dispatch

Here, the RPD problems characterized by a day ahead variable multilateral power transactions are solved for Indian Utility with 62- bus system. Alike the previous case studies, the restructured RPD issue was solving by V_g and t with unconstrained security constraint optimisation as case 1. This invoked dynamic voltage limit crossover problem. To solve the problem, different *var* compensators and some of their combinations has been proposed here as case 2-case 5 by controlling Q_C, x_{TCSC}, Q_{SMES} and hybrid combination of Q_C-Q_{SMES} respectively. In this regards, the other network parameters

were remaining unaltered. As an optimisation tool DERL technique was utilised here due to its different strength. The optimal parameters of the DERL method were chosen as $f_m \in \text{rand}(0,1)$, N_p = 40, C_R = 0.8, Gen_{max} = 100 after considering 100 trial runs. The operating ranges of the control variables such as V_g, t, Q_C and x_{TCSC} were given in Appendix Table A2, and Q_{SMES} were shown in Appendix B2. Moreover, power mismatch has been considered during the power transactions period. Before going to the detailed case studies, the background of power mismatches is elaborated.

7.4.3.2.1 Power Mismatch

In ideal deregulated power market scenario, the balanced interactions amongst the suppliers and consumers progressively lead to the market equilibrium. Here, the consumers purchase the power based on their load forecasting from the suppliers. Similarly, the suppliers provide the contract amount of power at the agreed time based on the exact demand of the consumers. In real market, however, these transactions are not that simple. Neither party can reliably satisfy its contractual obligations with perfect accuracy due to major reasons. First, the actual demand of a group of consumers is rarely found to be exactly equal to the value forecasted. Second, unpredictable problem such as a sudden mechanical or electrical failure often prevent the generating units to generate the contracted amount of power in time. These errors and undesirable events introduce gaps between load and generation in the real time deregulated power scenario. This gap is termed as power mismatch or power imbalances which are managed in terms of spot market. The spot market provides a mechanism for balancing load and generation. Besides the technical considerations such as balance between the load and generations, the spot market must operate in an economically efficient manner while influencing the global welfare. Therefore, the impact of power mismatch are technically and economically are illustrated in the following sections sequentially.

7.4.3.2.2 RPD based Case Studies with Power Mismatch

In the proposed multilateral power transactions, two power suppliers and four power consumers had participated. The participant buses of the Indian utility were chosen elsewhere [98]. The amount of power transactions by each participant were decided by planned bidding to achieve maximum economic efficiency which is discussed in detail in section 7.4.3.2.4. In this work, two studies of power mismatch during the variable power transactions in a day ahead inter-regional grid have been considered as in Table 48. In the first 12-h, multilateral power transactions (MPT) of 221 MW was traded between the power producers and the power consumers. In this case study, it had been considered an hourly power mismatch of 18 MW [11] with an additional 0.02 % loss variations occurred at the generation side while providing 203 ± 0.036 MW of power hourly to the consumers

[11]. Therefore the transaction authority would charge penalty in terms of balancing cost as given in equation (4) as available in Chapter 4. Here, an hourly variable spot price has been considered as described in detail in the section 7.4.3.2.4. Now, in the next 12-h of the day ahead power transactions at the inter-regional grid, MPT of 305 MW was contracted between the power suppliers and the consumers. In this case study, it had been found an hourly power mismatch of 26 MW [11]. Alike the previous hours, here 0.02% of additional loss variations over 26 MW have been considered. In this study, the consumers had drawn the extra amount of power to receive 331 ± 0.052 MW from the transaction network. Therefore, the transaction authority would arrange a spot pricing in the favour of the suppliers which was detailed in the section 7.4.3.2.4.

Table 48. Schedule of multilateral power transactions (MPT) for two case studies

No. of multilateral transactions	Buses as power supplier	Multi-lateral Power transactions by supplier (MW)		Buses as power Consumer	Multi-lateral Power transactions as power consumer	
		1h-12 h Case 1 of 221 MW	13h-24h Case 2 of 305 MW		1h-12h Case 1 of 221 MW	13h-24h Case 2 of 305 MW
T_1	36	71	110	12	50	80
T_2	42	150	195	24	50	90
T_3	-	-	-	54	50	80
T_4	-	-	-	60	71	55

In both the cases, it can be observed that the involvement of the spot pricing affects the global welfare which thereby needs improvement in terms of reduced merchandising surplus as invoked by the different *var* compensators. Therefore, the incorporation of the *var* compensators while solving the restructured RPD issues required major attention.

Before going to the detailed study, few assumptions are mentioned here to avoid repetition of similar results. Since, the variation in hourly power mismatch is very tiny i.e., 0.02 % of the total requirement, the technical parts of the RPD considering 18.0113 MW of average power mismatch for the first 12 hours and 26.0105 MW of average power mismatch for the next 12 hours were solved. These are more discussed in section 7.4.3.2.4.

- **Case 1: RPD Analysis without any Var Compensators**

As stated, initially by controlling V_g and t, the P_{LOSS} was found to be generated of a value of 64.2478 MW when MPT of 221 MW was traded. Moreover, the P_{LOSS} was derived as 64.1695 MW for the second study of MPTs of 305 MW power. Both of the losses were observed to converge globally at the earlier generations as presented in Figure 43 and 44. Besides the P_{LOSS} optimisations, the voltage profiles of the network during the MPTs were observed which demonstrated dynamic voltage limit crossover for both the cases as shown in Table 49. For the first case study, voltages of few buses have been observed to fluctuate near the boundary value. Amongst them four buses had violated the standard boundary limit of 0.95-1.10 p.u., which are shown in Table 49. Here, the operating range of the voltage profile has been found to vary within 0.9245 p.u. to 1.1105 p.u. during the power transactions. These further enhanced the voltage drops in the line. These increasing voltage drops caused increasing line current flow followed by huge power losses. These required *var* compensation to recover.

For the second study, the problem of dynamic voltage limit crossover has also been observed due to rapid fluctuation of the bus voltages during the multilateral power transactions. Even three of the buses likely the 13th, 20th, and the 49th buses were found violating the standard boundary limit of the network which are specified in Table 49. This voltage deviation generated increasing voltage drops leading to heavy currents and thereby huge power losses. These situations may also be solved by adequate *var* compensations.

Table 49. Dynamic voltage profile (p.u.) for a day-ahead double auction MPT

	1st case study of MPT 1				2nd case study of MPT 2		
Voltage deviated bus numbers	19	20	26	48	13	20	49
Case 1 based voltage value (p.u.)	0.9420	0.9287	0.9372	1.1105	0.9405	0.9496	0.9473
Case 2 based voltage value (p.u.)	1.0824	0.9610	0.9948	1.0215	0.9808	0.9588	1.0974
Case 3 based voltage value (p.u.)	1.0358	0.9545	0.9671	1.0083	0.9882	0.9559	1.0884
Case 4 based voltage value (p.u.)	0.9935	0.9705	1.0166	1.0850	1.0382	1.0607	1.0478
Case 5 based voltage value (p.u.)	0.970	0.9690	0.9876	1.0471	0.9969	0.9794	1.0777

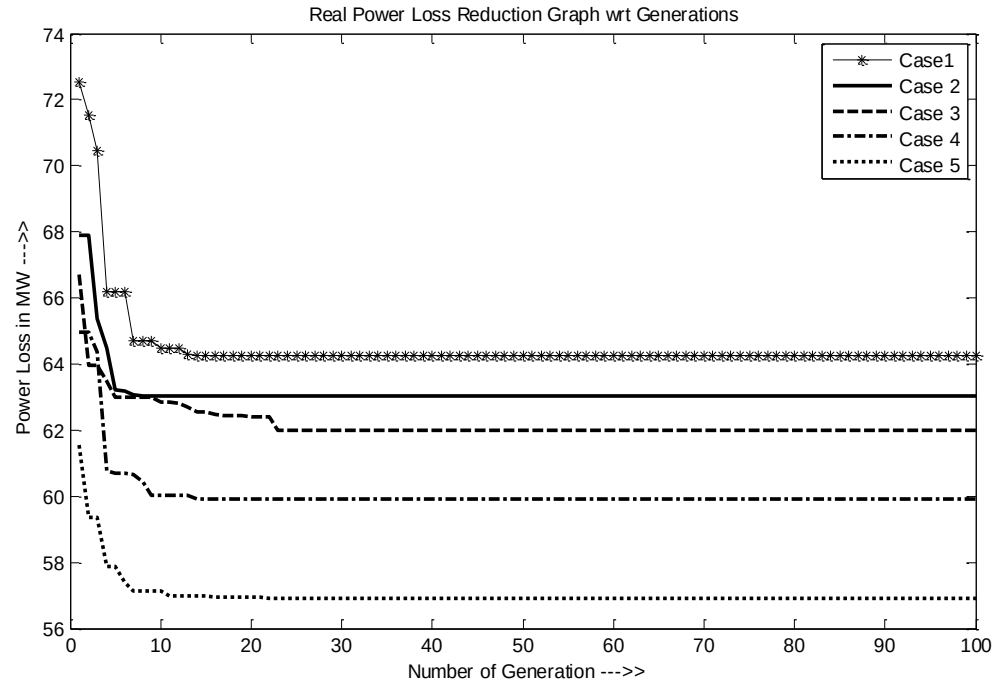

Figure 43. Power loss optimization curves by different *var* compensators for MPT (case 1) for real 62-bus network

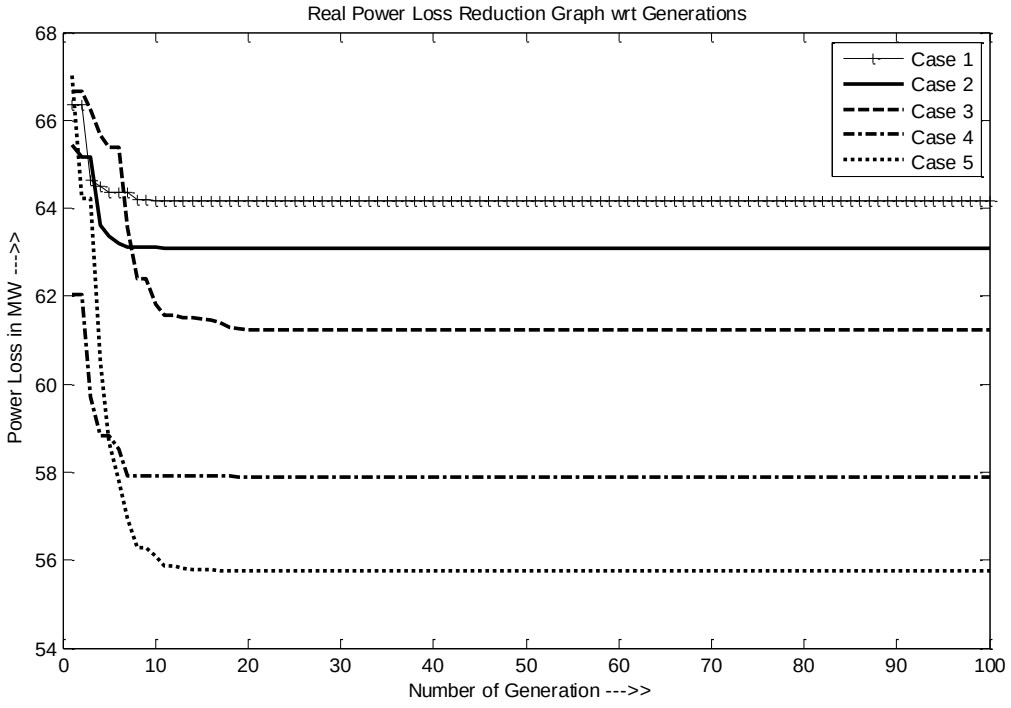

Figure 44. MPT (case 2) based power loss optimizations by different *var* compensators for real 62-bus network

Table 50. Different reactive power compensators based power loss optimization study

	Without any *var* compensators		Capacitor based solution		TCSC based solution		SMES based solution		Capacitor-SMES combination based solution	
Case studies on MPT	MPT 1	MPT 2	MPT 1	MPT 2	MPT 1	MPT 2	MPT 1	MPT 2	MPT 1	MPT 2
P_{LOSS} (MW)	64.2478	64.1695	63.0483	63.085	61.985	61.247	59.9155	57.895	56.902	55.743
% P_{LOSS} reduction w.r.t the case 1	-	-	1.867	1.690	3.522	4.554	6.743	9.778	11.433	13.132

- **Case 2: RPD Analysis by Capacitors**

Initially the RPD problem involving MPTs were solved by controlling V_g, t and one of the most commonly used fundamental *var* compensators likely capacitors Q_C. Here, eight positions (load buses) were optimally chosen by DERL method for capacitor placements. For the first case study of MPT, the P_{LOSS} was minimized to 63.0483 MW. Considering the hundred trial runs, the average and the worst value were obtained as 63.9946 MW and 64.0903 MW respectively. The best observation is plotted in Figure 43.

In this context, when the second study on MPT of 305 MW was traded, the power loss (P_{LOSS}) of the network was found to be optimized to 63.0858 MW. Considering hundred trial runs, the average and the worst value were obtained as 63.7884 MW and 63.9802 MW respectively. The best observation in this case is presented in Figure 44.

From both the Figure 43 and 44, it can be observed that during the 100 generations, several local optimum points were found to converge however the optimal P_{LOSS} had converged to the global optima. Moreover, the reduction of % P_{LOSS} w.r.t the case 1 had determined here in Table 50. It showed 1.867 and 1.690 percent of reduction indicating a small improvement towards the power loss

minimization for both the MPT 1 and MPT 2 respectively. The control variables were also found to be within stable operating limits amongst them the Q_C for both the cases are demonstrated in Table 51.

Table 51. Control variables as *var* compensators for MPT 1 and MPT 2 (i) Case 2 as Q_C (ii) Case 3 as x_{TCSC} (iii) Case 4 as Q_{SMES} (iv) Case 5 as Q_C –Q_{SMES}

Table 51. (i) Case 2 based Q_C as control variable for MPT1 and MPT 2

MPT 1	Bus Numbers	46	19	24	38	41	29	10	30
	Value in p.u.	2.2505	2.0170	1.2686	3.5805	0.3702	3.6327	0.6791	3.5295
MPT 2	Bus Numbers	11	12	13	15	24	39	45	56
	Value in p.u.	5.000	2.2027	3.3749	2.8797	0.150	4.9241	2.5456	0.150

In this connection to dynamic voltage limit crossover analysis, the voltage profile of the network was observed to vary within the stable operating limit of 0.95-1.10 p.u. in Table 49 for both the cases. However the operational margin did not reduced much. Moreover, the P_{LOSS} optimisations were required to improve more. Therefore, one of the improved *var* compensating devices namely TCSC was considered in place of capacitors for further simulation process.

- **Case 3: TCSC based RPD Analysis**

In the view of RPD problem characterized by MPTs, one of the important FACTs device namely TCSC was incorporated in six optimal positions (line where no transformers are connected). Considering, 221 MW of MPT, the P_{LOSS} was minimized to 61.9857 MW by controlling V_g, t and x_{TCSC}. In this work, the average and the worst value were obtained as 62.1659 MW and 62.887 MW respectively while considering hundred trial runs. Moreover, the reduction of % P_{LOSS} w.r.t case 1 was determined here as 3.532 shown in Table 50, which was also found improved by 1.68 % more compared to case 2. In this connection to MPT 2, the P_{LOSS} of the network was optimized to 61.247 MW by the optimal integration of the TCSC devices in the network. In this case, the average and the worst values were found as 63.686 MW and 63.14 MW respectively. The best P_{LOSS} value was reduced the % P_{LOSS} w.r.t case 1 as 4.554 shown in Table 50 and w.r.t case 2 as 2.9147 which indicated better responses compared to the previous cases. The best response in terms of P_{LOSS} optimization is plotted in Figure 43 and 44 respectively for MPT 1 and MPT 2. From both the Figure 43 and 44, it could be observed that during the 100 generations, the TCSC based optimal fitness functions were supposed to converge at several local optimum points although it converged to the

global optima due to efficient performance of the proposed DERL method. Moreover, the control variables were observed within the stable operating limits such that stability of the network remained uninterrupted. Here, the optimal values of the x_{TCSC} are shown in Table 51. (ii).

Table 51. (ii) Case 3 based x_{TCSC} as control variable for MPT1 and MPT 2

MPT 1	Line Numbers	17	27	29	67	77	79
	Value in p.u.	-0.0088	-0.0314	-0.0277	-0.0276	-0.0239	-0.0389
MPT 2	Line Numbers	26	41	47	49	66	84
	Value in p.u.	-0.0010	-0.0090	-0.0400	-0.0045	0.0079	-0.0388

Now, in the view of TCSC placement the dynamic voltage limit crossover issues of the network has been found to be within the stable operating limit of 0.95-1.09 p.u. for both the MPTs shown in Table 49. Therefore, it can be remarked that operating margin of the network was reduced compared to the case 1, 2 with a little improvement in loss reductions. Hence, to obtain more improvement for restructured RPD issue characterised by variable MPTs, the matter has been investigated by one of the promising dynamic *var* compensating devices namely SMES.

- **Case 4: SMES based RPD Analysis**

Alike the previous case, in this work SMES devices were optimally placed in six positions as one of the control variables to solve the RPD problem involving MPTs. Initially MPTs of 221 MW were considered in the network, for which minimum P_{LOSS} was obtained as 59.9155 MW by controlling V_g, t and Q_{SMES}. Moreover the average and the worst values were found as 61.3176 MW and 61.5 MW respectively after hundred trial runs. Here, the % P_{LOSS} reduction was determined to be 6.74311 w.r.t case 1 as given in Table 50. Further, the % P_{LOSS} reduction w.r.t case 2 and case 3 were determined as 4.9688 and 3.3398 respectively. In this connection to MPT 2 of 305 MW, the P_{LOSS} of the network was optimized to 57.895 MW by the incorporation of SMES device. In this case, the average and the worst values were found as 58.6373 MW and 60.09 MW respectively. Alike the other cases, the % P_{LOSS} reduction was estimated here as 9.778 w.r.t case 1 as shown in Table 50. Moreover, the % P_{LOSS} reductions were determined here as 8.2281, 5.4729 w.r.t case 2 and case 3 respectively. The best response in terms of P_{LOSS} is plotted in Figure 43 and 44 for both the MPTs respectively. Now, from both the Figure 43 and 44, it could be observed that during the 100 generations, the SMES based

optimal fitness functions were supposed to converge at several local optimum points although it converged to the global optima to efficient performance of the proposed DERL method. In this regards the optimal values of the Q_{SMES} are shown in Table 51. (iii) for both the MPTs which were also obtained to be within desired operating limit of the network.

Table 51. (iii) Case 4 based Q_{SMES} as control variable for MPT1 and MPT 2

MPT 1	Bus Numbers	7	13	22	29	35	60
	Value in p.u.	0.0357	0.0249	0.0214	0.0268	0.0301	0.0200
MPT 2	Bus Numbers	10	16	22	26	30	55
	Value in p.u.	0.0214	0.0418	0.0376	0.0239	0.0305	0.0204

Now, the dynamic voltage limit crossover analysis which is one of the prime parts of the proposed problem has been observed in terms of the voltage profile of the network for both the cases. Here, the operating margin of the network voltage was found to vary within the 0.967-1.085 p.u. including the disturbed ones of the case 1 as shown in Table 50. Therefore, the case 4 based *var* compensation was able to reduce the operating margin of the network with reducing power losses compared to case 1, 2 and 3. Although the singular SMES performed better compared to the other cases, its investment costs is very high. Therefore, to obtain cost-effective as well as sustainable solution, a hybrid combination of capacitor-SMES was further incorporated in the considered network to solve the proposed problem.

- **Case 5: Hybrid Capacitor-SMES based RPD Analysis**

In this work, finally a combination of four capacitor and three SMES devices were optimally fixed by the proposed DERL method to solve the RPD problem involving MPTs. Initially MPTs of 221 MW were considered in the network, for which the combined capacitor-SMES based *var* compensators helped to minimize the P_{LOSS} to 56.90 MW with other control variables likely V_g and t. Here, the average and the worst values were obtained 57.75 MW and 58.6262 MW respectively considering hundred trial runs. In this context, the % P_{LOSS} reduction was determined 11.4335 w.r.t case 1 as shown in Table 50. Further, the percent of P_{LOSS} reduction w.r.t the case 2, 3 and 4 based singular *var* compensations were obtained as 9.7517, 8.2046 and 5.032 respectively.

Now, for the 2nd study of MPT 2, the P_{LOSS} was found 55.7437 MW by controlling the proposed combined capacitor-SMES with V_g and t. In this case, the average and the worst value were obtained

as 57.0421 MW and 58.0212 MW respectively. Here, the % P_{LOSS} reduction was determined as 13.132 w.r.t case 1 as given in Table 50. In this connection, the % P_{LOSS} reduction w.r.t case 2, case 3 and case 4 were found as 11.2472, 8.5826 and 3.2897 respectively. The best results in terms of P_{LOSS} optimization are plotted in Figure 43 and 44 for both case cases respectively. Now, from both the Figure 43 and 44, it could be observed that during the 100 generations the fitness functions were supposed to converge at several local optimum points. However, these were found converged to the global optima due to efficient performance of the proposed DERL method. The optimal values of Q_C - Q_{SMES} for both the cases are provided in Table 51. (iv). This also showed to be within stable operating limit while maintaining desired stability of the network.

Table 51. (iv). Case 5 based Q_C -Q_{SMES} as control variable for MPT 1 and MPT 2

		Q_C				Q_{SMES}		
MPT 1	Bus Numbers	3	22	45	60	7	24	40
	Value in p.u.	2.0491	4.0387	2.2343	0.150	0.0326	0.0403	0.0265
MPT 2	Bus Numbers	15	16	26	61	10	11	22
	Value in p.u.	4.4405	1.4353	1.4682	0.150	0.0388	0.0420	0.0214

In this context, the operating margin of the voltage profile of the network has been observed to have 0.97-1.080 p.u. including the violated one as observed in case 1 shown in Table 49. This indicated a steady, stable and reduced operating margin to show the dynamic voltage profile within the stable operating limit in the view of restructured RPD analysis. In fact the operational range of the case 5 based voltage profile was found most promising compared to other cases with reduced losses.

Now, besides the technical analyses of the different *var* compensators for restructured RPD, the economics of the devices are required to be investigated for proper uses.

7.4.3.2.3 Economics of Comparable Reactive Power Compensators

Alike, the previous assumptions (as stated in sub-section 7.4.3.2.2), here the economics of the *var* compensators were also determined considering the power loss mismatch of 18.0113 MW for the first 12 hours and 26.0105 MW of power mismatch for the next 12 hours. In this work, the economics of the utilized *var* compensators were determined by equation (7-8, 11-21 and 23) as available in

Chapter 4. Here, the incentive return for power loss minimization was considered as 6800 Rs /MW h found elsewhere [177]. The economics including the investment cost of the *var* compensators (HIC_k) and the incentive return benefit (*Inc*) of both the case studies are shown in Table 52. According to MPT 1 as shown in Table 52, the HIC_{TCSC} was found 4309.609 Rs/ h. This was 1.664 times and 2.67 times higher compared to the HIC_{SMES} and $HIC_{Capacitor+SMES}$. In this connection, the case study 1 based HIC_{SMES} was obtained as 2587.955 Rs /h which was found 1.60 times higher compared to the $HIC_{Capacitor+SMES}$.

In this context, the 2nd case study on MPT, the HIC_{TCSC} and HIC_{SMES} were obtained nearly equal as given in Table 52. These data were obtained 1.661 and 1.719 times respectively more compared to the $HIC_{Capacitor+SMES}$ which was determined as 1619.825 Rs/ h. In this context, the investment cost of the capacitive *var* compensator was obtained very low compared to the advanced *var* compensators.

Table 52. Economics for the different reactive power compensators

		Case 1	Case 2	Case 3	Case 4
MPT 1	HIC_k	20.1766	4308.609	2587.955	1613.254
	$(P_{LOSS\_bVCP} - P_{LOSS\_aVCP}) \times Inc$ Rs/h	8156.6	15421.04	29459.64	49951.44
	NMB_k	8136.423	11112.43	26339.25	48338.19
MPT 2	HIC_k	24.7163	2750.95	2846.96075	1655.541
	$(P_{LOSS\_bVCP} - P_{LOSS\_aVCP}) \times Inc$ Rs/h	7369.16	19873	42666.6	57295.44
	NMB_k	7344.444	17122.04	39819.64	55639.9

k = case 1, case 2, case 3 and case 4, *NMB*=Net monetary benefit

Besides the investment cost of the different *var* compensators, the determination of incentive returns due to P_{LOSS} optimization was a vital issue to obtain net monetary benefit of the proposed transaction. According to the MPT 1, the case 3 has obtained 1.89 times more incentive benefit as 15421 Rs/ h. In this case study, singular SMES based case 4 received 29459.64 Rs/ h as incentive benefit which was 3.61 and 1.91 times more compared to case 2, case 3 based *var* compensations respectively. Finally, combined capacitor-SMES based case 5 achieved 49951.44 Rs/ h as incentive benefit which were 6.12, 3.24, and 1.70 times compared to case 2, case 3 and case 4 based incentive benefit respectively.

Similarly, in the context to MPT 2, the case 3 based incentive benefit was found as 19873 Rs/ h which was 2.70 times higher compared to case 2 as shown in Table 52. Moreover, the case 4 based incentive benefit was obtained as 42666.67 Rs/ h which was found to be 5.789 and 2.14 times higher compared to case 2 and case 3 respectively. In this regards, the case 5 based incentive benefit was determined as 57295.44 Rs/ h which was found 7.77, 2.88, 1.34 times more compared to the case 2, case 3 and case 4 based incentive benefits. While analyzing these observations, it was found that the combined capacitor-SMES based incentive return for both the MPTs have been achieved highest compared to other cases.

With these, the economics due to *var* compensation or the net monetary benefit (*NMB*) was determined for all the case studies as shown in Table 52. According to the first case study, it could be noticed that among the three set of *var* compensators, the combined capacitor-SMES provided highest $NMB_{Capacitor+SMES}$ of 48338.19 Rs/ h. This observation is almost six times higher than the $NMB_{Capacitor}$, 4.34 times higher than NMB_{TCSC} and 1.83 times higher than the NMB_{SMES}.

Similarly, for the MPT 2, the $NMB_{Capacitor+SMES}$ was found as 55639.90 Rs/ h as shown in Table 52. It has been found that the $NMB_{Capacitor+SMES}$ was obtained not only highest amongst the other cases, it was 7.5 times from the $NMB_{Capacitor}$. Moreover, the $NMB_{Capacitor+SMES}$ was found 3.24 times more than the NMB_{TCSC} and 1.40 times higher than the NMB_{SMES}.

Now, the economics of the *var* compensators helped to reduce the merchandising surplus as control by the transaction authority. Therefore, this played an important role on the global welfare improvement as well as the benefit improvements of the market participants of MPTs of the system under consideration.

7.4.3.2.4 Global Welfare Analysis considering Variable Spot Pricing

In this work, a day ahead inter-regional power network has been considered where two double auction power transactions have been considered. For 1-12h, MPT 1 took place and for 13-24h MPT 2 occurred where the two suppliers and four consumers bid twice. Their final bid prices with quantity are shown in Table 53. With the scheduling and drawling data, two market clearing curves have been drawn in Figure 45 and 46 which provided the MCP and MCV. Here, the bids were accepted as per the contracted power amount. The cost equations and the cost coefficients of the participants (two generators and four consumers) are given in Appendix Table C4.

Now, analyzing the bidding of the participants as well as market clearing for both the MPTs, the MCPs for the first 12-h has been derived as 257040 Rs/ MWh with 280 MW of MCV and for the next 12-h the MCP was obtained as 266900 Rs/ MWh with 350 MW of MCV.

Table 53. Final Bids of the market participants for 1-24-h variable double auction MPT

Hour	Supplier's offer price ($/ MW h) 1$ = 68 Rs on 27-01-2016	G_1 MW	G_2 MW	Total MW	Total MW	Consumer's offer price ($/ MW h) 1$ = 68 Rs on 27-01-2016	L_1 MW	L_2 MW	L_3 MW	L_4 MW	Total MW
1-12 h	3650	-	150	150	221	4410	50	-	-	-	50
	3690	71	-	71		4260	-	50	-	-	50
						4100	-	-	50	-	50
						3870	-	-	-	71	71
13-24 h	3880	110	-	110	305	4190	80	-	-	-	80
	3920	-	195	195		4000	-	90	-	-	90
						3940	-	-	-	55	55
						3930	-	-	80	-	80

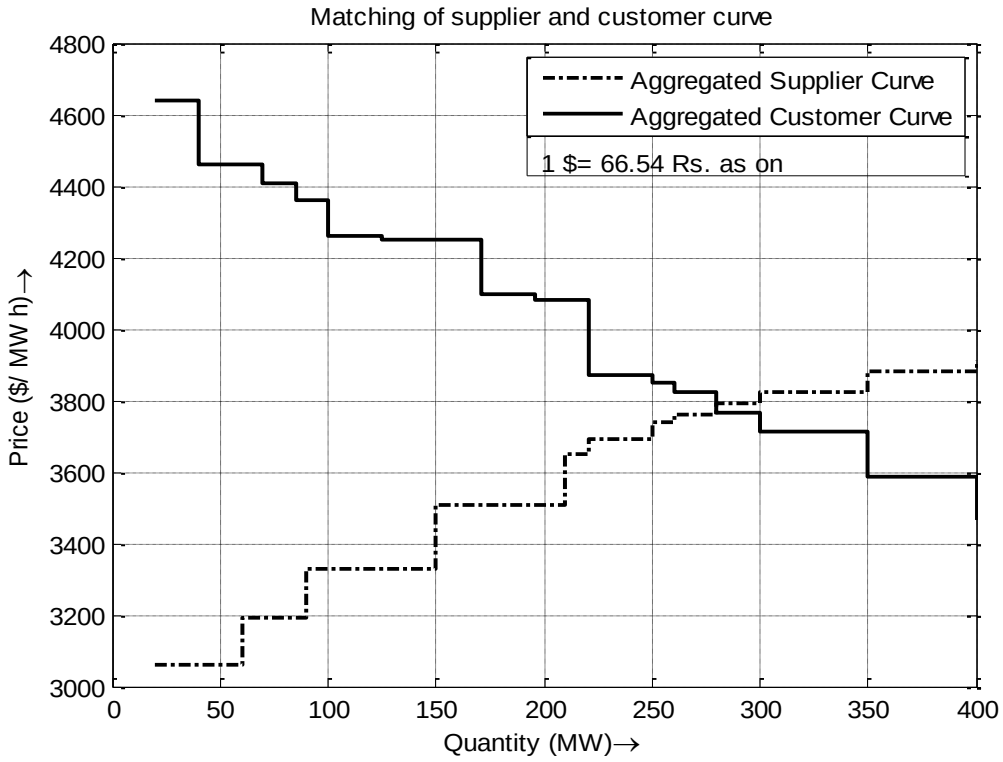

Figure 45. Market clearing data for 1st -12th hour

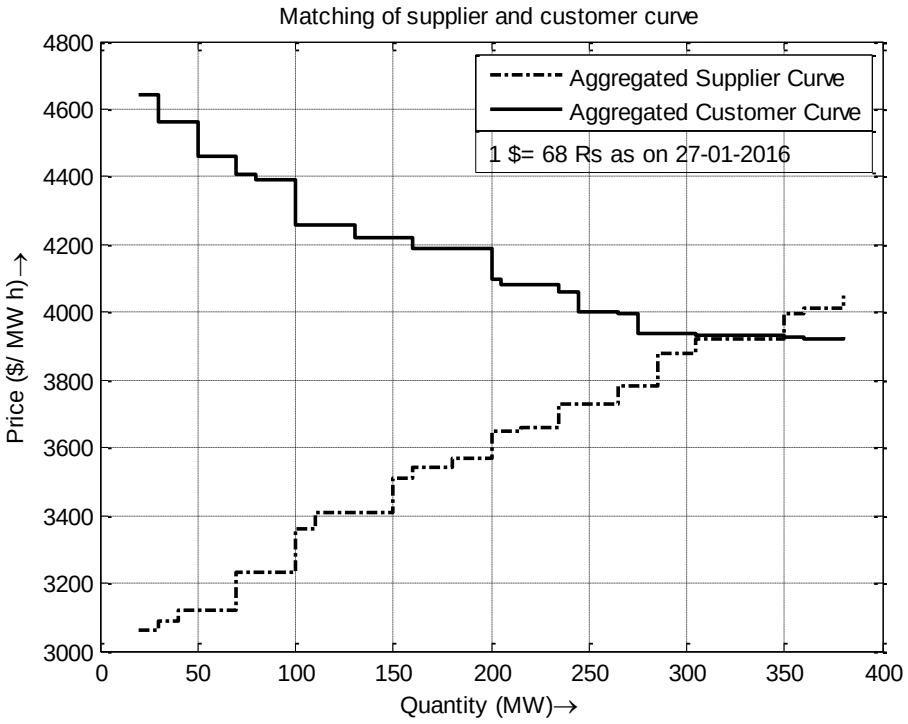

Figure 46. Market clearing data for 13th -24th hour

Since, hourly power mismatch has been occurred here, few data likely the hourly spot pricing and the balancing costs are required to be determined. These are shown in Table 54. Since, in a day ahead power scenario, operating point in terms of load management are different, the factors for the spot price due to power mismatch will be varying hourly. In this work, the range of the factor is considered as 0.5 to 1.6 times of the MCP in ascending order for the 1-12-h and 1.6 to 0.5 times of the MCP in descending order for the 13-24-h which are given in Table 54. In this context, the participant's benefits such as suppliers profit ($\sum_{k=1}^{ns} S\_Profit_k'$) and consumer's surplus ($\sum_{k=1}^{nc} C\_Surplus_k$) for the MPT1 has been determined as 6950280 Rs/ h and 7938320 Rs/ h respectively without considering any spot pricing.

For the MPT 2, the benefits of the participants such as $\sum_{k=1}^{ns} S\_Profit_k'$ and ($\sum_{k=1}^{nc} C\_Surplus_k$) were obtained as 9763100 Rs/ h and 6665700 Rs/ h respectively without considering any spot pricing. With these, the fundamental global welfare without balancing cost (*GW_WO_BC*) for MPT 1 and MPT 2 were found as 14888600 Rs/ h and 16437640 Rs/ h respectively when no spot pricing was considered.

Table 54. Hour wise spot price, *BC* and power mismatch data

Hour	1h	2h	3h	4h	5h	6h	7h	8h	9h	10h	11h	12h
Variable factor of Spot Price	0.5	0.6	0.7	0.8	0.9	1	1.1	1.2	1.3	1.4	1.5	1.6
Spot Price (Rs/ h)	128520	154224	179928	205632	231336	257040	282744	308448	334152	359856	385560	411264
Power Mismatch (MW) Average value= 18.0113 MW	18	18.001	18.004	17.996	18.002	17.998	18.005	18.02	18.024	18.022	18.03	18.034
BC (Rs/ h)	2313360	2776186.22	3239423.71	3700553	4164510.67	4626205.92	5090805.7	5558233	6022756	6485325	6951646.8	7416735
Hour	13h	14h	15h	16h	17h	18h	19h	20h	21h	22h	23h	24h
Variable factor of Spot Price	1.6	1.5	1.4	1.3	1.2	1.1	1	0.9	0.8	0.7	0.6	0.5
Spot Price (Rs/ h)	427040	400350	373660	346970	320280	293590	266900	240210	213520	186830	160140	133450
Power Mismatch (MW) Average value= 26.0105 MW	26	26.002	25.994	25.998	26.003	26.01	26.007	26.011	26.016	26.02	26.025	26.04
BC (Rs/ h)	11103040	10409901	9712918	9020526	8328241	7636276	6941268	6248102	5554936	4861317	4167644	3475038

Since, there was an hourly imbalance in the transacted power during the power trading, spot pricing in the form of balancing cost (*BC*) was considered in the proposed problem. After including the *BC*, the change in supplier's profit ($\sum_{k=1}^{ns} S\_Profit_k$) has been obtained and shown in Table 55. Now, considering the hourly variable supplier's profit and fixed consumer's benefit ($\sum_{k=1}^{nc} C\_Surplus_k$), the global welfare (*GW*) was determined and presented in the Table 55. Now, the $\sum_{k=1}^{ns} S\_Profit_k$, $\sum_{k=1}^{ns} S\_Profit_k'$ and *BC* for 1-12h were drawn in Figure 47. From the Figure 47, it can be observed that for each hour, $\sum_{k=1}^{ns} S\_Profit_k$ has been reducing from the $\sum_{k=1}^{ns} S\_Profit_k'$ in the first 12-hours. In these hours, the suppliers were unable to supply fully the contact power to the consumers and have faced an average power mismatch of 18.0113 MW hourly. Hence, the *BC* have been deducted from the $\sum_{k=1}^{ns} S\_Profit_k'$ w.r.t the hourly spot price available to the transaction authority. Although, the $\sum_{k=1}^{nc} C\_Surplus_k$ were improving here, due to negative effect of *BC* to the suppliers, the global welfare (*GW*) was further reduced as shown in Figure 48. Here, the highest $\sum_{k=1}^{ns} S\_Profit_k$ was obtained as 4636920 Rs/ h at 1-h and the minimum $\sum_{k=1}^{ns} S\_Profit_k$ was received as 466455 Rs/ h at 12-h. Since, the consumer's benefit were obtained positive for every hour, the hourly *GW* has been found positive with maximum value of 12575240 Rs/ h as in Figure 47.

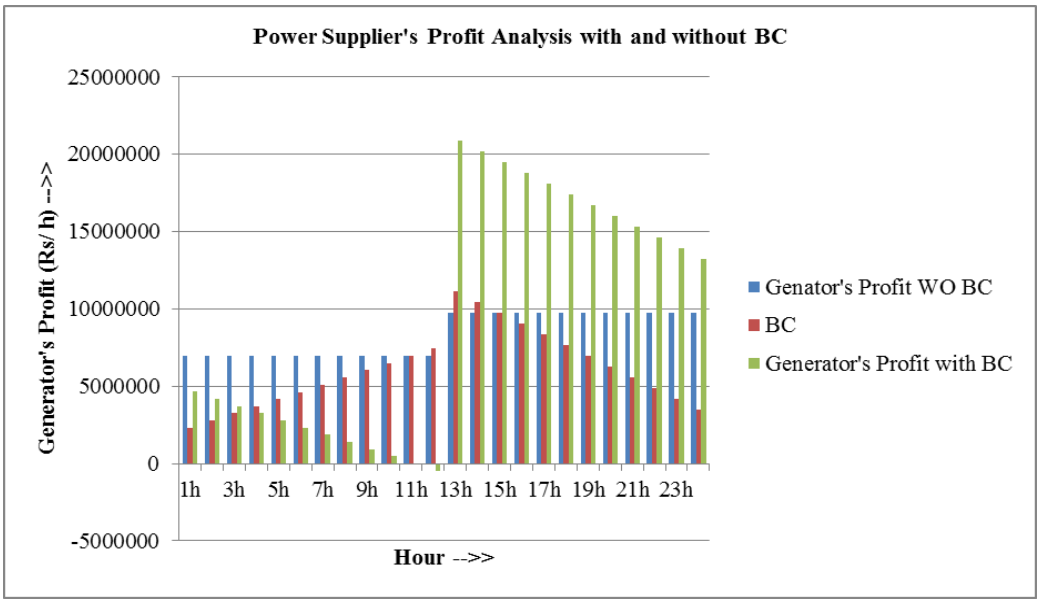

Figure 47. Hour wise variation of power supplier's profit, *BC*

Now, in the period of 13-24 h, the benefit of the participants were observed when the consumers have been drawn excess power of average value 26.0105 MW hourly. This helped to receive a *BC* favourably to the account of generator's profit as shown in Figure 47. According to Figure 47, the maximum $\sum_{k=1}^{ns} S\_Profit_k$ was obtained as 20866140 Rs/ h at 13-h which were 2.13 times more compared to generator's profit without *BC* ($\sum_{k=1}^{ns} S\_Profit_k'$). Moreover, the minimum value of the $\sum_{k=1}^{ns} S\_Profit_k$ was obtained as 19912678 Rs/ h at 24-h which were 1.356 times more compared to $\sum_{k=1}^{ns} S\_Profit_k'$. This further helped to improve the *GW* from the *GW_WO_BC* as shown in Figure 48. Although, $\sum_{k=1}^{nc} C\_Surplus_k$ was low here, the maximum *GW* was obtained as 27540680 Rs/ h which were also improved 1.675 times from the *GW_WO_BC*.

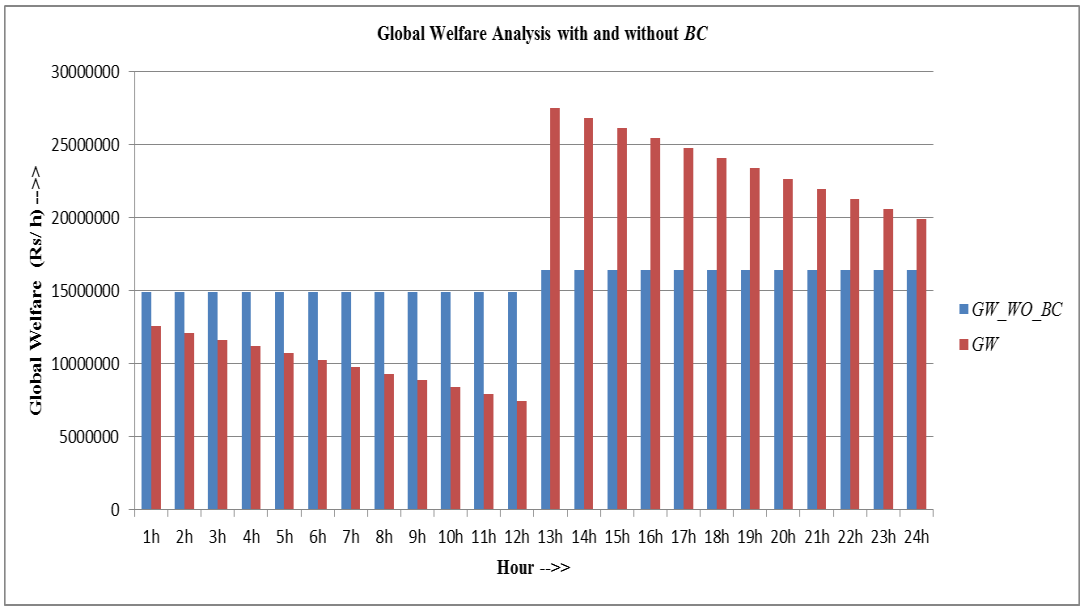

Figure 48. Variation of global welfare w.r.t hours without any *var* compensators

Now, the MEP for both the MPT 1 and MPT 2 has been observed from the Figure 45 and 46 which showed to have dead weight losses (*DWL*) i.e., the transactions were not Pareto efficient. For the MPT 1, the DWL_C for the consumers and DWL_S for the suppliers were obtained as 698360 Rs/ h and 456280 Rs/ h with a total *DWL* of 1154640 Rs/ h. In this regards, the DWL_C for the consumers and DWL_S for the suppliers of MPT 2 were obtained as 15300 Rs/ h each with a total *DWL* of 30600 Rs/ h. After comparing the two *DWL*s, it was found that case 2 based *DWL* was very small compared to the case 1. Moreover, the case 2 based *DWL* was obtained very minor compared to the *GW_WO_BC* as well as 12-h variable *GW*. Hence, it can be inferred that the MPT 2 however was not traded as the Pareto efficient transactions, the 12-h variable *GW* were achieved significant benefits in the deregulated power scenario.

Now, the 12-h variable *GW* can further be improved for both the power transactions by cumulating the economics of the *var* compensators to the fundamental *GW*. Here, the improved global welfare due to different *var* compensations was provided in Table 55 and presented in Figure 49. According to the hour wise representations as demonstrated in Figure 49, it was cleared that the economics of the *var* compensation helped to reduce the merchandising surplus. Therefore, it has increased the global welfare from the fundamental one. Amongst all the case studies, it was also obtained that the combined capacitor-SMES based *GW* has been achieved highest value. It was almost 0.384 % and 0.20 % improved compared to the fundamental GW without any *var* compensators for MPT 1 and MPT 2 respectively.

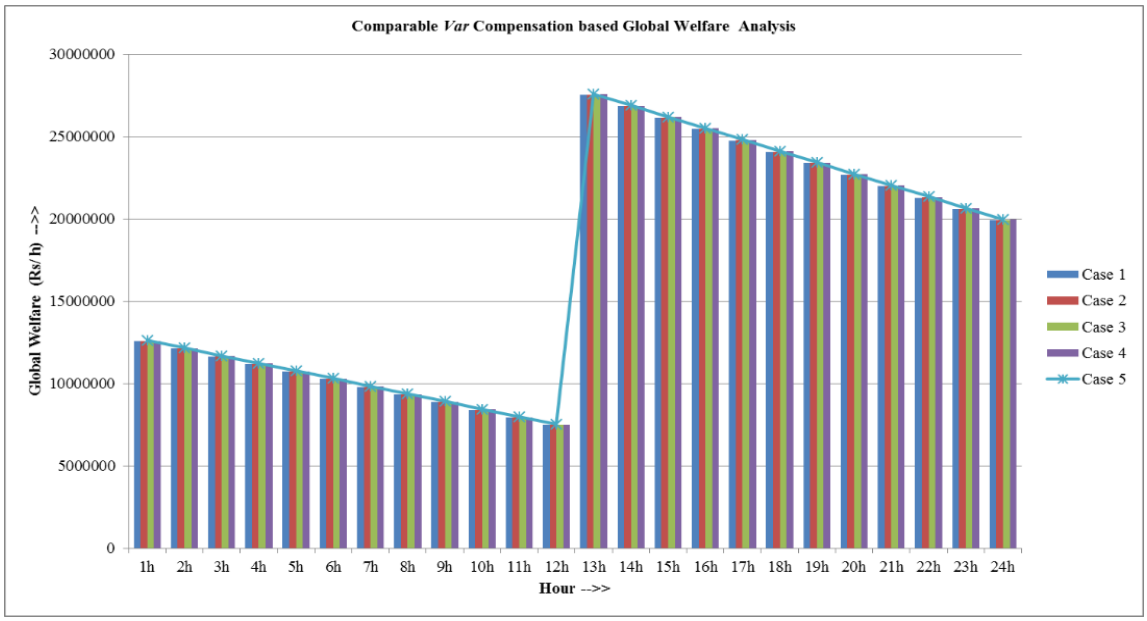

Figure 49. Hour wise global welfare for different *var* compensations

Table 55. Hour wise supplier's profit, global welfare for different cases on *var* compensations

Hour	1h	2h	3h	4h	5h	6h	7h	8h	9h	10h	11h	12h
$\sum_{k=1}^{ns} S\_Profit_k$ (Rs/ h)	4636920	4174093.78	3710856.29	3249727	2785769.33	2324074.08	1859474.3	1392047	927524.4	464955	-1366.8	-466455
GW (Rs/ h)	12575240	12112413.8	11649176.3	11188047	10724089.3	10262394.1	9797794.3	9330367	8865844	8403275	7936953.2	7471865
$\sum_{k=1}^{nc} C\_Profit_k + \sum_{k=1}^{ns} S\_Profit_k + NMB_{Capacitor}$ Rs/h	12583376	12120549.8	11657312.3	11196183	10732225.3	10270530.1	9805930.3	9338503	8873980	8411411	7945089.2	7480001
$\sum_{k=1}^{nc} C\_Profit_k + \sum_{k=1}^{ns} S\_Profit_k + NMB_{TCSC}$ Rs/h	12586352	12123525.8	11660288.3	11199159	10735201.3	10273506.1	9808906.3	9341479	8876956	8414387	7948065.2	7482977
$\sum_{k=1}^{nc} C\_Profit_k + \sum_{k=1}^{ns} S\_Profit_k + NMB_{SMES}$ Rs/h	12601579	12138752.8	11675515.3	11214386	10750428.3	10288733.1	9824133.3	9356706	8892183	8429614	7963292.2	7498204
$\sum_{k=1}^{nc} C\_Profit_k + \sum_{k=1}^{ns} S\_Profit_k + NMB_{Capacitor+SMES}$ Rs/h	12623578	12160751.8	11697514.3	11236385	10772427.3	10310732.1	9846132.3	9378705	8914182	8451613	7985291.2	7520203
Hour	13h	14h	15h	16h	17h	18h	19h	20h	21h	22h	23h	24h
$\sum_{k=1}^{ns} S\_Profit_k$ (Rs/ h)	20866140	20173001	19476018	18783626	18091341	17399376	16704368	16011202	15318036	14624417	13930744	13238138
GW (Rs/ h)	27540680	26847541	26150558	25458166	24765881	24073916	23378908	22685742	21992576	21298957	20605284	19912678
$\sum_{k=1}^{nc} C\_Profit_k + \sum_{k=1}^{ns} S\_Profit_k + NMB_{Capacitor}$ Rs/h	27548024	26854885	26157902	25465510	24773225	24081260	23386252	22693086	21999920	21306301	20612628	19920022

$\sum_{k=1}^{nc} C\_Profit_k + \sum_{k=1}^{ns} S\_Profit_k + NMB_{TCSC}$ Rs/h	27557802	26864663	26167680	25475288	24783003	24091038	23396030	22702864	22009698	21316079	20622406	19929800
$\sum_{k=1}^{nc} C\_Profit_k + \sum_{k=1}^{ns} S\_Profit_k + NMB_{SMES}$ Rs/h	27580500	26887361	26190378	25497986	24805701	24113736	23418728	22725562	22032396	21338777	20645104	19952498
$\sum_{k=1}^{nc} C\_Profit_k + \sum_{k=1}^{ns} S\_Profit_k + NMB_{Capacitor+SMES}$ Rs/h	27596320	26903181	26206198	25513806	24821521	24129556	23434548	22741382	22048216	21354597	20660924	19968318

From the aforementioned analysis considering an inter-regional advanced hybrid *var* compensation based multilateral power transaction data, the global welfare characterised by spot pricing issues in the view of Pareto efficiency can be summarised as:

1. The transactions characterised by power mismatch at the consumers side has improved the power supplier's profit as well as the global welfare of the network under considerations. Again the transactions characterised by power mismatch from supplier's side will reduce the power supplier's profit as well as the global welfare of the network under considerations.

2. Here, the balancing cost as generated due to hourly variable spot pricing has been found to control the variations in the global welfare.

3. Now, if these transactions are very close to the Pareto efficient point that would provide significant global welfare and vice-versa.

4. Moreover the global welfare has been found to be improved further by incorporating economics of the hybrid *var* compensators such as combined capacitor-SMES which are optimally chosen by the DERL method from different available compensators.

Therefore, the advanced economy as well as few developing economic countries like India might adopt these *var* compensators as suitable option for RPD solution in a day ahead inter-regional grid.

Chapter 8

8 Conclusion

In this work, RPD issue with different case studies were solved by several algorithms based on their operational efficiency. In the initial phase of study, the fundamental RPD was solved by controlling generator bus voltages, transformer tap settings and shunt capacitors placements. Moreover, as an optimisations technique SA, PSO, DELB, DERL and CSA were applied one by one to solve the proposed problem. However all the methods showed improvements compared to the previously applied other meta-heuristics based techniques. DERL and CSA have been finally utilised to solve different case studies on restructured RPD due to their different strengths. In this context, shunt capacitors as *var* compensator have been found working satisfactorily to solve the fundamental RPD issues. But when the complexities were imposed to the problem due to various uncertainties of the deregulated power scenario, shunt capacitors faced difficulties to provide desired results due to its static behaviour. In the restructured network, a number of power transactions frequently occurred. It has been observed that during the power transactions period, security constraints i.e., bus voltages were found fluctuating. Even some of them violated the prefixed boundary limit causing the dynamic voltage limit crossover followed by higher losses. These situations were handled here by incorporating different dynamic *var* compensators likely the Synchronous Condensers (SC), TCSC as FACTs, SMES as ESS and some of their combinations with capacitors. Amongst them some applications likely singular SMES, TCSC and combination of SMES and SC with capacitors have been observed to perform efficiently. Besides the technical issues, the economics of the *var* compensators were also addressed which helped to reduce the merchandising surplus or the congestion rent. This further improved the fundamental global welfare of the network involving the benefits of the different market participants. In this context, the fundamental global welfare can be obtained maximum if the power transactions occur at the Pareto efficient point. Even the transactions which were not Pareto efficient but very close to the Pareto efficient point, provided very significant global welfare. Now, the Pareto efficient power transactions have been arranged here by planned bidding of the market participants such as power suppliers and consumers. Three case studies were analysed on these issues considering IEEE 57, IEEE 118 bus systems by the DERL and CSA method. In these cases, it has been observed that the combined capacitor-SMES provided highest global welfare compared to the other *var* compensators. With an extension to the power transactions, the spot pricing due to power mismatches in the transactions were further considered for a real Indian scenario

of a 62 bus system. It has been observed that the balancing cost due to hour wise variable spot pricing affects the global welfare differently. In this context, the global welfare were further enhanced by cumulating the economics of the different *var* compensators. Alike the previous case studies, the combination of capacitor-SMES showed improved responses which were optimised by the DERL method. In this direction, the DERL and the CSA, both have generated fast and global converging responses for the RPD in different cases. All the control variables as well as the constraints remained within their dynamic voltage stable operating limits. Therefore, the system remained secured to some extent by the proposed methods.

Since, the proposed method works satisfactorily, we can draw few ideas inclusive of it to be formulated as future work of study.

Chapter 9

9 Future Scope

As an extension to the problem concerning restructured RPD, few other works associated with the present power scenario may be developed in future. Some of them are enumerated below:

1. It will be fruitful to consider network congestion w.r.t variable operating conditions of the network like the peak load, off peak load, outage of generators or loads etc.

2. Restructured RPD issues may be considered in terms of multi-objective optimisations comprising the minimisations of power loss and dynamic voltage instability, voltage security and reliability enhancement etc.

3. Besides the promising advanced *var* compensator namely SMES, few other promising devices namely Super-capacitor, flywheels, Polysulfide Bromide (PSB) Flow Battery, Lithium-ion (Li-ion) Batteries, Vanadium Redox Flow Battery (VRB), Zinc-Bromine (ZnBr) Flow Battery, may be incorporated to achieve even better results.

4. Competitions among the ancillary service providers may be considered in this context which is an important area to work in the backdrop of deregulated power scenario.

5. To improve the economics, hour wise variable double auction bidding may be utilised. Moreover, the effect on consumer's surplus may be observed considering variable spot pricing in two or more inter-regional grids.

6. Suitable strategies for optimal bidding can be adopted to achieve Pareto efficiency.

7. The efficiency of the meta-heuristics are always dependent on the improved global convergence criteria. Therefore investigations to obtain revised results by improved clever algorithms will definitely help to develop a motivated research work. In this context, hybridisation of two or more technique may bring a new path to the field of computational research.

References

[1]. Available online: http://www.eia.gov/cfapps/ipdbproject

[2]. Monthly all India installed generation capacity report 2015 from Central Electricity authority, Ministry of power, Government of India. Available online http://www.cea.nic.in/installed_capacity.

[3]. Statistical review of world energy. 2014.

[4]. International energy statistics. 2014.

[5]. India: overview, data & analysis. s.l. : U.S.Energy information administration, 2011.

[6]. Physical progress (achievements). s.l. : Ministry of new and renewable energy, Govt. of India, 2015. Available online: http://mnre.gov.in/mission-and-vision-2/achievements/.

[7]. L. L. Lai, and J. T. Ma., "Application of evolutionary programming to reactive power planning comparison with nonlinear programming approach", *IEEE Transaction on Power System*, Volume 12, Issue 1, 1997, Pages 198–206.

[8]. K. Y. Lee, Y. M. Park, J. L. Ortiz., "A united approach to optimal real and reactive power dispatch", *IEEE Transaction on Power Apparatus and Systems*, Volume 104, Issue 5, 1985, Pages 1147-1153.

[9]. L. L. Lai., "Power system restructuring and deregulation, Trading, performance and information technology", John Wiley & Sons ltd: 2007.

[10]. S. Rahimzadeh, M. H. Bina., "Looking for optimal number and placement of FACTs devices to manage the transmission congestion", *Energy Conversion and Management*, Volume 52, 2011, Pages 437-446.

[11]. D. S. Kirschen., "Fundamentals of Power System Economics". Wiley: 2007.

[12]. Executive summary of month of February 2014. s.l. : Central Electricity authority, ministry of power, Govt. of India., 2015. Available online:http://www.cea.nic.in/reports/monthly/executive_rep/mar15.pdf.

[13]. Google. wikipedia. [Online] http://en.wikipedia.org/wiki/Electricity_sector_in_India.

[14]. D. Devaraj, J. Preetha Roselyn., "Genetic algorithm based reactive power dispatch for voltage stability improvement", *International Journal of Electrical Power & Energy Systems*, Volume 32, Issue 10, December 2010, Pages 1151-1156.

[15]. M. Varadarajan, K. S. Swarup., "Network loss minimization with voltage security using differential evolution", *Electric Power Systems Research*, Volume 78, Issue 5, May 2008, Pages 815-823.

[16]. A. H. Khazali, M. Kalantar., "Optimal reactive power dispatch based on harmony search algorithm", *International Journal of Electrical Power & Energy Systems*, Volume 33, Issue 3, March 2011, Pages 684-692.

[17]. C. Wang, Y. Liu, Y. Zhao, Y. Chen., "A hybrid topology scale-free Gaussian-dynamic particle swarm optimization algorithm applied to real power loss minimization", *Engineering Applications of Artificial Intelligence*, Volume 32, June 2014, Pages 63-75.

[18]. B. Mandal, P. K. Roy., "Optimal reactive power dispatch using quasi-oppositional teaching learning based optimization", *International Journal of Electrical Power & Energy Systems*, Volume 53, December 2013, Pages 123-134.

[19]. S. Gopiya Naik, D. K. Khatod, M. P. Sharma., "Optimal allocation of combined DG and capacitor for real power loss minimization in distribution networks", *International Journal of Electrical Power & Energy Systems*, Volume 53, December 2013, Pages 967-973.

[20]. M. Martinez-Rojas, A. Sumper, O. Gomis-Bellmunt, A. Sudrià-Andreu., "Reactive power dispatch in wind farms using particle swarm optimization technique and feasible solutions search", *Applied Energy*, Volume 88, Issue 12, December 2011, Pages 4678-4686.

[21]. Y. A. Alturki, K. L. Lo., "Real and reactive power loss allocation in pool-based electricity markets", *International Journal of Electrical Power & Energy Systems*, Volume 32, Issue 4, May 2010, Pages 262-270.

[22]. S. S. Pourshafie, M. Mortazavi, M. Saniei, S. Saadati., "Optimal reactive power compensation in a deregulated distribution network", *Universities Power Engineering Conference (UPEC)*, 2009, Pages. 1 – 6.

[23]. M. Varadarajan, K. S. Swarup., "Differential evolutionary algorithm for optimal reactive power dispatch", *International Journal of Electrical Power & Energy Systems*, Volume 30, Issue 8, October 2008, Pages 435-441.

[24]. F. Hamzaoglu, E. B. Makram., "Minimization of series reactive power loss for the voltage instability problems", *Electric Power Systems Research*, Volume 50, Issue 3, 1 June 1999, Pages 175-181.

[25]. N. Amjady, M. Esmaili., "Voltage security assessment and vulnerable bus ranking of power systems", *Electric Power Systems Research*, Volume 64, Issue 3, March 2003, Pages 227-237.

[26]. O. A. Mousavi, M. Bozorg, R. Cherkaoui., "Preventive reactive power management for improving voltage stability margin", *Electric Power Systems Research*, Volume 96, March 2013, Pages 36-46.

[27]. M. K. Raoofat, M. Mohammadi., "Reactive power market management considering voltage control area reserve and system security", *Applied Energy*, Volume 88, Issue 11, November 2011, Pages 3832-3840.

[28]. C. F Yang, G. G. Lai, C. H. Lee, C. T. Su, G. W. Chang., "Optimal setting of reactive compensation devices with an improved voltage stability index for voltage stability enhancement", *International Journal of Electrical Power & Energy Systems*, Volume 37, Issue 1, May 2012, Pages 50-57.

[29]. C. A. Cañizares, C. Cavallo, M. Pozzi, S. Corsi., "Comparing secondary voltage regulation and shunt compensation for improving voltage stability and transfer capability in the Italian power system", *Electric Power Systems Research*, Volume 73, Issue 1, January 2005, Pages 67-76.

[30]. B. Naama, H. Bouzeboudja, A. Allali., "Solving the Economic Dispatch Problem by Using Tabu Search Algorithm", *Energy Procedia*, Volume 3234567890-36, 2013, Pages 694-701.

[31]. Z. Sahli, A. Hamouda, A. Bekrar, D. Trentesaux., "Hybrid PSO-tabu search for the optimal reactive power dispatch problem", *Industrial Electronics Society, IECON 2014 - 40th Annual Conference of the IEEE* , 2014.

[32]. M. Varadarajan, K.S. Swarup., "Differential evolution approach for optimal reactive power dispatch", *Applied Soft Computing*, Volume 8, Issue 4, September 2008, Pages 1549-1561.

[33]. P. Subbaraj, P.N. Rajnarayanan., "Optimal reactive power dispatch using self-adaptive real coded genetic algorithm", *Electric Power Systems Research*, Volume 79, Issue 2, February 2009, Pages 374-381.

[34]. A. A. Abou El Ela, M. A. Abido, S. R. Spea., "Differential evolution algorithm for optimal reactive power dispatch", *Electric Power Systems Research*, Volume 81, Issue 2, February 2011, Pages 458-464.

[35]. Q. H. Wu, Y. J. Cao, J. Y. Wen., "Optimal reactive power dispatch using an adaptive genetic algorithm", *International Journal of Electrical Power & Energy Systems*, Volume 20, Issue 8, November 1998, Pages 563-569.

[36]. C. A. Roa-Sepulveda, B. J. Pavez-Lazo., "A solution to the optimal power flow using simulated annealing", *International Journal of Electrical Power & Energy Systems*, Volume 25, Issue 1, 1 January 2003, Pages 47-57.

[37]. M. H. Gomes, J. T. Saraiva., "A market based active/reactive dispatch including transformer taps and reactor and capacitor banks using Simulated Annealing", *Electric Power Systems Research*, Volume 79, Issue 6, June 2009, Pages 959-972.

[38]. A. H. Khazali, M. Kalantar., "Optimal reactive power dispatch based on harmony search algorithm", *International Journal of Electrical Power & Energy Systems*, Volume 33, Issue 3, March 2011, Pages 684-692.

[39]. B. Jeddi, V. Vahidinasab., "A modified harmony search method for environmental/economic load dispatch of real-world power systems", *Energy Conversion and Management*, Volume 78, February 2014, Pages 661-675.

[40]. K. Mahadevan, P. S. Kannan., "Comprehensive learning particle swarm optimization for reactive power dispatch", *Applied Soft Computing*, Volume 10, Issue 2, March 2010, Pages 641-652.

[41]. D. C. Secui., "A new modified artificial bee colony algorithm for the economic dispatch problem", *Energy Conversion and Management*, Volume 89, 1 January 2015, Pages 43-6.2

[42]. C. M. Huang, Y. C. Huang., "Combined Differential Evolution Algorithm and Ant System for Optimal Reactive power Dispatch", *Energy Procedia*, Volume 14, 2012, Pages 1238-1243.

[43]. B. Canizes, J. Soares, P. Faria, Z. Vale., "Mixed integer non-linear programming and Artificial Neural Network based approach to ancillary services dispatch in competitive electricity markets", *Applied Energy*, Volume 108, August 2013, Pages 261-270.

[44]. A. R. Bahmanyar, A. Karami., "Power system voltage stability monitoring using artificial neural networks with a reduced set of inputs", *International Journal of Electrical Power & Energy Systems*, Volume 58, June 2014, Pages 246-256.

[45]. H. B. Aribia, N. Derbel, H. H. Abdallah., "The active–reactive ccomplete dispatch of an electrical network", *International Journal of Electrical Power & Energy Systems*, Volume 44, Issue 1, January 2013, Pages 236-248.

[46]. R. Mallipeddi, S. Jeyadevi, P. N. Suganthan, S. Baskar., "Efficient constraint handling for optimal reactive power dispatch problems", *Swarm and Evolutionary Computation*, Volume 5, August 2012, Pages 28-36.

[47]. X. Luo, J. Wang, M. Dooner, J. Clarke., "Overview of current development in electrical energy storage technologies and the application potential in power system operation", *Applied Energy* Volume 137, 2015, Pages 511–536.

[48]. N. S. Pearre, L. G. Swan., "Techno economic feasibility of grid storage: Mapping electrical services and energy storage technologies", *Applied Energy*, Volume 137, 2015, Pages 501–510.

[49]. C. J. Wu, C. H. Wang., "Damping of power system oscillations by an active and reactive power modulation superconducting magnetic energy storage unit", *Electric Power Systems Research*, Volume 24, Issue 1, July 1992, Pages 65-72.

[50]. J. Shi, Y. J. Tang, L. Ren, J. D. Li, S. J. Chen., "Application of SMES in wind farm to improve voltage stability", *Physica C: Superconductivity*, Volume 468, Issues 15–20, 15 September 2008, Pages 2100-2103.

[51]. K. S. Kwan, M. H. Tsai., "Superconducting magnetic energy storage for voltage stabilizer in electric power systems", *Proceedings of the IEEE International Symposium on Industrial Electronics*, Volume 2, 1992, Pages 509 – 513.

[52]. S. Banerjee, J. K. Chatterjee, S. C. Tripathy., "Application of magnetic energy storage unit as continuous VAr controller", *IEEE Transactions on Energy Conversion*, Volume 5, Issue 1, 1990, Pages 39 – 45.

[53]. Y. Mitani, Y. Murakami, K. Tsuji., "Experimental study on stabilization of model power transmission system by using four quadrant active and reactive power control by SMES", *IEEE Transactions on Magnetics*, Volume 23, Issue 2, 1987, Pages 541 – 544.

[54]. A. P. M. Reza, M. H. Ali, A. Abbas., "Voltage stabilization of VSI SMES capacitors and voltage sag compensation by SMES using novel switching strategies", *Energy*, Volume 35, 2010, Pages 3131-3142.

[55]. E. Acha, V. G. Agelidis, O. Anaya-Lara, T. J. E. Miller., "3-Transmission system compensation", *Power Electronic Control in Electrical Systems*, 2002, Pages 82-105.

[56]. M. El-Marsafawy., "Economical design of series capacitor compensation for long power transmission systems", *International Journal of Electrical Power & Energy Systems*, Volume 13, Issue 6, December 1991, Pages 321-329.

[57]. N. Kumar, M. P. Dave., "Application of static var system auxiliary controllers to improve the transient performance of series compensated long transmission lines", *Electric Power Systems Research*, Volume 34, Issue 2, August 1995, Pages 75-83.

[58]. U. Kılıç, K. Ayan, U. Arifoğlu., "Optimizing Reactive power flow of HVDC systems using genetic algorithm", *International Journal of Electrical* Power *& Energy Systems*, Volume 55, February 2014, Pages 1-12.

[59]. K. Srikrishna, R. Srinivasan., "Twin capacitor compensation of high voltage transmission line", *Electric Power Systems Research*, Volume 5, Issue 3, September 1982, Pages 191-198.

[60]. M. M. EL-Metwally, A. A. EL-Emary, M. EL-Azab., "Effect of load characteristics on maximum power transfer limit for HV compensated transmission lines", *International Journal of Electrical Power & Energy Systems*, Volume 26, Issue 7, September 2004, Pages 467-472.

[61]. K. Ramar, M. S. Raviprakasha., "Design of compensation schemes for long AC transmission lines for maximum power transfer limited by voltage stability", *International Journal of Electrical Power & Energy Systems*, Volume 17, Issue 2, April 1995, Pages 83-89.

[62]. B. Singh, D. O'Kelly., "Quasi-steady-state performance of a long shunt compensated transmission line," *Electric Power Systems Research*, Volume 26, Issue 2, February 1993, Pages 137-142.

[63]. M. Brucoli, M. L. Scala, F. Torelli, M. Trovato., "A co-ordinated compensation strategy involving synchronous generators and static VAR compensators in long distance AC transmission systems", *Electric Power Systems Research*, Volume 16, Issue 2, March 1989, Pages 89-99.

[64]. K. Wang, M. L. Crow., "Modern flexible AC transmission system (FACTS) devices", *Electricity Transmission, Distribution and Storage Systems*, 2013, Pages 174-205.

[65]. H. García, J. Segundo, M. Madrigal., "Harmonic analysis of power systems including thyristor-controlled series capacitor (TCSC) and its interaction with the transmission lines", *Electric Power Systems Research*, Volume 106, January 2014, Pages 151-159.

[66]. S. Bisanovic, M. Hajro, M. Samardzic., "One approach for reactive power control of capacitor banks in distribution and industrial network", *International Journal of Electrical Power & Energy Systems*, Volume 60, September 2014, Pages 67-73.

[67]. S. Kansal, V. Kumar, B.Tyagi., "Composite active and reactive power compensation of distribution networks", *Industrial and Information Systems (ICIIS), 2012* IEEE, 2012, Page(s): 1 – 6.

[68]. M. M. A. Salama, N. Manojlovic, V. H. Quintana, A. Y. Chikhani., "Real-time optimal reactive power control for distribution network", *International Journal of Electrical Power & Energy Systems*, Volume 18, Issue 3, March 1996, Pages 185-193.

[69]. D. Das., "Reactive power compensation for radial distribution network using genetic algorithm", *International Journal of Electrical Power & Energy Systems*, Volume 24, Issue 7, October 2002, Pages 573-581.

[70]. M. Ramalinga Raju, K. V. S. R. Murthy, K. Ravindra., "Direct search algorithm for capacitive compensation in radial distribution systems", *International Journal of Electrical Power & Energy Systems*, Volume 42, Issue 1, November 2012, Pages 24-30.

[71]. J. Vuletić, M. Todorovski., "Optimal capacitor placement in radial distribution systems using clustering based optimization", *International Journal of Electrical Power & Energy Systems*, Volume 62, November 2014, Pages 229-236.

[72]. A. Saraswat, A. Saini., "Multi-objective optimal reactive power dispatch considering voltage stability in power systems using HFMOEA", *Engineering Applications of Artificial Intelligence*, Volume 26, Issue 1, January 2013, Pages 390-404.

[73]. J. P. Roselyn, D. Devaraj, S. S. Dash., "Multi Objective Differential Evolution approach for voltage stability constrained reactive power planning problem", *International Journal of Electrical Power & Energy Systems*, Volume 59, July 2014, Pages 155-165.

[74]. L. Krichen, H. B. Aribia, H. H. Abdallah, A. Ouali., "ANN for multi-objective optimal reactive compensation of a power system with wind generators", *Electric Power Systems Research*, Volume 78, Issue 9, September 2008, Pages 1511-1519.

[75]. S. Cheng, M. Y. Chen., "Multi-objective reactive power optimization strategy for distribution system with penetration of distributed generation", *International Journal of Electrical Power & Energy Systems*, Volume 62, November 2014, Pages 221-228.

[76]. A. Ghasemi, K. Valipour, A. Tohidi., "Multi objective optimal reactive power dispatch using a new multi objective strategy", *International Journal of Electrical Power & Energy Systems*, Volume 57, May 2014, Pages 318-334.

[77]. R. Wang, Y. Yang, B. Bin, X. Wang, J. Huang, S. Zeng., "Application of optimization Algorithm on Simulating the Fisher Fishing in Multi-objective Optimal reactive power", *Energy Procedia*, Volume 17, Part B, 2012, Pages 1482-1489.

[78]. X. Wang, Y. Zhang., "Multi-Objective reactive power optimization based on the Fuzzy Adaptive Particle Swarm Algorithm", *Procedia Engineering*, Volume 16, 2011, Pages 230-238.

[79]. D. F. Pires, C. H. Antunes, A. G. Martins., "NSGA-II with local search for a multi-objective reactive power compensation problem", *International Journal of Electrical Power & Energy Systems*, Volume 43, Issue 1, December 2012, Pages 313-324.

[80]. L. Ara, A. Kazemi, S. Gahramani, M. Behshad., "Optimal reactive power flow using multi-objective mathematical programming", *Scientia Iranica*, Volume 19, Issue 6, December 2012, Pages 1829-1836.

[81]. C. H. Antunes, D. F. Pires, C. Barrico, Á. Gomes, A. G. Martins., "A multi-objective evolutionary algorithm for reactive power compensation in distribution networks", *Applied Energy*, Volume 86, Issues 7–8, July–August 2009, Pages 977-984.

[82]. H. R. E. H. Bouchekara, M. A. Abido, M. Boucherma., "Optimal power flow using Teaching-Learning-Based Optimization technique", *Electric Power Systems Research*, Volume 114, September 2014, Pages 49-59.

[83]. A. A. Abou El Ela, M. A. Abido, S. R. Spea., "Optimal power flow using differential evolution algorithm", *Electric Power Systems Research*, Volume 80, Issue 7, July 2010, Pages 878-885.

[84]. M. Kolenc, I. Papič, B. Blažič., "Coordinated reactive power control to achieve minimal operating costs", *International Journal of Electrical Power& Energy Systems*, Volume 63, December 2014, Pages 1000-1007.

[85]. F. Dong, L. Huang, B. P. Lam, X. Xu., "Practical applications of Preventive Security Constrained Optimal Power Flow", *Power and Energy Society General Meeting, IEEE* 2012, Pages 1 – 5.

[86]. A. Bhattacharya, P. K. Chattopadhyay., "Application of biogeography-based optimization to solve different optimal power flow problems", *IET, Generation, Transmission & Distribution*, Volume 5, Issue 1, 2011, Pages 70 – 80.

[87]. Y. Amrane, M. Boudour, M. Belazzoug., "A new Optimal reactive power planning based on Differential Search Algorithm", *International Journal of Electrical Power& Energy Systems*, Volume 64, January 2015, Pages 551-561.

[88]. N. Sinha, L. L. Lai, P. K. Ghosh., "GA based algorithm for optimum allocation of reactive power under deregulated environment", *Electric Utility Deregulation and Restructuring and Power Technologies, DRPT* 2008. Third International Conference on 2008 , Pages 926 – 932.

[89]. J. W. Chang, F. C. Graves, D. M. Murphy., "Transmission Management in the Deregulated Electric Industry: A Case Study on Reactive Power", *The Electricity Journal*, Volume 16, Issue 8, October 2003, Pages 61-73.

[90]. N. Mithulanantshan, N. Acharya., "A proposal for investment recovery of FACTS devices in deregulated electricity markets", *Electric Power Systems Research*, Volume 77, Issues 5–6, April 2007, Pages 695-703.

[91]. S. Porkar, P. Poure, A. Abbaspour-Tehrani-fard, S. Saadate., "A novel optimal distribution system planning framework implementing distributed generation in a deregulated electricity market", *Electric Power Systems Research*, Volume 80, Issue 7, July 2010, Pages 828-837.

[92]. L. Augugliaro, M. G. Dusonchet, E. Ippolito, R. Sanseverino., "Multiobjective design of distributed reactive power production in a deregulated electric market", *International Journal of Electrical Power & Energy Systems*, Volume 27, Issue 3, March 2005, Pages 205-214.

[93]. H. S. Rabiee, N. Amjady., "Multiobjective clearing of reactive power market in deregulated power systems", *Applied Energy*, Volume 86, Issue 9, September 2009, Pages 1555-1564.

[94]. D. F. Galiana, M. Phelan., "Allocation of transmission losses to bilateral contracts in a competitive environment", *IEEE Transactions on Power Systems*, Vol. 15, No.1, February 2000, Pages. 143.

[95]. I. J. Raglend, P. Karthikeyan, S. S. Sowjanya, D. P. Kothari., "Comparison of intelligent techniques to solve economic load dispatch with bilateral and multilateral transactions", *TENCON 2008*, IEEE 2008, Pages: 1 – 6.

[96]. P. Venkatesh, R. Gnanadass, N. P. Padhy., "Comparison and Application of Evolutionary Programming Techniques to combined Economic Emission Dispatch with Line Flow Constraints", *IEEE Transactions on Power Systems*, Volume 18, Issue 2, 2003, Pages 688-697.

[97]. M. Ilic, E. Hsieh, P. Ramanan., "Transmission pricing of distributed multilateral energy transactions to ensure system security and guide economic dispatch", *IEEE Transactions on Power Systems*, Volume 18, Issue 2, 2003, Pages: 428 – 434.

[98]. R. Gnanadass, N. P. Padhy., "A New Approach for Transmission Embedded Cost Allocation in Restructured Power Market", *Journal of Energy & Environment*, Volume 4, 2005, Pages 37 – 47.

[99]. F. F. Wu, P. Varaiya., "Coordinated multilateral trades for electric power networks: Theory and implementation", *Electrical Power and Energy System*, Volume 21, Issue 2, 1999, Pages 75–102.

[100]. K. Liu, N. Yixin, F. F. Wu, T. S. Bi., "Decentralized Congestion Management for Multilateral Transactions Based on Optimal Resource Allocation", *IEEE Transactions on Power Systems*, Volume 22, Issue 4, 2007, Pages 1835 – 1842.

[101]. S. Visalakshi, S. Baskar., "Covariance matrix adapted evolution strategy based decentralised congestion management for multilateral transactions", *IET, Generation, Transmission & Distribution*, Volume 4, Issue 3, 2010, Pages 400 – 417.

[102]. K. Daroj, B. Eua-arporn., "Real Power Loss Allocation for Transactions in Bilateral Markets", *Power System Technology, 2006. PowerCon 2006*. Pages 1 – 8

[103]. M. De, N. B. D. Choudhury, S. K. Goswami., "Transaction based power flow solution and transmission loss allocation using neural network", *Power Electronics, Drives and Energy Systems (PEDES) & 2010 Power India*, 2010, Pages: 1 – 6.

[104]. R. Haque, N. Chowdhury., "An artificial neural network based transmission loss allocation for bilateral contracts", *Electrical and Computer Engineering, 2005.* Pages 2203 – 2207.

[105]. X. Zhang, D. P. Manjure, E. B. Makram., "Optimal choice of bilateral contract transaction for minimizing total transmission loss", *Power Engineering Society Winter Meeting, IEEE,* Volume 2, 2002, Pages 1338 - 1343.

[106]. M. De, N. B. D. Choudhury, S. K. Goswami., "A modified approach to transmission loss allocation using proportional sharing method for transaction based power system operation", *EUROCON, IEEE* 2013 , Page(s): 1278 – 1284

[107]. G. Gross, T. Shu., "A physical-flow-based approach to allocating transmission losses in a transaction framework", *IEEE Transactions on Power Systems,* Volume 15, Issue 2, 2000, Pages 631 – 637.

[108]. M. Kyung-Il, H. Sang-Hyeon, L. Su-won, M. Young-Hyun., "Transmission Loss Allocation Algorithm Using Path-Integral Based on Transaction Strategy", *IEEE Transactions on Power Systems,* Volume 25, Issue 1, 2010, Page(s): 195 – 205.

[109]. M. H. Gomes, J. T. Saraiva., "Allocation of reactive power support, active loss balancing and demand interruption ancillary services in MicroGrids", *Electric Power Systems Research*, Volume 80, Issue 10, October 2010, Pages 1267-1276.

[110]. A. G. Madureira, J. A. Peças Lopes., "Ancillary services market framework for voltage control in distribution networks with microgrids", *Electric Power Systems Research*, Volume 86, May 2012, Pages 1-7.

[111]. W. Ongsakul, K. Chayakulkheeree., "Constrained optimal power dispatch for electricity and ancillary services auctions", *Electric Power Systems Research*, Volume 66, Issue 3, September 2003, Pages 193-204.

[112]. A. L. Costa, A. Simões Costa., "Energy and ancillary service dispatch through dynamic optimal power flow, *Electric Power Systems Research*, Volume 77, Issue 8, June 2007, Pages 1047-1055.

[113]. J. H. T. Hernandez, M. J. Guzman, G. G. Alcaraz., "Ancillary reactive power service allocation cost in deregulated markets: a methodology", *International Journal of Electrical Power & Energy Systems*, Volume 27, Issues 5–6, June–July 2005, Pages 371-378.

[114]. E. E. El-Araby, N. Yorino., "A hybrid PSO technique for procuring VAR ancillary service in the deregulated electricity markets", *International Journal of Electrical Power & Energy Systems*, Volume 32, Issue 6, July 2010, Pages 664-670.

[115]. E. R. Samani, H. Seifi, M. K. Sheikh-El-Eslami., "A framework for PSS pricing as an ancillary service in a competitive electricity market", *International Journal of Electrical Power & Energy Systems*, Volume 46, March 2013, Pages 221-227.

[116]. E. L. Miguélez, I. E. Cortés, L. R. Rodríguez, G. L. Camino., "An overview of ancillary services in Spain", *Electric Power Systems Research*, Volume 78, Issue 3, March 2008, Pages 515-523.

[117]. R. Raineri, S. Ríos, D. Schiele., "Technical and economic aspects of ancillary services markets in the electric power industry: an international comparison", *Energy Policy*, Volume 34, Issue 13, September 2006, Pages 1540-1555.

[118]. S. Jena, B. C. Babu, G. Mishra, A. K. Naik., "Reactive power compensation in inverter-interfaced distributed generation", *International Conference on Energy, Automation, and Signal (ICEAS),* 2011, Pages 1 – 6.

[119]. M. A. Mahmud, M. J. Hossain, H. R. Pota, A. B. M. Nasiruzzaman., "Voltage control of distribution networks with distributed generation using reactive power compensation", *IECON 2011 - 37th Annual Conference on IEEE Industrial Electronics Society* 2011, Pages 985 – 990.

[120]. L. Xiyi, Y. Jiangang, M. Tian, G. Lei., "Innovative Smart Grid Te91. Inductive reactive power compensation optimization for 10kV distribution network with distributed generations", *Chinese Automation Congress (CAC),* 2013, Pages 87 – 91.

[121]. N. K. Roy, H. R. Pota, M. J. Hossain., "Reactive power management of distribution networks with wind generation for improving voltage stability", *Renewable Energy*, Volume 58, October 2013, Pages 85-94.

[122]. A. K. Singh, S. K. Parida., "Congestion management with distributed generation and its impact on electricity market", *International Journal of Electrical Power & Energy Systems*, Volume 48, June 2013, Pages 39-47.

[123]. P. P. Su, S. Su, L. Xi, F. Li-quan., "Study on Fuzzy Dynamic Programming for Optimization of Reactive Power Compensation of Power System Including Distributed Generation", *International Conference on Intelligent Computation Technology and Automation (ICICTA)*, 2008, Volume 1, 2008, Pages 931 – 935.

[124]. Y. Chen, A. Luo, Z. Shuai, S. Xie., "Robust predictive dual-loop control strategy with reactive power compensation for single-phase grid-connected distributed generation system". *Power Electronics, IET*, Volume 6, Issue 7, 2013, Pages 1320 – 1328.

[125]. K. Bhumkittipich, W. Phuangpornpitak., "Optimal Placement and Sizing of Distributed Generation for Power Loss Reduction Using Particle Swarm Optimization", *Energy Procedia*, Volume 34, 2013, Pages 307-317.

[126]. E. Samahy, K. Bhattacharya, C. Can0izares, M. F. Anjos, P. Jiuping., "A Procurement Market Model for Reactive Power Services Considering System Security", *IEEE Transactions on Power Systems*, Volume 23, Issue 1, 2008, Pages 137 – 149.

[127]. A. Rabiee, H. Shayanfar, N. Amjady., "Coupled energy and reactive power market clearing considering power system security", *Energy Conversion and Management*, Volume 50, Issue 4, April 2009, Pages 907-915.

[128]. J. Aghaei, H. A. Shayanfar, N. Amjady., "Joint market clearing in a stochastic framework considering power system security", *Applied Energy*, Volume 86, Issue 9, September 2009, Pages 1675-1682.

[129]. K. M. Raoofat, M. Mohammadi., "Reactive power market management considering voltage control area reserve and system security", *Applied Energy*, Volume 88, Issue 11, November 2011, Pages 3832-3840.

[130]. H. Ying-Tung , C. Hsiao-Dong, L. Chun-Chang, C. Yuan-Lin., "A computer package for optimal multi-objective VAr planning in large scale power systems", *IEEE Transactions on Power Systems*, Volume 9, Issue 2, 1994, Pages 668 – 676.

[131]. H. A. Hejazi, H. R. Mohabati, S. H. Hosseinian, M. Abedi., "Differential Evolution Algorithm for Security-Constrained Energy and Reserve Optimization Considering Credible Contingencies", *IEEE Transactions on Power Systems*, Volume 26, Issue 3, 2011, Pages 1145 – 1155.

[132]. P. Acharjee., "Application of efficient self-adaptive differential evolutionary algorithm for voltage stability analysis under practical security constraints", *Applied Mathematics and Computation*, Volume 219, Issue 23, 1 August 2013, Pages 10882-10897.

[133]. X. R. Li, C. W. Yu, W. H. Chen., "A novel value based reactive power procurement scheme in electricity markets", *International Journal of Electrical Power & Energy Systems*, Volume 43, Issue 1, December 2012, Pages 910-914.

[134]. C. Y. Chung, T. S. Chung, C. W. Yu, X. J. Lin., "Cost-based reactive power pricing with voltage security consideration in restructured power systems", *Electric Power Systems Research*, Volume 70, Issue 2, July 2004, Pages 85-91.

[135]. N. Amjady, V. Vahidinasab., "Security-constrained self-scheduling of generation companies in day-ahead electricity markets considering financial risk", *Energy Conversion and Management*, Volume 65, January 2013, Pages 164-172.

[136]. H. Shangyou, A. Papalexopoulos., "Reactive power pricing and management", *IEEE Transactions on Power Systems*, Volume 12 , Issue 1, 1997, Pages 95 – 104.

[137]. D. Chattopadhyay, K. Bhattacharya, J. Parikh., "Optimal reactive power planning and its spot-pricing: an integrated approach", *IEEE Transactions on Power Systems*, Volume 10, Issue 4, 1995, Pages 2014 – 2020.

[138]. J. B. Gil, T. G. S. Román, J. J. Alba Rios, P. S., Martin., "Reactive power pricing: a conceptual framework for remuneration and charging procedures", *IEEE Transactions on Power Systems*, Volume 15, Issue 2, 2000, Pages 483 – 489.

[139]. A. Ketabi, A. Alibabaee, R. Feuillet., "Application of the ant colony search algorithm to reactive power pricing in an open electricity market", *International Journal of Electrical Power & Energy Systems*, Volume 32, Issue 6, July 2010, Pages 622-628.

[140]. G. A. Vaidya, N. Gopalakrishnan, Y. P. Nerkar., "Reactive power pricing structure for hydroelectric power station in condenser mode operation", *International Journal of Electrical Power & Energy Systems*, Volume 33, Issue 8, October 2011, Pages 1420-1428.

[141]. A. P S. Meliopoulos, G. J Cokkinides, M. A Asa'd., "Issues for reactive power and voltage control pricing in a deregulated environment", *Decision Support Systems*, Volume 30, Issue 3, January 2001, Pages 303-310.

[142]. M. J. Rider, V. L. Paucar., "Application of a nonlinear reactive power pricing model for competitive electric markets", *IEE Proceedings-Generation, Transmission and Distribution*, Volume 151 , Issue 3, 2004 , Pages 407 – 414.

[143]. K. S. Verma, H. O. Gupta., "Impact on real and reactive power pricing in open power market using unified power flow controller", *IEEE Transactions on Power Systems*, Volume 21, Issue 1, 2006, Pages 365 – 371.

[144]. M. H. R. Gomes, J. T. Saraiva., "Active/reactive bid based dispatch models to be used in electricity markets", *Electric Power Systems Research*, Volume 78, Issue 1, January 2008, Pages 106-121.

[145]. A. Badri, S. Jadid, M. Rashidinejad, M. P. Moghaddam., "Optimal bidding strategies in oligopoly markets considering bilateral contracts and transmission constraints", *Electric Power Systems Research*, Volume 78, Issue 6, June 2008, Pages 1089-1098.

[146]. G. Duan, Z. Y. Dong, W. Bai, X. F. Wang., "Power flow based monetary flow method for electricity transmission and wheeling pricing", *Electric Power Systems Research*, Volume 74, Issue 2, May 2005, Pages 293-305.

[147]. M. K. Kim, J. K. Park, Y. W. Nam., "Market-clearing for pricing system security based on voltage stability criteria", *Energy*, Volume 36, Issue 2, February 2011, Pages 1255-1264.

[148]. M. Dotoli, N. Epicoco, M. Falagario, F. Sciancalepore, N. Costantino., "A Nash equilibrium simulation model for the competitiveness evaluation of the auction based day ahead electricity market", *Computers in Industry*, Volume 65, Issue 4, May 2014, Pages 774-785.

[149]. S. P. Karthikeyan, I. J. Raglend, D. P. Kothari., "A review on market power in deregulated electricity market", *International Journal of Electrical Power & Energy Systems*, Volume 48, June 2013, Pages 139-147.

[150]. M. Prabavathi, R. Gnanadass., "Energy bidding strategies for restructured electricity market". *International Journal of Electrical Power and Energy Systems*, Volume 64, 2015, Pages 956-966.

[151]. S. Nielsen, P. Sorknæs, P. A. Ostergaard., "Electricity market auction settings in a future Danish electricity system with a high penetration of renewable energy sources– A comparison of marginal pricing and pay-as-bid", *Energy*, Volume 36, Issue 7, July 2011, Pages 4434-4444.

[152]. N. Acharya, N. Mithulananthan., "Influence of TCSC on congestion and spot price in electricity market with bilateral contract", *International Journal of Electric Power Systems Research*, Volume 77, Issue 8, June 2007, Pages 1010-1018.

[153]. H. Wu, C. W. Yu, N. Xu, X. J. Lin., "An OPF based approach for assessing the minimal reactive power support for generators in deregulated power systems", *International Journal of Electrical Power & Energy Systems*, Volume 30, Issue 1, January 2008, Pages 23-30.

[154]. X. R. Li, C. W. Yu, W. H. Chen., "A novel value based reactive power procurement scheme in electricity markets", *International Journal of Electrical Power & Energy Systems*, Volume 43, Issue 1, December 2012, Pages 910-914.

[155]. L. D. Arya, P. Singh, L. S. Titare., "Anticipatory reactive power reserve maximization using differential evolution", *International Journal of Electrical Power & Energy Systems*, Volume 35, Issue 1, February 2012, Pages 66-73.

[156]. L. D. Arya, L. S. Titare, D. P. Kothari., "Improved particle swarm optimization applied to reactive power reserve maximization", *International Journal of Electrical Power & Energy Systems*, Volume 32, Issue 5, June 2010, Pages 368-374.

[157]. W. Xu, Y. Zhang, L. C. P. Da Silva, P. Kundur., "Assessing the value of generator reactive power support for transmission access", *IEE Proceedings- Generation, Transmission and Distribution*, Volume 148 ,Issue 4 , 2001, Pages 337 – 342.

[158]. W. Xu, Y. Zhang, L. C. P. da Silva, P. Kundur, A. A. Warrack., "Valuation of dynamic reactive power support services for transmission access", *IEEE Transactions on Power Systems*,Volume 16 , Issue 4, 2001, Pages 719 – 728.

[159]. W. Xu, Y. Zhang, L. C. P. Da Silva, P. Kundur., "Competitive procurement of dynamic reactive power support service for transmission access", *Power Engineering Society Summer Meeting, 2000. IEEE*, Volume 1, 2000, Pages 543 – 548.

[160]. X. Ma, A. A El-Keib, T. A. Haskew., "Marginal cost-based pricing of wheeling transactions and independent power producers considering security constraints", *Electric Power Systems Research*, Volume 48, Issue 2, 15 December 1998, Pages 73-78.

[161]. S. M. H. Nabavi, A. Kazemi, M. A. S. Masoum., "Social welfare maximization with fuzzy based genetic algorithm by TCSC and SSSC in double-sided auction market", *Scientia Iranica*, Volume 19, Issue 3, June 2012, Pages 745-758.

[162]. X. J. Lin, C. W. Yu, A. K. David, C. Y. Chung, H. Wu, N. Xu., "A novel market-based reactive power management scheme", *International Journal of Electrical Power & Energy Systems*, Volume 28, Issue 2, February 2006, Pages 127-132.

[163]. A. Kumar, S. C. Srivastava, S. N. Singh., "Congestion management in competitive power market: A bibliographical survey", *Electric Power Systems Research*, Volume 76, Issues 1–3, September 2005, Pages 153-164.

[164]. F. Hussin, M.Y. Hassan, K. L. Lo., "Transmission Congestion Management Assessment in Deregulated Electricity Market", 2006, Pages 250 – 255.

[165]. S. N. Singh, K. David., "Congestion management in dynamic security constrained open power markets", *Computers & Electrical Engineering*, Volume 29, Issue 5, July 2003, Pages 575-588.

[166]. Y. T. Yuan, Q. Wan., "A New Method for Assessing Ancillary Service of FACTS in Congestion Management", *Power Engineering Society General Meeting*, 2007, Pages 1 – 7.

[167]. E. Muneender, D. M. Vinodkumar., "Real Coded Genetic Algorithm based dynamic Congestion Management in open power markets", *Transmission and Distribution Conference and Exposition (T&D), IEEE PES* 2012, Pages 1 – 5.

[168]. E. Muneender, D. M.V., "Optimal real and reactive power dispatch for zonalcongestion management problem for multi congestion case using Adaptive Fuzzy PSO", *TENCON 2009 IEEE* 2009, Pages 1 – 6.

[169]. M. A. Rahim, I. Musirin, I. Z. Abidin, M. M. Othman, D. Joshi., "Congestion management based optimization technique using bee colony", *Power Engineering and Optimization Conference (PEOCO)*, 2010, Pages 184 – 188.

[170]. M. Esmaili, N. Amjady, H. A. Shayanfar., "Multi-objective congestion management by modified augmented ε-constraint method", *Applied Energy*, Volume 88, Issue 3, March 2011, Pages 755-766.

[171]. M. Esmaili, H. A. Shayanfar, N. Amjady., "Multi-objective congestion management incorporating voltage and transient stabilities", *Energy*, Volume 34, Issue 9, September 2009, Pages 1401-1412.

[172]. Y. Wang, H. Cheng, C. Wang, Z. Hu, L. Yao, Z. Ma, Z. Zhu., "Pareto optimality-based multi-objective transmission planning considering transmission congestion", *Electric Power Systems Research*, Volume 78, Issue 9, September 2008, Pages 1619-1626.

[173]. P. Preedavichit, S. C. Srivastava., "Optimal reactive power dispatch considering FACTS devices", *Electric Power Systems Research*, Volume 46, Issue 3, 1 September 1998, Pages 251-257.

[174]. N. R. H. Abdullah, I. Musirin, M. M. Othman., "Thyristor Controlled Series Compensator planning using Evolutionary Programming for transmission loss minimization for system under contingencies", *Power and Energy (PECON)*, 2010, Pages 18 – 23.

[175]. S. Nagalakshmi, N. Kamaraj., "Comparison of computational intelligence algorithms for loadability enhancement of restructured power system with FACTs devices", *Swarm and Evolutionary Computation*, Volume 5, August 2012, Pages 17-27.

[176]. J. B. Edward, N. Rajasekar, K. Sathiyasekar, N. Senthilnathan, R. Sarjila., "An enhanced bacterial foraging algorithm approach for optimal power flow problem including FACTs devices considering system loadability", *ISA Transactions*, Volume 52, Issue 5, September 2013, Pages 622-628.

[177]. H. Besharat, S. A. Taher., "Congestion management by determining optimal location of TCSC in deregulated power system", *International Journal of Electrical Power & Energy Systems*, Volume 30, Issue 10, December 2008, Pages 563-568.

[178]. N. Acharya, N. Mithulananthan., "Locating series FACTS devices for Congestion management in deregulated electricity markets". *Electric Power Systems Research*, Volume 77, Issues 3–4, March 2007, Pages 352-360.

[179]. S. N. Singh, A. K. David., "Optimal location of FACTs devices for congestion management", *Electric Power Systems Research*, Volume 58, Issue 2, 21 June 2001, Pages 71-79.

[180]. G. I. Rashed, H. I. Shaheen, X. Z. Duan, S. J. Cheng., "Evolutionary optimization techniques for optimal location and parameter setting of TCSC under single line contingency", *Applied Mathematics and Computation*, Volume 205, Issue 1, 1 November 2008, Pages 133-147.

[181]. P. Bhasaputra, W. Ongsakul., "Optimal placement of multi-type FACTS devices by hybrid TS/SA approach", *Circuits and Systems, 2003. ISCAS '03. 2003*, Volume 3, Pages III-375 - III-378.

[182]. R. Jordehi, M. Joorabian., "Optimal placement of Multi-type FACTS devices in power systems using evolution strategies", *Power Engineering and Optimization Conference (PEOCO), 2011*, Page(s): 352 – 357.

[183]. B. Bhattacharyya, V. K. Gupta., "Fuzzy based evolutionary algorithm for reactive power optimisation with FACTS devices", *International Journal of Electrical Power & Energy Systems*, Volume 61, October 2014, Pages 39-47.

[184]. W. Ongsakul, P. Bhasaputra., "Optimal power flow with FACTs devices by hybrid TS/SA approach", *International Journal of Electrical Power & Energy Systems*, Volume 24, Issue 10, December 2002, Pages 851-857.

[185]. S. A. Jumaat, I. Musirin, M. M. Othman, H. Mokhlis., "Placement and sizing of thyristor controlled series compensator using PSO based technique for loss minimization", *Power Engineering and Optimization Conference (PEDCO) Melaka, Malaysia, 2012 IEEE*, 2012 , Pages 285 – 290.

[186]. Y. R. Sood, R. Singh., "Optimal model of congestion management in deregulated environment of power sector with promotion of renewable energy sources", *Renewable Energy*, Volume 35, Issue 8, August 2010, Pages 1828-1836.

[187]. A. Kumar, C. Sekhar., "Congestion management with FACTS devices in deregulated electricity markets ensuring loadability limit", *International Journal of Electrical Power & Energy Systems*, Volume 46, March 2013, Pages 258-273.

[188]. C. Venkaiah, D. M. V. Kumar., "Fuzzy adaptive bacterial foraging congestion management using sensitivity based optimal active power re-scheduling of generators", *Applied Soft Computing*, Volume 11, Issue 8, December 2011, Pages 4921-4930.

[189]. N. Amjady, M. Hakimi., "Dynamic voltage stability constrained congestion management framework for deregulated electricity markets", *Energy Conversion and Management*, Volume 58, June 2012, Pages 66-75.

[190]. M. Esmaili, H. A. Shayanfar, N. Amjady., "Congestion management considering voltage security of power systems", *Energy Conversion and Management*, Volume 50, Issue 10, October 2009, Pages 2562-2569.

[191]. Q. Wang, J. D. McCalley, W. Li., "Voltage instability performance of risk-based security constrained optimal power flow", *Electric Power Systems Research*, Volume 116, November 2014, Pages 45-53.

[192]. J. Conejo, F. Milano, R. Garcia-Bertrand., "Congestion management ensuring voltage stability",*IEEE Transactions on Power Systems*, Volume 21, Issue 1 2006, Pages 357 – 364.

[193]. M. R. Kargarian., "Stochastic reactive power market with volatility of wind power considering voltage security", *Energy*, Volume 36, Issue 5, May 2011, Pages 2565-2571.

[194]. M. Esmaili, H. A. Shayanfar, N. Amjady., "Congestion management enhancing transient stability of power systems", *Applied Energy*, Volume 87, Issue 3, March 2010, Pages 971-981.

[195]. T. Hsiao, C. Lu., "Application assessment of system protection schemes for power network congestion management", *Energy Conversion and Management*, Volume 51, Issue 12, December 2010, Pages 2655-2662.

[196]. M. B. Nappu, A. Arief, R. C. Bansal., "Transmission management for congested power system: A review of concepts, technical challenges and development of a new methodology", *Renewable and Sustainable Energy Reviews*, Volume 38, October 2014, Pages 572-580.

[197]. X. Wang, J. Zhuang., "Balancing congestion and security in the presence of strategic applicants with private information", *European Journal of Operational Research*, Volume 212, Issue 1, 1 July 2011, Pages 100-111.

[198]. A. K. Singh, S. K. Parida., "Congestion management with distributed generation and its impact on electricity market", *International Journal of Electrical Power & Energy Systems*, Volume 48, June 2013, Pages 39-47.

[199]. A. Kumar, R. K. Mittapalli., "Congestion management with generic load model in hybrid electricity markets with FACTS devices", *International Journal of Electrical Power & Energy Systems*, Volume 57, May 2014, Pages 49-63.

[200]. G. B. Shrestha, W. Feng., "Effects of series compensation on spot price power markets", *International Journal of Electrical Power & Energy Systems*, Volume 27, Issues 5–6, June–July 2005, Pages 428-436.

[201]. D. Chattopadhyay, B. B. Chakrabarti, E. G. Read., "A spot pricing mechanism for voltage stability", *International Journal of Electrical Power & Energy Systems*, Volume 25, Issue 9, November 2003, Pages 725-734.

[202]. K. Xie, Y. H. Song, D. Zhang, Y. Nakanishi, C. Nakazawa., "Calculation and decomposition of spot price using interior point nonlinear optimisation methods", *International Journal of Electrical Power & Energy Systems*, Volume 26, Issue 5, June 2004, Pages 349-356.

[203]. K. Bradbury, L. Pratson, D. Patiño-Echeverri., "Economic viability of energy storage systems based on price arbitrage potential in real-time U.S. electricity markets", *Applied Energy*, Volume 114, 2014, Pages 512–519.

[204]. M. Zheng, C. J. Meinrenken, K. S. Lackner., "Smart households: Dispatch strategies and economic analysis of distributed energy storage for residential peak shaving", *Applied Energy*, Volume 147, 2015; Pages 246–257.

[205]. M. A. F. Ghazvini, J. Soares, N. Horta, R. Neves, R. Castro, Z. Vale., "A multi-objective model for scheduling of short-term incentive-based demand response programs offered by electricity retailers", *Applied Energy*, Volume 151, 2015, Pages 102–118.

[206]. K. Balamurugan, R. Muralisachithanandam, V. Dharmalingam., "Performance comparison of evolutionary programming and differential evolution approaches for social welfare maximization by placement of multi type FACTs devices in pool electricity market", *Internation Journal of Electrical Power and Energy Systems*, Volume 67, 2015, Pages 517-528.

[207]. B. Jiang, A. M. Farid, K. Youcef-Toumi., "Demand side management in a day-ahead wholesale market: A comparison of industrial & social welfare approaches", *Applied Energy*, Volume 156, 2015, Pages 642–654.

[208]. H. Ahmadi, J. R., "Marti. Distribution System Optimization Based on a Linear Power-Flow Formulation", *IEEE Transactions on Power Delivery*, Volume 30, Issue 1, 2015, Pages 25 – 33.

[209]. H. Vu, P. Pruvot, C. Launay, Y. Harmand., "An improved voltage control on large-scale power system", *IEEE Transactions on Power Systems*, Volume 11, Issue 3, 1996, Pages 1295 – 1303.

[210]. J. Skliutas, D. LaForest, R. D'Aquila, D. Derr, E. Kronbeck., "Next-Generation Synchronous Condenser Installation at the VELCO Granite Substation", *IEEE proceedings* 2009, Pages 1-8.

[211]. S. Kalsi, D. Madura, R. Howard, G. Snitcbler, T. MacDonald, D. Bradshaw, I. Grant, M. lngram., "Superconducting dynamic synchronous condenser for improved grid voltage support", *IEEE proceedings* 2003, Pages 742-747.

[212]. K. R. Padiyar., "FACTs Controllers in Power Transmission and Distribution", *New Age International (P) Ltd, Publishers*. 2007.

[213]. V. K. Sood., "HVDC and FACTS Controllers Applications of Static Converters in Power Systems", *Kluwer Academic Publishers*. 2004.

[214]. X. Luo, J. Wang, M. Dooner, J. Clarke., "Overview of current development in electrical energy storage technologies and the application potential in power system operation", *Applied Energy*, Volume 137, 2015, Pages 511–536.

[215]. A. Marini, M. A. Latify, M. S. Ghazizadeh, A. Salemnia., "Long-term chronological load modelling in power system studies with energy storage systems", *Applied Energy*, Volume 156, 2015, Pages 436–448.

[216]. K. Bhattacharya, M. H. J. Bollen, J. E. Daalder., "Operation of restructured power systems", *Kluwer Academic Publishers*, 2011.

[217]. A. Sode-Yome, N. Mithulananthan., "Comparison of shunt capacitor, SVC and STATCOM in static voltage stability margin enhancement", *International Jjournal of Electrical Engineering Education*. Volume 41, Issue 2, 2005, Pages 158-170.

[218]. S. Hao, A. Papalexopoulos., "Reactive Power Pricing and Management", *IEEE Transactions on Power Systems*, Volume 12, Issue 1, 1997, Pages 95-101.

[219]. P. K. Tiwari, R. S. Yog., "An Efficient Approach for Optimal Allocation and Parameters Determination of TCSC with Investment Cost Recovery under Competitive Power Market", *IEEE Transactions on Power System*. Volume 28, Issue 3, 2013, Pages 2475-2484.

[220]. V. Karasik, K. Dixon, C. Weber, B. Batchelder, G. Campbell, P. Ribeiro., "SMES for power utility applications: A review of technical and cost considerations", *IEEE Transaction on Applied Superconductivity*. Volume 9, Issue 2, 1999, Pages 541-546.

[221]. A. Friedman, N. Shaked, E. Perel, F. Gartzman, M. Sinvani, Y. Wolfus, D. Kottick, J. Furman, Y. Yeshurun., "HT-SMES operating at liquid nitrogen temperatures for electric power quality improvement demonstrating", *IEEE Transactions on Applied Superconductivity*. Volume 13, Issue 2, 2003, Pages 1875-78.

[222]. H. Sadat., "Power System Analysis", *McGraw-Hill Publishing Company Limited* New Delhi, India, 14th reprint 2008.

[223]. M. Wahde., "Biologically Inspired Optimization Methods An Introduction", *WIT Press* 2008

[224]. E. G. Talbi., "Metaheuristics from Design to implementation", *John Wiley & Sons*. 2009.

[225]. J. Brownlee., "Clever Algorithms: Nature-Inspired Programming Recipes", 2011. *Available online http://www.CleverAlgorithms.com*

[226]. Y. Amrane, M. Boudour, A. A. Ladjici, A. Elmaouhab., "Optimal VAR control for real power loss minimization using differential evolution algorithm", *International Journal of Electrical Power & Energy Systems*. Volume 66, 2015, Pages 262-271.

[227]. K. K. Mandal, N. Chakraborty., "Short-term combined economic emission scheduling of hydrothermal power systems with cascaded reservoirs using differential evolution", *Energy Conversion and Management*. Volume 50, Issue 1, 2009, Pages 97-104.

[228]. K. Rajesh, A. Bhuvanesh, S. Kannan, C. Thangaraj., "Least cost generation expansion planning with solar power plant using Differential Evolution algorithm", *Renewable Energy*, Volume 85, 2016, Pages 677-686.

[229]. C. H. Liang, C. Y. Chung, K. P. Wong, X. Z. Duan, C. T. Tse., "Study of differential evolution for optimal reactive power flow", *IET Generation Transmission Distribution*, Volume 1, Issue 2, 2007, Pages 253-260.

[230]. J. Brest., "Self-adapting control parameters in differential evolution: A comparative study on numerical benchmark problems", *IEEE Transaction on Evolutionary Computation*, Volume 10, Issue 6, 2006, Pages 646–657.

[231]. W. U. Yanling, L. U. Jiangang, S. U. N. Youxian., "An Improved Differential Evolution for Optimization of Chemical Process", *Chinese Journal of Chemical Engineering*, Volume 16, Issue 2, 2008, Pages 228-234.

[232]. P. Kaelo, M. M. Ali., "A numerical study of some modified differential evolution algorithms", *European Journal of Operational Research*, Volume 169, 2006, Pages 1176-1184.

[233]. T. T. Nguyen, D. N. Vo, A. V. Truong, "Cuckoo search algorithm for short-term hydrothermal scheduling", *Applied Energy*, Volume 132, 2014, Pages 276-287.

[234]. S. K. Fateen, A. B. Petriciolet., "A note on effective phase stability calculations using a Gradient-Based Cuckoo Search algorithm", *Fluid Phase Equilibria*, Volume 375, 2014, Pages 360-366.

[235]. P. Dash, L. C. Saikia, N. Sinha., "Comparison of performances of several Cuckoo search algorithm based 2DOF controllers in AGC of multi-area thermal system", *International Journal of Electrical Power & Energy Systems*, Volume 55, 2014, Pages 429-436.

[236]. M. K. Kim., "Short-term price forecasting of Nordic power market by combination Levenberg–Marquardt and cuckoo search algorithms", *IET Generation, Transmission & Distribution.* Volume 9, Issue 13, 2015, Pages 1553– 1563.

[237]. D. N. Vo, P. Schegner, W. Ongsakul., "Cuckoo search algorithm for non-convex economic dispatch", *IET Generation, Transmission & Distribution*, Volume 8, Issue 15, 2014, 873– 894.

[238]. S. Kirkpatrick, C. D. Gelatt, M. P. Vecchi., "Optimization by simulated annealing", *Science*, Volume 220, Issue 4598, 1983, Pages 671–680.

[239]. N. Metropolis, A. W. Rosenbluth, M. N. Rosenbluth, A. H. Teller, E. Teller., "Equations of State Calculations by Fast Computing Machines", *Journal of Chemical Physics*, Volume 21, Issue 6, 1953, Pages 1087-1092.

[240]. R. C. Eberhart, J. Kennedy., "A new optimizer using particle swarm theory", In *Proceedings of the sixth international symposium on micro machine and human science*, 1995, Pages 39–43.

[241]. J. Kennedy, R. C. Eberhart., "Particle swarm optimization", In *Proceedings IEEE int'l conf. on neural networks Vol. IV*, 1995, Pages 1942–1948.

[242]. M. Clerc., "The swarm and the queen: towards a deterministic and adaptive particle swarm optimization", *In Proceedings ICEC, Washington, DC*, 1999, Pages 1951–1957.

[243]. R. Storn, K. Price., "Differential evolution: A simple and efficient adaptive scheme for global optimization over continuous spaces", *Technical Report TR-95-012, International Computer Science Institute*, Berkeley, CA, 1995.

[244]. X. S. Yang, S. Deb., "Cuckoo search via Lévy flights", *World Congress on Nature & Biologically Inspired Computing (NaBIC 2009). IEEE Publications.* Pages 210–214.

[245]. Power system test case archive, 2006, Decembar [Online], Available: http://www.ww.washington.edu/research/pstca

[246]. S. Ghosh, S. P. Ghoshal, S. Ghosh, "Optimal sizing and placement of distributed generation in a network system", *International Journal of Electrical Power & Energy Systems*, Volume 32, Issue 8, October 2010, Pages 849-856.

[247]. H. Yoshida, Y. Fukuyama, K. Kawata, S. Takayama, Y. Nakanishi, "A particle swarm optimization for reactive power and voltage control considering voltage security assessment", *IEEE Transaction on Power System*, Volume 15, Issue 4, 2000, Pages. 1232-39.

[248]. Standard PSO 2007 (SPSO-07) on the Particle Swarm Central, Programs section, (2007). [Online]. Available: http://www.particleswarm.info

[249]. K. Deb., "Multi-objective optimisation using evolutionary algorithms", *John Wiley & Sons*, 2001.

[250]. M. Ghasemi, M. Taghizadeh, S. Ghavidel, J. Aghaei, A. Abbasian., "Solving optimal reactive power dispatch problem using a novel teaching-learning-based optimization algorithm", *Engineering Applications of Artificial Intelligence*, volume 39, 2015, Pages. 100-108.

[251]. M. Ghasemi, S. Ghavidel, M. M. Ghanbarian, A. Habibi, "A new hybrid algorithm for optimal reactive power dispatch problem with discrete and continuous control variables", *Applied Soft Computing*, Volume 22, 2014, Pages. 126-140.

[252]. R. Prathiba, M. Balasingh, M. Karuppasamypandiyan., "Optimal selection and allocation of generator for static ATC using differential evolution algorithm", *International Journal of Engineering and Technology (IJET).* Volume 6, Issue 2, 2014, Pages 948-959.

Appendixes

Appendix A.

Table A. 1. Operating ranges of the different control variables of the RPD for the standard *IEEE* bus systems

Sl No.	Control Variables	Units	IEEE 14-Bus System	IEEE 30-Bus System	IEEE 57-Bus System	IEEE 118-Bus System
1.	Load bus voltage (V_L)	p. u	For all these networks, the range of V_L is considered as: $0.95 \leq V_L \leq 1.10$			
2.	Generator bus voltage (V_g)	p. u	For all these networks, the range of V_g is considered as: $0.95 \leq V_g \leq 1.10$			
3.	Transformer tap settings (t)	p. u	For all these networks, the range of t is considered as: $0.90 \leq t \leq 1.10$			
4.	Shunt capacitors (Q_c)	p. u	$0.06 \leq Q_C \leq 0.1800$	Case 1: $0.06 \leq Q_C \leq 0.3000$ Case 2: $0.0 \leq Q_C \leq 5.00$ Case 3: $0.0 \leq Q_C \leq 5.00$	$0.05 \leq Q_{C18} \leq 0.20$ $0.06 \leq Q_{C25} \leq 0.30$ $0.06 \leq Q_{C53} \leq 0.30$	$0.0 \leq Q_{c34} \leq 14.0$ $0.0 \leq Q_{c44}, Q_{c45}, Q_{c46}, Q_{c83} \leq 10.0$ $0.0 \leq Q_{c48} \leq 15.0$ $0.0 \leq Q_{c74} \leq 12.0$ $0.0 \leq Q_{c79}, Q_{c82}, Q_{c105} \leq 20.0$ $0.0 \leq Q_{c107}, Q_{c110} \leq 6.0$

Table A. 2. Operating ranges of the different control variables of the RPD problem for the Indian 62-bus network

Sl No.	Control Variables	Units	Indian 62-bus network
1.	Load bus voltage (V_L)	p. u	$0.95 \leq V_L \leq 1.10$
2.	Generator bus voltage (V_g)	p. u	$0.95 \leq V_g \leq 1.10$
3.	Transformer tap settings (t)	p. u	$0.90 \leq t \leq 1.10$
4.	Var compensators (shunt capacitor, TCSC)	p. u	$0.150 \leq Q_C \leq 5.00$ $-0.04 \leq X_{TCSC} \leq 0.0265$

Appendix B.

- B1. Rating of the Synchronous Condensers:

Here reactive power output from Synchronous Condensers (SC) (Q_{SC}) is considered as 25 MVar as maximum capability [210].

- B2. Rating of the SMES:

The E, P_{SMES} and Q_{SMES} is considered as 4 MJ, 8.64 MW and 4.184 MVar respectively [52].

Appendix C.

Table C. 1 Constants of three generators ($G_{1,2,3}$) and consumers ($L_{1,2,3}$) during bilateral transaction for the IEEE 118-bus system

Generator/consumers	Operating Range	Fuel constants of the generators/consumers are considered here as coefficient of bid price $(aP^2 + bP + c)$		
		a (\$/MW^{2}h)	b(\$/MWh)	c(\$/h)
G_1	$30 \le P_{G1\_BiLat} \le 110$	0.025	16.0	500
G_2	$10 \le P_{G2\_BiLat} \le 186$	0.015	12.0	300
G_3	$44 \le P_{G3\_BiLat} \le 250$	0.01	8.0	400
L_1	$50 \le P_{L1\_BiLat} \le 200$	0.006248	-8.216	2000
L_2	$50 \le P_{L2\_BiLat} \le 280$	0.0082	-7.216	2300
L_3	$16 \le P_{L3\_BiLat} \le 50$	0.0062	-10.216	3800

Table C. 2. Constants of two generators and consumers during 12-h variable bilateral transaction for the IEEE 57 bus system

Generator/ Consumers	Operating Range	Fuel constants of the generators/consumers are considered here as coefficient of bid price $(aP^2 + bP + c)$		
		a(\$/MW^{2}h)	b(\$/MWh)	c(\$/h)
G_1	$P^{\min}_{G1\_BiLat\_i^{hour}} \le P_{G1\_BiLat\_i^{hour}} \le P^{\max}_{G1\_BiLat\_i^{hour}}$	0.01295	2.453	2500
G_2	$P^{\min}_{G2\_BiLat\_i^{hour}} \le P_{G2\_BiLat\_i^{hour}} \le P^{\max}_{G2\_BiLat\_i^{hour}}$	0.01195	2.253	2000
L_1	$P^{\min}_{L1\_BiLat\_i^{hour}} \le P_{L1\_BiLat\_i^{hour}} \le P^{\max}_{L1\_BiLat\_i^{hour}}$	0.00625	-8.216	5000
L_2	$P^{\min}_{L2\_BiLat\_i^{hour}} \le P_{L2\_BiLat\_i^{hour}} \le P^{\max}_{L2\_BiLat\_i^{hour}}$	0.00525	-7.216	4700

Here, $P^{\min}_{G1\_BiLat\_i^{hour}}$ and $P^{\min}_{G2\_BiLat\_i^{hour}}$ is the minimum value of the generations of two producers at the specified hour, $P_{G1\_BiLat\_i^{hour}}$ and $P_{G2\_BiLat\_i^{hour}}$ is the produced power at specified hour, $P^{\max}_{G1\_BiLat\_i^{hour}}$ and $P^{\max}_{G2\_BiLat\_i^{hour}}$ is the maximum value of the generation of the two producers at the specified hour.

$P^{\min}_{L1\_BiLat\_i^{hour}}$ and $P^{\min}_{L2\_BiLat\_i^{hour}}$ is the minimum value of the consumption of two consumers at the specified hour, $P_{L1\_BiLat\_i^{hour}}$ and $P_{L2\_BiLat\_i^{hour}}$ is the consumer power at specified hour, $P^{\max}_{L1\_BiLat\_i^{hour}}$ and $P^{\max}_{L2\_BiLat\_i^{hour}}$ is the maximum value of the consumption of two consumers at the specified hour.

Table C. 3. Constants of three generators and two consumers during multilateral transaction for the IEEE 118-bus system

Generator /consumers	Operating Range	Fuel constants of the generators/consumers are considered here as coefficient of bid price $(aP^2 + bP + c)$		
		a(\$/MW^{2}h)	b(\$/MWh)	c(\$/h)
G_1	$6 \le P_{G1\_MultiLat} \le 40$	0.025	16.0	500
G_2	$10 \le P_{G2\_MultiLat} \le 60$	0.015	12.0	300
G_3	$10 \le P_{G3\_MultiLat} \le 108$	0.01	8.0	400
L_1	$8 \le P_{L1\_MultiLat} \le 58$	0.006248	-8.216	2000
L_2	$20 \le P_{L2\_MultiLat} \le 150$	0.008248	-7.216	2300

Table C. 4. Constants of two generators and four utilities during 24-h variable multilateral power transaction for the Indian Utility 62-bus system

Generator / Consumers	Operating Range	Fuel constants of the generators/consumers are considered here as coefficient of bid price $(aP^2 + bP + c)$		
		a(\$/MW^{2}h)	b(\$/MWh)	c(\$/h)
G_1	$P^{\min}_{G1\_MultiLat\_i^{hour}} \le P_{G1\_MultiLat\_i^{hour}} \le P^{\max}_{G1\_MultiLat\_i^{hour}}$	0.01295	2.453	2500
G_2	$P^{\min}_{G2\_MultiLat\_i^{hour}} \le P_{G2\_MultiLat\_i^{hour}} \le P^{\max}_{G2\_MultiLat\_i^{hour}}$	0.01195	2.353	2000
L_1	$P^{\min}_{L1\_MultiLat\_i^{hour}} \le P_{L1\_MultiLat\_i^{hour}} \le P^{\max}_{L1\_MultiLat\_i^{hour}}$	0.006245	-8.216	4800
L_2	$P^{\min}_{L2\_MultiLat\_i^{hour}} \le P_{L2\_MultiLat\_i^{hour}} \le P^{\max}_{L2\_MultiLat\_i^{hour}}$	0.005248	-7.216	4600
L_3	$P^{\min}_{L2\_MultiLat\_i^{hour}} \le P_{L2\_MultiLat\_i^{hour}} \le P^{\max}_{L2\_MultiLat\_i^{hour}}$	0.004248	-6.216	4400
L_4	$P^{\min}_{L2\_MultiLat\_i^{hour}} \le P_{L2\_MultiLat\_i^{hour}} \le P^{\max}_{L2\_MultiLat\_i^{hour}}$	0.007248	-5.216	4200

Here, $P^{\min}_{G1\_MultiLat\_i^{hour}}$ and $P^{\min}_{G2\_MultiLat\_i^{hour}}$ is the minimum value of generations the two producers at the specified hour, $P_{G1\_MultiLat\_i^{hour}}$ and $P_{G2\_MultiLat\_i^{hour}}$ is the produced power at specified hour, $P^{\max}_{G1\_MultiLat\_i^{hour}}$ and $P^{\max}_{G2\_MultiLat\_i^{hour}}$ is the maximum value of the generation of two producers at the specified hour.

$P^{\min}_{L1\_MultiLat\_i^{hour}}$, $P^{\min}_{L2\_MultiLat\_i^{hour}}$, $P^{\min}_{L3\_MultiLat\_i^{hour}}$ and $P^{\min}_{L4\_MultiLat\_i^{hour}}$ is the minimum value consumption of the four consumers at the specified hour, $P_{L1\_MultiLat\_i^{hour}}$, $P_{L2\_MultiLat\_i^{hour}}$, $P_{L3\_MultiLat\_i^{hour}}$ and $P_{L4\_MultiLat\_i^{hour}}$ is the consumer power at specified hour, $P^{\max}_{L1\_MultiLat\_i^{hour}}$, $P^{\max}_{L2\_MultiLat\_i^{hour}}$, $P^{\max}_{L3\_MultiLat\_i^{hour}}$ and $P^{\max}_{L4\_MultiLat\_i^{hour}}$ is the maximum value of the consumption four consumers at the specified hour. All the above values are for multilateral transactions.